AD-A160 734

**Final Report
for the period
1 April 1984 to
31 January 1985**

Antiproton Annihilation Propulsion

September 1985

University of Dayton
Research Institute
Dayton, Ohio 45469

UDR-TR-85-55
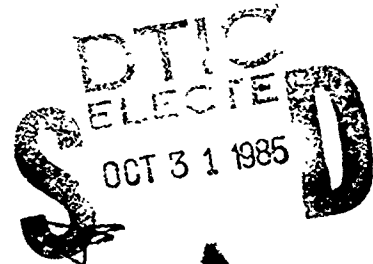F04611-83-C-0046

Author:
R. L. Forward

Forward Unlimited
34 Carriage Square
Oxnard, CA 93030

Approved for Public Release   RI-32901

prepared for the: **Air Force
Rocket Propulsion
Laboratory**

Air Force Space Technology Center
Space Division, Air Force Systems Command
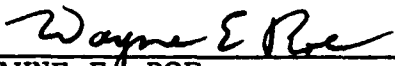Edwards Air Force Base,
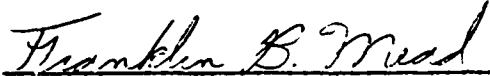California 93523-5000

85 10 31 063

NOTICE

This report was submitted by the University of Dayton Research Institute, Dayton, Ohio 45469 USA under Contract Number F04611-83-C-0046, Job Order Number 2308 M3 RC with the Air Force Rocket Propulsion Laboratory, Edwards Air Force Base, California 93523 USA. The report includes work done from 1 April 1984 to 31 January 1985. The research was performed at the Air Force Rocket Propulsion Laboratory, Edwards Air Force Base, California. The Principal Investigator was Dr. Robert L. Forward. The Project Manager was Mr. Wayne E. Roe, and the Task Manager was Dr. Franklin B. Mead, Jr.

This technical report is approved for release and distribution in accordance with the distribution statement on the cover and on the DD Form 1473.
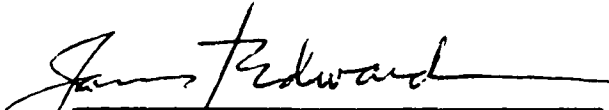

WAYNE E. ROE
Research Coordinator

FRANKLIN B. MEAD
Project Manager

FOR THE DIRECTOR

JAMES T. EDWARDS
Chief, Plans and Programs

EDWARD L. IBBOTSON, Lt Col, USAF
Deputy Chief, Liquid Rocket Division

AD-A160734

REPORT DOCUMENTATION PAGE

1a. REPORT SECURITY CLASSIFICATION	1b. RESTRICTIVE MARKINGS
Unclassified	

2a. SECURITY CLASSIFICATION AUTHORITY	3. DISTRIBUTION/AVAILABILITY OF REPORT
	Approved for Public Release:
2b. DECLASSIFICATION/DOWNGRADING SCHEDULE	Distribution is Unlimited.

4. PERFORMING ORGANIZATION REPORT NUMBER(S)	5. MONITORING ORGANIZATION REPORT NUMBER(S)
UDR-TR-85-55	AFRPL-TR-85-034

6a. NAME OF PERFORMING ORGANIZATION	6b. OFFICE SYMBOL (If applicable)	7a. NAME OF MONITORING ORGANIZATION
Forward Unlimited, subcontractor to University of Dayton		Air Force Rocket Propulsion Lab.

6c. ADDRESS (City. State and ZIP Code)	7b. ADDRESS (City. State and ZIP Code)
Oxnard, CA 93030/Dayton, OH 45469	AFRPL/XRX, Stop 24
	Edwards Air Force Base, CA 93523-5000

8a. NAME OF FUNDING/SPONSORING ORGANIZATION	8b. OFFICE SYMBOL (If applicable)	9. PROCUREMENT INSTRUMENT IDENTIFICATION NUMBER
AFRPL		F04611-83-C-0046

8c. ADDRESS (City, State and ZIP Code)	10. SOURCE OF FUNDING NOS.			
AFRPL/XRX, Stop 24 Edwards Air Force Base, CA 93523-5000	PROGRAM ELEMENT NO.	PROJECT NO.	TASK NO.	WORK UNIT NO.
11. TITLE (Include Security Classification) ANTIPROTON ANNIHILATION PROPULSION (U)	62302F	2308	M3	RC

12. PERSONAL AUTHOR(S)
Forward, Robert L.

13a. TYPE OF REPORT	13b. TIME COVERED	14. DATE OF REPORT (Yr., Mo., Day)	15. PAGE COUNT
Final	FROM 84/4/1 TO 85/1/31	85/9	212

16. SUPPLEMENTARY NOTATION

17.	COSATI CODES		18. SUBJECT TERMS (Continue on reverse if necessary and identify by block number)
FIELD	GROUP	SUB. GR.	Antimatter Propulsion, Antiproton Propulsion, Advanced Propulsion.
21	03		

19. ABSTRACT (Continue on reverse if necessary and identify by block number)

Antiproton annihilation propulsion is a new form of space propulsion, where milligrams of antimatter are used to heat tons of reaction fluid to high temperatures. The hot reaction fluid is exhausted from a nozzle to produce high thrust at high specific impulse. This study was to determine the physical, engineering, and economic feasibility of antiproton annihilation propulsion. The conclusion of the study is that antiproton propulsion is feasible, but expensive. Because the low mass of the antimatter fuel more than compensates for its high price, comparative mission studies show that antimatter fuel can be cost effective in space, where even normal chemical fuel is expensive because its mass must be lifted into orbit before it can be used. Antiproton annihilation propulsion is mission enabling, in that it allows missions to be performed that cannot be performed by any other propulsion system.

20. DISTRIBUTION/AVAILABILITY OF ABSTRACT	21. ABSTRACT SECURITY CLASSIFICATION
UNCLASSIFIED/UNLIMITED ☒ SAME AS RPT. ☐ DTIC USERS ☐	Unclassified

22a. NAME OF RESPONSIBLE INDIVIDUAL	22b. TELEPHONE NUMBER (Include Area Code)	22c. OFFICE SYMBOL
Wayne E. Roe	(805) 277-5206	XRX

DD FORM 1473, 83 APR   EDITION OF 1 JAN 73 IS OBSOLETE.

TABLE OF CONTENTS

QUALITY
INSPECTED
5

iii

LIST OF FIGURES

v

LIST OF TABLES

INTRODUCTION AND SUMMARY

Antiproton annihilation propulsion is a new form of space propulsion in which milligrams of antimatter are used to heat tons of reaction fluid to high temperatures. The hot reaction fluid is then exhausted from a nozzle to produce high thrust at high specific impulse (1000 to 3500 s).

This study was contracted by the Air Force Rocket Propulsion Laboratory to determine the physical, engineering, and economic feasibility of antiproton annihilation propulsion. The conclusion of the study is that antiproton annihilation propulsion is feasible, but expensive.

Antimatter fuel has to be manufactured. It is probable that the efficiency of production will always be low, so the price will be high. Antimatter is a very lightweight form of fuel, however, since the antimatter converts all of its mass to energy upon annihilation with normal matter. Because its low mass more than compensates for its high price, comparative mission studies show that antimatter fuel can be cost effective in space, where even normal chemical fuel is expensive because its mass must be lifted into low earth orbit before it can be used.

For propulsion applications the antimatter should be in the form of antiprotons. Unlike antielectrons (positrons), the antiproton does not convert into gamma rays upon annihilation. Instead, two-thirds of the annihilation energy is emitted as charged particles (pions) whose kinetic energy can be converted into thrust by interaction with a magnetic field nozzle or a working fluid.

Antiproton annihilation propulsion is mission enabling, in that it allows missions to be performed that cannot be performed by any other propulsion system. The most striking example of such an "impossible" mission is a simple sortie mission that involves leaving an orbiting base, inspecting a spacecraft in a counter-rotating orbit, then returning to base a few hours later. This can be done with an antiproton powered vehicle that has a mass ratio of 3:1. To carry out a similar mission, a chemical rocket would have to have an unachievable mass ratio of 500:1, while an electric propulsion system would require days instead of hours to complete the task.

Antiprotons are already being generated, captured, cooled, and
stored at a number of particle physics laboratories around the
world, albeit in small quantities. The rest of this report
discusses in detail the techniques for the efficient
generation, long-term storage, and effective utilization of
milligram quantities of antiprotons for space propulsion.

Since the fields of particle physics, laser physics, and
molecular beam physics are not included in the educational
background of the usual propulsion professional, this report
contains more than the usual amount of tutorial material and
a great number of bibliographic references. It is hoped that
this tutorial material will be useful to those attempting to
make antimatter propulsion a reality.

Section 1 describes the present facilities for the production
of antimatter in the form of antiprotons. The major producer
is the European Center for Nuclear Research (CERN) which has
been producing, capturing, and storing antiprotons in magnetic
storage rings for a number of years. Antiproton production
facilities are also under construction at the Fermi National
Accelerator Laboratory in the U.S. and at the Institute for
High Energy Physics in the USSR.

Antiprotons are produced by accelerating normal matter protons
to high speed and smashing them into a heavy metal target.
The interaction causes new particles to be made, among them a
small number of antiprotons. The antiprotons are focused with
a magnetic lens, captured in a collecting ring, then cooled
off and slowed down by other rings, and finally accumulated in
a storage ring. In the present facilities they are later
accelerated back up to high energies and smashed head-on into
normal protons to carry out high-energy particle physics
experiments.

Sections 1.5 and 1.6 show that the production efficiencies of
the present machines are extremely low. Due to space, time,
and funding restrictions, only a small fraction (~0.1%) of the
antiprotons generated in the target are captured.

Section 2 is a tutorial summary of the present methods for
generating, capturing, cooling, and storing of antiprotons.
The present methods all have problems with efficiency. Some
of the problems are inherent in the physics, some are due to
the engineering limitations of the present designs, and some
are just due to a lack of time or money.

Section 3 is a detailed discussion of the limitations of the
present antiproton production techniques and methods for
improving the antiproton production efficiencies. If the
improvements were to be made, the antiproton production
efficiency in terms of number of antiprotons captured per

2

incident protons hitting the target could be raised from the present $\bar{p}/p=4\times10^{-7}$ at CERN and 3×10^{-5} at Fermilab to a production ratio of $\bar{p}/p=5\times10^{-2}$. Then, if the proton accelerator were optimized for energy efficiency, the overall energy efficiency could be raised to 2.5×10^{-4}. Although an energy efficiency of 0.025% does not seem very efficient, it is adequate to allow the production of antimatter at a cost of 10M$/mg, at which point antimatter becomes cost effective for space propulsion.

The present methods for storing antiprotons are not suitable for space propulsion. The storage rings are too massive and the antimatter they can hold is too diffuse. Section 4 discusses the various techniques for adding a positron to the antiproton to make antihydrogen atoms, then combining two antihydrogen atoms to make an antihydrogen molecule. Section 5 then shows how electromagnetic fields and laser photons can be used to control, slow down, and cool antihydrogen atoms and molecules.

Section 6 shows the same laser techniques can be used to stop the antihydrogen molecules and put them in a trap. The laser also cools the gas until it has the temperature of a millidegree Kelvin. The supercooled gas is then turned into a crystal of antihydrogen ice and the antihydrogen ice ball is levitated in an electrostatic or magnetostatic trap until ready for use. If the antihydrogen ice ball is kept below 2 K, its vapor pressure is so low (4×10^{-18} Torr) that it can be kept indefinitely. Section 6.5 contains a detailed energy balance for the iceball assuming that some annihilation reactions are going on inside the storage chamber. The amount of energy deposited by the expected reactions is less than the cooling to the chamber walls.

Section 7 goes into detail on the reaction products to be expected from the annihilation of the antiprotons and how they can be utilized to provide thrust. On the average there are 3 charged pions with an average kinetic energy of 250 MeV and 1.5 neutral pions that turn into 3 gamma rays with an average energy of 200 MeV. The charged pions have a relatively short lifetime, but in a properly designed engine, they last long enough to transfer most of their kinetic energy into the working fluid. The present estimates are that one third of the annihilation energy from the antimatter fuel ends up as kinetic energy in the vehicle. In a typical antiproton rocket design where the working fluid was hydrogen gas, 1 mg of antimatter was equivalent to 6 metric tons of propellant.

Section 8 discusses the effect of antiproton annihilation propulsion on space mission design. First it is shown that no matter what the mission characteristic velocity or the antimatter rocket efficiency, the optimum mass ratio of an

3

antimatter rocket is never greater than 5:1. For most
missions near earth and in the solar system it is 2.5:1. This
contrasts strongly with chemically fueled missions, where mass
ratios are much greater.

Section 8.4 and Appendix B contain a comparative cost study of
a storable chemical fuel propulsion system, a liquid
oxygen/liquid hydrogen propulsion system, a nuclear thermal
hydrogen propulsion system, and an antiproton annihilation
propulsion system. Since hauling chemical fuel into low earth
orbit costs 5K$/kg or 5M$/T, it is shown that if antimatter
fuel costs 10M$/mg or less it is more cost effective than any
chemical propulsion system for any mission characteristic
velocity greater than 5 km/s. If the price of antimatter fuel
could be brought down to less than 1M$/mg, then any mission in
the solar system, including a rendezvous mission to the rings
deep down in the gravity well of Saturn becomes possible.

Section 9 contains the basic conclusion that antiproton
annihilation propulsion is feasible, but expensive. It then
recommends a number of research and engineering studies that
need to be undertaken to verify that antimatter propulsion is
indeed feasible and to obtain a better estimate of the
antimatter production efficiencies and costs. Section 9.6 is
included for the skeptics. Here are listed those areas of
technology that are considered the weakest. These are the
areas where a "show stopper" may lurk. If found and proven,
it would mean that antiproton annihilation propulsion is
either not possible or too difficult or expensive to pursue.

Section 10 contains a lengthy bibliography of all of the
pertinent papers in particle physics, nuclear physics, atomic
physics, laser physics, molecular beam physics, and antimatter
propulsion engineering that might be useful for someone
intending to work further in the field.

SECTION 1

PRESENT ANTIPROTON PRODUCTION FACILITIES

In this section we describe the present facilities for the
production of antimatter in the form of antiprotons. As we
will see, antiprotons are being made, collected, and stored
today. Thus, the production of antimatter is no longer a
question of technical feasibility, but a question of economic
feasibility.

The present methods for producing antimatter are highly
inefficient and extremely expensive, but they don't have to
be. Before we can start considering the use of antimatter for
propulsion, however, we will need to identify efficient
methods for making and storing antimatter that will produce
significant quantities of antimatter at a reasonable cost. To
start, let us see what is being done now in the production,
capture, and storage of antimatter.

1.1 BACKGROUND

Antimatter in the form of antiprotons is being made and stored
today, albeit in small quantities. The only known major
producer is the Organisation Européenne pour la Recherche
Nucléaire (formerly the Center for European Nuclear Research
or CERN) in Europe.[1.1] Fermilab in the U.S. has started
construction of their antiproton facility and expects to be in
operation in 1985.[1.2] In 1980, it was reported[1.3] that the
Institute for High Energy Physics (IHEP) in the USSR was
constructing an antiproton production facility, but no further
information on construction progress has been published since.

In these facilities, the antiprotons are generated by sending
a high-energy beam of protons into a metal target as is shown
in Figure 1-1. When the relativistic protons strike the dense
metal nuclei, their kinetic energy, which is many times their
rest-mass energy, is converted into a spray of particles, some
of which are antiprotons. A magnetic field focuser and
selector separates the antiprotons from the resulting debris,
decelerates it, and directs it to a storage ring.

When the antiprotons are generated, they have a wide spread of
energies. Before they can be used further, it is necessary to
"cool" the beam so that all the antiprotons have the same
energy. Two techniques for reducing the spread in velocity
have been demonstrated. They are called electron cooling and
stochastic cooling and are described in Sections 2.3 and 2.4.

5

RELATIVISTIC
PROTON BEAM
~100 GeV

METAL

DEBRIS

TARGET

INCLUDING
ANTIPROTONS

BENDING
MAGNET
FOCUSER
AND
SELECTOR

"COOL" ANTIPROTONS
100 ±0.001 MeV

ANTIPROTON
COOLER AND
STORAGE
RING

ANTIPROTON
DECELERATOR

RELATIVISTIC
ANTIPROTONS
10 GeV

SUBRELATIVISTIC
ANTIPROTONS
100 ±10 MeV
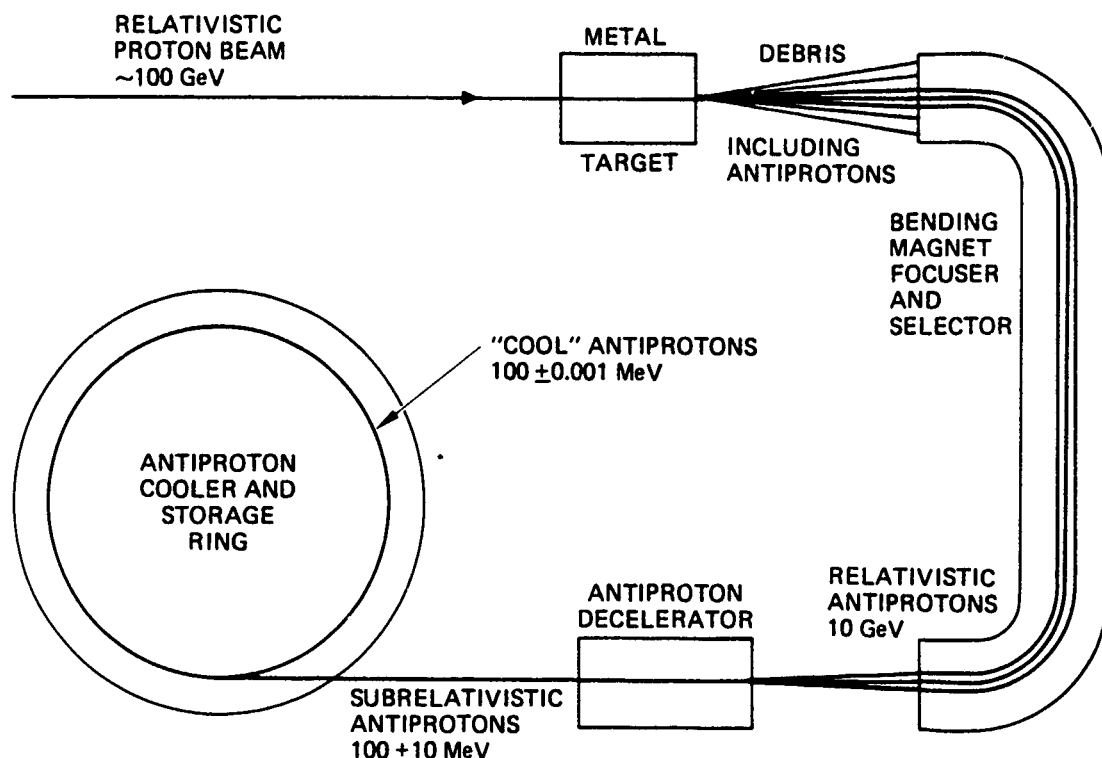
Fig. 1-1   Producing, capturing, and storing antiprotons.

These cooled antiprotons could then go through another stage
of deceleration and cooling to bring them down to speeds
suitable for capture and control by other techniques. The
present accelerator at CERN generates 3.5 GeV antiprotons
using a 26 GeV proton beam and has stored up to 10^{12}
antiprotons in their magnetic ring "racetrack" antiproton
accumulator.[1.4]

To give some scale to what has already been accomplished, 10^{12}
antiprotons have a mass of 1.7 picograms. When this amount of
antimatter is annihilated with an equivalent amount of normal
matter, it will release 300 joules, a significant quantity of
energy from an engineering viewpoint. To obtain this
"firecracker" amount of annihilation energy required the use
of multimillion dollar machines that used an enormous amount
of electric energy. Yet it is important to recognize that
scientists, working in basic physics, using research tools not
designed for the job, have produced and continue to produce
significant quantities of annihilation energy.

References:

1.1CERN Proton Synchrotron Staff, "The CERN PS complex as an antiproton source," IEEE Trans. **NS-30**, 2039-2041 (1983).

1.2J. Peoples, "The Fermilab antiproton source," IEEE Trans. **NS-30**, 1970-1975 (1983).

1.3T.A. Vsevolozhskaya, B. Grishanov, Ya. Derbenev, N. Dikansky, I. Meshkov, V. Parkhomchuk, D. Pesrikov, G. Sil'vestrov, A. Skrinsky, "Antiproton source for the accelerator-storage complex, UNK-IHEP," Fermilab Report FN-353 8000.00 (June 1981), a translation of INP Preprint 80-182 (December 1980).

1.4D.B. Cline, C. Rubbia, and S. van der Meer, "The search for intermediate vector bosons," Scientific American **247**, No. 3, 48-59 (March 1982).

1.2 ANTIPROTON PHYSICS AT CERN

The only facility in the world presently making significant quantities of antiprotons is the European Organization for Nuclear Research or CERN, outside Geneva, Switzerland. CERN operates three large machines used for elementary particle physics. These are the Proton Synchrotron (PS), the Intersecting Storage Rings (ISR), and the 7 km circumference Super Proton Synchrotron (SPS). There are also two smaller machines used for antiproton collection and research, the Antiproton Accumulator (AA) and the Low Energy Antiproton Ring (LEAR). The CERN complex will grow in the future with the addition of an Antiproton Collector (AC) and a Large Electron-Positron (LEP) ring that will be 28 km in circumference.

1.2.1 Present Status of CERN facility.

The heart of the complex is the Proton Synchrotron, the original CERN machine that has matured into a complex tool. As is shown in Figure 1-2, protons are accelerated by the Linear Accelerator (linac) to 50 MeV and injected into the Booster which accelerates them to the near relativistic energy of 0.8 GeV. The kinetic energy of the proton is now comparable to its rest mass energy of 0.938 GeV. The Booster then sends the protons to the Proton Synchrotron, which further accelerates them up to 26 GeV. These 26 GeV protons can be sent to the ISR or the SPS to carry out particle physics experiments, or can be switched to a target area to make antiprotons.
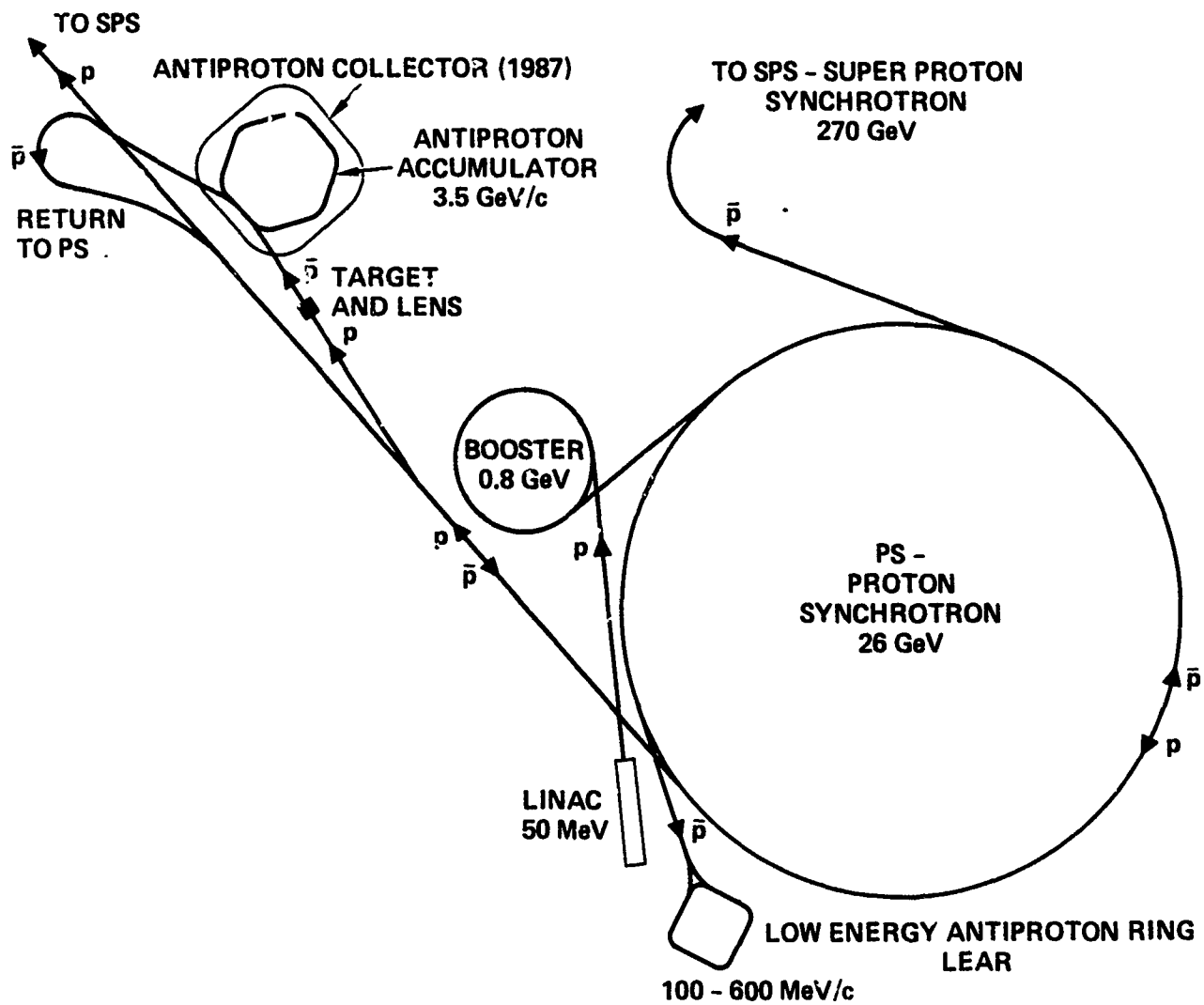
Fig. 1-2 Producing antiprotons at CERN.

Antiprotons are produced by focusing the 26 GeV protons down to a 2 mm beam and inserting them into a 3 mm diameter, 11 cm long copper wire target. The protons collide with the copper nuclei in the wire and the kinetic energy of the collision produces a spray of particles, mostly pions and kaons, some protons and neutrons from the original nuclei, and an occasional antiproton. The production rates are discussed further in Section 2.1.

The spectrum of the antiprotons is peaked around a momentum of 3.5 GeV/c (energy of 3 GeV). The antiprotons with that momentum are focused by a short focal length pulsed magnetic horn designed to capture a momentum bite of 1.5% at angles up to 50 mrad.[1.5] The focused antiproton beam is then transported to the Antiproton Accumulator by a normal quadrupole focusing channel. Although the AA was designed to have an acceptance of 100π mm-mrad (2 mm by 50 mrad), in practice the acceptance has been found to only be 70π mm-mrad.

The antiprotons are injected into the outer half of the AA ring where their momentum spread is reduced by a stochastic precooling system to the point where they can be moved to the inner part of the ring and deposited in the tail of the stack of antiprotons accumulating there. About 7×10^6 antiprotons are injected in each burst and are precooled before the next burst arrives, 2.4 s later.[1.5] The antiprotons in the stack undergo further stochastic cooling and slowly build up into an intense core of about 10^{11} antiprotons.

The scientists at CERN have discovered an effect which limits the density of the antiprotons that can be stored and kept cool in a single accumulator ring. The effect, called intramodulation blow-up, is due to intrabeam scattering. It is related to the space charge limit in stationary collections of ions and is independent of beam energy. The intramodulation blow-up is an exponentially increasing expansion of the beam which must be kept down by stochastic cooling. With the present cooling system, the intrabeam scattering expansion will equal the stochastic cooling compression at a beam intensity of 6×10^{11} $\bar{p}$. This effect must be taken into account in the design of the accumulators and coolers for an antiproton factory since it will limit the number of antiprotons that can be held at one time in a stochastic cooler before the antiproton ions must be decelerated further or turned into neutral hydrogen.

For particle physics experiments at high energies, the 3 GeV antiprotons are extracted from the AA and sent to the PS, where they are accelerated up to 26 GeV. These high-energy antiprotons are then sent to the SPS where they and an oppositely directed beam of 26 GeV protons are simultaneously accelerated up to as much as 270 GeV each and collided at

9

center of mass energies of 540 GeV to produce new particles such as the W and Z^0 vector bosons that are the carriers of the weak force. (Finding these particles won the 1984 Nobel Prize in Physics for Simon van der Meer and Carlo Rubbia of CERN).

For particle physics experiments at intermediate energies, the 26 GeV antiprotons from the PS are sent to one of the storage rings of the ISR, where they undergo further cooling. Once optimized, the transfer efficiency from the AA stack through the PS to the ISR approaches 100%. The ISR has a good vacuum system and has stored an $1.998+0.0025$ ma beam of antiprotons with no detectable loss for 55 hours, leading to an estimate for the antiproton lifetime of greater than 30,000 hr.[1.6] One experimental run on the ISR lasted for 2 weeks. For particle physics experiments, the second ring of the ISR is filled with protons, and experiments are carried out at the eight regions where the two counter-circulating beams intersect each other.

For particle physics experiments at low energies, the 3 GeV antiprotons are <u>decelerated</u> by the PS down to 200 MeV and sent to the LEAR. Here they are decelerated to an energy of 50 MeV and are further cooled by stochastic cooling. The antiprotons are then used for various experiments such as the measurement of the production rates for some of the more exotic products of the proton-antiproton annihilation process and the X-rays emitted by a protonic atom (a proton and antiproton orbiting about each other just before annihilation) as it drops from one excited state to the next.[1.7]

A typical "fill" of the LEAR ring is 10^{10} antiprotons, and the beam is used for a number of hours by many different experiments. Many of the antiprotons, however, do not interact with the experiments and as many as 10^9 of them end up in the beam dump. These "dumped" antiprotons might be a source for antiprotons needed for experiments on freezing and storage of antihydrogen for propulsion.

References:

[1.5]R. Billinge, "CERN's p$\bar{p}$ source," CERN Publication 84-09, Proc. Fourth Topical Workshop on Proton-Antiproton Collider Physics, Berne, 5-8 March 1984, pp. 357-364 (8 August 1984).

[1.6]P.J. Bryant, "Antiprotons in the ISR," IEEE Trans. Nuclear Sci. **NS-30**, 2047-2049 (August 1983)

[1.7]K. Kilian, "Physics with antiprotons at LEAR," CERN Publication 84-09, Proc. Fourth Topical Workshop on Proton-Antiproton Collider Physics, Berne, 5-8 March 1984, pp. 324-341 (8 August 1984).

1.2.2 Future Plans at CERN

Since Fermilab has no present plans to decelerate the
antiprotons at their facility, the only source of antiprotons
for the next few years will be the Low Energy Antiproton Ring
(LEAR) at CERN. Thus it is important to know what the future
plans are for antiproton generation, collection, and storage.

The present CERN antiproton facility, although remarkable in
its present capabilities, falls short of the original
expectations of the designers. First, the CERN facility is
limited in its production capability by the energy limits of
the available proton accelerator, the Proton Synchrotron (PS).
The PS has an upper limit to its energy of about 28 GeV. For
producing antiprotons it is operated at a momentum of
26 GeV/c. This is not too far from the antiproton production
threshold of 8.8 GeV/c. Thus, the initial production is 10
times lower than Fermilab, which will use 120 GeV protons, and
20 times lower than the energy optimum at a proton energy of
200 GeV. There is no reasonable way that the proton energy
can be increased, so CERN is stuck with the present proton
energy and its effect on the production rate.

The PS operates at a current intensity of 1.2×10^{13} protons for
each 2.4 s cycle. The cycle time per pulse is fixed by the
design parameters of the PS. Efforts are being made to
increase the current intensity to 2×10^{13} protons/pulse.[1.8]
The increased beam intensity will have an effect on the choice
of the target, since the present targets are being stressed
close to their limit.

To increase the brightness of the antiproton source, the CERN
engineers are looking at a number of modifications to the
present techniques. One is to reduce the radius of the
primary beam by focusing the protons onto the target with a
magnetic lens. For a fixed acceptance of the Antiproton
Accumulator in mm-mrad, this means that antiprotons can be
captured over a wider angular range.

The decreased beam size and increased current means that the
energy density on the target will be increased. The present
targets are copper, which have been found to be capable of
standing the present energy deposition rates. It may be
necessary to use tungsten targets although the yield per
incident proton is slightly less than the yield for copper.
An alternative would be to use rotating or liquid metal
targets.

A second modification being considered at CERN is to pass a
high current through or just outside the target to create an
azimuthal field in and around it. The antiprotons, instead of
spreading out in angle, will tend to follow along the magnetic

11

field lines until they reach the end of the target. This, in effect, turns the antiproton source from a rod source to a disk source.

A third modification is to decrease the focal length of the magnetic lens following the target so as to be able to collect antiprotons at larger production angles. Replacing the present magnetic horn with a lithium lens[1.9] is one possibility being considered. An alternative possibility is to use a non-linear magnetic lens that selectively collects some particles at higher energies. Another, which is not presently being considered by CERN, is to use an array of lenses with longer focal lengths.

CERN has carried out calculations on a target system using a prefocusing lithium lens 2 cm in diameter by 15 cm long and pulsed at 350 kA, a current carrying copper target 1.8 mm diameter by 17 cm long pulsed at 225 kA, followed by a collecting lithium lens 4 cm in diameter by 15 cm long pulsed at 800 kA. This system would multiply the present target yield by a factor of 22.[1.10] The output emittance, however, would be too big to enter the present AA.

A major disappointment to CERN was that the beam acceptance of the Antiproton Accumulator did not reach the design goals. The CERN engineers will continue to look for the source of the decrease in acceptance and attempt to correct it. Meanwhile they will bypass the problem by adding an antiproton preconditioning ring called the Antiproton Collector (AC or ACOL). The AC will be optimized for collecting the antiprotons, while the AA will be reworked to optimize it for stacking and storing of the collected antiprotons.

The AA will be shut down in late 1986 and will be combined in late 1987 with the AC. The AC will be designed to have twice the transverse acceptance of the AA in both planes and four times the momentum acceptance (6%).[1.11] The AC will carry out a phase space "compression" of the incoming antiproton pulse using a combination of longitudinal and transverse stochastic beam cooling and bunch manipulation in phase space.

The antiprotons arrive in 5 short bunches and it is possible to exchange momentum spread against bunch length by using a technique called bunch "rotation". This process uses a RF cavity pulsed at 1 MV for a fraction of a millisecond. After this bunch rotation, the bunches smear out into a continuous beam and the transverse emittances will be cooled from 200π down to 3π mm-mrad by fast horizontal and vertical stochastic cooling systems. Longitudinal cooling will then be applied to reduce the momentum spread of 6% by an order of magnitude.[1.11]

The precooled beam will then be transferred to the AA. The transfer should be highly efficient since the momentum spread and the transverse emittances of the preconditioned beam are now small enough to easily fit into the present AA acceptances. The stochastic cooling systems in the AA will be upgraded to handle the higher antiproton flux. Primarily this means increased bandwidth (2-4 GHz) and increased power (10 kW) in the sensing and kicker circuits. This amount of power is quite expensive in this frequency range. The AA will also be modified by removing the precooling circuits and movable shutters so that it will be a reliable machine for cooling, stacking, and storage of the antiprotons until they are needed for experiments.

References:

1.8 E. Jones, S. van der Meer, R. Rohner, J.C. Schnuriger, and T.R. Sherwood, "Antiproton production and collection for the CERN antiproton accumulator," IEEE Trans. Nuclear Sci. **NS-30**, 2778-2780 (August 1983).

1.9 B.F. Bayanov, J.N. Petrov, G.I. Silvestrov, J.A. MacLachlan, and G.L. Nicholls, "A lithium lens for axially symmetric focusing of high energy particle beams," Nucl. Instr. & Methods, **190**, 9-14 (1981).

1.10 B. Autin, "The future of the antiproton accumulator," pp. 573-582, Proc. Workshop on Proton-Antiproton Physics and the W discovery," La Plagne (1983).

1.11 S. van der Meer, "Practical and foreseeable limitations in usable luminosity for the collider," CERN Publication 83-04, Proc. Third Topical Workshop on Proton-Antiproton Collider Physics, Rome, 12-14 January 1983, pp. 555-561 (10 May 1983).

1.3 ANTIPROTON PHYSICS AT FERMILAB

The particle physics facilities at the Fermi National Accelerator Laboratory consist of the Booster, the 400 GeV Main Ring, and the superconducting 1 TeV Tevatron in the same tunnel as the Main Ring. To collect the antiprotons needed for p$\bar{\text{p}}$ collision experiments Fermilab is constructing a Target Station followed by a Debuncher and an Accumulator shown in Figure 1-3.[1.12] The antiproton source will come on line in 1985 and be operational in 1986. There are no plans for decelerating the antiprotons to subrelativistic velocities.

In the Fermilab complex, every two seconds a batch of 2×10^{12} protons in 82 rf bunches are accelerated by the Main Ring to 120 GeV, then rotated by rf pulsing to convert the long pulses into short pulses. The short proton bunches strike a 5 cm long tungsten target, producing 82 equally spaced short antiproton bunches. The 8 GeV antiprotons near the peak of the antiproton spectrum are collected by a lithium lens 2 cm in diameter by 15 cm long, that is pulsed with a current of 500 kA to produce a magnetic gradient of 1000 T/m. The focused antiprotons near 8 GeV are diverted 3° by a pulsed dipole magnet and then transported to the Debuncher. The combination of lens and Debuncher acceptance collects the 7×10^7 antiprotons near 8 GeV within a momentum spread of 3% and beam emittances of 20π mm-mrad in each plane.

In the Debuncher the antiproton bunches are rotated so that the narrow pulse length and the large momentum spread have been transformed into a small momentum spread and a long pulse length. After the rf manipulations, the horizontal and vertical transverse emittances are stochastically cooled in the Debuncher from 20 to 7π mm-mrad during the two seconds before the next antiprotons are to be injected.

The antiprotons are then extracted from the Debuncher and injected into the Accumulator. Successive batches are accumulated by rf stacking each batch at the edge of the stack. Between injection cycles, the stack is stochastically cooled using a combination of longitudinal and transverse cooling. Some antiprotons are lost during transfer and rf stacking, and some diffuse away from the stack into the chamber walls. Allowing for losses, 6×10^7 antiprotons are stacked in each pulse. In 4 hours, the core will grow to 4.3×10^{11} antiprotons. During this time the transverse cooling systems will have reduced the horizontal and vertical emittances to 2π mm-mrad.

14
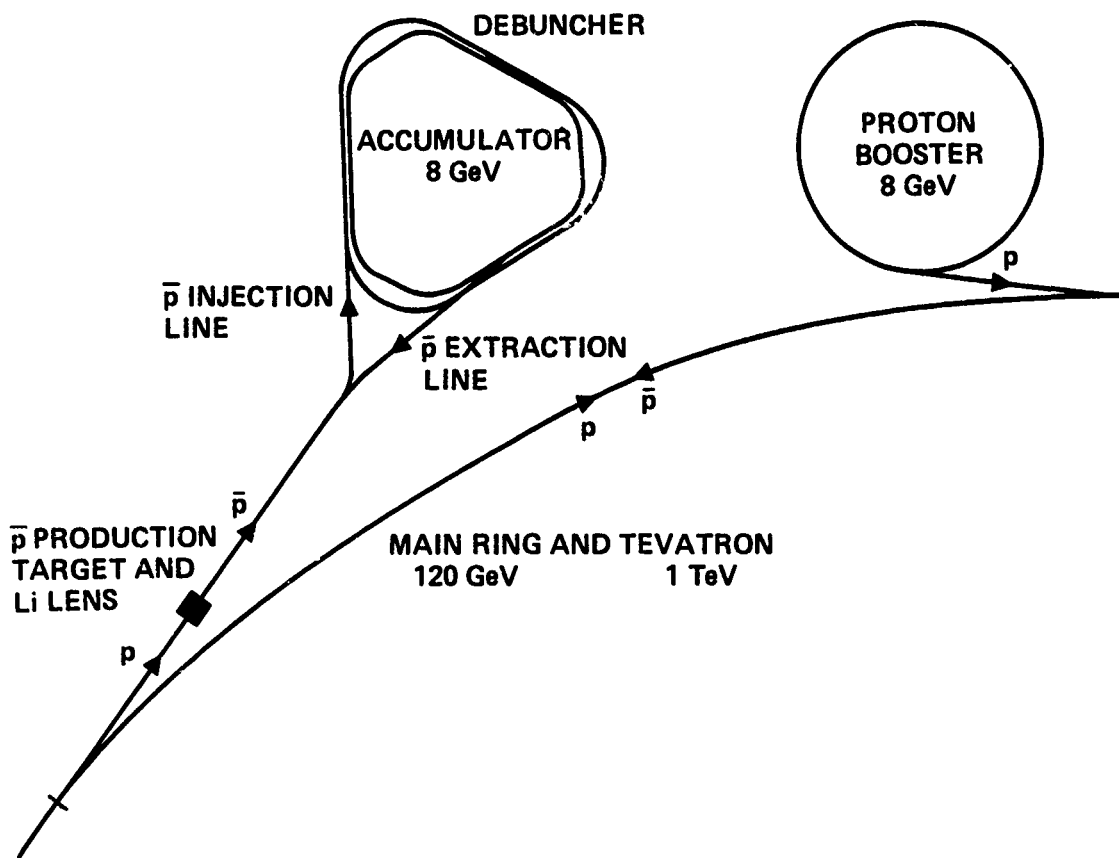
Fig. 1-3   Antiproton production facility at Fermilab.

After the Accumulator is full, antiproton bunches of the
desired intensity are individually extracted from the core,
transferred to the Main Ring, accelerated to 150 GeV and
injected into the Tevatron for p$\bar{\text{p}}$ collision experiments (and,
it is hoped, some Nobel prizes in the late 1980's).

Future plans at Fermilab include adding momentum precooling to
the Debuncher, improving the stochastic cooling in the
Accumulator, improving the Main Ring extraction for antiproton
production, and installing intermediate energy electron
cooling in the Accumulator.

The cost of the antiproton generation, collection, and storage
facility, including the modifications to the existing
accelerators, the p$\bar{\text{p}}$ interaction area, and overhead is 124 M$.
Of this amount, 62.5 M$ is for the building of the antiproton
source.[1.13] The overall cost of the 1 TeV Tevatron is
estimated at 300 M$.[1.14]

References:

[1.12]Fermilab staff, **Design Report: Tevatron 1 Project**, Fermi
National Accelerator Laboratory, Batavia, Illinois (September
1984).

[1.13]J.P. Marriner, "The Fermilab $\bar{\text{p}}$p collider," pp. 583-592,
Proc. Workshop on Proton-Antiproton Physics and the W
discovery," La Plagne (1983).

[1.14]Physics Today editors, "Fermilab's superconducting
synchrotron strives for 1 TeV," Search and Discovery Section,
Physics Today, 37, No. 3, 17-20 (March 1984).

1.4 ANTIPROTON PHYSICS AT IHEP

High-energy particle physics in the USSR is carried out at the Institute for High Energy Physics (IHEP) in Serpukhov, Novosibirsk. The major machine is the U-70 proton synchrotron with a maximum energy of 70 GeV with a beam intensity of 7×10^{12} protons/cycle and a cycle duration of 7 s. This machine has been used for particle physics experiments including measurements of the production spectrum of hadrons (including antiprotons) in the collision of 70 GeV protons with heavy nuclei including Al, Be, Cu, C, Sn, and Pb.[1.15]

The future plans for the particle physics research at IHEP are to construct by 1989 an electron-positron collider (VLEPP) with an initial center of mass energy of 300 GeV. This will later be upgraded to 1000 GeV. By 1990 it is planned to have one ring of the Accelerating and Storage Complex (UNK) operating with protons and antiprotons with a center of mass energy of 6000 GeV (6 TeV) and a $3 \times 10^{30}/cm^2 \cdot s$ luminosity.[1.16] The UNK tunnel will be 19.3 km in circumference (6 km diameter) and contains two rings. The first uses conventional magnets and will accelerate the 70 GeV protons from the U-70 to 400 GeV. A second ring will use superconducting magnets and provide energies from 400 to 3000 GeV. The 400 and 3000 GeV proton beams can be collided to provide a center of mass energy of 2.2 TeV. A third superconducting intersecting ring will be added later to provide proton-proton collisions at 6 TeV with a substantially higher luminosity of $10^{32}/cm^2 \cdot s$.[1.17]

The antiproton source for the UNK will use the 70 GeV protons from the U-70 machine. A new booster for the U-70 will increase the beam intensity to 5×10^{13} protons/cycle. The proton beam is focused down to 0.5 mm by a 100 kG lithium lens 5 mm in diameter and 10 cm long. The peak of the antiproton spectrum is about 5.5 GeV. The antiprotons from the target are collected by a 170 kG lithium lens 2 cm in diameter by 15 cm long. This lens is able to collect antiprotons with a linear angle of 0.1 rad (solid angle of 0.0314 sterrad).

As shown in Figure 1-4, the antiprotons go to the synchrotron-decelerator where rotation of the antiproton bunches decreases their momentum spread. This is followed by deceleration of the antiprotons to 400 MeV. The antiprotons are then sent to the cooler-accumulator where they are cooled and stored. The cooler-accumulator is in a race-track configuration with two half-rings with a radius of 40 m at the end and two straight sections 100 m long. Electron beam cooling is used in the cooler-accumulator. A 218 MeV electron beam is generated in one end, travels around the track and is collected near the source. With the source and the collector at the same potential, most of the electron beam energy is recycled.[1.18]

17

P   70 GeV

TARGET AND LENSES

P̄   5.5 GeV

U-70
PROTON
SYNCHROTRON

P

P̄

SYNCHROTRON
DECELERATOR

P̄   P̄   400 MeV

ANTIPROTON LOOP

ELECTRON LOOP

e⁻

COOLER-ACCUMULATOR

STRAIGHT
COOLING
SECTIONS
(100 m)

e⁻   e⁻

ELECTRON SOURCE   ELECTRON
COLLECTOR

P̄
ANTIPROTON
LOOP
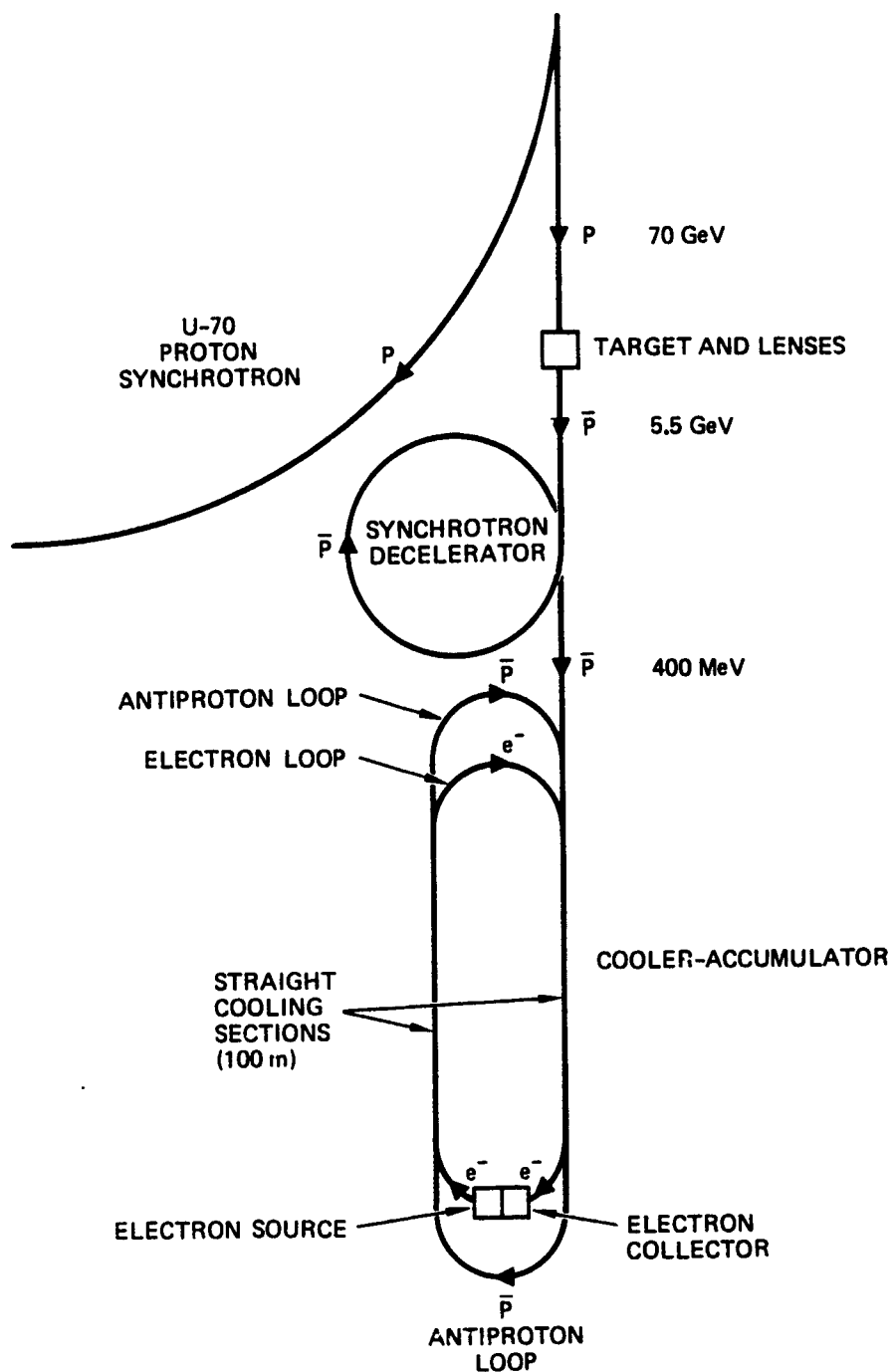
Fig. 1-4   Antiproton production facility at IHEP.

The 400 MeV antiprotons are injected into the cooler-accumulator ring in the straight section where they travel along with the 218 MeV electrons and are cooled by coulomb interaction with the low temperature electron beam. At the ends of the track, the antiprotons, with their greater momentum, exit from the ring to be turned around by the antiproton bending magnet channel and sent back in the other straight section for further cooling.

There are several plans for future improvement of the antiproton source.[1.18] One concept increases the proton beam intensity by stacking up 7 bunches of protons by sending sequential bunches to delay lines of differing lengths. A second concept involves decreasing the momentum spread of each bunch and stacking four bunches in the length of one present bunch. A third concept uses a multiple target system where the proton beam passes through several targets in succession. The antiprotons produced in a target (and other targets upstream) are refocused on the next target by a lithium lens. Thus, the "image" of all the targets are superimposed. If successful, these concepts and others could improve the antiproton production rate by a factor of 140.[1.18] The production rate would then be 6×10^9 $\bar{p}$/s or 300 ng/year.

It is interesting to note that there have been no significant publications on antiproton sources by USSR scientists since 1981.

References:

[1.15] V.V. Abramov, et al., "Production of hadrons with transverse momentum 0.5-2.5 GeV/c in 70-GeV proton-nucleus collisions," Sov. J. Nucl. Phys. 31, 343-346 (1980).

[1.16] B.E. Balakin and A.N. Skrinsky, "Project VLEPP," Akademiya Nauk USSR, Vestnik, No. 3, 66-77 (1983).

[1.17] A.I. Ageyev, et al., "The IHEP accelerating and storage complex (UNK) status report," pp. 60-70, Proc. 11th Int. Conf. High Energy Accelerators, Geneva (1980).

[1.18] T.A. Vsevolozskaya, B. Grishanov, Ya. Derbenev, N. Dikansky, I. Meshkov, V. Parkhomchuk, D. Pesrikov, G. Sil'vestrov, A. Skrinsky, "Antiproton source for the accelerator-storage complex, UNK-IHEP," Fermilab Report FN-353 8000.00 (June 1981), a translation of INP Preprint 80-182 (December 1980).

1.5   COMPARISON OF ANTIPROTON PRODUCTION FACILITIES

The three antiproton production facilities are compared in
Table 1-1. Fermilab has the highest proton energy, while CERN
partially makes up for the lower production at its low proton
energy by having over five times as many protons per second
hitting the production target. CERN was the first to be
operational and had some problems meeting the initial goals
in angular and momentum capture. The numbers for Fermilab and
IHEP are still design goals and it will be interesting to see
how close the actual machine performance comes to the goals.

If the Fermilab and IHEP machines achieve their production and
capture goals, then the production rate for the number of
antiprotons captured for every incident proton will be 40 to
110 times that of the present CERN accomplishments. Of
course, with the addition of the Antiproton Collector in 1987,
CERN hopes to close that production gap somewhat. Still, in
all the machines, the production rate is only a few parts in a
million antiprotons per proton. When we calculate the
efficiency in terms of energy rather than number of particles
the differences between the machine efficiencies become
smaller because of the higher energy in the initial protons in
the FNAL and IHEP machines.

The energy efficiency for the machines shown in the last line
of Table 1-1 is the ratio of the energy that would be obtained
by annihilation of the captured antiproton with a proton
($2mc^2$), divided by the beam energy of all the protons that it
took to generate that one captured antiproton. As we can see,
the energy efficiency from proton beam energy to annihilation
energy varies from 3×10^{-8} for CERN to 1.3×10^{-6} for IHEP. If
we then assume that a typical synchrotron has an energy
efficiency from ac power to beam power of 5% (or less), then
the present total energy efficiency for producing antiprotons
is only a few parts in a billion.

It is this extremely low production efficiency for the CERN
machine that has led many experts to categorically state that
the capture and storage of antiprotons for later use as an
energy source is pure science fiction and will never become
practical. The following sections discuss each of the various
inefficiencies in the present machine designs that lead to
this parts-per-billion total efficiency and outline what hopes
there are to improve the efficiencies in each area to bring
the total production efficiency up to some more reasonable
number, like a part in 10^{-4}.

Table 1-1   Comparison of Antiproton Production Facilities.

	CERN (EUROPE)	FNAL (USA)	IHEP (USSR)
PROTON ENERGY (GeV)	26	120	70
PROTONS/CYCLE (x 10^{12})	13	2	7
CYCLE DURATION (sec)	2.4	2	7
ANTIPROTON ENERGY (GeV)	3.5	8	5.5
ANGULAR CAPTURE (mm - mrad)	70π	20π	60π
MOMENTUM CAPTURE ($\Delta P/P$)	1.5%	3%	6%
ANTIPROTONS/PROTON (x 10^{-6})	0.4	30	46
$\epsilon = 2 \times \bar{p}$ ENERGY/p ENERGY (x 10^{-7})	0.3	4	13

1.6 EFFICIENCY OF PRESENT ANTIPROTON PRODUCTION FACILITIES

The capture efficiencies of the present antiproton facilities
are abysmally low. The present magnetic lenses and collector
rings capture only a very small fraction of the antiprotons
that are generated in the target. The reason for this is
summarized by Figure 1.5 from a recent paper on the efficiency
of the proposed Fermilab collector system.[1.19]

The upper part of the figure shows the total number of
antiprotons generated per GeV of antiproton momentum per
steradian of solid angle at the central portion of the
antiproton beam. Integrating the curve over the antiproton
momenta shows that each proton produces 7.7 antiprotons per
steradian. The half-width of the angular spectrum is unknown
since the angular spectrum has never been measured.

If the magnetic lens had a wide enough angular capture
(<100 mrad), then probably that would be enough to capture
nearly all the antiprotons. Their total number is estimated
at 4.7×10^{-2} antiprotons per proton (see Section 2.1). The
estimated momentum spectrum of these antiprotons is the middle
curve in Figure 1-5.

21
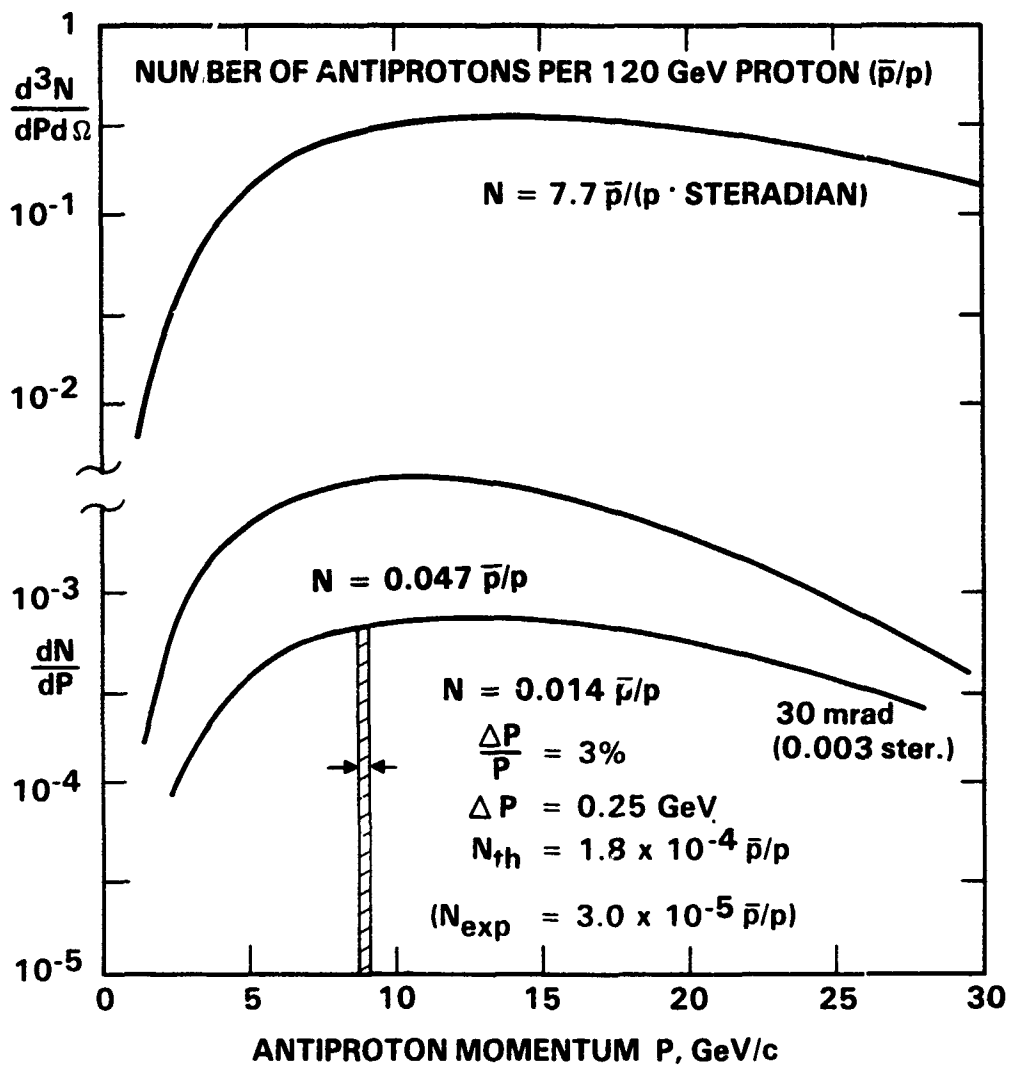
Fig. 1-5 Present antiproton capture efficiencies.

The Fermilab magnetic lens, as presently designed, is going to have an angular capture range of 30 mrad. Thus the spectrum of antiprotons it can capture is shown by the bottom line of Figure 1-5. When the 30 mrad curve is integrated over the antiproton momenta we find a total of only 0.014 antiprotons per proton in this narrow angular acceptance. This is only 30% of the total number of antiprotons generated by the target.

Then, of this small angular spread the Fermilab collector-debuncher is only able to capture those with a momentum (velocity) spread of 3% or 0.27 GeV/c around the momentum design center of 8.9 GeV. Even under ideal conditions, with this momentum capture bandwidth, they would expect to capture only about 1.8×10^{-4} antiprotons per proton. This is only 1.3% of the protons that were collected by the lens and only 0.4% of those generated in the target. In practice, the Fermilab group expects that after target losses, transfer losses, and other losses they will only get 1/6th of the ideal figure and are hoping to ultimately collect 3×10^{-5} $\bar{p}/p$ or 0.06% of the antiprotons generated in the target.

It is obvious that to increase the efficiency of antiproton production, one of the areas needing improvement is the angular and especially the momentum capture efficiencies of the collection system. We will discuss these further in Section 3.

References:

1.19Hojvat, C., and Van Ginneken, A., "Calculation of Antiproton Yields for the Fermilab Antiproton Source," Nuclear Instrumentation and Methods, Vol. 206, 1983, pp. 67-83.

SECTION 2

SOME ANTIPROTON PRODUCTION FUNDAMENTALS

In this section we will expand upon some of the fundamental techniques for the generation, capture, cooling, and trapping of antiprotons that were discussed briefly in Section 1.

2.1 GENERATION OF ANTIPROTONS

At present, the best known technique for producing antiprotons is to send a beam of high-energy protons into a metal target. The protons strike the protons and neutrons in the nuclei of the target and various reactions occur which produce gamma ays, pions, kaons, and baryons, including antiprotons. Although the absolute production rate of antiprotons is unknown to roughly a factor of two, the relative production rate of antiprotons to the total inelastic cross section is known and is shown in Figure 2-1.[2.1]

The curve is a fit of a specific model to the available experimental data for the relative cross section at the peak in the forward direction. There are two curves, one for protons hitting a hydrogen target and the other for a lead target. The lead data is not significantly different from the data for other heavy metal target nuclei. The total inelastic cross section is dominated by the pion production. At 200 Gev the ratio of the antiproton production cross-section to the total inelastic cross-section is about 0.04. This low production ratio is one of the major factors in the total production efficiency and cannot be increased by engineering improvements.

The best available data on the total antiproton production rate is a 1973 paper[2.2] based on p-p reactions in colliding beam experiments. Because the colliding beam experiments are symmetric in the laboratory frame, all the emitted particles have the same angular distributions, and the production ratios do not have the angular biases that occur when measurements are made using protons hitting a stationary target nucleus.

A typical measurement made at a center of mass squared energy $s=485$ GeV^2 (equivalent to a proton hitting a stationary target nucleon at an energy of 258 GeV), gave 3.56 π^+, 2.98 π^-, 3.5 π^0, 0.35 K^+, 0.24 K^-, 1.28 p^+, and only 0.061 p^-. Thus for every antiproton emitted, there are about 165 pions and 10 kaons.

25
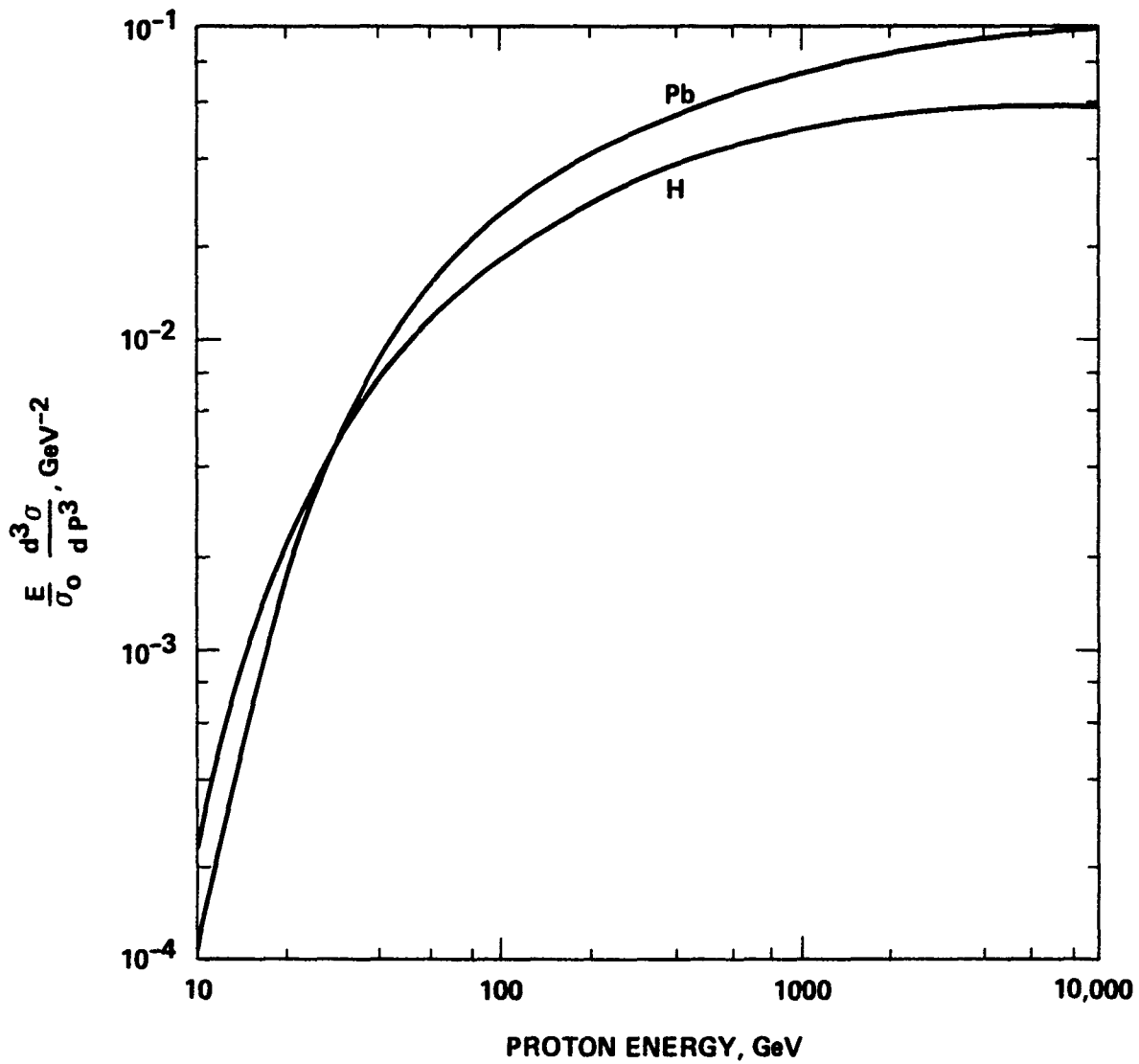
Fig. 2-1 Relative antiproton production rates
for hydrogen and heavy metal targets.

26

A plot of the available data on the total antiproton multiplicity of the reaction p-p is shown in Figure 2-2. The dots are the available data points and the curve is a smooth fit to the data. If we now take Figure 2-1, which shows the difference between the antiproton production rates in hydrogen and a heavy metal, we can use the ratio of p-Pb to p-p at each energy to make an estimate for the total antiproton production for protons striking a stationary heavy metal target. This is the top curve in Figure 2-2. It must be emphasized that this estimate is not very accurate. It could be off by as much as a factor of two. Note that at 200 GeV, the total antiproton production rate in a lead target is 0.085 antiprotons per incident proton. This is a factor of two less than an estimate made in a previous report on antiproton propulsion.[2.3]

Now that we have an estimate of the total production, we can estimate how well present antiproton collectors perform in collecting the total number of antiprotons generated. If the target is long, there will be some absorption of the antiprotons in the target, but this is compensated somewhat by additional antiprotons produced by secondary reactions of the emitted particles from the first p-N collision with other target nuclei. For example, the secondary reaction antiprotons are 22% of the total antiproton flux for a 6 cm tungsten target bombarded by 120 GeV protons.[2.1] The antiprotons come out of the target with a spread in angle and momentum. As the energy of the incident proton beam is increased, the total number of antiprotons produced increases, and the a ,le into which they are concentrated becomes smaller, making it easier to collect them, but the spread in longitudinal momentum becomes larger, requiring that the collector accept a larger momentum spread to capture the same percentage of generated antiprotons.

References:

[2.1] C. Hojvat and A. van Ginneken, "Calculation of antiproton yields for the Fermilab antiproton source," Nucl. Inst. & Methods **206**, 67-83 (1983).

[2.2] M. Antinucci, A. Bertin, P. Capiluppi, M. D'Agostino-Bruno, A.M. Rossi, G. Vannini, G. Giacomelli, and A. Bussiere, "Multiplicities of charged particles up to ISR energies," Lett. Nuovo Cimento **6**, 121-127 (1973).

[2.3] R.L. Forward, Alternate Propulsion Energy Sources, p. 1-8, AFRPL-TR-83-067, Final Report on Contract F04611-83-C-0013, Air Force Rocket Propulsion Lab, Edwards, CA 93523 (Dec 1983)
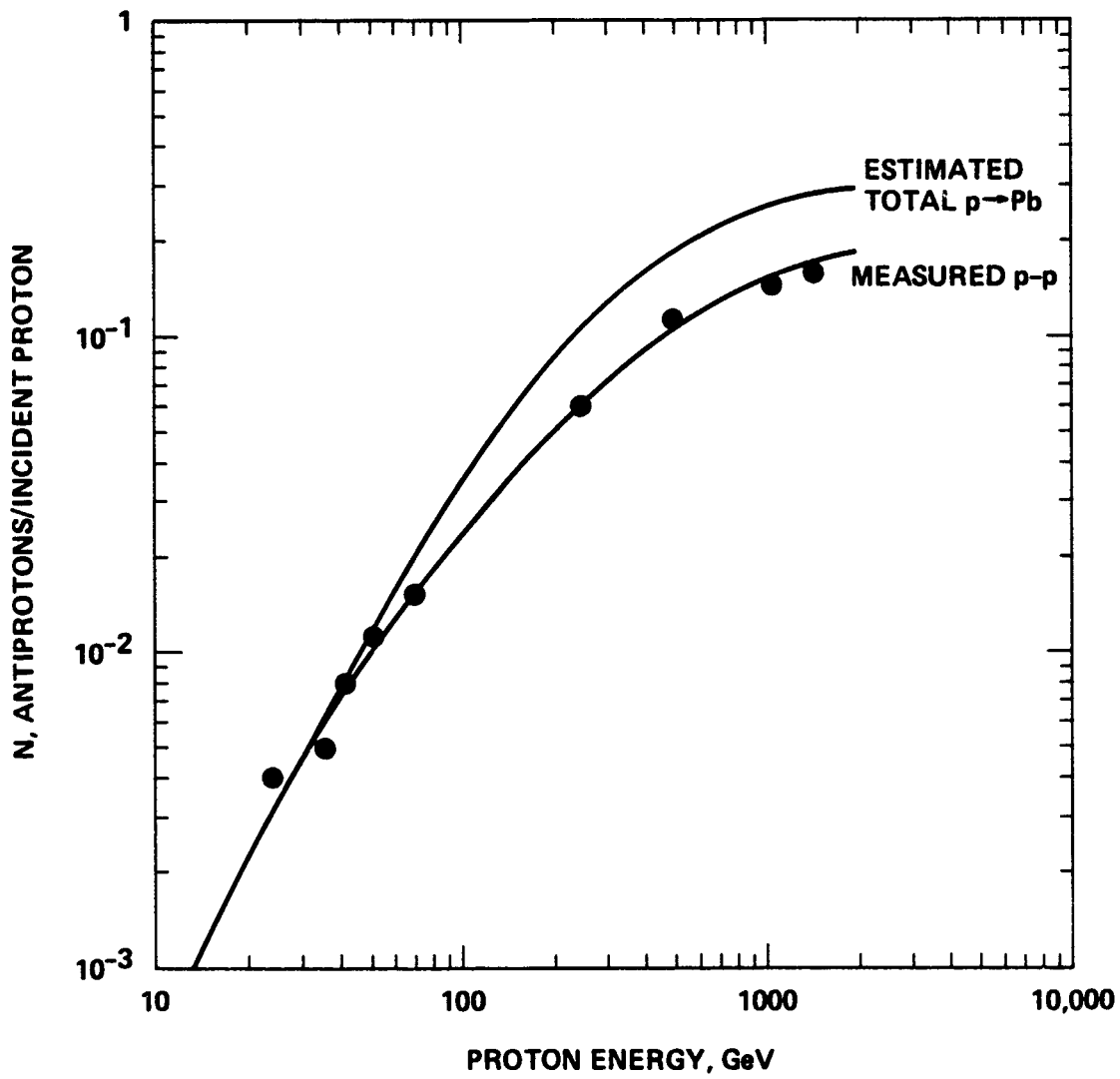
Fig. 2-2 Total antiproton production rates.

28

2.2. ANGULAR CAPTURE BY MAGNETIC LENSES

We will now look at the problem of angular capture. The spray of antiprotons coming from the target are focused by a magnetic lens into the aperture of the collector ring that will manipulate, cool, and accumulate the antiprotons.

The standard lens used in particle accelerators is a magnetic quadrupole. It consists of four long magnetic pole pieces wound with coils of alternating polarity just outside the beam transport tube. The magnetic quadrupole focuses in one axis while causing a slight defocusing in the orthogonal axis. A series of quadrupoles of orthogonal orientation, however, can produce a net focusing of the beam in all orientations. The off-axis aberrations of a quadrupole magnetic lens are severe.

To obtain symmetric focusing, it is necessary to produce a magnetic field along the beam with a radially increasing gradient. So far, the only meth)ds found to achieve this field configuration have required that the particle beam pass through a portion of the current conductors.

Conceptually, the lithium lens is the simplest of the symmetric lenses, although its development came later. These lenses consist of long lithium cylinders placed directly in the particle beam path that carry a large pulsed current from one end to the other.[2.4] Provided the diameter of the lithium lens is not too much greater than the electromagnetic skin depth at the frequencies corresponding to the pulse width, the current distribution in the lithium cylinder is uniform. A uniform current distribution gives an azimuthal magnetic field within the conductor that increases linearly with radius, giving a constant radial gradient.

A typical lens designed for focusing an 80 GeV proton beam to a spot size of 0.1 mm radius is 5 mm in diameter, 10 cm long, and is excited at a 13 Hz repetition rate by a 60 µs pulse of 160 kA to produce a magnetic field of 10 T (100 kG) and a magnetic field gradient of 4000 T/m.[2.4] Because the beam must go though the material in the lens, the magnetic design of the lens is compromised by requirements that the beam not destroy the lens and the lens not destroy the beam. This is especially critical in the design of a lens for antiprotons. For example, a longer lens needs less drive current but absorbs more antiprotons.

Since the metal targets for antiproton production are also long and thin, they can be pulsed with current to provide self-focusing.[2.5] Although this has not been implemented yet in any system, it is an obvious next step since the target has to be in the beam anyway.

The lenses presently in use at CERN, Fermilab, and elsewhere are parabolic horns.[2.6] These are usually made of aluminum, or beryllium copper, and consist of two elongated parabolic horns connected at the center at the narrowed down "mouthpiece". The wall thickness varies inversely with distance from the axis and is 0.5 mm at the maximum radius at the bell of the horn. The current runs from one horn rim through the connection at the "mouthpieces" to the other horn rim. There is no magnetic field inside the horn, while the magnetic field outside the horn drops off as $1/r$. The center of the beam passes through the center axis of the horn, but any off axis particles pass through the conductor of the horn to enter the region containing the magnetic field. The parabolic shape of the horn means that a particle a distance r from the axis will travel a distance r^2 outside the horn, giving a net magnetic interaction that varies as r.[2.7] This constant magnetic gradient force then bends the particle back to the focal point. Real (thick) lenses have horn shapes that are not exactly parabolic and are different sizes at the entry and exit ends.

After the antiprotons have been focused by the magnetic lens they are diverted a few degrees by a pulsed dipole magnet that selects negatively charged particles with energies near the peak of the antiproton production spectrum. The antiprotons not selected, the remnants of the incident protons, and the other interaction products continue on towards the beam dump. The selected antiprotons pass through a channel in the beam dump into a transport line leading to the collector ring.

References:

[2.4] B.F. Bayanov, J.N. Petrov, G.I. Silvestrov, J.A. MacLachlan, and G.L. Nicholls, "A lithium lens for axially symmetric focusing of high-energy particle beams," Nucl. Instr. & Methods, **190**, 9-14 (1981).

[2.5] B. Autin, "The future of the antiproton accumulator," pp. 573-582, Proc. Workshop on Proton-Antiproton Physics and the W discovery, La Plagne (1983).

[2.6] B.F. Bayanov, A.D. Chernyakin, V.N. Karasyuc, G.I. Sil'vestrov, T.A. Vsevolozhskaya, V.G. Volohov, G.S. Willewald, "The antiproton target station on the basis of lithium lenses," pp. 362-368, Proc. 11th Int. Conf. High Energy Accelerators, Geneva (1980).

[2.7] T.A. Vsevolozskaya and G.I. Sil'vestrov, "Optical properties of fast parabolic lenses," Zh. Tekh. Fiz. **43**, 61-70 (1973) [English translation Sov. Phys. Tech. Phys. **18**, 38-43 (1973)].

2.3 MOMENTUM CAPTURE BY COLLECTING RINGS

As was pointed out in Section 1.6, one of the major reasons for the low efficiencies in the present antiproton production facilities is the low momentum capture capabilities of the present collecting rings. The efficiency of a collecting ring is usually given in terms of dp/p or the momentum spread dp accepted by the ring divided by the center momentum p of the ring (usually the peak of the antiproton spectrum).

Since the antiproton spectrum is presently unknown, and the spectrum is usually modified by the magnetic lens, the use of the present figure of merit is understandable, but it usually implies a better capture efficiency for the ring than it really delivers. A better figure of merit would be the momentum spread accepted by the ring divided by the half-width Dp of the antiproton spectrum. For example, at CERN, dp/p=1.5%, but dp/Dp is significantly less at 1%. At Fermilab, the quoted dp/p=3% for the capture portion of the debuncher ring means that at a capture momentum of p=8.9 GeV/c the momentum bite is dp=0.25 GeV/c. Since the estimated half-width of the total antiproton spectrum is Dp=22 GeV/c, the real capture efficiency is only dp/Dp=1.2%. Thus, though the Fermilab collecting ring has a quoted momentum capture efficiency that is twice that of CERN, the actual momentum capture efficiency is only 20% better.

It is very difficult to build a ring that can accept a wide spread in the momentum of the particles. Particles with different momenta have different radii of curvature in the magnetic field of the bending magnets. If the magnetic field strength is adjusted so that the radius of curvature of a particle is equal to the radius of curvature of the beam line, then a particle with a different momentum will have a different radius of curvature and hit the wall of the beam line.

Conceptually, one could make a beam line that is much wider than it is tall so that it could hold particles with a wider spread in momentum. This is in fact done, but there is a practical limit to the width imposed by a combination of pressure forces on the top and bottom of the vacuum line, the amount of vacuum volume to be pumped, and the size of the magnets. The present state-of-the art in collector rings is represented by the IHEP Synchrotron Decelerator and the new CERN Antiproton Collector, which both have a dp/p=6%.

2.4 ELECTRON COOLING OF ANTIPROTON BEAMS

In carrying out almost any experiments with beams of charged particles, it is of fundamental importance to be able to compress the beams, to decrease the size of the beam as well as narrow the momentum spread of the particles in the beam in both magnitude and direction. In other words, it would be desirable to "cool" the flux of fast charged particles, lowering their effective "temperature" about the average motion of the beam.

In electron cooling of an antiproton beam, a beam of monoenergetic electrons with a velocity equal to the average velocity of the antiprotons is made to travel along with the antiproton beam.[2.8] Then, in the rest system of the electron beam, the "hot" antiproton gas is within the "cold" electron gas and is cooled in all directions as the result of Coulomb collisions. As a result, the phase space of the antiproton beam decreases in all degrees of freedom and the beam is compressed. The compression continues in principle until the antiproton temperature in the center-of-mass system becomes equal to the electron temperature. Since the antiprotons are much heavier than the electrons, the resultant decrease in the velocity spread for the antiprotons goes as the square root of the mass ratio. For an easily achieved velocity spread ratio of $dp/p = 10^{-3}$ for the electrons, the resultant velocity spread for the antiprotons is 2×10^{-5}.

Electron cooling has been demonstrated at CERN[2.9] and Fermilab[2.10] using protons and electrons. The recombination reaction rate is small enough that this gives a good simulation of electron cooling of antiprotons. At Fermilab a 200 MeV proton beam with an initial momentum spread of $dp/p = 3 \times 10^{-3}$ was cooled with a 110 keV beam of electrons with a energy spread of 1 eV transverse and 8×10^{-5} eV longitudinal. With 1 A of electrons, the protons reached a momentum spread of $dp/p = 1 \times 10^{-5}$ in 4 s of cooling. Transverse cooling by a factor of 25 was also achieved in less than 20 s of cooling time.[2.10] Electron cooling can be made very efficient. The electrons can be circulated in a ring and "cooled" using a "wiggler" section[2.11] or up to 98% of the electron energy can be recovered using a well designed depressed collector.[2.12]

Despite the experimental success of electron cooling, it is not used much in practice. It was originally felt that stochastic cooling would be most effective when the antiprotons were at relativistic energies, while electron cooling would be more effective at subrelativistic energies. It has turned out that stochastic cooling has been found to be effective at all energies of present interest.

Electron cooling has also been found to have catastrophic failure modes. For this, as well as other reasons, stochastic cooling is usually the choice for cooling of antiproton beams. This may change as new machines such as the Extra Low ENergy Antiproton (ELENA) ring are built to take the 5 MeV antiprotons from LEAR and decelerate them down to 200 keV.[2.13]

References:

[2.8] G.I. Budker and A.N. Skrinsky, "Electron cooling and new possibilities in elementary particle physics," Usp. Fiz. Nauk 124, 561-595 (1978) [English translation Sov. Phys. Usp. 21, 277-296 (1978).

[2.9] M. Bell, J. Chaney, H. Herr, F. Krienen, P. Møller-Petersen, and G. Petrucci, "Electron cooling in ICE at CERN," Nuclear Instr. & Methods 190, 237-255 (1981).

[2.10] T. Ellison, W. Kells, V. Kerner, F. Mills, R. Peters, T. Rathbun, D. Young, P.M. McIntyre, "Electron cooling and accumulation of 200-MeV protons at Fermilab," IEEE Trans. Nuclear Sci. NS-30, 2636-2638 (1983).

[2.11] H. Herr and C. Rubbia, "High energy cooling of protons and antiprotons for the SPS collider," pp. 825-829, Proc. 11th Int. Conf. on High Energy Accelerators, Geneva, Switzerland (1980).

[2.12] L. Hütten, H. Poth, and A. Wolf, "The electron cooling device for LEAR," pp. 605-618, Physics at LEAR with Low-Energy Cooled Antiprotons, Workshop on Physics at LEAR with Low-Energy Cooled Antiprotons, Erice, Sicily, Italy, 9-16 May 1982, U. Gastaldi and R. Klapisch, ed., Plenum Press, NY (1984).

[2.13] H. Herr, "A small deceleration ring for extra low energy antiprotons (ELENA)," pp. 633-642, Physics at LEAR with Low-Energy Cooled Antiprotons, Workshop on Physics at LEAR with Low-Energy Cooled Antiprotons, Erice, Sicily, Italy, 9-16 May 1982, U. Gastaldi and R. Klapisch, ed., Plenum Press, NY (1984).

2.5 STOCHASTIC COOLING OF ANTIPROTON BEAMS

It is not possible to compress a beam of charged particles by
any known combination of external electromagnetic forces which
only act on the beam as a whole and which do not depend upon
the motion of the individual particles of the beam. By means
of focusing and acceleration in any combination one can only
change the shape of the phase space occupied by the beam
particles but cannot change its magnitude or increase the
phase density. This is a special case of Liouville's theorem,
that the density of the particles of a beam in six-dimensional
phase space (the space of generalized coordinates and
conjugate momenta) is a constant and is determined by the
initial conditions.

Stochastic cooling is the damping of the momentum spread and
the transverse oscillations of a particle beam by an
electronic feedback system. In its simplest form, a pickup
electrode detects the instantaneous transverse position or
momentum of a fluctuation in the average current of the
particles in a storage ring due to particle bunching. The
signal is amplified, delayed, and phase shifted, then sent
across the ring to a kicker which applies a force to the bunch
that is designed to damp out the fluctuation.

Stochastic cooling is not a violation of Liouville's theorem.
It works only if the number of particles available is small
and there is a lot of empty phase space. During stochastic
cooling, a "capsule" of phase space is formed around each one
of the particles. Liouville's theorem then applies to the
phase space inside those capsules. The capsules are then
moved around freely in the rest of the (empty) phase space and
brought closer together to achieve a denser packing. The
phase space around each particle is the same, except the empty
phase space has been removed. Although there is an apparent
violation of the Liouville theorem, there is no violation in
reality because the initial phase space was so sparsely
populated.

If there were only a single particle in the ring, it is
obvious that the transverse oscillations and momentum offset
of the particle could be damped using electronic feedback. In
stochastic cooling of many particles in a beam, the cooling of
a single particle is hampered by the presence of the other
particles in the dense cool core, which create a noise signal
(Schottky noise) that heats the single particle. For a
properly designed system, however, the net effect over many
turns is that cooling is achieved.[2.14]

In addition to the Schottky noise created by the "cool"
particles in the beam, another major noise source is the
thermal noise generated by the resistive terminations in the

pickups and the noise figure of the preamplifiers. A series of notch filters are used to protect the cool dense core of the stacked particles from the broadband thermal noise. What is typically done is to have two cooling systems, one of which operates at low gain appropriate for cooling of the dense core and another with the high gain needed to manipulate the newly injected antiprotons in the low density part of the stack. The high gain system has a number of notch filters which prohibit power from being transmitted at the harmonics of the revolution frequencies of the dense core.[2.15] To decrease the thermal noise contribution of the pickup terminations, the termination resistors at CERN are now cooled to cryogenic temperatures (18 K).[2.16]

In the Antiproton Accumulator at CERN, the stochastic precooler system has a signal bandwidth from 150-500 MHz, 192 pickups with 2 db noise figure preamplifiers, 50 power amplifiers that operate at 2 kW total, and 200 kickers. They are able to reduce the momentum spread from a dp/p of 1.5% to 0.17% in just 2 seconds. The horizontal and vertical transverse cooling systems operate over a bandwidth from 1 to 2 GHz and in 15 to 30 minutes can reduce the transverse emittance from 100π to 5π mm-mrad.[2.17]

In the Fermilab Debuncher, the stochastic precooler is designed for transverse cooling only, since the debunching process will take care of the momentum compression. It will operate over a bandwidth of 2 to 4 GHz, use 128 pairs of pickups and kickers, driven by 8 microwave traveling wave tubes operating at 500 W, to reduce the emittance from 20π to $<5\pi$ mm-mrad in the 2 s system cycle time.[2.14]

Stochastic cooling has a significant energy requirement. At CERN the power requirement for the stochastic cooling in the Antiproton Accumulator is 1/4 mW per $\bar{p}$/s.[2.18] Since the AA handles 1.4×10^6 $\bar{p}$/s, the total power requirement on the stochastic cooling electronics is 350 W of expensive microwave power. Unlike decelerating a particle beam, where the coherent energy of the beam can actually be extracted out of the beam slowing apparatus as rf power, stochastic cooling is working with the random, incoherent energy differences between the particles and requires the input of energy. This is because stochastic cooling uses an active damping technique in which the energy difference between initial energy and the final energy of the antiprotons in the beam is "cancelled" by the insertion of an equal amount of energy from the electronics. The need for extensive amounts of stochastic cooling energy will be an important cost factor in the design of a facility for producing large numbers of antiprotons.

35

References:

[2.14]Fermilab staff, <u>Design Report: Tevatron 1 Project</u>, p. 4-13 to p. 4-16, Fermi National Accelerator Lab, Batavia, Illinois (September 1984).

[2.15]R.P. Johnson and J. Marriner, "Stochastic stacking without filters," Fermilab p̄ Note 226, Fermi National Accelerator Lab, Batavia, Illinois (17 August 1982).

[2.16]G. Carron, R. Johnson, S. van der Meer, C. Taylor, and L. Thorndahl, "Recent experience with antiproton cooling," IEEE Trans. Nucl. Sci. NS-30, 2587-2589 (1983).

[2.17]S. van der Meer, "Stochastic cooling in the CERN antiproton accumulator," IEEE Trans. Nuclear Science, NS-28, 1194-1998 (1981).

[2.18]R. Billinge, CERN, Switzerland (personal communication).

2.6 STORING OF ANTIPROTONS

Once the antiprotons have been slowed down to subrelativistic energies they can be stored as ions for long periods of time (many days) in various traps using a combination of electric, magnetic, electrodynamic, gravity, and/or inertial fields. The present technique is to build a magnetic storage ring using a combination of inertial forces and static magnetic fields that keep the antiproton ions circulating about the ring. The low-energy antiproton ring (LEAR) at CERN is the best example of this type of trap.

For antiproton annihilation propulsion this type of trap has two major problems. Because of the magnets and vacuum system, the present designs are bulky and heavy. It might be possible, however, to produce a compact design with the antiproton beam wound up into an endless spiral somewhat like a continuously playing magnetic tape cartridge.

The other problem is the relatively low ion current the present machines can carry. A phenomenon called intrabeam scattering, which is the particle beam version of space charge forces, puts a practical upper limit of about 10^{12} ions to the number of antiproton ions that can be stored in present machine designs. At about that number of ions the expansion of the beam due to intrabeam scattering is just compensated by the shrinking of the beam from the stochastic cooling systems. Obtaining beam control forces from the stochastic cooling process is very costly since it requires wide bandwidth microwave power generators.

A number of experimenters have now proposed to decelerate the
antiproton ions down to almost zero velocity and put them into
a Penning trap.[2.19-2.21] The Penning trap uses only static
electric and magnetic fields and can trap nonmagnetic charged
ions.[2.22] A properly constructed trap kept at cryogenic
temperatures is completely stable and can hold one or more
ions for long periods of time.

A Penning trap has demonstrated it can even hold antimatter.
A trap at the University of Washington has kept a single
positron trapped for a month.[2.23] This indicates that the
number of residual normal matter gas molecules in a
cryogenically cooled ultrahigh vacuum Penning trap is
extremely small. How good the vacuum is, however, is unknown,
since the cross section for the annihilation of a positron
with the bound electron on a slowly moving atom is unknown.
The present estimates are that a UHV sealed Penning trap at
5 K will have a vacuum of $<<10^{-14}$ torr.[2.20]

As is shown in Figure 2-3, the Penning trap consists of a
small trapping region containing an axial magnetic field and
bounded by three electrodes. There is a central ring
electrode with a hyperbolic inner surface shape and two cap
electrodes, also with carefully machined hyperbolic shapes.
For the storage of negative ions (negatively charged
antiprotons), the ring electrode is positively charged and the
cap electrodes are negatively charged.

When a charged ion is inserted into the Penning trap, it has
energy and in general is moving both radially and axially.
The radial motion in the strong magnetic field is converted
into a tight circle that is much smaller than the dimensions
of the trap. This is the cyclotron motion shown in the
diagram above the drawing of the Penning trap in Figure 2-3.
The axial motion of the negatively charged antiprotons is
restrained by the repulsion of the negatively charged cap
electrodes. This sends the antiprotons back through the
center of the trap to the other electrode, causing the axial
oscillations shown in the upper diagram of Figure 2-3. The
positively charged ring electrode attracts the antiprotons
radially outward. But as the antiprotons attempt to drift
outward, their motion is curved by the magnetic field into the
large circle shown as the magnetron motion in Figure 2-3.
Thus, if the initial energy of the antiproton is small enough,
the antiproton is trapped.
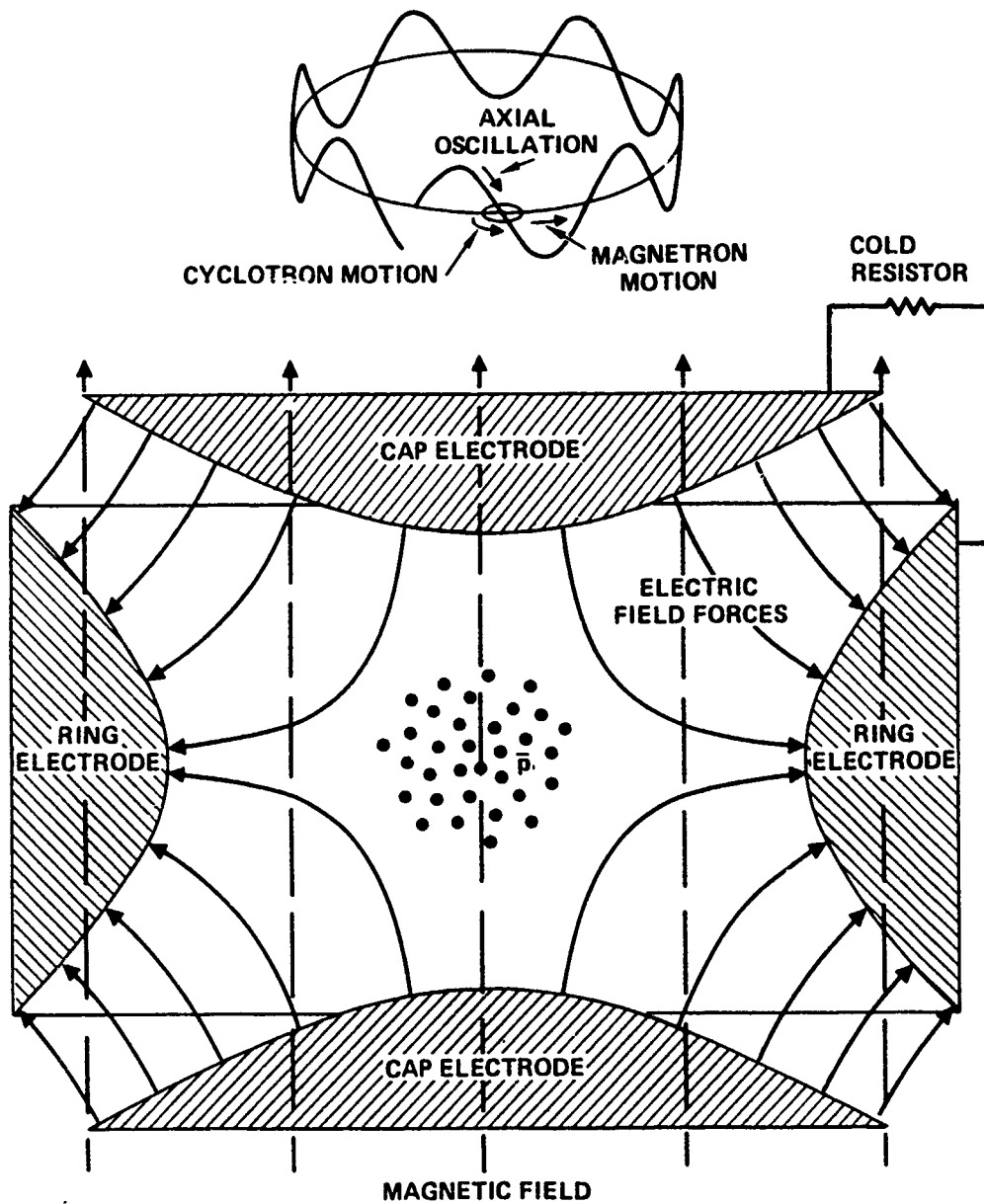
Fig. 2-3 Penning trap for antiproton ions.

The motion of the antiproton between the electrodes causes image voltages in the electrodes, which cause currents to flow between the two cap electrodes, and between each of the cap electrodes and the ring electrode. As shown in Figure 2-3, a resistor placed between the cap electrode and the ring electrode will dissipate these currents, extracting energy out of the antiproton. The damping from this external resistor is strong enough that positrons inserted into the trap immediately lose enough energy to stay in the trap.[2.24] This approach is not suitable with externally injected antiprotons, however, because the damping rates go inversely as the mass of the trapped particle. It will be necessary to vary the trapping voltages to trap the antiproton initially, then using the damping resistor for further cooling.

If the resistor is kept at cryogenic temperatures, the amount of random Johnson noise voltage that it generates is kept small so that it doesn't excite the antiproton. Thus, if the resistor is kept in a cryogenic bath, the energy in the antiproton will be damped out over a period of a number of seconds until its kinetic energy is equivalent to the temperature of the bath.[2.19, 2.24] In this manner, the last bit of kinetic energy can be extracted from the antiproton without touching it.

An alternative cooling method is to use an electron buffer gas, trapped in the center of the same trap and cooled to cryogenic temperatures via coupling to an external circuit.[2.20] Antiprotons oscillating through this electron buffer gas will scatter from the cold electrons and transfer energy to them and thus to their external resistor damping circuit. The cooling time is estimated to be 5 s.

The limit to the number of antiproton ions that can be stored in such a trap is determined by the space charge limit. Estimates of the number density vary from 10^{11} $\bar{p}$/cc for a 2 cm radius trap[2.19] to 10^{14} $\bar{p}$/cc for a 50 cm radius trap.[2.21] If a trap that large could be built, it would hold about a milligram of antiprotons.

The ability of a Penning trap to store antiproton ions for long periods of time will be tested in the next few years. Both the University of Washington[2.20] and the Los Alamos National Laboratory[2.21] are mounting efforts to trap one or more of the slow antiprotons available at LEAR. It is suspected that the Italian group will proceed with their plans also.

The University of Washington program will use one of their cryogenic Penning traps modified by thinning the center portion of one of the cap electrodes down to about 0.25 mm. This will maintain the ultrahigh vacuum capability that they have demonstrated in their sealed traps. The thinned portion of the electrode will act as a stopping foil for the medium energy (100 keV) antiprotons. With the thickness adjusted to equal the average range of the antiprotons in cap electrode material, some of the antiprotons will emerge from the other side with just the proper energy to be caught in the trap.

The intention of the University of Washington experiment is to trap only a few antiprotons and measure the mass to high precision. As a byproduct, however, the lifetime of the antiproton in the trap will put a good upper limit to the quality of the vacuum in the trap.

The LANL experiment is more ambitious. They are fabricating a radio frequency quadrupole (RFQ) decelerator that will decelerate the beam of antiprotons from LEAR down to the trap energy and deposit a large number (up to 10^{10} antiprotons) in the trap.

References:

2.19 N. Beverini, L. Bracci, V. Lagomarsino, G. Manuzio, R. Parodi, and G. Torelli, "A Penning trap to store antiprotons," pp. 771-778, **Physics at LEAR**, U. Gastaldi and R. Klapisch, ed., Plenum Press, NY (1984).

2.20 W. Kells, G. Gabrielse, and K. Helmerson, "On achieving cold antiprotons in a Penning trap," FERMILAB-Conf-84/68-E, Fermi National Accelerator Lab, Batavia, Illinois (August 1984). [Preprint submitted to the IX Int. Conf. on Atomic Physics, Seattle, Washington (23-27 July 1984).]

2.21 L. Campbell, W.R. Gibbs, T. Goldman, D.B. Holtkamp, M.V. Hynes, N.S.P. King, M.M. Nieto, A. Picklesimer, and T.P. Wangler, "Basic research in atomic, nuclear and particle physics," LA-UR-84-3572, Los Alamos National Lab, Los Alamos, New Mexico (1984).

2.22 P. Ekstrom and D. Wineland, "The isolated electron," Sci. Am. **243**, 105-121 (August 1980).

2.23 G. Gabrielse, personal communication (1985).

2.24 P.B. Schwinberg, R.S. Van Dyck, Jr., and H.G. Dehmelt, "New comparison of the positron and electron g factors," Phys. Rev. Lett. **47**, 1679-1682 (1981).

SECTION 3

IMPROVING ANTIPROTON PRODUCTION EFFICIENCIES

There are a number of obvious ways to improve the efficiency
of antiproton production over the present methods. It should
be realized that the present production facilities were
designed under a number of restrictions. They had to use
existing proton accelerators, fit onto the existing sites, and
not use up too much precious time on the main machine. Above
all, they had to be built as fast as possible so that some
laboratory in some other country didn't reach the next highest
interaction energy region first, find the next batch of new
"elementary" particle resonances, and win that year's Nobel
prize in Physics.

The original motivation behind the production of antimatter at
these laboratories was very pragmatic. It was not for the
study of the properties of antimatter, although some of that
work is now going on at CERN since the antiprotons are
available. The reason antimatter sources were built was to
reach a higher center-of-mass energy by colliding two particle
beams head-on. Beam-beam collisions produce much more
interaction energy than a proton beam hitting a stationary
target (see Appendix A). The present proton machines can be
used in a colliding beam mode with minor modifications if they
are loaded with two beams, one of protons and one of
antiprotons, orbiting in different directions.

To obtain the same results with two colliding proton beams
would have required building a second proton ring that
intersects with the first one at a number of points (like the
ISR at CERN). It is interesting to note that the reason the
three different national facilities have tackled the very
difficult task of making, collecting, cooling, and storing
antimatter is that they realized it was cheaper to make an
antiproton facility for producing antimatter than to build
another proton ring.

A good part of the effort on this study contract was to
determine the reasons behind the low efficiencies of the
present facilities. Some of the low efficiencies are
inherent, such as the number of antiprotons per proton from a
target. Most of the other low efficiencies are just artifacts
of the particular choices forced on the particular facility,
and there are obvious ways to improve these efficiencies by
large factors. These will be discussed in the following
subsections.

41

3.1 ALTERNATE ANTIPROTON PRODUCTION TECHNIQUES

A survey was undertaken to find alternate methods of producing antiprotons other than by high-energy protons striking a heavy nuclei target.

3.1.1 Colliding Particle Beams

It is known that colliding proton beams produce antiprotons.[3.1] Because the center of mass energy in a colliding proton beam configuration is higher than in a proton beam-target configuration, the energy efficiency for production of antiprotons per proton is significantly higher for the colliding beam case. Unless methods for significantly improving the luminosity of the beams are found, however, the absolute rate of production will remain small.

It should also be remembered that in the true colliding beam case, the antiprotons are emitted isotropically, making them more difficult to collect. This can be rectified somewhat by making one beam more energetic than the other so the resulting products come out in a directional spray.

The colliding beams do not have to be protons. Colliding beams of positrons and electrons at 29 GeV center of mass energy produce 10.7 pions, 1.4 kaons, 0.3 protons and 0.3 antiprotons per annihilation event.[3.2] Again, this method suffers from the same low luminosity and wide angular distribution problems as the colliding proton beam technique.

To get around the low luminosity problem, which is basically caused by space charge repulsion between the particles in the beam, it has been proposed to use colliding beams of heavy ions such as uranium with energies so high (2.5 TeV) that each nucleon has 10 GeV or ten times its rest mass energy.[3.3]

Because of the small charge to mass ratio of singly charged uranium, calculations show that for a 100 m diameter colliding beam facility with an intersection area of 1 cm^2, the production rate could be as high as 10^{18} $\bar{p}$/s (1 gm/wk) without exceeding the space charge limit. Thus, the real limit in these machines is not space charge, but the available power. There are problems with this concept because of the isotropic distribution of the antiprotons and the large amounts of nuclear debris from the U-U interactions that would have to be filtered out. However, as design studies start on antiproton factories, colliding heavy ions beams should definitely be one of the candidate systems.

42

3.1.2 Laser Induced Pair Production

It has been proposed to make antiprotons by laser-induced pair production.[3.4] The original antiproton-proton production threshold estimate of 10^{17} W/cm^2 for CO_2 laser radiation in that paper has since been increased to 3×10^{23} W/cm^2 by the author.[3.5] This is still far from the capabilities of even the most optimistic laser designs. Perhaps self-focusing of the laser light in plasmas[3.6] or other exotic effects might bring the goal closer.

Even then, unless some unexpected resonance cross-section is found near the proton-antiproton energy threshold, it is expected that with laser production, just as is observed in production of antiprotons with high-energy particles, for every antiproton produced most of the energy will go into the production of many positron-electron, pion, kaon and other particle pairs.

References

[3.1]M. Antinucci, A. Bertin, P. Capiluppi, M. D'Agostino-Bruno, A.M. Rossi, G. Vannini, G. Giacomelli, and A. Bussiere, "Multiplicities of charged particles up to ISR Energies," Lett. Nuovo Cimento 6, 121-127 (1972).

[3.2]H. Aihara and TPC Collaboration, "Charged hadron production in e^+e^- annihilation at 29 GeV," LBL-17142 preprint, Lawrence Berkeley Lab, Berkeley, California 94720 (December 1983) [submitted to Physical Review Letters].

[3.3]G. Chapline, "Antimatter Breeders?" J. British Interplanetary Soc., 35, 423-424 (1982).

[3.4]H. Hora, "Estimates for the efficient production of antihydrogen by lasers of very high intensities," Opto-Electronics 5, 491-501 (1973).

[3.5]H. Hora, personal communication (23 November 1983).

[3.6]H. Hora, "Theory of relativistic self-focusing of laser radiation in plasmas," J. Opt. Soc. Am. 65, 882-886 (1975).

3.2 MAXIMIZING THE ANTIPROTON PRODUCTION RATE

Data on the antiproton production spectrum of high-energy
protons impacting heavy metal targets is available only for
small angles about the forward direction. These data are
sufficient for the design of the present antiproton collector
systems that only attempt to capture the antiprotons emitted
around the forward peak.

In order to design systems that will capture a higher
percentage of the antiprotons, it will be necessary to know
the antiproton spectrum as a function of angle and incident
proton energy over a greater angular spread. Such data does
not seem to exist and there are no present plans to make these
measurements, since obtaining the data would require an
extensive amount of time on the large synchrotron machines.
The particle physics community prefers to use the machine time
to study issues more important to particle physics. As a
result of this lack of detailed knowledge of the spectrum, the
total number of antiprotons generated is also unknown (to
probably a factor of two).

In Section 2.1, Figure 2-2, an estimate was made of the total
antiproton production efficiency for protons hitting a heavy
metal target as a function of proton energy. This is the
upper curve in Figure 3-1. If we now take the upper curve and
divide it by the energy of the proton making the antiprotons,
we obtain the bottom curve. This is the energy efficiency for
producing antiprotons. Note that it has a broad peak around
200 GeV. Although the number of antiprotons produced
continues to increase as the incident proton energy is
increased, above 200 GeV the gain in production is not enough
to offset the increased proton energy required.

From Figure 3-1 we see that the maximum energy efficiency
production rate occurs for an incident proton energy of
200 GeV and is 0.085 antiprotons/proton. (There are roughly
5 K mesons, 50 pi mesons, and large numbers of positrons and
electrons produced for each antiproton generated.) This
antiproton production rate is 2 times the production at the
Fermilab energy of 120 GeV and 20 times the production at the
CERN energy of 26 GeV. It should be emphasized that the
curves in Figure 3-1 are based on sparse data and that actual
measurements of antiproton production spectra as a function of
angle and proton energy are needed before any major
engineering studies on antiproton production are done.

44
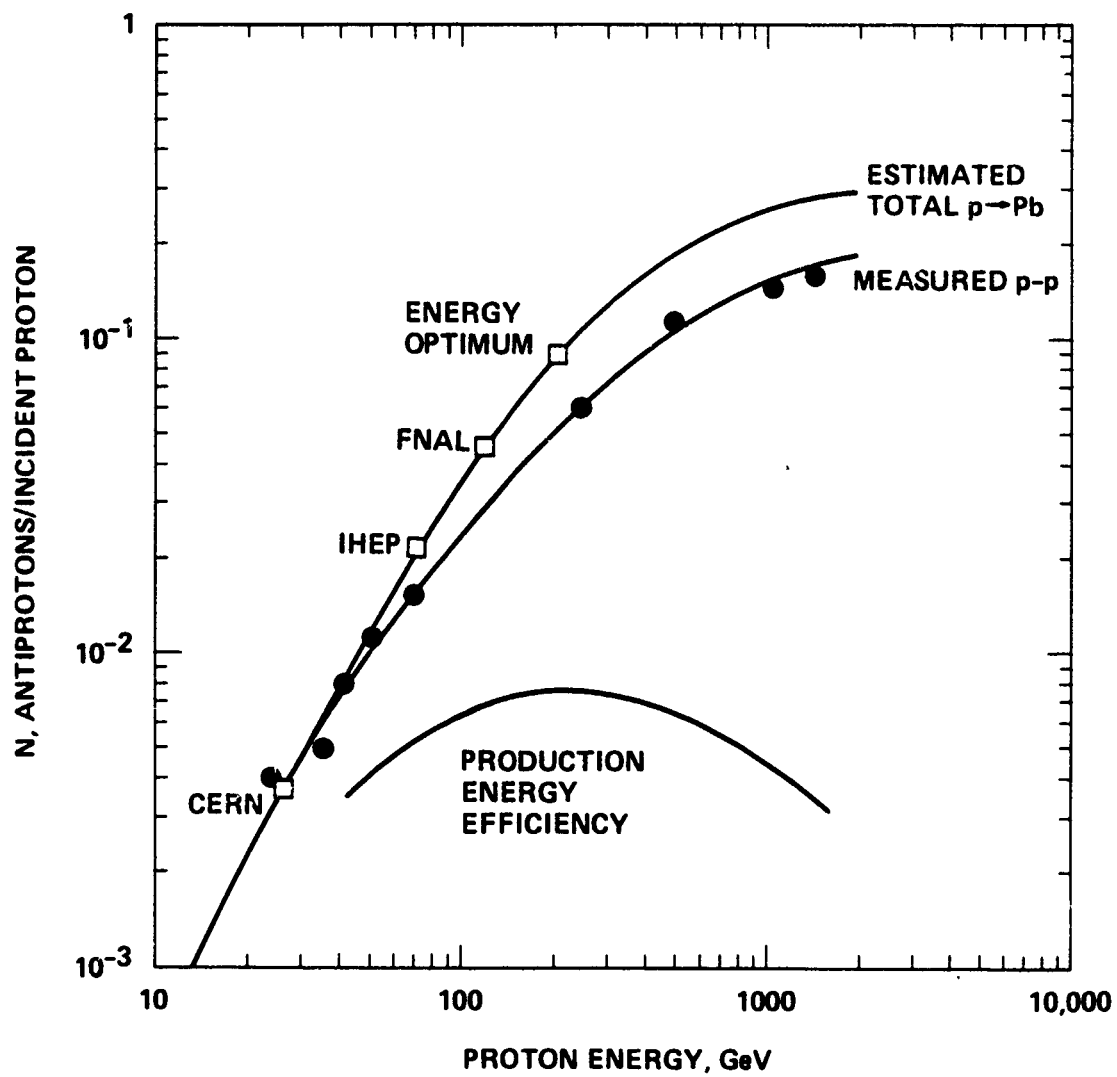
Fig. 3-1 Total antiproton production rates and efficiencies.

3.3 IMPROVING TARGET EFFICIENCY

The present targets for antiproton production are long wires of beryllium, copper, or tungsten a few millimeters in diameter and a length designed to optimize the tradeoff between a longer length to maximize the proton interaction and a shorter length to minimize the antiproton absorption. The first improvement to the present targets would be to have them carry a current so that the antiprotons produced would have a tendency to stay near the target axis. This would in effect convert the antiproton source from a rod source to a disk source at the exit plane of the target. An alternative is to break up the target into multiple targets and use magnetic lenses between each section to refocus the antiprotons.[3.7]

At Fermilab, designs have been carried out on rotating targets.[3.8] The length of the tungsten targets at Fermilab is only 5 cm, so a disk target will be of reasonable size and can be rotated at high enough speeds to minimize the local heating problem. At IHEP designs have been carried out on targets made of a flat jet of mercury with a width of 0.5 to 3 mm and 60 cm long.[3.9] The flowing mercury solves the target cooling problem for the proton beam intensities expected at IHEP. Beryllium foil windows are used to separate the mercury target vacuum chamber from the main vacuum system.

For an antiproton factory, a major problem area needing invention, materials experimentation, and study is the development of a suitable target design. Rotating and liquid targets are a potential solution to this problem, but further work needs to be done to find the best target-lens configuration for high power production.

References:

[3.7] J.A. MacLachlan, "Current carrying targets and multitarget arrays for high luminosity secondary beams," FN-334, 8055.000, Fermi National Accelerator Lab, Batavia, Illinois (April 1982).

[3.8] Fermilab staff, "Design Report: Tevatron 1 Project," p. 3-4 and Figures 3-6 and 3-7, Fermi National Accelerator Lab, Batavia, Illinois (September 1984).

[3.9] B.F. Bayanov, A.D. Chernyakin, V.N. Karasyuc, G.I. Silvestrov, T.A. Vsevolozskaya, V.G. Volohov, G.S. Willewald, "The antiproton target station on the basis of lithium lenses," pp. 362-368, Proc. 11th Int. Conf. High Energy Accelerators, Geneva (1980).

3.4 IMPROVING ACCELERATOR EFFICIENCY

The present machines that are used for accelerating protons to
relativistic speeds are synchrotrons. The design of these
machines enables protons to be accelerated to very high
energies using a reasonable amount of hardware and site
acreage. The synchrotron is built in a large circle and the
protons travel around through the machine many times, gaining
energy with each cycle. The upper limit to the energy is
primarily determined by the maximum strength of the magnetic
fields in the bending magnets that keep the proton beam
turning in a circle. The synchrotron provides the particle
physicist with high-energy protons at a very precisely known
energy. It is an ideal tool for studying elementary particle
physics. The average current that the synchrotron can handle
is small, however, and the efficiency is only a few percent.

There is an alternate machine for producing high-energy
protons, that can handle high average currents and has high
energy efficiency. It is called the linear accelerator or
linac. As its name implies, the linear accelerator is a long,
straight machine. The protons only pass through it once. The
linac consists of a series of RF cavities which set up
electric fields that accelerate the protons, drift tubes to
isolate the protons when the RF fields reverse phase, and
alternating polarity quadrupole focusing magnets to keep the
proton beam from spreading.

By using the alternating gradient focusing concept, it has
become possible to accelerate very intense beams (up to one
ampere) to very high energies. The energy limit is economic,
not technical. It is known that machines can be built to
handle over 250 mA, since it has been demonstrated in the
first section of the linac injector at Fermilab, which is the
only section where current limitations would occur.
Acceleration to higher energies only requires more RF power.

Because of their high average current capability, linacs have
been considered for an unconventional type of nuclear reactor,
called an accelerator breeder or electrothermal reactor. The
linac is used to accelerate protons to about 1 GeV and the
beam is sent into a target made of unenriched or even depleted
uranium. The protons cause spallation reactions to occur,
which produce up to 100 neutrons per incident 1 GeV proton.
The neutrons react with the ^{238}U to produce ^{239}Pu as well as
6 GeV of thermal energy, which can be used to make electricity
to help run the linac. Originally considered as an alternate
method of making plutonium for weapons, these types of
reactors received considerable study in the 1950's and 1960's,
but as the supply of uranium ore became more secure, effort on
the accelerator breeder stopped. The last major meeting on
the subject was held in 1977.[3.10]

47

What came out of the meeting was the realization that high
current linacs could be built and that with the availability
of new high efficiency (75%) klystrons, their AC "wallplug"
power to proton beam power efficiencies could exceed 50%. At
these efficiencies the thermal energy released in the reactor
could supply enough electrical power to keep the linac running
so that the reactor would be self-sustaining. The output of
the reactor would then be the plutonium. One specific design
of such a system would use 600 MW of electrical power to drive
a 50% efficient linac. The linac would then produce a 300 MW
proton beam. The proton beam would be sent into an
electronuclear reactor where it would release over 1500 MW of
thermal energy. The thermal energy would then be used to
operate a thermal power plant. At 40% efficiency, the power
plant would produce the 600 MW of electricity needed to run
the linac, and the cycle would be closed.

The Chalk River, Canada linac program[3.10] has been studying
100% duty factor linacs, with the goal of producing a linac
capable of of 300 mA _average_ current at 1 GeV (0.3 GW beam
power) for use in an accelerator breeder. They have several
designs for a proton ion source that are capable of delivering
a 300 mA beam of satisfactory emittance, so ion sources are
not a limitation.

The acceleration limit of a linac (the energy increase per
meter) is determined by the sparking limit in the cavity. The
sparking limit is inversely proportional to the wavelength.
Present machines operating at 200 MHz usually operate at
1 MeV/m, and there are designs for higher frequency machines
that will operate at 5 MeV/m.

A linac for an antiproton factory with a proton energy of
200 GeV would be 40 km long. This is a little longer than the
28 km LEP ring presently under construction at CERN and 1/5th
the size of the 200 km Supercollider being proposed as the
next large particle accelerator in the US. If run at a power
level of 10 GW, the proton current required would only be
50 mA, which is less than the 300 mA of the Chalk River
design. By skimming off the antiprotons and using the
remaining particles to run a closed electronuclear breeder
cycle, such a factory would require no outside power source
and would essentially be turning depleted uranium into
plutonium and antiprotons.

References:

[3.10] H.J.C. Kouts, Chairman, **Proceedings of an Information
Meeting on Accelerator Breeding**, Brookhaven National
Laboratory, Upton, New York, 18-19 Jan 1977.

3.5 IMPROVING ANGULAR CAPTURE EFFICIENCY

The present angular capture efficiencies of the magnetic lens collection systems are already quite good, with up to 30% of the antiprotons collected and directed into the aperture of the collecting ring. The present designs, however, were optimized for the antiproton energies expected at the particular facility and the particular conditions in the target area (such as power supply limitations, tunnel size, etc.).

The estimated number of antiprotons collected as a function of antiproton momentum has been calculated for both 30 mrad and 60 mrad angular acceptance at a number of incident proton beam energies.[3.11] These curves were then integrated to obtain an estimate of the total number of antiprotons collected by the two lens acceptances. These estimates are plotted in Figure 3-2 along with the estimate of the total number of antiprotons obtained from protons hitting heavy metal targets (see Figure 2-2).

As is shown in Figure 3-2, the limitation on angular acceptance to 30 mrad means that only 55% of the antiprotons generated are being captured by the lens at the higher energies and even less at the lower energies. If the angular capture could be increased to 60 mrad or more, then the angular capture efficiency could reach a value of 80% or greater.

Also shown in Figure 3-2 is the energy efficiency of the antiproton production process. Each of the top three curves was multiplied by the energy that would be released by the annihilation of the antiproton ($2mc^2=1.876$ GeV) and divided by the energy of the incident proton to produce an energy efficiency estimate. This energy efficiency estimate gives us a rough guide to the choice of the optimum proton energy for production. We can see from the bottom three curves that, if we can capture all the antiprotons, the optimum energy for the proton beam is 200 GeV. If our angular acceptance is limited for some reason, it pays to go to slightly higher energies. (This is intuitively obvious since at higher energies the antiprotons are more concentrated in the forward direction.)

These "optimum energy" estimates, however, do not take into account the fact that the antiproton longitudinal momentum is spread over a wider band at higher energies. The best operating point must take this and a number of other factors into account, but it looks as though a proton beam energy from 100 to 500 GeV will give the best overall energy efficiency for antiproton production. We will assume for now that 200 GeV is an optimum energy for the incident proton beam.
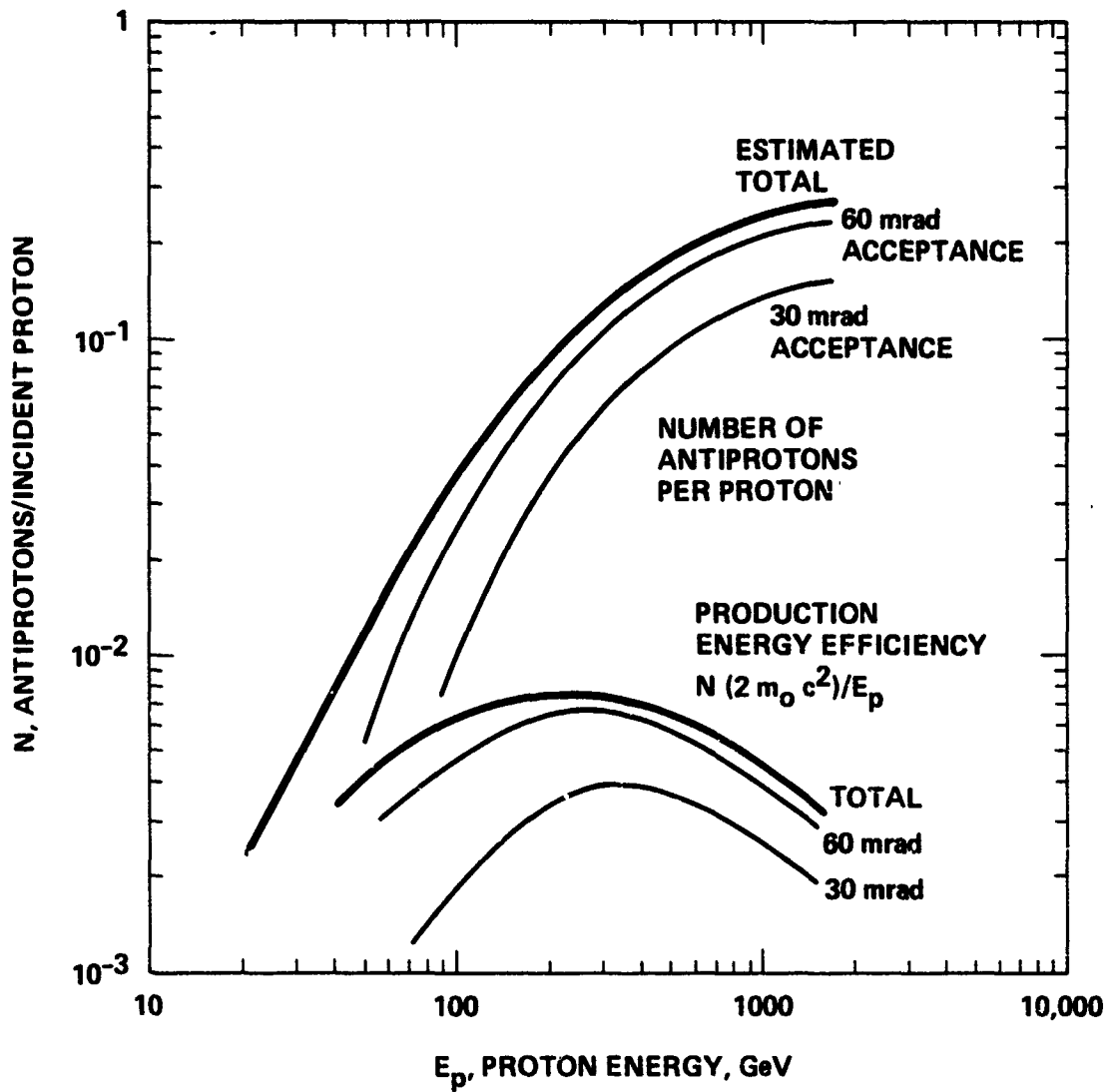
Fig. 3-2 Antiproton production vs. angular capture.

50

All of the studies to date have assumed that only a single, on-axis lens would be used to capture the antiprotons. Because the antiprotons are being emitted over a wide angle, this immediately leads to the requirement of a short focal length for the lens so it can capture these wide angle antiprotons. Research needs to be done on the feasibility and comparative merits of an array of lenses. Since each lens has to capture only the antiprotons in a small portion of the emitted beam solid angle, the focal length requirements can be relaxed. The support hardware for the lenses will cause interception losses, however, and realistic tradeoff studies need to be done between the number of lenses and the lens design parameters. If a multiple lens approach looks desirable, then invention is needed on low-loss devices for separating the wide angle antiproton beam into multiple beams to minimize the interception losses of the multiple lens hardware.

Most present magnetic lens designs require the antiproton beam to pass through the material of the lens. This causes significant losses in the antiproton spectrum. This is not true for the magnetic quadrupole lens, but it does not focus well in all orientations. Invention is needed to develop new lens designs with low loss and good focusing.

Another method for construction of a magnetic lens similar to that of the lithium lens would be to carry the current for the lens in a cylinder of ionized plasma instead of lithium metal. The problem of the current or beam heating up the lens would be gone and it is likely that absorption of the antiprotons in the lens would be less. A plasma lens would have its own problems, such as all the various plasma instabilities that would be driven by the high currents needed. The concept is still in the preliminary idea stage at CERN and to date there have been no publications concerning its feasibility.

The present single magnetic lens concepts have already achieved angular capture efficiencies of 30% or greater and there are many ideas for new lens concepts with greatly improved performance. It is therefore reasonable to expect that after modest investment in invention, engineering, and testing, there should be new magnetic lens designs capable of capture angles of 60 mrad even at higher antiproton momentum levels and capture efficiencies of 85% or greater.

References:

[3.11]C. Hojvat and A. Van Ginneken, "Calculation of antiproton yields for the Fermilab antiproton source," Nucl. Instr. & Methods **206**, 67-83 (1983).

3.6 IMPROVING MOMENTUM CAPTURE EFFICIENCY

We now will look at the problem of momentum capture. When the antiprotons come from the target, they not only have a wide spread in angle, they also have a wide spread in momentum. It is this wide spread in resultant antiproton momentum and the difficulty of making an antiproton collection ring with a wide momentum acceptance that leads to the extremely low inefficiencies in present antiproton "factories".

For example, at CERN, the present momentum acceptance in a Antiproton Accumulator is only $dp/p=1.5\%$. For a peak momentum of $p=3.5$ GeV/c, this translates into a momentum bite of only $dp=0.05$GeV/c. Thus, only 1% of the 5 GeV/c half-width of the antiproton momentum spectrum is captured.

If we assume that an antiproton factory has an incident proton beam at 200 GeV energy and a 60 mrad angular acceptance, then the flux of antiprotons per proton per unit antiproton momentum is shown in Figure 3-3.[3.11] The antiproton flux peaks at 12.5 GeV/c antiproton momentum and spreads from 1 GeV/c to 50 GeV/c, with a half-width of 22 GeV/c.

The present state-of-the-art in collection rings for antiprotons is a momentum acceptance of about $dp/p=6\%$. Even if this could be raised to 8%, the momentum bite at an antiproton momentum of $p=12.5$ GeV/c would still be only $dp=1$ GeV/c and would capture only 4.5% of the antiprotons.

The obvious solution is to build a multiplicity of rings. They would be identical copies of each other, with the same radius of curvature and sharing the same tunnel (since the tunnel costs are a major portion of the expense of a ring). Each ring would have the strength of the magnetic fields in its bending magnets set at a different level to keep a different antiproton momentum circulating through its vacuum pipe. If each ring could handle a momentum bite of 1 GeV/c, then as we see in Figure 3-3, 16 rings could capture 61% of the antiproton momentum spectrum and 27 rings could capture 84% of the antiprotons.

Separating the antiproton beam into different momentum buckets should not be too difficult. The magnetic focusing lens has chromatic aberration. Each level of antiproton momentum is focused at a different focal point. A string of diverter magnets can deflect the different antiproton momenta in different directions, where they can be channeled to the proper collecting ring.
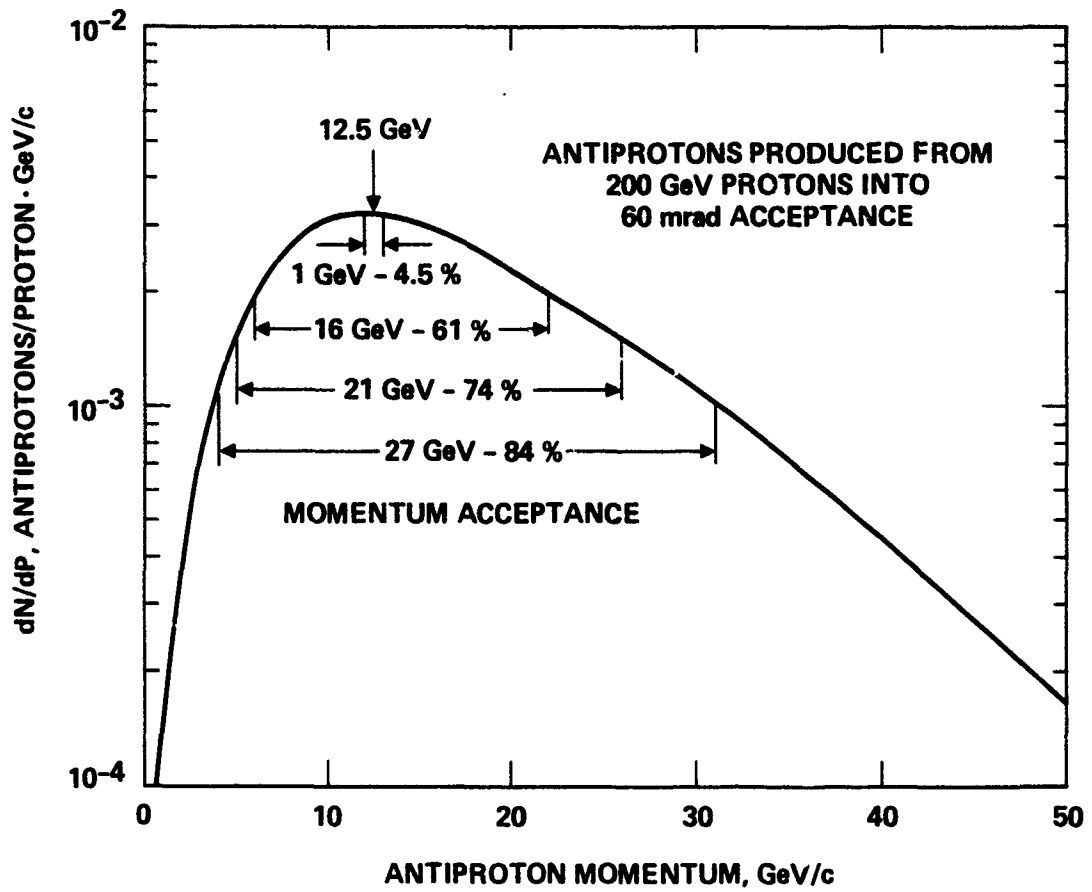
Fig. 3-3 Antiprotons vs. momentum spread.

3.7 SYSTEM EFFICIENCY ESTIMATES

From the previous sections we can see that there are a number
of ways to improve the efficiency of antiproton production
over the present techniques. The first obvious improvement is
to use a linear accelerator or other high-current, high-
efficiency machine to produce the protons instead of a
synchrotron. A linear accelerator with its energy efficiency
from ac mains to beam energy of 50% will be more than an order
of magnitude better than the present synchrotrons.

The next significant improvement is to use a higher proton
energy so that more antiprotons are produced in the target.
As is shown in Table 3-1, by going to 200 GeV, the number of
antiprotons produced can be increased by a factor of 20 from
the 3.8×10^{-3} $\bar{p}/p$ at CERN to 8.5×10^{-2} $\bar{p}/p$.

The present magnetic lenses are relatively efficient in
capturing the resulting antiprotons in angle. Yet by
improving the design and going to multiple lens collectors, we
should be able to improve the angular capture efficiency by a
factor of 3 or 4 to 85%.

Another place where a significant improvement can be made is
in the momentum capture efficiency. The single ring
collectors at CERN, Fermilab, and IHEP are severely limited by
inherent difficulties with matching the magnetic and vacuum
pipe acceptances to the emittances of the lenses. With a
large enough tunnel and enough money to build copies of the
collectors, each tuned to accept a different momentum range,
it should be possible to improve the capture efficiencies
significantly. Whether it will be possible to go from the
present few percent to a desirable 85% is unknown. Studies of
the feasibility of separating a beam of antiprotons into
separate beams at different momenta are needed.

There are many losses as the antiproton beam is generated,
collected, and switched around from one device to another.
The handling efficiencies in the present facilities are not
bad, but improvement in this area is also needed.

As we can see from Table 3-1, if all these efficiencies can be
achieved, the total production efficiency of antiprotons can
be raised from the present 4×10^{-7} $\bar{p}/p$ at CERN by more than
five orders of magnitude to 5×10^{-2} $\bar{p}/p$. With an efficient
linear accelerator replacing the low-efficiency synchrotron,
the energy efficiency can rise even more from its present
value of 1.4×10^{-9} to 2.5×10^{-4}.

Table 3-1   Antiproton Production Efficiencies

	CERN	Fermilab	Goal
Incident Proton Energy (GeV)	26	120	200
Generation Efficiency ($\bar{p}/p$)	0.4%	4.7%	8.5%
Angular Capture Efficiency	20%	30%	85%
Momentum Capture Efficiency	1%	1.2%	85%
Handling Efficiency	5%	18%	80%
Total Production Efficiency ($\bar{p}/p$)	4×10^{-7}	3×10^{-5}	5×10^{-2}
Overall Energy Efficiency	1.4×10^{-9}	2.5×10^{-8}	2.5×10^{-4}

3.8   CONCEPTUAL ANTIPROTON FACTORY

In Figure 3-4 is shown a conceptual design for an antiproton factory which would utilize the technologies being developed at CERN, Fermilab, and IHEP, but on a much larger scale and with the design optimized for energy efficiency. First, the proton accelerator should be a high-current rf linear accelerator (linac) with a wallplug efficiency of 50%, rather than the low-current, low-efficiency, but high-energy resolution synchrotron preferred as a research tool by particle physicists.

There would be more than one proton beam with each beam operated at the optimum beam current for the particular target design chosen. Each proton beam would strike a metal target and the resulting particles would be sorted by an array of wide-angle collecting lenses to extract the antiprotons and positrons. The positrons with the right energy would be picked off and sent to the antihydrogen generator, while all the antiprotons possible would be sorted by energy and sent to a stack of stochastic coolers, each optimized for a particular central antiproton momentum.

After stochastic cooling, the stack of beams at different energies would go to a decelerator stack that would reduce all the antiproton energies to the same subrelativistic energy (200 MeV). The combined beam would then be sent to a subrelativistic cooling ring using either stochastic or electron cooling before being further decelerated and sent on to the antihydrogen generator where the antiprotons are combined with the positrons to make antihydrogen atoms.

55
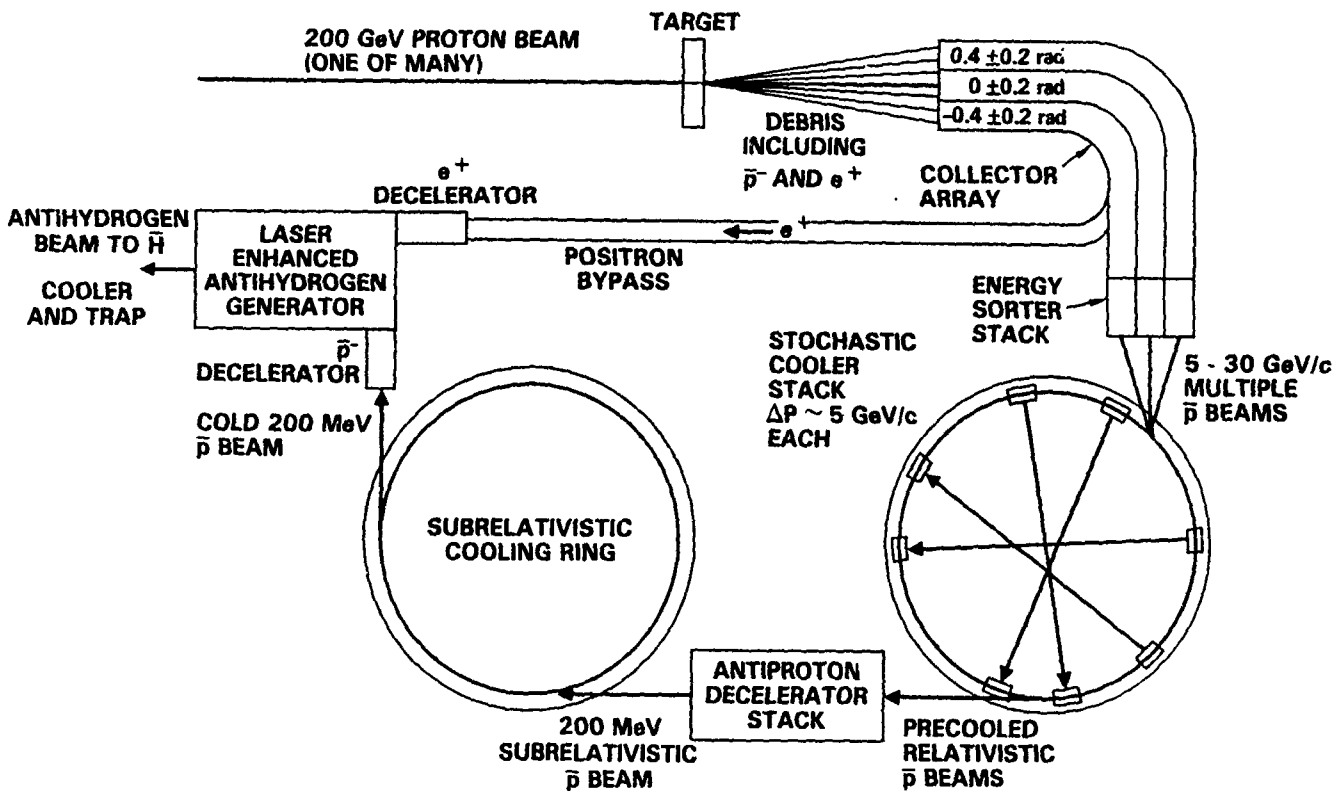
Fig. 3-4 Antiproton factory (one segment).

56

3.9 COST ESTIMATES

Cost estimates of major facilities requiring new technology are notorious for their inaccuracy. It is possible, however, to get a first cut at the operational cost of producing antimatter in a prototype production facility by making some assumptions about the energy efficiency of the production and the cost of energy.

A milligram of antiproton fuel would be a useful quantity to consider for antiproton propulsion since annihilation with a milligram of protons would give an energy output equivalent to the burning of 6 tons of liquid hydrogen/liquid oxygen rocket fuel. One milligram of antiprotons contains 6×10^{20} $\bar{p}$. Thus, if the antiproton-to-proton production ratic is 5%, the factory would have to produce 1.2×10^{22} protons, each with 200 GeV of energy or a total of 3.8×10^{14} J.

If the protons were accelerated with a linear accelerator with an ac mains to beam power of 50%, then the linac would require 7.7×10^{14} J of energy or in electrical power terms, 2×10^8 kW-hr. If we had to buy that electrical energy at 0.05$/kW-hr, then the cost of the antiprotons is found to be an optimistic 10M$/mg.

Liquid oxygen and liquid hydrogen, being cryogenic fuels, are expensive. But their production costs certainly are much less than 10M$ for 6 metric tons. Thus, it is obvious that unless the cost of producing antimatter comes down significantly, antimatter will never be a cost competitive method of storing energy on the surface of the earth where hydrogen and oxygen are easily obtained. We shall see in Section 8, however, that even at 10M$/mg, antimatter is a cost effective fuel in space. In space, mass costs money, and the low mass of an antiproton propulsion system makes it much more attractive than any chemical propulsion system for the more difficult space missions.

SECTION 4

GENERATION OF ANTIHYDROGEN

In this section we will discuss methods for the generation of antihydrogen atoms and molecules, given that a supply of antiprotons is available as a result of the research discussed in the previous sections. These investigations into the generation of antihydrogen are ideally suited for relatively inexpensive near-term experimental research efforts, since in nearly every case, the research can be carried out using normal protons, normal electrons, and normal hydrogen atoms, ions, and molecules. If performed at a university, the research projects would be ideal thesis topics.

There is one caveat. The techniques used during the research must not allow the protons, electrons, or hydrogen to come into contact with other forms of matter. This includes residual gas atoms in the vacuum system. To be a valid simulation, the research should be carried out in ultra-high vacuum (UHV) systems, not standard vacuum systems. In some experiments, the UHV systems must be cryogenically cooled.

In each investigation, the effect of background gas on the antimatter version of the experiment should be taken into account. If the technique being studied allows for the loss of protons, electrons, or hydrogen from the sample, the effects of the radiation from the annihilation of the equivalent antiprotons, positrons, and antihydrogen with the walls should be calculated. As the investigations progress, it may be found that the use of atomic and molecular hydrogen ions, or excited states of either ions or neutral particles may give better results than the use of neutral atoms or molecules. Where possible, these alternate pathways will be indicated in the following list of potential research projects.

The research projects discussed in this section are relatively independent of each other and can be carried out in any order. The equipment needed is similar to that used in modern atomic and molecular beam experiments. In many of the projects, there will be a requirement for high-strength electric, magnetic, and photon fields to produce significant interaction rates. There will also be a need for sophisticated diagnostic tools that can interrogate the state of individual particles and an ultrahigh vacuum to maintain the quality of the atomic and molecular beams. Thus, it is essential that adequate equipment funds be budgeted to provide the apparatus needed to carry out the experiments.

59

4.1 CONVERSION OF ANTIPROTONS TO ATOMIC ANTIHYDROGEN

It will probably be found desirable to store the antiprotons as some form of antihydrogen rather than as antiproton ions. The first step is to convert the antiprotons into atomic antihydrogen by adding a positron.

4.1) $$p^- + e^+ \longrightarrow \bar{H} + h\nu$$
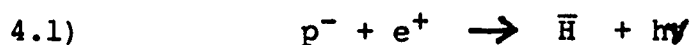
Since the antiproton and positron attract each other, the reaction will take place spontaneously. The system will emit photons as the electron jumps from one state to the next on its way to the ground state. If there is a large velocity difference between the antiproton and positron, however, the cross section can be small and the conversion rate slow. It may be found necessary to enhance the conversion rate by using electromagnetic stimulation or possibly a catalyst made of some form of antihydrogen.

If the antiprotons are obtained as trapped and cooled ions in an ion trap, such as a Penning trap, then a straightforward approach would be to convert the trap into one that would hold and cool both positive and negative ions. A simple example is the Paul trap. As is shown in Figure 4.1, a Paul trap has the same electrode configuration as the Penning trap, but uses rf electric fields instead of static electric and magnetic fields to form the trapping region. A Paul trap could hold both antiprotons and positrons and cool them until their relative velocities were low enough that the conversion to hydrogen takes place naturally.

There are a number of obvious research questions concerning the recombination process that need to be investigated. Efficient methods for injecting the antiprotons and positrons and removing the neutral antihydrogen need to be found. The effect of high ion densities on the trapping lifetime and the recombination rate needs to be evaluated. The use of rf modulation or laser radiation to enhance the various reactions needs to be studied. Also, the effectiveness of magnetic fields or laser beams to trap and manipulate the neutral antihydrogen atoms and ions needs to be determined.

Then, the conversion rate of the neutral atomic hydrogen to positively charged atomic antihydrogen ions, or antihydrogen molecules with positive, negative, or neutral charge needs to be measured and the efficacy of these antihydrogen atoms or molecules in acting as a "catalyst" to enhance subsequent conversions needs to be determined.

60
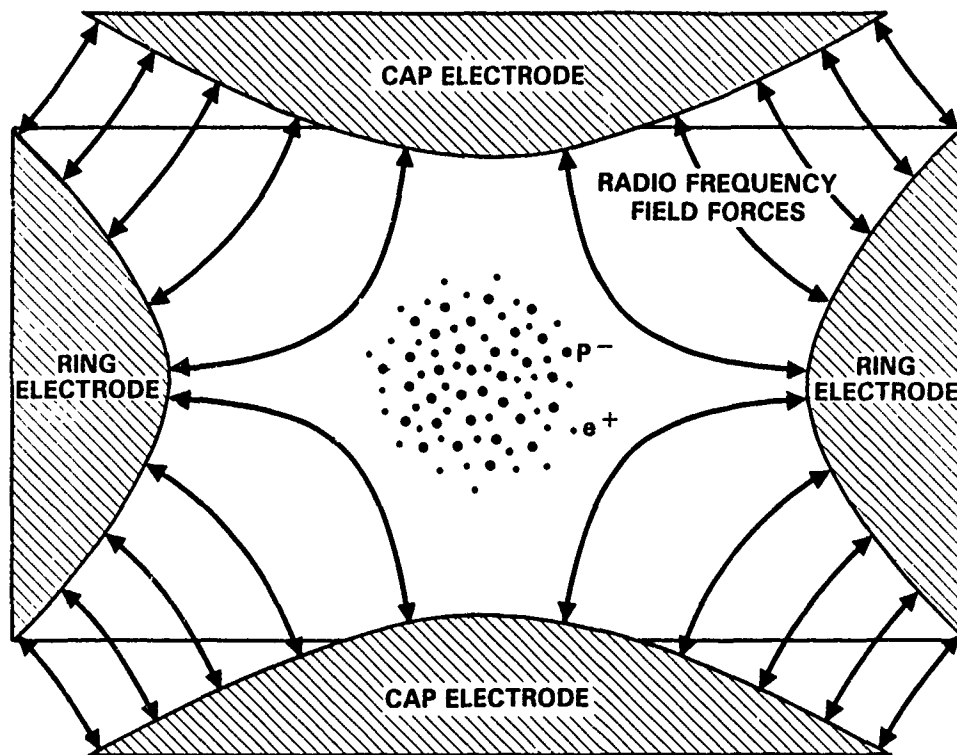
Fig. 4-1 Paul trap for positive and negative ions.

For example, after the first antihydrogen atom is formed, it
may be desirable to deliberately enhance the addition of a
positron to it to form an atomic antihydrogen ion. The
antihydrogen ion can then be used in a charge exchange
reaction with an antiproton ion. In this manner, the
antihydrogen ion acts as a catalyst to breed new antihydrogen
atoms that act as catalysts for further reactions:

4.2) $\overline{H} + e^+ + h\nu_1 \longrightarrow \overline{H}^+ + 2h\nu_1$

4.3) $\overline{H}^+ + p^- + h\nu_2 \longrightarrow \overline{H} + \overline{H} + 2h\nu_2$
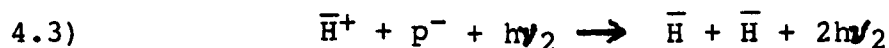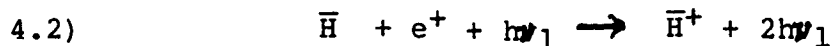
Research on the reaction given by Equation 4.3 for normal
hydrogen ions has been proposed as a method for neutralizing a
hydrogen particle beam.[4.1] Any results from that study of
hydrogen ions will have relevance to the antihydrogen problem.

61

If this research on conversion of trapped antiprotons to antihydrogen shows promise, thought needs to be given to methods for converting this "batch" process to a "flow" process suitable for a high throughput antiproton "factory".

Instead of a trap, the antiprotons may be available in the form of a low-energy, low-temperature beam. The research task here is to combine this antiproton beam with a positron beam and have it convert into an atomic antihydrogen beam. This experiment has already been carried out at CERN using normal matter during the process of studying the concept of electronic cooling. (See Section 2.3 on Electron Cooling of Antiprotons.) Electron cooling was first tested by mixing a cold electron beam with a hot proton beam. During the tests it was noted that some of the electrons recombined with the protons to produce hydrogen atoms.[4.2] The recombination rates were low, however, so the concept of using lasers to enhance the recombination was developed.[4.3], [4.4] A conceptual system that incorporates this concept is shown in Figure 4.2.
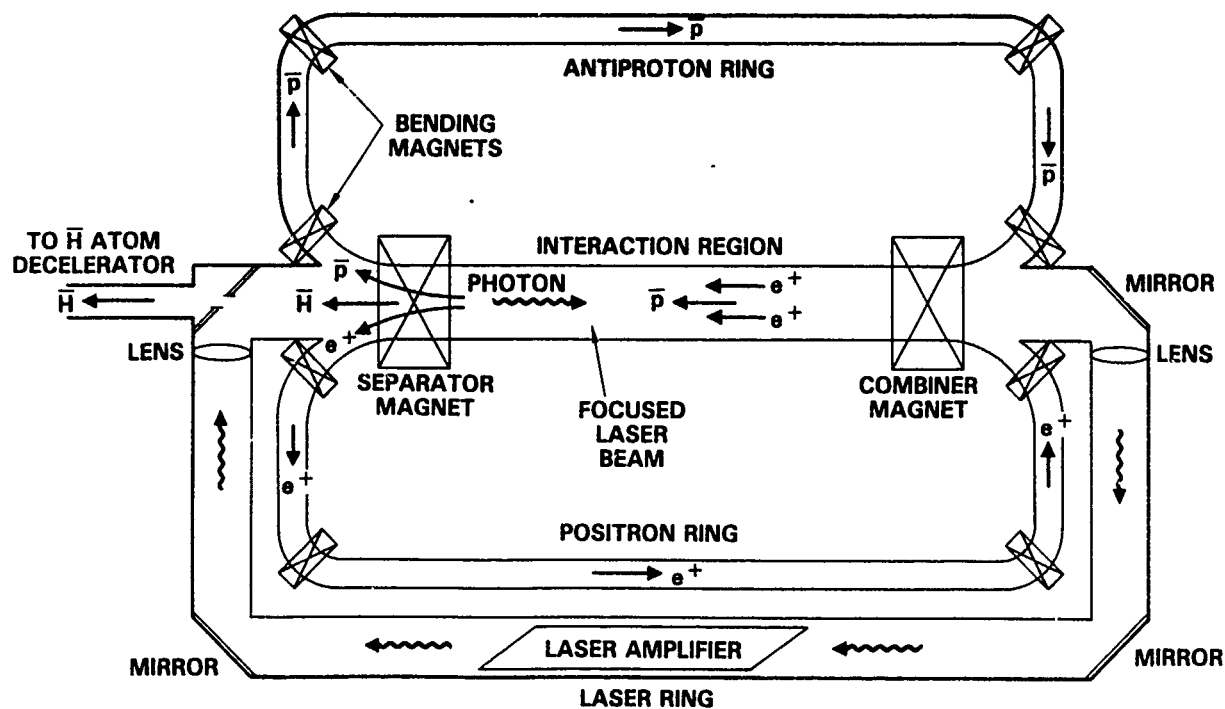
Fig. 4.2 Laser-enhanced antihydrogen formation.

The apparatus for laser-enhanced antihydrogen formation consists of three storage rings coupled at a straight section. One storage ring contains the antiprotons. This would be very similar to the Low Energy Antiproton Ring (LEAR) at CERN and would incorporate stochastic cooling to keep the velocity spread of the antiprotons low. There would be a second ring for the cooling and storage of the positrons. In the combined straight section there would be magnets that would separate the oppositely charged moving particles at one end and recombine them at the other so they are moving in the same direction with very low relative velocity. A laser, tuned to the optimum frequency to enhance the recombination, would then be sent up the combined beam to stimulate the recombination of the antiproton and the positron into antihydrogen. The neutral antihydrogen atoms would pass through the magnet section without being bent and would exit as a neutral antihydrogen atomic beam. The neutral antihydrogen beam would then be manipulated using lasers as described in the section on laser cooling and trapping.

In this apparatus, the basic reaction in Equation 4.1 is stimulated by irradiation with light corresponding to a transition from the continuum into a bound atomic state.

$$4.4) \qquad p^- + e^+ + h\nu \longrightarrow \bar{H} + 2h\nu$$

The proposed CERN experiment[4.3] will be carried out with antiprotons in the LEAR storage ring. These antiprotons are typically at an energy of 100 MeV. Although this is "low energy" to a particle physicist, the velocities are high enough that the frequency of the laser light coming up the beams of antiprotons and positrons is significantly Doppler shifted. The CERN experimenters will use visible light lasers, but the light will be Doppler shifted to the ultraviolet frequencies needed to stimulate the recombination. At lower antiproton energies, coherent ultraviolet sources such as those discussed in the section on cooling and trapping of neutral particles will be needed.

The experiment proposal to produce and study antihydrogen has not received a high rating from the CERN experiment evaluation committee because it is not elementary particle physics. In the probable view of the committee, it is not even a physics experiment, it is a trivial chemistry experiment. The recombination of an electron with a nucleus is a well understood atomic process and the mere demonstration of the process with antimatter is of marginal value. Thus, the experiment will have to wait a number of years while more important science questions are answered with the limited supply of antiprotons available in LEAR.

Thus, to obtain any near term results on the controlled production of antihydrogen, it will be necessary to design and carry out experiments using normal matter (protons and electrons). The objective of the research would be to investigate the interaction of the protons with the electrons under the influence of other protons, electrons, hydrogen atoms, and electromagnetic fields, and to optimize the conversion of the protons and electrons into atomic hydrogen. The resultant hydrogen atoms should emerge from the process under "control". That is, they should be stationary, or in a reasonably collimated beam with a small velocity spread.

References:

4.1 D.G. Steel, J.F. Lam, R.A. McFarlane, "Studies of laser enhanced relativistic ion beam neutralization." White Paper, Hughes Research Laboratories, Malibu, California (October 1983).

4.2 M. Bell and J.S. Bell, "Capture of cooling electrons by cool protons," Particle Accelerators, 12, 49-52 (1982).

4.3 R. Neumann, H. Poth, A. Winnacker, and A. Wolf, "Laser-enhanced electron-ion capture and antihydrogen formation," Z. Phys. A, 313, 253-262 (1983).

4.4 H. Herr, D. Mohnl, and A. Winnacker, "Production of and experimentation with antihydrogen at LEAR," pp. 659-676, **Physics at LEAR with Low-Energy Cooled Antiprotons**, Workshop on Physics at LEAR with Low-Energy Cooled Antiprotons, Erice, Sicily, Italy, 9-16 May 1982, U. Gastaldi and R. Klapisch, Ed., Plenum Press, NY (1984).

4.2 CONVERSION OF ANTIHYDROGEN ATOMS TO MOLECULES

Once we have atomic hydrogen in some controllable form, the next step is to produce molecular hydrogen. Atomic hydrogen easily converts to molecular hydrogen since the process releases energy. A third body is needed, however, to carry off the energy. Under normal laboratory conditions, the third body is the wall or other atoms or molecules. We do not want the antihydrogen to touch the walls or to have antihydrogen atoms or molecules leaving the reaction with too much energy. To keep control of the process, it will be necessary to supply the "third body" in the form of one or more photons.

4.2.1 Atomic to Molecular Hydrogen Reactions

In addition to neutral molecular hydrogen, both H_2^+, a molecule of hydrogen missing an electron, and H_2^-, a molecule of hydrogen with an additional electron are known to be stable, so the antimatter analogs should be stable. Thus, there are many reactions that could be investigated in this research project. Some of them are listed below:

4.5) $H^O + H^O + h\nu \longrightarrow H_2 + nh\nu$

4.6) $H^O + H^O + h\nu \longrightarrow H_2^+ + nh\nu + e^-$

4.7) $H^- + p^+ + h\nu \longrightarrow H_2 + nh\nu$

4.8) $H^- + p^+ + h\nu \longrightarrow H_2^+ + nh\nu + e^-$

4.9) $H^- + H^- + h\nu \longrightarrow H_2^- + nh\nu + e^-$

4.10) $H^- + H^- + h\nu \longrightarrow H_2 + nh\nu + 2e^-$

4.11) $H^O + H^- + h\nu \longrightarrow H_2^- + nh\nu$

4.12) $H^O + H^- + h\nu \longrightarrow H_2 + nh\nu + e^-$

4.13) $H^O + H^- + h\nu \longrightarrow H_2^+ + nh\nu + 2e^-$
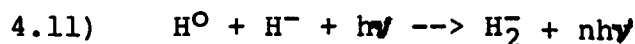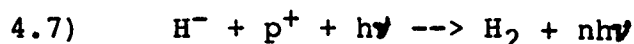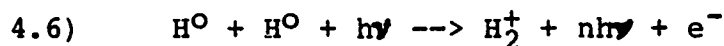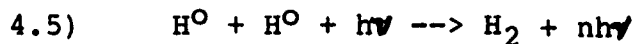
Some of these reactions involve the loss of positrons. This may be an acceptable loss, depending upon the results of the investigations. For example, the availability of a positron to act as a third body to aid in conservation of both energy and momentum in the reaction may give these reactions a much higher conversion rate than those that have only photons emitted after the formation of the molecule.

All of these processes have modifications where one or more of the hydrogen atoms or the resultant hydrogen molecules are in an excited state. It might be found advantageous to excite one or both of the initial hydrogen atoms before the two are brought near each other, rather than having to supply the photon energy at the exact instant the two atoms approach each other. Also, exciting one or both of the atoms to a very high level to produce a "Rydberg" atom would increase the physical size, thus increasing the cross-section.

By using polarized hydrogen atoms and polarized laser beams combined with magnetic fields, it may be possible to produce neutral hydrogen molecules in the desired ground level parahydrogen state. If that research is successful, then research on the conversion of hydrogen to parahydrogen would not be needed.

4.2.2 Orthohydrogen and Parahydrogen Molecules

Molecular hydrogen is usually found as a mixture of two
different states. The ground state is called parahydrogen and
consists of two bound hydrogen atoms with the nuclear magnetic
moments or spins of the two proton nuclei pointing in opposite
directions (I=0). Since the two electrons in the ground state
are required by the Fermi exclusion principle to have their
spins oppositely directed (J=0), the atom has zero net
magnetic moment (M=0).

The first energy level of molecular hydrogen is created when
the spins of the two protons are aligned with each other
(I=1). This form, called orthohydrogen, has net magnetic
moment (M=1) and is highly metastable at low temperatures. It
is only 170.5 K (0.0147 eV) above the ground state and
conversion to the ground state can only take place when a
magnetic gradient perturbs the magnetic moments of the two
protons, causing one of them to flip over. The flipping can
be caused by the magnetic field from another orthohydrogen
molecule or by a magnetic catalyst such as nickel or iron.

The hydrogen molecule is a "homonuclear" molecule in that it
contains two identical nuclei. Since the molecule looks
identical if the molecule is rotated so the two nuclei are
interchanged, the rules of quantum mechanics only allow
alternate energy levels to exist. As is shown in Figure 4-3,
for parahydrogen the allowed levels are the even rotational
states (J=0,2,4...), while for orthohydrogen it is the odd
numbered states (J=1,3,5...).[2.23] There are no restrictions
on the vibrational states.

Since the energy levels for both ortho and parahydrogen are
separated by two units of angular momentum, transitions
between two rotational states cannot be excited by a single
photon, which only carries one unit of angular momentum. Even
collisions cannot produce a transition between the rotational
states.

Transitions can be produced, however, by Raman scattering,
which involves two photons, the incoming photon and the
scattered photon. It also might be possible to produce two-
photon transitions using the nonlinear effects that arise when
the molecule is irradiated with intense beams of laser photons
at exactly half the transition energy. The orthohydrogen
molecule also has an electric quadrupole moment which can be
coupled into by a strong magnetic field.

66
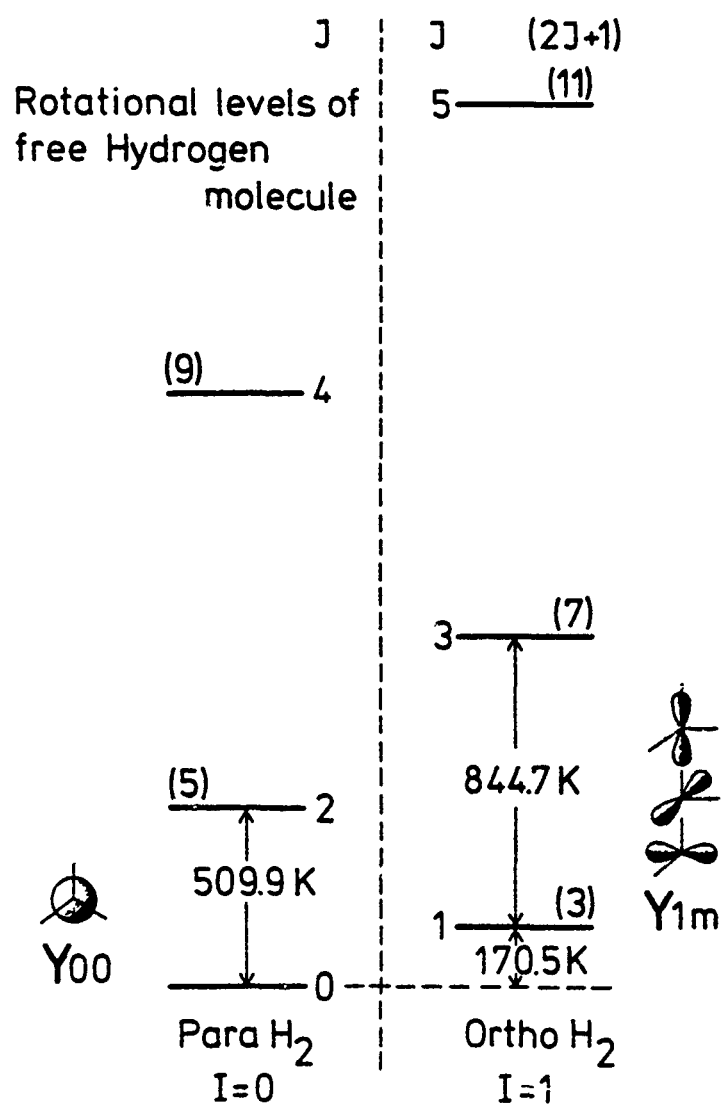
Fig. 4-3   Molecular hydrogen rotational energy levels.

67

Because of the small energy difference between the ortho and para states the orthohydrogen form is populated by thermal excitation at elevated temperatures. Hydrogen gas at room temperature consists of 75% orthohydrogen and 25% parahydrogen since the first ortho state with J=1 has three possible magnetic orientations (M=0,+1), while the para ground state with J=0 has only one. When the mixture is rapidly cooled and turned into a liquid or solid, this initial 3:1 mixture ratio is "frozen in".

In the liquid or solid state, the orthohydrogen slowly converts to parahydrogen, releasing energy. This energy must be removed from the hydrogen or the liquid or solid will rise in temperature and the hydrogen will evaporate. Since the conversion process requires that two orthohydrogen molecules approach each other closely enough that the magnetic field of one causes the other to flip, the absolute rate of conversion decreases as the density of the orthohydrogen molecules decrease, so the process is never really complete. The conversion rate in the solid state has been measured as 1.9%/hr or a 1/e decay time of about 2 days.[4.5]

At present, the method for producing pure parahydrogen from the mixed form is to pass the liquid hydrogen over a magnetic salt. The conversion process is quite rapid and very pure samples of parahydrogen can be prepared that way. It will not be possible to use matter in the form of magnetic salts to convert antiorthohydrogen to antiparahydrogen, so it will be necessary to find some other way to do it.

One approach is to prepare the antihydrogen initially in the para state by controlling the molecular formation using polarized beams of atoms and/or lasers combined with strong applied electric and magnetic fields. Another is to convert the orthohydrogen while it is still a gas using Raman or nonlinear two-photon transitions. If nothing else works, one could allow it to form as a low temperature mixed state solid and cool the solid electronically for the number of days needed for the conversion energy release to decrease to an amount that can be handled by infrared radiation to the cold walls of the containing vessel.

References:

[4.5]I.F. Silvera, "The solid molecular hydrogens in the condensed phase: Fundamentals and static properties," Rev. Mod. Phys. 32, 393-452 (1980).

SECTION 5

SLOWING AND COOLING OF ANTIHYDROGEN

As was pointed out in Section 4, antihydrogen can either be
produced in a trap from stationary antiprotons and positrons,
or it can be produced "on the fly" in the form of an
antihydrogen beam. Slowing and cooling of the antihydrogen
will be necessary if the process of producing the antihydrogen
introduces some excursions in its direction and velocity.

5.1 ELECTRONIC SLOWING AND COOLING OF ANTIHYDROGEN IONS

If the resulting antihydrogen is a positive hydrogen ion with
an extra positron (or a negative molecular hydrogen ion with a
missing positron), then it can be guided by magnetic fields
and slowed by radio frequency fields or electrostatic
gradients in a process that is essentially the inverse of the
well known electrostatic and rf accelerator techniques.

A beam of atomic hydrogen ions can also be cooled by the
stochastic cooling technique where fluctuations in the beam
current are sensed and used to create feedback signals. When
these signals are applied to the beam by an electromagnetic
"kicker," they damp the fluctuations in the beam and produce
cooling. As discussed in Section 2.4 this technique has been
successfully demonstrated with protons and antiprotons
(although not with negative atomic hydrogen ions) at CERN and
Fermilab.

An alternate cooling technique for a beam of antihydrogen ions
is to combine them with a beam of co-propagating positrons
that have been generated with a very low spread in velocity.
Those ions that are moving too fast will be decelerated by
collisions with the positrons, and those ions that are moving
too slowly will be accelerated. As discussed in Section 2.3,
cooling of protons and antiprotons has been successfully
demonstrated at CERN using electrons.

Although electron beams can be used to cool antiprotons, since
electrons and antiprotons do not annihilate each other,
electron beams cannot be used to cool antihydrogen positive
ions. The electrons will annihilate with the positrons in the
antihydrogen ion. For atomic antihydrogen ions it will be
necessary to use a cold beam of positrons. A cold beam of
positrons will be significantly harder to generate than a cold
beam of electrons.

69

5.2 LASER SLOWING AND COOLING OF NEUTRAL ANTIHYDROGEN

Beams of neutral atoms or molecules can be separated into different species, directed into different directions, slowed to zero velocity, cooled to millidegrees, and manipulated into traps solely with the use of photons, typically those from carefully tuned lasers. Thus, it is possible to handle neutral particles of antimatter such as antihydrogen atoms and molecules, without touching them with normal matter.

There are two types of pressure forces caused by the interaction of photons with neutral particles. One is called dipole resonance-radiation pressure and the other is called spontaneous resonance-radiation pressure. They both can exert significant forces on a neutral particle and often both effects are in operation at the same time in an experiment.

The dipole resonance-radiation pressure arises from the optically induced dipole field of the particle when it is placed in an optical field gradient. The induced dipole field is caused by <u>stimulated</u> light-scattering processes. The pressure is proportional to the <u>gradient</u> of the optical field and the forces are transverse to the direction of the laser beam. This force is dispersive in character because of the sign change of the atomic polarizability on either side of resonance.

The dipole forces become appreciable when the laser energy is concentrated in a region, for example by focusing it to create a region of high intensity. When the laser is tuned below the atomic resonance frequency of a particle, the particle tends to be pulled into the the high intensity region. When the laser is tuned above the atomic resonance, the particles tend to be expelled. Focal spot diameters of about 60 μm and a 30-fold increase of the on-axis atomic beam intensity have been obtained using the dipole resonance-radiation force.[5.1] For defocusing, the on-axis intensity can be reduced to less than 1% of its original value. Deflection angles of 5 mrad have also been demonstrated.[5.2]

The spontaneous resonance-radiation pressure arises from spontaneous light scattering as the neutral particle is irradiated by the photons from a laser beam. The force on the atom is along the direction of the laser beam and is proportional to the intensity of the beam. Spontaneous forces have been used to deflect atoms, cool atomic vapors, produce density gradients in a vapor, and separate isotopes. They cannot be used to make optical traps because of an optical equivalent to the Earnshaw theorem.[5.3] The basic mechanism by which the laser manipulation of neutral atoms by spontaneous forces takes place is shown in Figure 5-1.
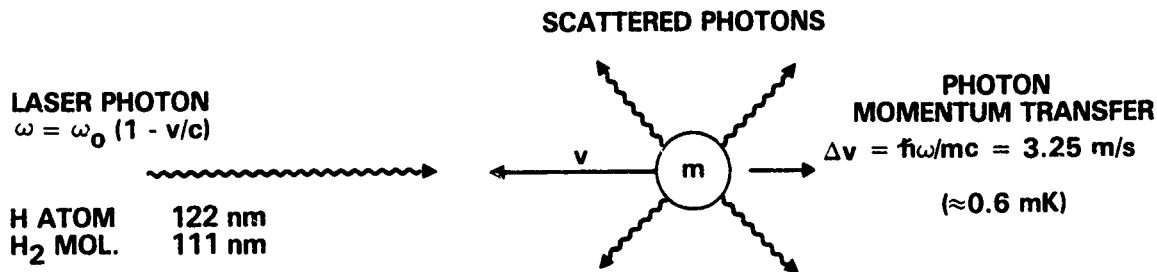
Fig. 5-1 Laser slowing of a neutral particle.

In Figure 5-1, a neutral particle of mass m is moving with a velocity v towards a laser beam. A typical velocity would be v=10,000 m/s. This corresponds to an energy for a hydrogen molecule with mass $m=3.34 \times 10^{-27}$ kg of:

5.1) $\qquad E = mv^2/2$

$\qquad\qquad = 1.67 \times 10^{-19}$ J

$\qquad\qquad = 12,100$ K

$\qquad\qquad = 1.04$ eV $\qquad$.

The neutral particles will generally be in their ground state. They can be excited to a higher state by a laser tuned to the resonance frequency corresponding to the transition to that state. The laser photons needed to excite the first excited states for atomic and molecular (anti)hydrogen are in the vacuum ultraviolet (VUV) region:

71

	Atomic (anti)hydrogen	Molecular (anti)hydrogen
λ =	121.6 nm	110.9 nm
f =	2.47×10^{15} Hz	2.72×10^{15} Hz
E = hf =	10.2 eV	11.2 eV

In order to be on resonance the laser must be tuned to a frequency f just below the atomic resonance f_o by an amount corresponding to the velocity v of the particle:

5.2) $$f = f_o(1-v/c) \quad .$$

The moving particle will then see the photon Doppler shifted upward into resonance and absorption will take place with a high probability. When the particle absorbs the photon and jumps to the excited state, the photon will impart momentum and energy to the particle, slowing it down by an amount:

5.3)   dv = hf/mc = 3.27 m/s for atomic (anti)hydrogen

$$= 1.80 \text{ m/s for molecular (anti)hydrogen}$$

Thus, it takes many thousands of absorptions of laser photons to slow a typical particle down to near zero speed. After each excitation process, the particle spontaneously re-emits a photon. The frequency of the photon is the natural resonance frequency so the emitted photon has more energy than the absorbed photon. The energy difference, of course, comes from the decrease in kinetic energy of the particle.

The spontaneously emitted photons impart a kick to the particle when they leave, but the spontaneous photons are emitted randomly in all directions. Thus, on the average, there is no net momentum transfer to the particle by the spontaneous emission process. The reradiation does, of course, contribute to a random walk of the momentum of the particle about its initial value, causing some transverse heating as the particle is slowed in the longitudinal direction.

In the usual particle beam, the particles have a range of energies and a single frequency laser will cause spontaneous radiation pressure only on those atoms with the right velocity. Also, as the atom is slowed, it will drop out of resonance with the laser. Thus, it is necessary to keep the laser and particle in tune with each other.

References:

[5.1] D.B. Pearson, R.R. Freeman, J.E. Bjorkholm, and A. Ashkin, "Focusing and defocusing of neutral atomic beams using resonance-radiation pressure," Appl. Phys. Lett. **36**, 99-101 (1980).

[5.2] J.E. Bjorkholm, R.R. Freeman, and D.B. Pearson, "Efficient transverse deflection of neutral atomic beams using spontaneous resonance-radiation pressure," Phys. Rev. **23A**, 491-497 (1981).

[5.3] A. Ashkin and J.P. Gordon, "Stability of radiation-pressure particle traps: an optical Earnshaw theorem," Optics Lett. **8**, 511-513 (1983).

5.2.1 Laser Chirp Tuning

One approach is to use a tunable laser and start with the laser frequency well below the natural frequency. Photons of this low frequency will interact with the high-speed particles in the beam, slowing them down. The frequency of the laser is now increased so that the slowed atoms <u>plus</u> those atoms with a lower initial velocity are both slowed. As the laser continues to "chirp" upward in frequency, it "sweeps" the velocity of all the particles downward. Thus, not only are all the particles in a beam slowed down, they are all slowed down to the same velocity.

An example of the potential efficiency of this process is shown in Figure 5-2. A Monte Carlo simulation was carried out calculating the effect of a chirped laser on a beam of sodium atoms.[5.4] The sodium atoms come from an oven with a wide spread in initial longitudinal and transverse velocity. As is shown in the "before cooling" and "after cooling" scatter diagrams, the chirped laser sweeps all the atoms but two down to zero longitudinal velocity. Thus, theoretically, this method of slowing atoms should be highly efficient.

This slowing technique has been recently demonstrated on a beam of sodium atoms.[5.5] A 10 mW laser was frequency swept with a broadband electro-optic phase modulator using a $LiTaO_3$ crystal in a traveling-wave configuration driven by 5 W of microwave power. The modulator chirped at a rate of about 1.5 GHz/s and put about 34% of the laser light into the down-shifted sideband.
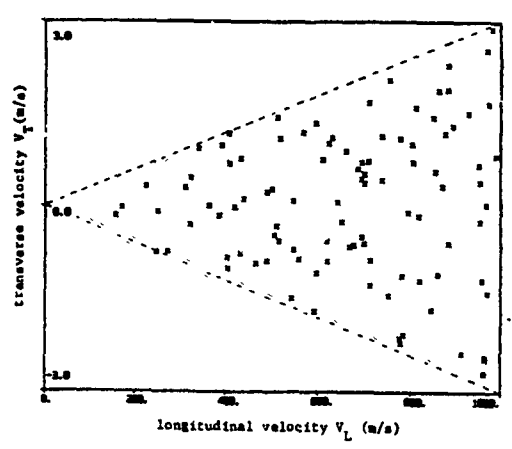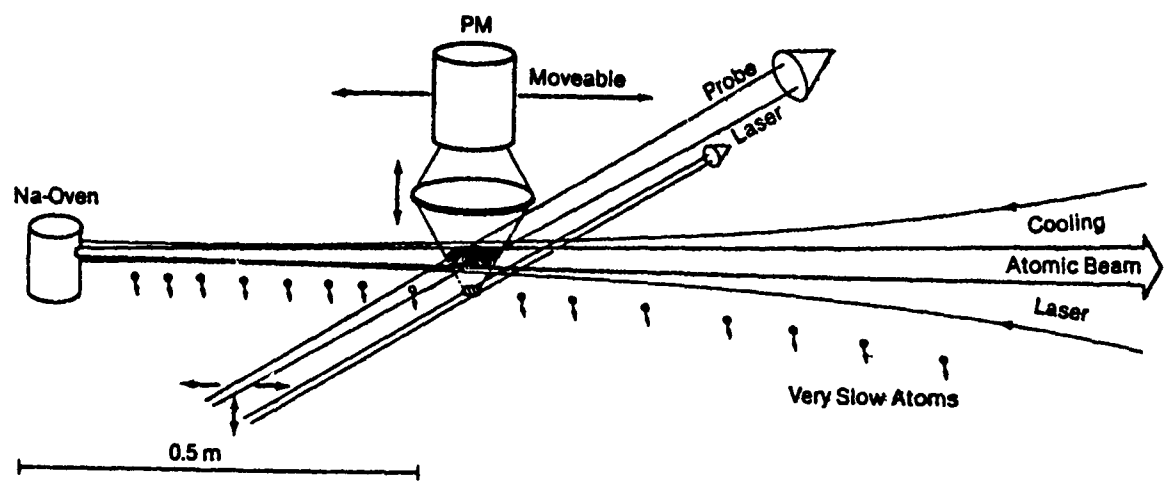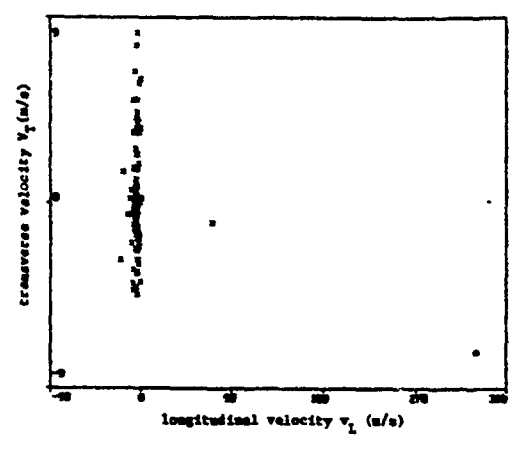
BEFORE COOLING   AFTER COOLING

Fig. 5-2 Particle slowing using chirped laser frequency.

74

The chirped laser light brought the sodium beam to a stop and converted it into a slowly expanding cloud of sodium atoms with a density of about 10^6 atoms/cc and an expansion velocity of about 6 m/s. This is equivalent to a kinetic temperature of about 50 mK. In one experiment, the laser was deliberately over-shifted in frequency and the atoms in the beam were actually brought to a stop, then pushed back in the opposite direction.

References:

[5.4]R. Blatt, W. Ertmer, and J.L. Hall, "Cooling of an atomic beam with frequency-sweep techniques," pp. 142-153, **Laser-Cooled and Trapped Atoms**, NBS SP-653, W.D. Phillips (editor) (1983).

[5.5]W. Ertmer, R. Blatt, J.L. Hall, and M. Zhu, "Laser manipulation of atomic beam velocities: Demonstration of stopped atoms and velocity reversal," Phys. Rev. Lett. **54**, 996-999 (1985).

5.2.2 Magnetic State Tuning

An alternate technique for lining up the atomic resonance of the moving atom with the laser frequency is to use the Zeeman shift to "tune" the separation of the atomic levels with a magnetic field.[5.6] As is shown in Figure 5-3, the sodium atoms from an oven were sent down the bore of a multi-layer solenoid with a tapered magnetic field. The length of the solenoid and strength of the field were chosen so that sodium atoms with an initial velocity of 1000 m/s could be stopped in about 1 m with a deceleration about half the theoretical maximum given by the spontaneous decay lifetime t_{sp}:

5.4)
$$a_{max} = hf/2mct_{sp}$$

When a given atom reaches a point in the solenoid where the combined Zeeman and Doppler shifts place it in resonance with the fixed frequency slowing laser, the atom absorbs photons and begins to decelerate. As long as the magnetic field does not change so rapidly that the rate of Zeeman shift change exceeds the possible rate of Doppler shift change, the atoms will stay in resonance, slowing continuously as they travel down the varying field of the solenoid. The cooling laser beam is arranged to be converging so as to cool the beam transversely as well as longitudinally.
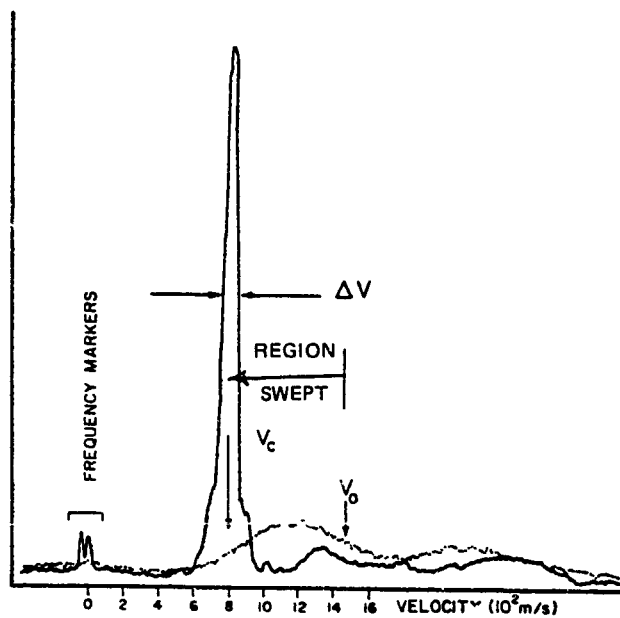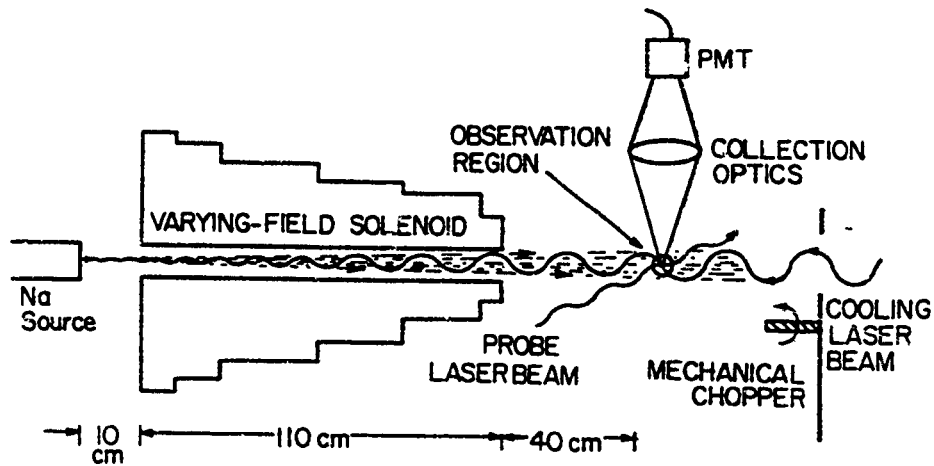
Fig. 5-3 Particle slowing using variable magnetic field.

In practice, instead of bringing the atoms to a halt inside the solenoid, the frequency of the laser is chosen so that the atoms are all brought to some low finite velocity. This is shown in Figure 5-3, where the atoms in the initial distribution with a broad peak from 800 to 1400 m/s were all swept to a common velocity of 800 m/s.

After the initial cooling has taken place, the slowly moving atoms now drift out of the end of the solenoid and are brought to a stop some distance away by a short decelerating pulse from the cooling laser. Recent results[5,7] using this double pulse technique have produced a cloud of free sodium atoms at rest in the laboratory with a density of about 10^5 atoms/cc and a velocity spread of about 15 m/s. This corresponds to a kinetic temperature of less than 100 mK.

References:

[5.6]W.D. Phillips, J.V. Prodan, and H.J. Metcalf, "Neutral atomic beam cooling experiments at NBS," pp. 1-8, **Laser—Cooled and Trapped Atoms**, NBS SP-653, W.D. Phillips (editor) (1983).

[5.7]J. Prodan, A. Migdall, W.D. Phillips, I. So, H. Metcalf, and J. Dalibard, "Stopping atoms with laser light," Phys. Rev. Lett. **54**, 992-995 (1985).

5.2.3 Pi-Pulse Laser Cooling of Neutral Antihydrogen

In the standard procedure for laser cooling of neutral atoms, the atoms are illuminated with counterpropagating laser beams which are tuned to the lower portion of the atomic resonance line. Cooling results from the transfer of momentum from the photons to the atoms during a resonant absorption-fluorescence reradiation event. The cooling rate for this process is limited by the natural decay of the atom due to spontaneous radiation.

The maximum cooling rate occurs at laser power levels which saturate the transition. An increase of laser power above saturation does not increase the cooling rate. The first photon absorbed will cause a transfer of momentum of -hk to the atom as the photon is absorbed, raising the atom to its excited state. A second photon, however, will cause simulated emission from the excited state back down to the ground state, and since the stimulated photon will be emitted in the direction of the original photon beam, the transfer of momentum to the atom will be +hk, cancelling out the original momentum transfer from the absorption.

This limitation on the cooling rate can be overcome by alternating the direction and detuning of two separate upward-stimulating and downward-stimulating photon beams. Thus, a net momentum transfer to the atom can be made to occur at transition rates greater than the spontaneous decay rate. This can be done by using an alternating series of oppositely directed and detuned population inverting (pi) pulses.

A pi-pulse is a short, intense pulse of radiation of electric field strength E and duration t_p such that when it interacts with an atom with a transition electrical dipole moment μ , the relationship[5.8]

$$5.5) \qquad 2t_p \left| \mu \cdot E / \hbar \right| = \pi$$

holds. As long as the pulse duration is much shorter than the natural spontaneous decay time of the atom, such a pi-pulse has a unit probability of causing a transition between two states whose energy difference matches the radiation frequency.

The use of pi-pulses for transverse deflection of an atomic beam is shown in Figure 5-4. The atomic beam is assumed to start in the ground state. First, an upward-going pi-pulse is absorbed, exciting the atom to the upper state and transferring an increment of momentum hk to the atom. Next, a downward-going pi-pulse passes by the excited atom. It is not absorbed, since the atom is in its excited state; instead, the pi-pulse stimulates the atom to emit a photon downward, resulting in another recoil momentum transfer of hk for a net momentum transfer of 2hk. Thus, a train of alternating N pi-pulses will result in a momentum transfer of Nhk to the atom.

By providing alternate pulses with the proper detuning, the pi-pulses can be used not only for atom deflection, but for atom cooling. The shaping of the pi-pulses in amplitude, frequency, and length[5.9], as well as the interval between alternate pi-pulses[5.10] are all variables that can optimize their use for a particular application. In some applications, the pi-pulses can be "reused" by reflecting them off stationary or moving mirrors[5.9] or by using optical cavities.

There is always some amount of spontaneous emission present during pi-pulse operation. If the length of the pi-pulse is short compared to the spontaneous emission decay time, the effect is small, but does put some limits on the cooling rate and limiting temperature that can be reached.[5.10]

COOLING RATE MUCH FASTER THAN CW RATE

Pi-PULSE DURATION T_p MUCH SHORTER THAN DECAY TIME T_2

$$T_p \ll T_2 = 2A^{-1}$$
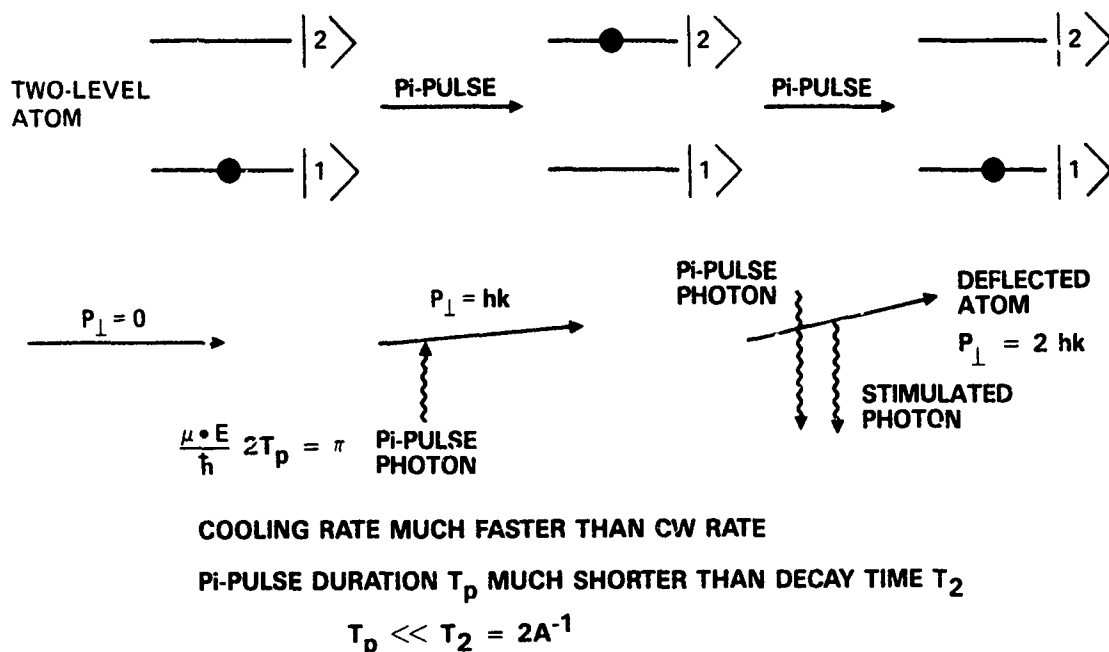
Fig. 5-4 Pi-pulse deflection and cooling of atoms.

In general, pi-pulse cooling of atomic hydrogen is orders of magnitude faster than standard laser cooling for beam temperatures of 100 K or greater, and becomes comparable to standard cooling for beam temperatures below 1 K.

Pi-pulse cooling will be especially useful in cooling of molecular hydrogen. Right above the ground state of molecular hydrogen there are a great number of rotational and vibrational states. Since the hydrogen molecule is homonuclear, only the even states are allowed. These states are metastable, since the transition to the ground state requires a change of two units of angular momentum and a photon only carries one unit.

The presence of these states makes it difficult to use standard laser cooling where the laser photon excites the molecule from the ground state to the first excited electronic state, but we depend upon spontaneous emission to return the mclecule to the ground state. The spontaneous emission could instead cause a transition to one of the metastable vibrational or rotational levels and the molecule would be out of resonance with the cooling laser and would no longer be cooled. With pi-pulse cooling, tne excited molecule will be "driven" to the ground state, bypassing the metastable rotational and vibrational states.

79

When pi-pulse cooling is used with atomic or molecular
hydrogen, the simple two-state picture is no longer rigorously
valid. For both atomic and molecular hydrogen, the two-state
picture is modified since there is a finite probability that a
hydrogen atom or molecule in its excited state can be excited
by a second pi-pulse into the continuum, causing the atom or
molecule to be ionized. Because the density of states in the
continuum is small, this rate will be small. How small is
unknown, however, and experiments are underway to measure this
double-photon ionization rate.[5.11]

References

[5.8]H. Friedman and A.D. Wilson, "Isotope separation by
radiation pressure of coherent pi pulses," Appl. Phys. Lett.
28, 270-273 (1976).

[5.9]I. Nebenzahl and A. Szöke, "Deflection of atomic beams by
resonance radiaion using stimulated emission," Appl. Phys.
Lett. **25**, 327-329 (1974)

[5.10]A.J. Palmer and J.F. Lam, "Radiation cooling with pi-
pulses," Paper WG1, Annual Meeting Optical Soc. Am., San Diego
(1984) [submitted to J. Opt. Soc. Am.].

[5.11]R.A. McFarlane, D.G. Steel, R.S. Turley, J.F. Lam, and
A.J. Palmer, "Experimental and theoretical studies of laser
cooling and emittance control of neutral beams," Hughes
Research, Malibu, California 90265, Annual report on contract
F49620-82-C-0004, AFOSR, Bolling AFB, DC 20332 (Ort 1984).

5.2.4 Optical Transitions in Atomic and Molecular Hydrogen.

Most of the research on cooling and trapping of neutral
particles has taken place with sodium atoms or other particles
with optical transitions in the visible region where tunable
lasers are available. In order to slow and cool antihydrogen
atoms and molecules, these techniques will need to be extended
into the vacuum ultraviolet (VUV) region of the spectrum.
What are needed are tunable sources of VUV photons suitable
for the transitions expected in atomic and molecular hydrogen.

Partial energy level diagrams for atomic and molecular
hydrogen are shown in Figure 5-5. The spectrum for atomic
hydrogen in Figure 5-5(a) is very simple since we are only
dealing with a single electron about a single proton. The
major transition that will be used for cooling is the Lyman
alpha line with a wavelength of 121.57 nm.

The spectrum for molecular hydrogen shown in Figure 5-5(b) is much more complicated since there are many excited states of the molecule as well as excited states in each of the two atoms making up the molecule.[5.12] The major transition that will be used for cooling is the 110.9 nm VUV line. At the bottom of Figure 5-5(b) are some of the vibrationally excited molecular states that exist just above the ground state of the electronic transitions. Each electronic transition state in the diagram has a similar set of vibrational as well as rotational states. Thus, unlike the hydrogen atom, the hydrogen molecule has a multiplicity of possible transitions and many of them have been observed to produce laser action.

The major laser lines for molecular hydrogen are in the ultraviolet and go from the first excited state to one of the vibrational levels in the ground state (B→X). This transition gives 39 lines that range from 127.95 nm (0-3)P(2) to 164.60 nm (4-11)P(4).[5.13] The C→X transition is also active with 11 lines observed ranging from 109.82 nm (0-2)R(0) to 125.20 nm (6-10)R(0).

There are also some short infrared lines observed that go from one excited state to another, such as the 11,159 nm transition from E→B. Thus, one source for the laser radiation needed for laser cooling of molecular hydrogen could come from molecular hydrogen lasers.[5.14] These will not be easily tunable, however, and it might ultimately be found better to use nonlinear optical mixing to produce a tunable coherent vacuum ultraviolet light source.

References

[5.12]G. Herzberg, **Molecula Spectra and Molecular Structure - I. Spectra of Diatomic Mo ecules**, 2nd Ed., D. Van Nostrand, Princeton, NJ (1950).

[5.13]M.J. Weber, Ed., **CRC Handbook of Laser Science and Technology**, pp. 282-286, CRC Press, Boca Raton, Florida.

[5.14]L.N. Breusova, I.N. Knyazev, V.G. Movshev, and T.B. Fogel'son, "Vacuum ultraviolet H$_2$ laser with a sealed gas-discharge cell," Kvant. Elektron. 6, 2458-2460 (1979) [English translation Sov. J. Quantum Elec. 9, 1452-1453 (1979)].
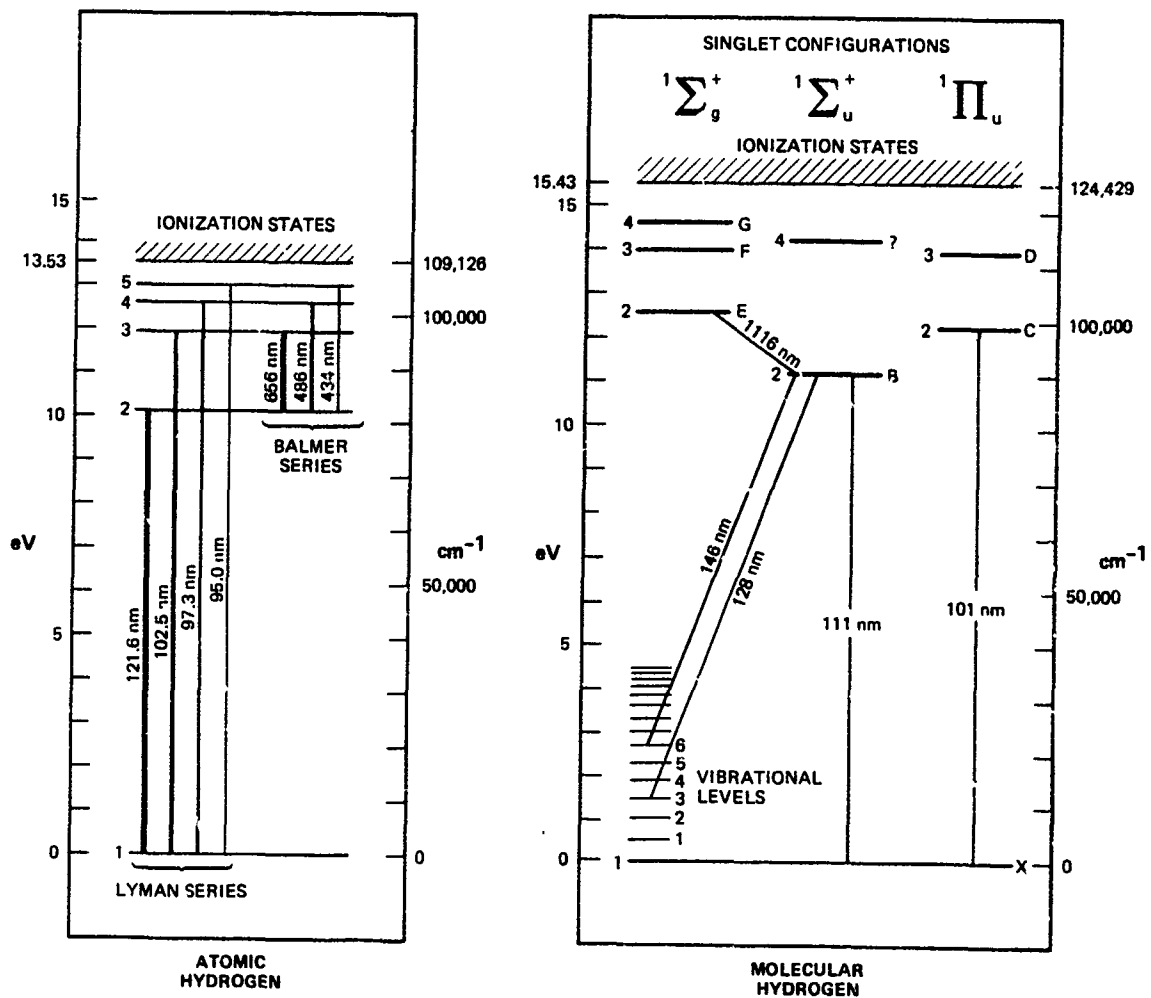
Fig. 5-5   Energy levels of atomic and molecular hydrogen.

5.2.5 Non-Laser Sources of Monochromatic Radiation

An alternate way to produce the desired tunable VUV photons
for the cooling and trapping of atomic and molecular hydrogen
is to manufacture the photons by nonlinear optical mixing.
The concept of optical doubling and tripling is well known in
laser technology.

In this procedure, a high intensity source of photons, such as
the 1064 nm infrared photons from a YAG laser, is focused
into an optically nonlinear crystal. The light intensities
drive the optical material far into their nonlinear range and
frequency doubling takes place with high efficiency, producing
one 532 nm wavelength photon out for every two 1064 nm photons
put in. With proper attention paid to choosing the crystal
axis so that the two colors of light have the same velocity in
the crystal, the efficiency of conversion can approach 100%.

By using a more general version of nonlinear mixing called
four-wave mixing, it is possible to mix two or more photons to
produce an output photon with an energy that is the sum of the
input photon frequencies. The nonlinear material does not
have to be a crystal, but can be any nonlinear optical
phenomena including a convenient optical transition in some
atom or molecule that is near the desired sum frequency.

In Figure 5-6(a) is shown one method for making a tunable
Lyman alpha source of narrow band, spatially coherent
photons.[5.15] It is not a laser, since no stimulated emission
is taking place. Two tunable dye lasers make photons at the
frequencies of 545.37 nm and 625.52 nm. These low-power
signals are then amplified by dye laser amplifiers pumped by
532 nm photons from a frequency doubled 1064 nm YAG laser.
The 625.52 nm photons are frequency doubled to 312.76 nm by a
nonlinear crystal and sent to a cell of mercury vapor which
acts as the last nonlinear medium.

As is shown in Figure 5-6(b), mercury has a convenient optical
transition line that allows two of the 312.76 nm photons and
one 545.37 nm photon to add to produce one 121.57 nm photon.
This photon is tunable around the atomic hydrogen Lyman alpha
transition frequency since the original dye laser signal
sources are tunable. A similar technique can be used to
produce the 110.9 nm photons needed for cooling and trapping
of molecular hydrogen.

References:

[5.15]D.G. Steel, Hughes Research Laboratories, Malibu,
California, personal communication.

(a)

POWER LIMITED
BY TWO-PHOTON
SATURATION
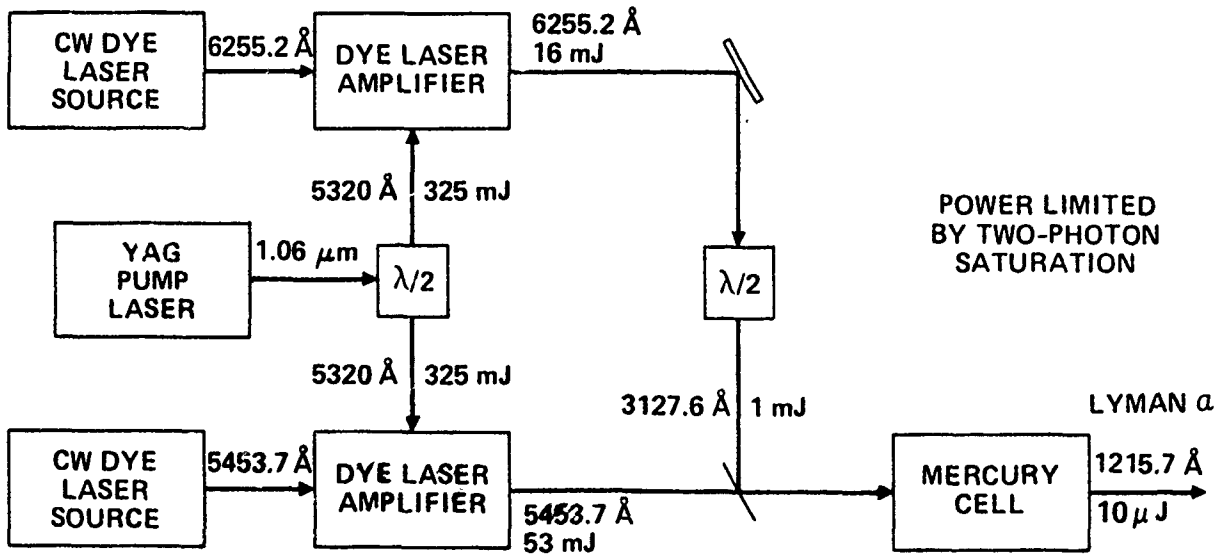
(b)
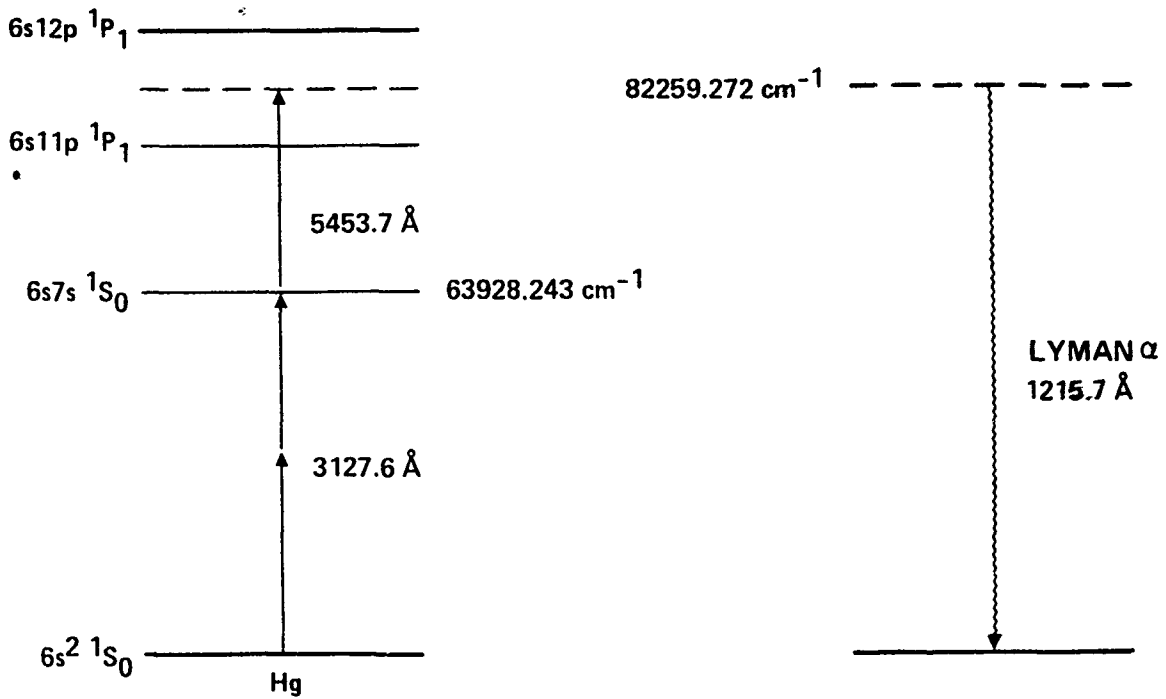
Fig. 5-6   Tunable Lyman alpha source using four-wave mixing.

84

SECTION 6

TRAPPING AND STORING ANTIHYDROGEN

6.1 TRAPPING OF ATOMIC ANTIHYDROGEN

The hydrogen atom consists of a proton and an orbiting electron. Both the proton and the electron have a magnetic moment and can interact with an applied magnetic field. The proton magnetic moment or nuclear magneton is given by:

6.1) $$\mu_n = eh/4\pi Mc = 5.05 \times 10^{-24} \text{ erg/G} \quad \text{(cgs)}$$

$$= eh/4\pi M = 5.05 \times 10^{-27} \text{ J/T} \quad \text{(MKS)}$$

where e is the electronic charge, h is Planck's constant, c is the speed of light, and M is the mass of the proton.

The electron mass m is 1836 times smaller than the proton mass, while the angular momentum and charge are the same. Thus the electron magnetic moment or Bohr magneton is 1836 times larger than the nuclear magneton:

6.2) $$\mu_e = eh/4\pi mc = 0.927 \times 10^{-20} \text{ erg/G} \quad \text{(cgs)}$$

$$= eh/4\pi m = 0.927 \times 10^{-23} \text{ J/T} \quad \text{(MKS)}$$

When a hydrogen atom is put into a magnetic field, the magnetic moments can align with the magnetic field either in the parallel (low energy) direction or antiparallel (high energy) direction and are said to be polarized. Those atoms with both magnetic moments in the same direction are called doubly polarized hydrogen.[6.1]

Atoms in the lower energy states are drawn into the magnetic field by the magnetic field gradients, while atoms in the higher energy states are repelled. The magnetic trap is not stable. The axial gradient in the magnetic field holds the atoms along the axial direction, but the atoms can drift radially across the magnetic field lines and strike the walls. A wall coating of superfluid liquid helium is used to reflect the polarized atoms back into the trap without flipping their spins.[6.1]

85

A collection of cold doubly polarized atoms in a magnetic
field will have a tendency to stay in the atomic form since
the electrons have the same spin orientation. If the atoms
attempted to form a molecule with the two electrons in the
ground state, the Pauli exclusion principal would be violated.
If the two atoms are kept cold, they cannot form the ground
state and do not have enough energy to form in an excited
molecular state, and so remain as separate atoms.

The maximum density of doubly spin-polarized atomic hydrogen
achieved to date has been 2×10^{18} atoms/cc in a very small
"bubble" in liquid helium at 0.7 K.[6.2] Densities of this
magnitude would be of interest for storing atomic antihydrogen
since 12 mg of spin-stabilized antihydrogen could be stored in
a 10 cm sphere. Unfortunately, the lifetimes at these
densities were only a few minutes and were limited by wall
losses and three-body dipolar recombination processes.

Other experimenters have demonstrated confinement times of
4 hr for densities of 8×10^{16} atoms/cc with a 10 T magnetic
field and a temperature of 0.3 K. The lifetime increases
dramatically with increasing magnetic field since the atoms
are kept away from the walls. The lifetime also increases
with decreasing density, which lowers the probability of a
three-body recombination.[6.3] If the lifetime problems could
be solved, even a density of 10^{15} atoms/cc would be
interesting for antiproton annihilation propulsion, since
10 mg of antihydrogen could be stored in a one-meter sphere.

The need for normal matter walls made of helium to complete
the trap makes the present trapping methods unusable for
antimatter. New ideas for magnetic traps to contain spin
polarized atomic antihydrogen are needed. Since static fields
are not stable, some kind of dynamic field arrangement needs
to be invented. It is conceivable that some kind of
alternating magnetic field configuration using an analogy to
the Paul rf electrostatic trap might work.

One configuration proposed for the trapping of spin polarized
atoms is the hybrid laser-magnet trap.[6.4] As is shown in
Figure 6-1, a strong magnetic field provides axial trapping of
the spin polarized atoms, while the radial trapping is
provided by a laser cavity operated in the TEM_{01}^{*} mode. This
mode is circular with a null in the center and most of the
radiation is confined to a cylinder. It is a natural mode of
some laser cavities. If the laser is tuned slightly to the
"blue" of the atomic resonance frequency, the atom will
experience a relatively strong "transverse dipole" force
pushing it into the central region of lower light intensity.
With an 11 T (110 kG) magnet and a highly reflecting cavity to
store the light energy, the "depth" of the trap is estimated
to be around 7 K.[6.4]
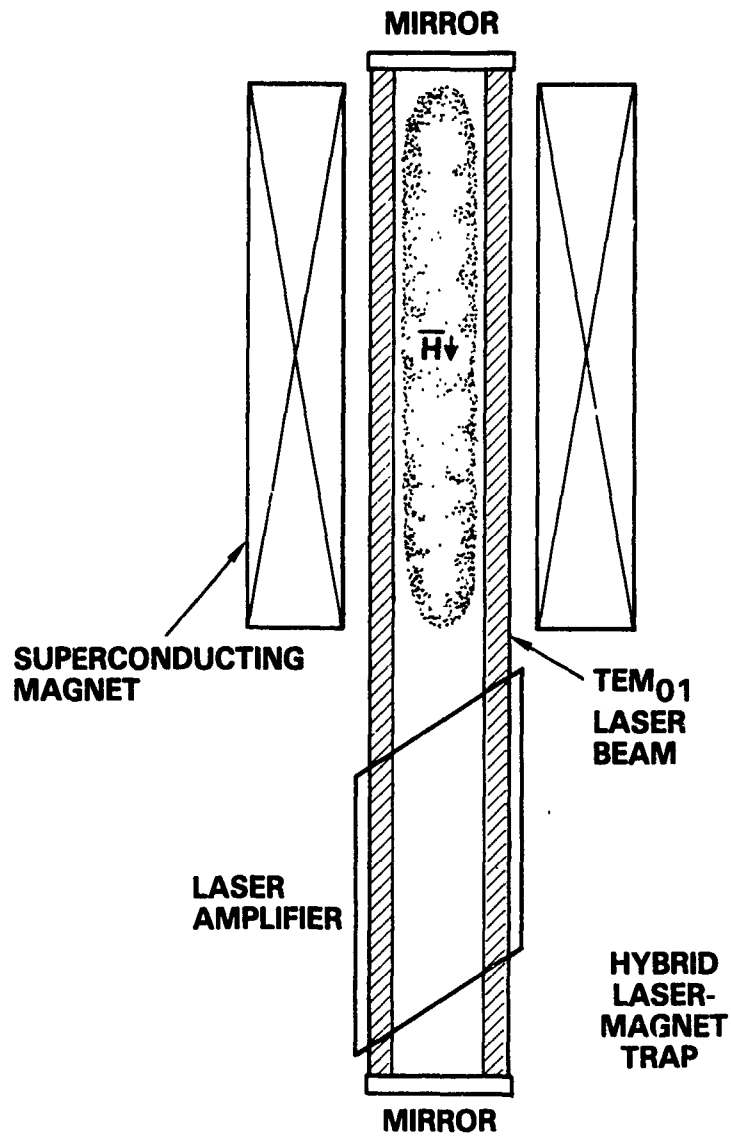
Fig. 6-1 <u>Laser-magnet trap for polarized antihydrogen atoms.</u>

87

References:

6.1 I.F. Silvera and J. Walraven, "The stabilization of atomic hydrogen," Scientific Am. **246**, 66-74 (January 1982).

6.2 R. Sprik, J.T.M. Walraven, and I.F. Silvera, "Compression of spin-polarized hydrogen to high density," Phys. Rev. Lett. **51**, 479-482 (1983).

6.3 H.F. Hess, D.A. Bell, G.P. Kochanski, R.W. Cline, D. Kleppner, and T.J. Greytak, "Observation of three-body recombination in spin-polarized hydrogen," Phys. Rev. Lett. **51**, 483-486 (1983).

6.4 W.C. Stwalley, "A hybrid laser-magnet trap for spin-polarized atoms," pp. 95-102, **Laser Cooled and Trapped Atoms,** W.D. Phillips, ed., National Bureau of Standards SP-653 (1983).

6.2 TRAPPING OF ANTIHYDROGEN

Lasers can be used not only for slowing, cooling, and stopping of particles, but for trapping them. One example of an optical trap is shown in Figure 6-2. This trap uses both the scattering force due to spontaneous emission and the ponderomotive force from the coupling of the induced atomic dipole to the optical field gradient.

In Figure 6-2 two opposing TEM_{oo} mode cw laser beams are focused at the two focal points F_1 and F_2 located symmetrically about the trapping point E.[6.5] The beams grow in radius from w_o from the waist at the focal points to 13 w_o in going 1 cm from the focal point to the trapping point. Each beam is tuned some 50 times the natural linewidth below the resonance frequency. For sodium atoms and 590 nm yellow light, w_o=12 μm and the cw laser power is 200 mW.

The trapping point at E is a point of stable equilibrium since any displacement of an atom from E results in a restoring force. There is an axial spontaneous scattering restoring force due to the oppositely directed laser beams and a radial restoring dipole force due to the radial optical field gradient.

To trap the atoms after they have entered the trap requires damping. Damping due to the Doppler shift occurs when the laser is tuned below resonance since the moving atoms interact more strongly with the opposing beam.
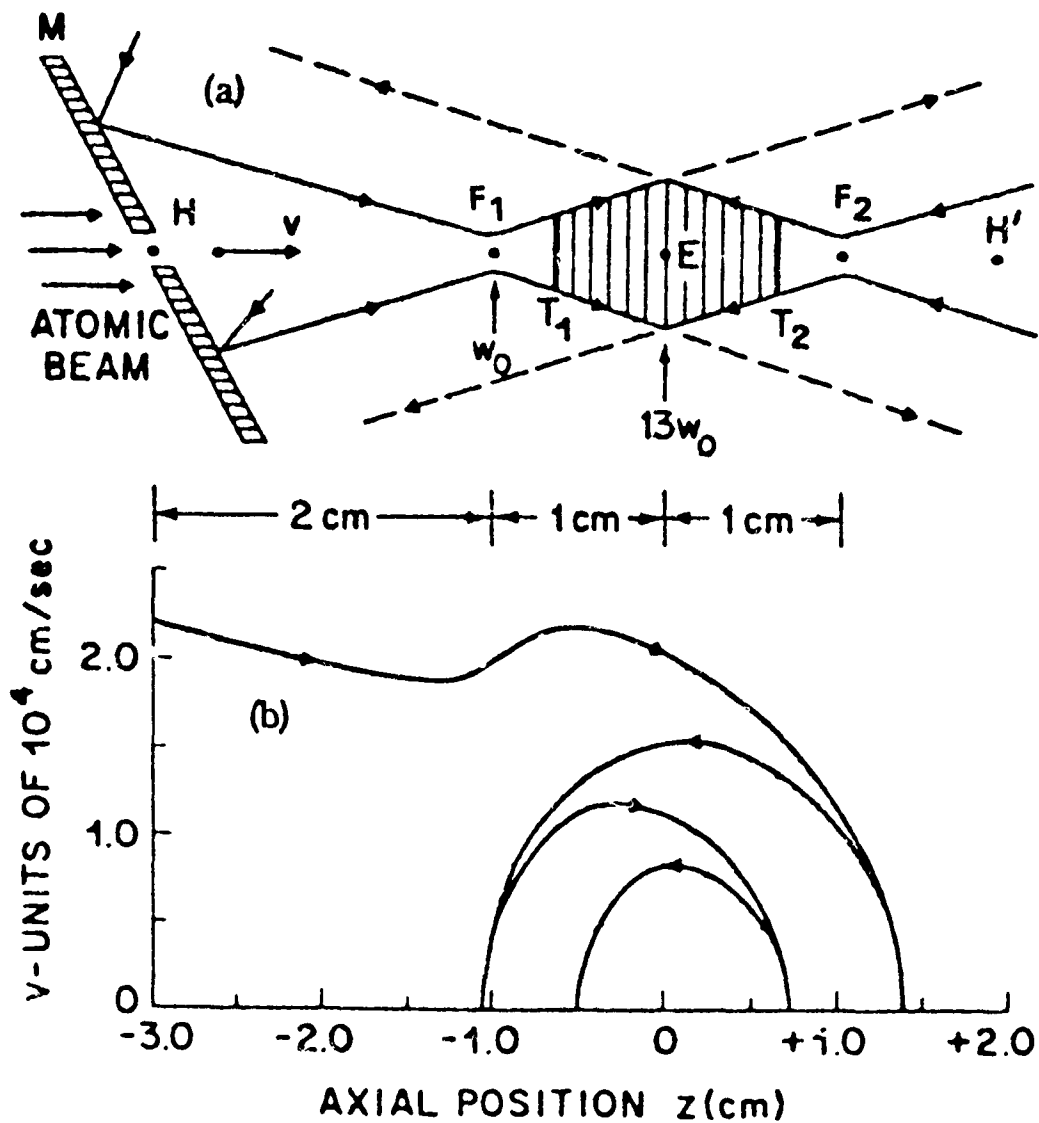
Fig. 6-2 Trapping of atoms by resonance radiation pressure.

The atoms are inserted into the trap through the hole H in the mirror M. An atom entering the trap with a velocity v=200 m/s stops at a point some 4 mm beyond F_2. It then rebounds and executes a damped oscillation about E, cooling off as it is trapped. Several cycles are shown in Figure 6-2(b).

The original optical trap design was later analyzed in more detail.[6.6] It was found that the concept produces rapid damping of fast atoms injected into the trap, but slow atoms held in these traps are not optimally damped because of large detuning. It was then found that the addition of a damping beam decreases the trapping force, while the presence of a trapping beam decreases the damping force. In addition, the trapping beam causes an optical Stark shift of the atomic resonance, which further complicates the damping process.

Despite these problems, an optical trap using optimally tuned trapping and damping beams was predicted to result in traps capable of confining sodium atoms at temperatures as low as 0.1 mK in optical potential well as deep as 0.1 meV, within a dimension as small as $\lambda/35$, with negligible probability of escape by tunneling or thermal excitation.

There are a number of methods to use a multiplicity of damping and trapping beams to improve the trap. One proposal is to alternate the cooling and trapping beams in time so that they do not conflict with each other. Another is to have the cooling beam and the trapping beam at different frequencies and have them cause transitions between different states. A third is to use right- and left-handed circularly polarized light for a transition from a J=0 state to the M=+1 and M=-1 levels of a J=1 state.[6.6] Some of these concepts may be applicable to the problem of trapping of hydrogen atoms and molecules.

Estimates have been made[6.7] that by using these traps, up to 3×10^7 atoms can be cooled down to less than a millidegree Kelvin and be confined to a dimension as small as $\lambda/35$. At these temperatures the gas density approaches that of a solid and the atoms may convert into the condensed phase. For sodium atoms, the condensed phase is a metal and the trapping mechanism no longer will operate. For antihydrogen the condensed phase will be a transparent dielectric material and the laser trapping will still be operative, although the details of the trapping mechanism will be different.

A neutral highly transparent dielectric particle has been trapped, levitated, and manipulated using an alternating light beam approach.[6.8] The actual particle used in the experiments was a sphere of silicon oil 9 μm diameter and weighing about 0.6 ng. The damping was supplied by air. The particle was suspended and trapped by an optical trap similar to that shown in Figure 6-2, but as is shown in Figure 6-3, the directions of the trapping beams were reversed periodically.

There is a direct analogy between the dc trap of Figure 6-2 and the ac trap of Figure 6-3, and the dc Penning ion trap in Figure 2-3 and the ac Paul ion trap in Figure 4-1. In the ac traps, the dynamic stability is governed by the Mathieu equations and avoids the consequences of the Earnshaw stability theorem for static field traps.

The alternating field trap has only been demonstrated on air-damped silicon oil drops. The technique should be applicable, however, not only to macroscopic Rayleigh-sized particles, but to neutral atoms and molecules. For atoms, large-volume traps with dimensions of 1 cc are predicted with greatly reduced optical cooling problems and well depths as great at 1 K.[6.8]

Since liquid and solid antihydrogen are transparent dielectric materials, it is quite likely that these types of optical traps can not only be used to cool and compress the antihydrogen molecular vapor to densities approaching that of the condensed phase, but also maintain the trapping action on the particles after the condensation has taken place.

References

[6.5]A. Ashkin, "Trapping of atoms by resonance radiation pressure," Phys. Rev. Lett. **40**, 729-732 (1978).

[6.6]A. Ashkin and J.P. Gordon, "Cooling and trapping of atoms by resonance radiation pressure," Optics Lett. **4**, 161-163 (1979).

[6.7]J. Dalibard, S. Reynaud, and C. Cohen-Tannoudji, "Proposals of stable optical traps for neutral atoms," Optics Comm. **47**, 395-399 (1983).

[6.8]A. Askin and J.M. Dziedzic, "Observation of radiation-pressure trapping of particles by alternating light beams," Phys. Rev. Lett. **54**, 1245-1248 (1985).
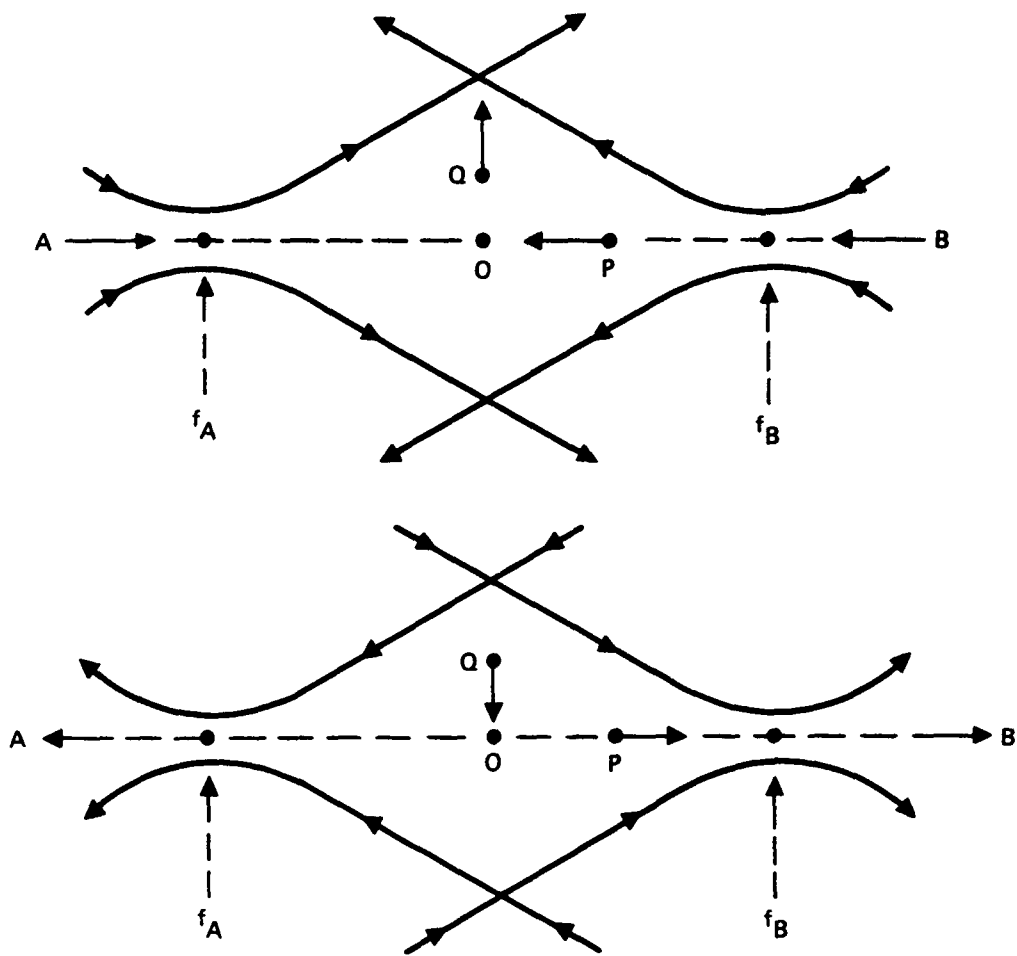
Fig. 6-3 <u>Geometry of alternating-beam optical trap</u>.

92

6.3 CONVERSION OF ANTIHYDROGEN GAS TO ICE

Trapping the parahydrogen gas will leave the molecules at very low kinetic energies, equivalent to millikelvin or microkelvin. The next step is to convert the gas into either amorphous or crystalline ice by inverse sublimation. Research is needed on techniques to induce the process of nucleation directly from the gas without involving a wall.

The experiments would investigate the effect of various electromagnetic fields on the nucleation process, including the precursor phase where two, three, and multiple-molecule collisions produce the dendritic "snowflake" clusters that precede the formation of the crystalline solid. It may be that "shock" waves of density fluctuations set up by the laser trapping fields are sufficient to induce the nucleation. Molecular hydrogen ions and specially selected excited states may aid in the nucleation and growth of these clusters into crystals. The rate of crystal growth should be measured as a function of the temperature and effective pressure of the trapped molecular gas.

Since the process of forming the solid releases energy, it will also be necessary to investigate methods for extracting the heat from the solid. A straightforward approach is to allow the solid to evaporate a molecule containing the energy from a number of fusions, then cool the molecule with the laser slowing and cooling process. The cooled molecule would then be directed back into the cold gas. Alternate techniques could conceivably use active laser or magnetic "cooling" techniques that work through a nonlinear optical or magnetic property of the parahydrogen solid. All of the research should concentrate on techniques that leave the solid at temperatures of 1 K or lower.

It is important to remember that, as shown in Figure 6-4, there are many paths that lead from the generation of an antiproton beam to the generation of a frozen ball of molecular antihydrogen. The antiprotons can be trapped in a Paul trap, turned into antihydrogen atoms by the addition of positrons, trapped with Lyman alpha laser beams, converted into magnetic field-trapped antihydrogen molecules, tickled into forming an iceball by positron beams and laser beams, then grown into a charged microcrystal.

Alternatively, the antiproton beam can be converted into an atomic antihydrogen beam, then a molecular antihydrogen beam, all on the fly; then the antihydrogen molecules are slowed, cooled, trapped, and turned into ice with VUV laser beams. A few extra positrons will prepare the crystal for levitation in an electrostatic trap.

93
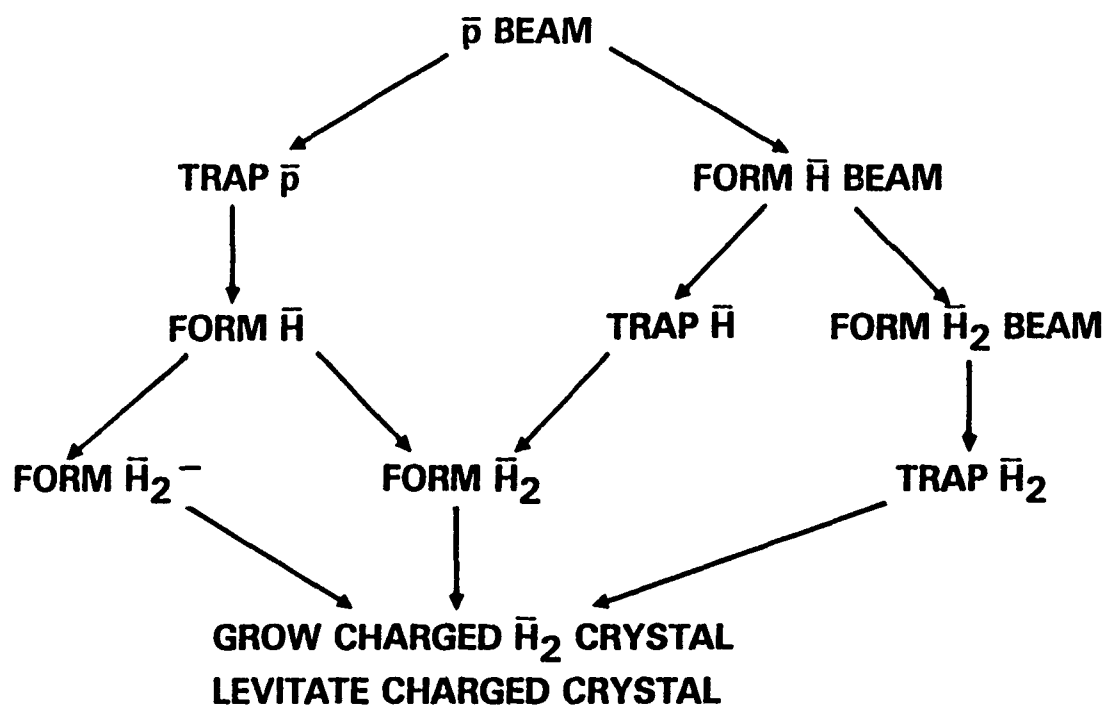
Fig. 6-4 Many paths from antiprotons to antihydrogen ice.

6.4 LEVITATION OF ANTIHYDROGEN ICE

The techniques for trapping parahydrogen gas and the subsequent formation of solid parahydrogen may turn out t. be relatively simple, or they may require complex ultrahigh vacuum chambers with many ports and windows, high-power lasers, and heavy electric or magnetic field generators. Once the small microcrystals or larger ice balls of parahydrogen ice are formed, however, they can be transferred to a compact lightweight vacuum system that uses simple magnetic or electric traps for levitation.

The magnetic susceptibility of solid hydrogen depends upon its state. The orthohydrogen form has both of the protons in its nucleus with their magnetic moments pointing in the same direction, so it has a positive magnetic moment. The parahydrogen form has its two protons and its two electrons with their spins oriented in opposite directions so the particle spins cancel out. The only magnetic susceptibility left comes from the "currents" caused by orbital motion of the electrons around the nucleus.

94

As a magnetic field is applied to these "superconducting" currents, the current tends to increase, driving the impressed magnetic field out of the molecule. This gives the parahydrogen molecule a negative or diamagnetic susceptibility. Diamagnetic substances are attracted to the minimum in a magnetic field. Even with purely static magnetic field, the configuration is stable, unlike levitation systems based on repulsion of paramagnetic or ferromagnetic materials, which seek a field maximum and are unstable.

The magnetic susceptibility of solid parahydrogen has not yet been measured.[6.9] The theoretical prediction of the magnetic susceptibility of a one-gram formula weight of molecular hydrogen is -3.98×10^{-6} cgs units.[6.10] This can be compared to a value of -6.0×10^{-6} cgs for carbon atoms in the form of graphite.

There have been many demonstrations of the stable levitation of many grams of graphite in the gravity field of earth using nonsuperconducting magnets. In one specific example, a ring shaped rotor weighing 3.843 g and containing only 0.933 g of graphite was levitated in the 0.2 cm gap between two opposed ring shaped permanent magnets with a magnetic field of 11,600 G (1.16 T).[6.11]

One straightforward configuration for a magnetic trap that would be compatible with a cryogenically cooled vacuum chamber would be a pair of superconducting rings carrying opposed persistent currents as shown in Figure 6-5.

It is recommended that a research project be started on the magnetic properties of hydrogen. This research project would measure the magnetic susceptibility of parahydrogen at low temperatures as a function of temperature, particle size, and orthohydrogen contamination. The next step would be to demonstrate that the magnetic field gradients from persistent currents in a set of superconducting coils are sufficiently strong to levitate the parahydrogen at moderately high acceleration levels.

This research is not path critical, since there exists a known technique, active electrostatic levitation, that can support a charged ball of low density parahydrogen with ease at high acceleration levels. The passive magnetic levitation technique would be preferred, however, since it would be safer than any active technique, as well as making the storage container extremely simple, compact, and independent of electric power.

95

SUPERCONDUCTING RINGS WITH PERSISTENT CURRENT

DIAMAGNETIC BALL OF ANTIHYDROGEN

DIAMAGNETICS ATTRACTED TO FIELD MINIMUM
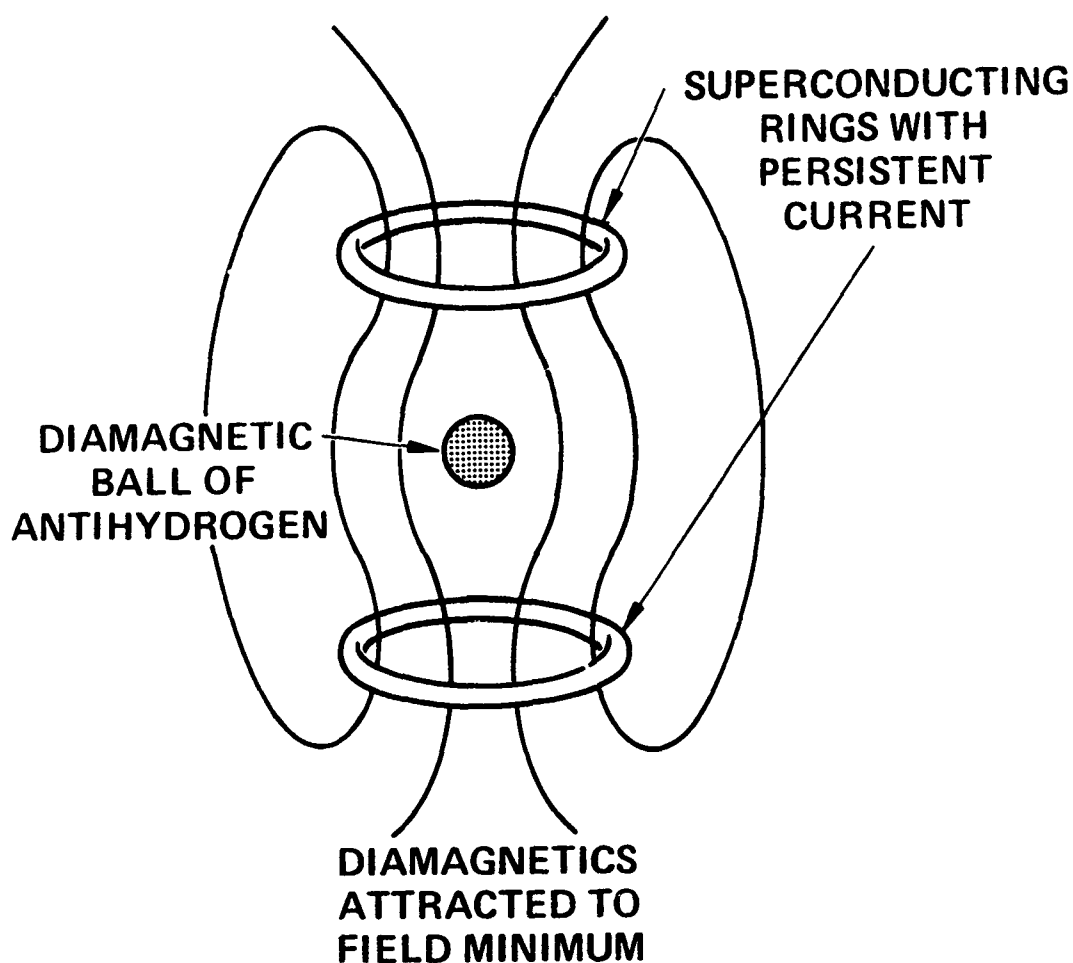
Fig. 6-5 Magnetostatic trap for antiparahydrogen ice.

An alternate method of levitating antihydrogen ice is to use electrostatic levitation. The ice particles need to be slightly charged, either positive or negative. This can be accomplished either by charging the ice positive by addition of extra positrons or charging it negative by annihilating some of the positrons with electrons from an electron gun or driving off the positrons with ultraviolet light.

The well known Earnshaw Theorem states: "A charged body placed in an electric field of force cannot rest in stable equilibrium under the influence of the electric forces alone."[6.12] This means that an electric levitation system has to have an active means of maintaining sufficient charge on the antihydrogen ice particles, as well as an active position control loop to maintain the particles in the center of the trap.

If the direction of acceleration is constant, a charged ball can be levitated between electrically charged plates as is shown in Figure 6-6, provided that the plates have a slight curvature. Such a trap has been constructed at the Jet Propulsion Laboratory[6.13] and has levitated a 20-mg ball of water ice in the one gee field of the earth. The density of water at 1.0 g/cc is 13 times that of antihydrogen ice at 0.0763 g/cc. Thus, the present JPL trap with its present voltage levels could levitate a 1.5-mg ball of antihydrogen ice of the same size, surface area, and surface charge at a vehicle acceleration of 13 gees.

References:

[6.9]N.A. Olien, NBS, personal communication (1984).

[6.10]R.C. Weast, **CRC Handbook of Chemistry and Physics**, 63rd Edition, p. E-119, CRC Press (1983).

[6.11]R.D. Waldron, "Diamagnetic levitation using pyrolytic graphite," Rev. Sci. Instr. 37, 29-34 (1966).

[6.12]J. Jeans, Sir, **The Mathematical Theory of Electricity and Magnetism**, Cambridge Press, UK (1925).

[6.13]W-K Rhim, M.M. Saffren, and D.D. Elleman, "Development electrostatic levitator at JPL," pp. 115-119, **Material Processing in the Reduced Gravity Environment of Space**, G.E. Rindone, ed., Elsevier (1982).
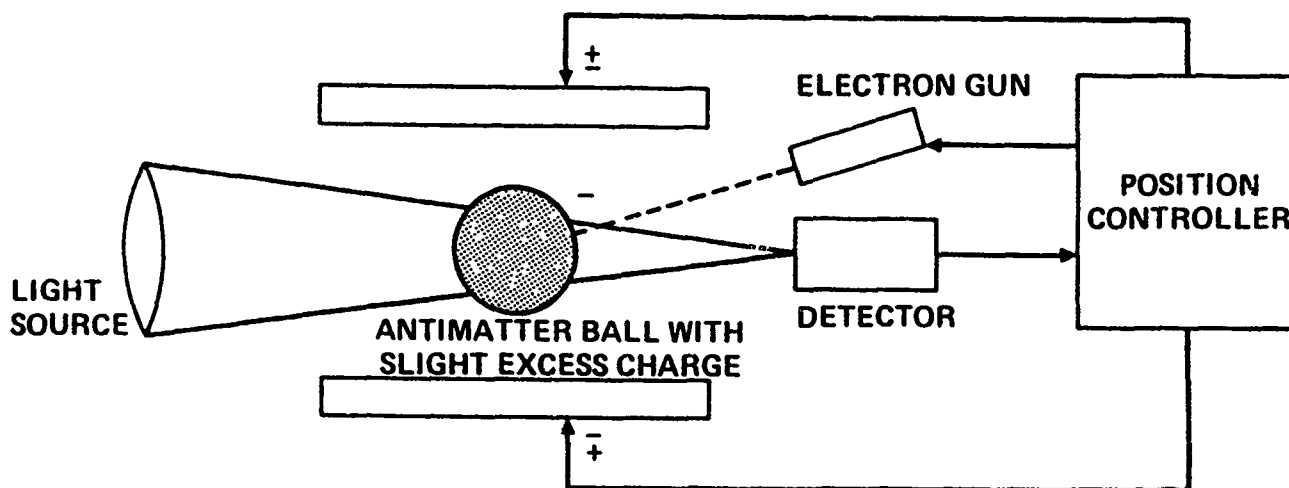
Fig. 6-6   Active electric levitation of antihydrogen ice.

6.5 ANTIHYDROGEN ICE BALL ENERGY BALANCE

As has been shown in previous sections, there are a number of active techniques to remove energy from antihydrogen so that it will turn into a cold vapor, condense, and form antihydrogen ice. Since laser cooling, for instance, will leave the antihydrogen at a temperature well below a millidegree, the antihydrogen ice will start out cold.

In this section we will determine whether the initially cold antihydrogen ice can be kept cold by passive cooling techniques despite unavoidable heating due to annihilation processes. For example, antihydrogen molecules could evaporate off the ice ball and drift over to annihilate on the walls of the chamber.

Then there could be hydrogen molecules or other normal molecules knocked off the walls of the vacuum chamber by those annihilation processes or cosmic rays that would drift across the vacuum chamber to annihilate on the surface of the antihydrogen ice ball.

6.5.1 Infrared Radiation Passive Cooling

The passive cooling technique we will use for this analysis is infrared radiation to the walls of the cold containment chamber as is shown in Figure 6-7. The amount of thermal power P radiated from an object of temperature T, area A, and emissivity E to the surroundings at temperature t and emissivity e is given by the relation:

$$6.3) \quad P = \sigma A(E\ T^4 - e\ t^4)$$

where the Stefan-Boltzmann constant is

$$6.4) \quad \sigma = 5.67 \times 10^{-8}\ W/m^2 \cdot K^4$$

At the temperatures we will be discussing, the peak of the infrared radiation is in the very long infrared or short microwave region. At a temperature of 2 K, for example, the peak of the infrared radiation is at 1.4 mm wavelength. Very little is known about the emissive properties of materials in this region.
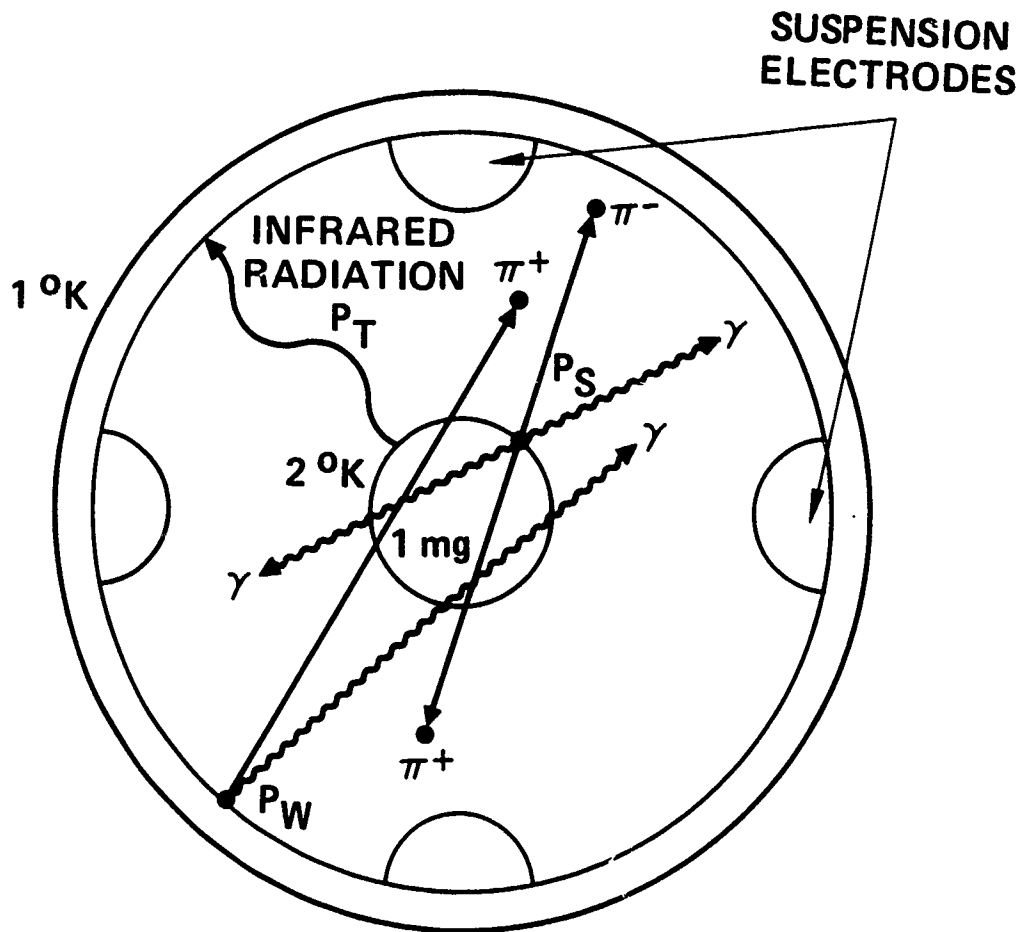
Fig. 6-7   Energy balance for antihydrogen ice ball.

99

Also, the iceball and the vacuum cavity are comparable in size to the infrared wavelengths, which will complicate the interaction. Obviously, further research is needed in this area. For now, we will assume that the infrared radiation power is given by Equation 6.3.

If we assume a 1-mg ball of antihydrogen ice at a density of $p=0.08$ gm/cc, then the radius of the ball is $r=0.15$ cm and the surface area is $A=0.28$ cm^2. The emissivity of hydrogen ice in the long infrared is unknown, so we will assume a grey body with $E=0.5$, and that the walls of the chamber can be made black with an emissivity of $e=1$. The vacuum chamber will be assumed to be 2 cm in radius.

To get maximum cooling power, the antihydrogen iceball should be as warm as possible and the walls of the chamber should be as cold as possible. As is shown in the section on the properties of hydrogen ice in Appendix A,[6.14] the vapor pressure of solid hydrogen drops precipitously below 4 K. We will choose a tentative equilibrium temperature for the antihydrogen ice of 2 K. At this temperature, the vapor pressure is only 4×10^{-18} Torr or roughly 0.1 atom/cc.

The velocity of the evaporated molecules at the sublimation temperature of 14 K is 340 m/sec. This gives a flux of 3400 mol/cm^2·s, which means that 950 antihydrogen molecules per second leave the 0.28 cm^2 surface area of the antihydrogen iceball to strike the walls of the chamber and annihilate. The temperature of the walls of the chamber has to be less than the temperature of the ice ball to obtain infrared radiation cooling. To make it easier on the cryogenic cooling system (which will be a magnetic dilution or paramagnetic refrigerator), we will assume a wall temperature of 1 K.

The major outgassing contaminant in vacuum systems is hydrogen. The vapor pressure of hydrogen at 1 K is 8.3×10^{-39} Torr, which is completely negligible. If helium leakage proves to be a problem, the temperature of the chamber walls should be lowered to 0.1 K, where the vapor pressure of helium is 10^{-47} Torr.

With the ice ball at 2 K and the walls of the chamber at 1 K, the cooling power for a 2.8×10^{-5} m^2 area ball with emissivity $E=0.5$ is:

6.5) $$P_c = 11 \times 10^{-12} \text{ W} = 11 \text{ pW.}$$

6.5.2 Energy Deposited by Annihilation Particles

Energy from annihilations can be deposited in the antihydrogen ice ball by the 0.511 MeV gamma rays from positron-electron annihilation, the 250 MeV charged pions from the $p\bar{p}$ annihilation, and the 200 MeV gamma rays from the decay of the neutral pions from the $p\bar{p}$ annihilation. Because the pion decay gamma rays are so much more energetic, we will ignore the positron-electron annihilation gamma rays.

For 200 MeV gamma rays, the attenuation coefficient in matter is roughly constant at $\mu/p = 0.1$ cm^2/g. Since the density of antihydrogen is $\rho = 0.0763$ gm/cm^3, the attenuation per unit path length is only $\mu = 0.0076/cm$. Thus, instead of causing intense local heating, most of the gamma rays pass right through the iceball and continue on through the chamber wall to deposit their energy in the outside shield.

The fraction of the total average gamma ray energy of $E_g = 200$ MeV deposited in traversing the $d = 0.3$ cm diameter of the iceball is only:

$$6.6) \qquad dE_g = (1 - e^{-\mu d})E_g = = 460 \text{ keV} = 7.4 \times 10^{-14} \text{ J} \quad .$$

For the 250 MeV charged pions, the stopping power is essentially flat at $S = 15$ $MeV/(g/cm^2)$. The pions will leave a small amount of their energy in the iceball and chamber walls and deposit the rest in the outside shield. The energy deposited along a charged pion track traveling $d = 0.3$ cm through an antihydrogen ice ball with density $\rho = 0.0763$ gm/cm^3 is:

$$6.7) \qquad dE_p = S\rho d = 340 \text{ keV} = 5.5 \times 10^{-14} \text{ J} \quad .$$

We will make the assumption that there are 3.0 charged pions and 1.5 neutral pions per annihilation of each antiproton (see Section 7.3 on Particle Production from Antiproton Annihilation). Thus, the annihilation of each antihydrogen molecule will produce 6.0 250 MeV charged pions and 6.0 200 MeV gamma rays (plus 4.0 0.511 MeV positron-electron annihilation gamma rays which we will ignore).

Since the annihilation gamma rays and pions have such great penetrating power, failure of the antihydrogen trap will probably result in a "meltdown" of the antihydrogen container and shielding rather than a violent explosion. A trap failure would be extremely serious, however, and further studies need to be done on antimatter trap failure modes.

6.5.3 Heat Input from Annihilations on Chamber Wall

If the annihilation takes place from a sublimated antihydrogen molecule hitting the chamber wall, the reaction products will be emitted in all directions. If we assume the chamber is R=2 cm in radius, then the r=0.15 cm radius ice ball will intercept

6.8) $a/A = \pi r^2/4\pi R^2 = r^2/4R^2 = 1.41 \times 10^{-3}$

of the particles. Although most of the particles will not pass through the whole diameter of the ice ball, we will use the worst case example. The total energy deposited in the iceball for each antiproton annihilation on the wall of the chamber is then:

6.9) $dE_w = (6\ dE_g + 6\ dE_p)a/A = 1.3 \times 10^{-15}$ J

The 950 molecules per second leaving the ice ball will thus produce a total heating power in the ice ball of:

6.10) $P_w = 1.2 \times 10^{-12}$ W = 1.2 pW

This heating power due to wall annihilations is significantly less than the cooling power of 11 pW, so the evaporation of antihydrogen from the ice ball at 2 K will not cause excessive heating.

6.5.4 Heat Input from Annihilations on Surface

Although thermal analysis indicates that there should be no significant number of normal molecules left in a cryogenically cooled chamber, there could conceivably still be some normal molecules released by nonthermal processes such as natural radioactivity or cosmic rays. These normal molecules will annihilate right on the surface of the antihydrogen ice ball. We will want to estimate how many of these annihilations per second the passive cooling system will be able to handle.

In a surface annihilation half the particles will pass through the ice ball and the other half will head toward the chamber walls and pass through. The energy deposited in the ice ball for each annihilation on the surface is then:

6.11) $dE_s = (3\ dE_g + 3\ dE_p) = 4.6 \times 10^{-13}$ J

Although there should be no molecules left in a well-made vacuum chamber held at 1 K, we see that up to 10 annihilations per second can take place right on the surface of an antihydrogen ice ball without the heating power exceeding radiative cooling power at 2 K.

102

Obtaining a better estimate of this heating source will require research on hypervacuums in cryogenically cooled chambers. Probably the best way to obtain this information is to trap a few antiprotons from the Low Energy Antiproton Ring at CERN in a cryogenically cooled Penning trap and observe their lifetime.

We know that a single antielectron (positron) has been kept in a cryogenically cooled Penning trap for a month.[6.15] But the annihilation cross section for a free positron and a bound electron at these very low energies is not known well enough to establish a firm lower bound on the vacuum level in the trap. Plans are underway to trap an antiproton at LEAR in 1986-7 which should provide information on hypervacuums as well as the various properties of the antiproton itself.[6.16]

6.5.5 Cooling Rate.

If the heating power from annihilations can be made significantly smaller than the infrared cooling power, the ice ball should cool off. As is noted in Appendix A on the properties of solid hydrogen, the specific heat of antihydrogen at these low temperatures is quite small and decreases rapidly with temperature. At 2 K the heat capacity is $C=4.8 \times 10^{-3}$ cal/mole·K or 1.0×10^{-2} J/gm·K. Thus, a cooling power of $P_c = dE_c/dt = 10$ pW for a 1 mg antihydrogen ice ball would produce a cooling rate of:

6.12) $\qquad dT/dt = (C\ m)^{-1}\ dE/dt = 1 \times 10^{-6}$ K/s

or about 0.1 K/day. As the antihydrogen cooled below the assumed 2 K, the evaporation rate of antihydrogen, being an inverse exponential function of the temperature, would drop rapidly and one of the main sources of heat would become less important. As the temperature dropped, however, the infrared cooling power would also drop, but only as the fourth power of the temperature. The temperature of the ice ball would finally stabilize somewhere below 2 K and above the temperature of the chamber walls.

6.5.6 Alternate Cooling Methods

It may turn out that the emissivity of antihydrogen is too low in the long infrared region to allow significant cooling power by emission of radiation. In that case, alternate cooling methods will have to be found. Three possible examples are laser cooling, electrodynamic cooling, and magnetodynamic cooling.

In laser cooling, the storage cavity would be larger and laser beams would be used to intercept the antihydrogen molecules evaporating from the surface of the ice ball. The lasers would cool off the molecules and direct them back into the iceball using the techniques discussed in the section on laser slowing and cooling of antihydrogen.

In electrodynamic cooling, the iceball would be kept highly electrostatically charged. The vibrational excitation of the normal modes of the antihydrogen iceball by the internal heat would cause vibrational motion of the excess positrons on the surface of the iceball. These vibrating charges would cause changes in the image charges in the suspension electrodes. The changing currents in the electrode control circuits would then be damped out with a cryogenically cooled resistor as is presently done with trapped ions in a Penning trap,[6.17] or an active "cold damping" circuit.[6.18]

In magnetodynamic cooling, the entire trap region would be imbedded in a strong magnetic field. The antihydrogen, being diamagnetic, would be coupled to the magnetic field lines. Heat vibrations in the normal modes would then cause fluctuations in the magnetic field, which in turn would cause fluctuations in the current running through the magnet. These current fluctuations could then be damped out with a passive cryogenically cold resistor or an active "cold damping" circuit.

References:

[6.14] J.C. Mullins, W.T. Ziegler, and B.S. Kirk, "The thermodynamic properties of parahydrogen from 1 to 22 K," Georgia Institute of Technology, Atlanta, Georgia, Technical Report No. 1, Project No. A-593, Contract No. CST-7339 with National Bureau of Standards, Boulder, Colorado (1 November 1961).

[6.15] G. Gabrielse, Univ. of Washington, personal communication.

[6.16] W. Kells, G. Gabrielse, and K. Helmerson, "On achieving cold antiprotons in a Penning trap," Fermilab Preprint No. Conf-84/68-E, 8055.000, Fermi National Accelerator Lab, Batavia, Illinois (August 1984).

[6.17] P.B. Schwinberg, R.S. Van Dyck, Jr., and H.G. Dehmelt, "New comparison of the positron and electron g factors," Phys. Ref. Lett. 47, 1679-1682 (1981).

[6.18] R.L. Forward and G.D. Thurmond, "Network for simulating low-noise-temperature resistors," U.S. Patent 4,176,331 (27 November 1979).

SECTION 7

ANTIPROTON ANNIHILATION PROPULSION

This section discusses how we might go about building and using a high-specific-impulse, high-thrust propulsion system based on the generation, storage, and utilization of antiprotons. It will be shown that antiproton propulsion is technically feasible, but difficult and expensive. Yet, despite the high cost of antimatter, it may be a cost-effective fuel in space, where any fuel is expensive.

7.1 ANTIMATTER PROPULSION

It has long been realized that antimatter would be a valuable propulsion energy source because it allows for the complete conversion of mass to energy. Early studies of the concept by Sänger[7.1] assumed that the antimatter would be antielectrons (positrons), which interact with electrons to produce 0.511 MeV gamma rays. Sänger unsuccessfully tried to invent electron-gas mirrors to direct these short wavelength gamma rays to produce a photon rocket.

The antiproton is much more suitable than the antielectron for propulsion systems. The annihilation of an antiproton by a proton (or neutron) does not produce gamma rays immediately. Instead, as we show in more detail in Section 7.3, the products of the annihilation are from three to seven pions. On the average there are 3.0 charged pions and 1.5 neutral pions.

As is shown schematically in Figure 7-1, the neutral pions have a lifetime of only 90 attoseconds and almost immediately convert into two high energy (200 MeV) gamma rays. The charged pions have a normal half-life of 26 nanoseconds, but because they are moving at 94% the speed of light, their lives are lengthened to 70 nanoseconds. Thus, they travel an average of 21 meters before they decay. This time and interaction length is easily long enough to collect the charged pions in a thrust chamber constructed of magnetic fields and to direct the isotropic microexplosion into directed thrust. Even after the charged pions decay, they decay into energetic charged muons, which have even longer lifetimes and interaction lengths for further conversion into thrust. Thus, if sufficient quantities of antiprotons could be made and stored, then, according to presently known physical principles, they can be used as a highly efficient propulsion fuel.

105

Because of the extreme difficulty in obtaining significant quantities of antimatter, the idea of an antimatter rocket has usually remained in the "science fiction" category. Any papers before 1980 [see 27 references in section 02.01 of bibliography by Mallove, et al.[7.2]] were usually concerned with interstellar missions and glossed over the problems of generating, storing, and using the antimatter.

Recent progress in particle physics on methods for obtaining intense antiproton beams, however, has caused those in the space propulsion community to take another look at the concept of antimatter propulsion to see if the concept can be removed from the "science fiction" category to the "technically difficult and very costly" category, at which point the military services or NASA could begin considering its use. The last five years have seen the presentation of a number of papers on antimatter propulsion,[7.3-7.8] including a special issue of the Journal of the British Interplanetary Society on the subject of antimatter propulsion.[7.9]

Fig. 7-1 Schematic of an idealized antiproton rocket.

106

References:

7.1 Sänger, E., "The Theory of Photon Pockets," Ing. Arch. 21, 213 ff. (1953).

7.2 Mallove, E.F., Forward, R.L., Paprotny, Z., and Lehmann, J., "Interstellar Travel and Communication: A Bibliography," J. British Interplanetary Soc. 33, 201-248 (1980) [entire issue].

7.3 Forward, R.L., "Interstellar Flight Systems," AIAA Paper 80-0823, AIAA Int. Meeting, Baltimore, Md., (6-8 May 1980).

7.4 Cassenti, B.N., "Antimatter Propulsion for OTV Applications," AIAA Paper 84-1485, 20th Joint Prop. Conf., Cincinnati, Ohio (June 1984).

7.5 Cassenti, B.N., "Optimization of Relativistic Antimatter Rockets," J. British Interplanetary Soc. 37, 483-490 (1984).

7.6 Vulpetti, G., "A Propulsion-Oriented Synthesis of the Antiproton-Nucleon Annihilation Experimental Results," J. British Interplanetary Soc. 37, 124-134 (1984).

7.7 Vulpetti, G., "An Approach to the Modeling of Matter-Antimatter Propulsion Systems," J. British Interplanetary Soc. 37, 403-409 (1984).

7.8 R.L. Forward, "Antiproton annihilation propulsion," AIAA Paper 84-1482, 20th Joint Prop. Conf., Cincinnati, Ohio (11-13 June 1984) [To be published in J. Propulsion and Power].

7.9 Special issue on antimatter propulsion, J. British Interplanetary Soc. 35, 387-424 (September 1982).

7.2 EXTRACTION OF ANTIMATTER FROM STORAGE

There are a number of techniques for extracting the antihydrogen from the storage trap and directing it into the rocket engine under control. If the antihydrogen is in the form of an electrostatically suspended ball many milligrams in size, then as is shown in Figure 7-2, the antiprotons can be extracted from the ice ball by irradiating the ice with ultraviolet, driving off the positrons, extracting the excess antiprotons by field emission with a high intensity electric field, then directing them to the thrust chamber.[7.10]

It might be more desirable to form the antihydrogen as a cloud of charged microcrystals, each crystal a microgram in mass and containing the energy equivalent of 20 kg of chemical fuel. Then, using a directed beam of ultraviolet light to drive off

a few more positrons, an individual microcrystal could be preferentially extracted from the microcrystal cloud using electric fields, and directed down a vacuum line to the thrust chamber. Since the position of the charged microcrystal in the injection line can be sensed, mechanical shutters can allow the passage of the microcrystal without breaking the storage chamber vacuum.

References:

7.10 Morgan, D.L., "Concepts for the Design of an Antimatter Annihilation Rocket," J. British Interplanetary Soc. **35**, 405-412 (1982).
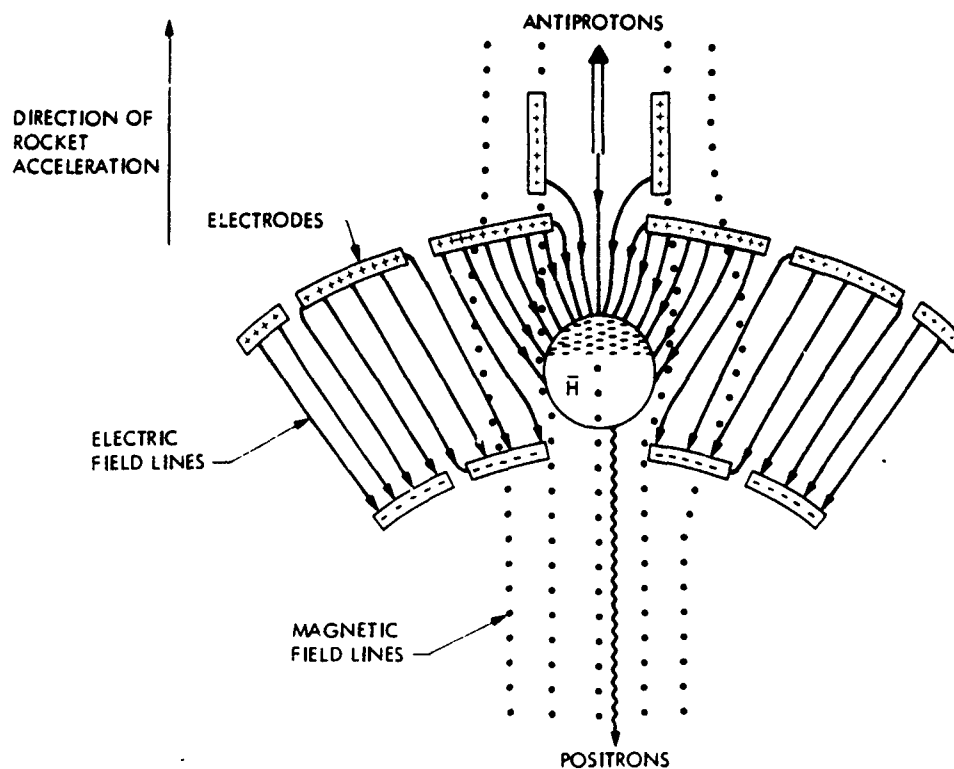
Fig. 7-2   Extraction of antiprotons from storage.

7.3 PARTICLE PRODUCTION FROM ANTIPROTON ANNIHILATION

When the antiprotons reach the rocket chamber, they will be annihilated with the protons in normal hydrogen to release the rest mass energy of both particles. There is a popular misconception that the annihilation of antimatter with matter produces prompt high-energy gamma rays. This is true for the annihilation of positrons with electrons, which produces two 0.511 MeV gamma rays. It is not true for the annihilation of baryons.

When an antiproton annihilates with a proton, the predominant reaction products (98%) are pions. A recent survey of the literature[7.11] found that on the average there are 3.0 charged pions, 1.5 neutral pions, 0.05 charged kaons, 0.03 neutral kaons, and 0.02 prompt gamma rays. The branching ratios are given by Table 7-1:

Table 7-1 Branching Ratios of p̄p annihilation products

Probability	π^+	π^-	π^0	K^+	K^-	K^0	γ
0.345	1	1	2				
0.213	2	2	2				
0.187	2	2	1				
0.078	1	1	1				
0.058	2	2					
0.019	3	3					
0.016	3	3	1				
0.0133			1	1	1		
0.0133		1		1		1	
0.0103	1	1	1			1	
0.0091	2	1			1		
0.0076			3				
0.0050							2
0.0047			3			1	
0.0042	1		2		1		
0.0036			2				2
0.0032	1	1					
0.0030	3	3	2				
0.0005	1	1	2				1
0.9938	1.49	1.49	1.52	0.026	0.026	0.028	0.018

This estimate of the branching ratio should be compared with other estimates such as the ones by Agnew, et al. from antiproton annihilations in propane in 1960,[7.12] by Lawrence Berkeley Laboratory in 1972,[7.13] and by Vulpetti based on recent work at CERN and Columbia.[7.14]

	π^+	π^-	π^0	K^+	K^-	K^0
Agnew	1.53	1.53	1.60			
LBL	1.5	1.5	2.0			
Vulpetti	1.53	1.53	1.96	0.012	0.012	0.026

It is obvious that more work needs to be done to pin down the exact values for the neutral pions and the kaons.

The neutral pions have a lifetime of only 90 attoseconds and almost immediately convert into two high-energy gamma rays. The charged pions have a normal lifetime of 26 nanoseconds, but because the relativistic time contraction at their velocity of 94% of the speed of light, their lifetimes are lengthened to 70 nanoseconds. Thus, unless they are stopped by interaction with matter, they will travel an average of 21 meters before they decay. The energy spectra of the charged pions and gamma rays are shown in Figure 7-3.[7.11] The average energy of the gamma rays is 200 MeV, while the average energy of the charged pions is 250 MeV.

In the annihilation process of antiprotons or antihydrogen with normal atoms or molecules, it should be appreciated that the relevant cross sections are not the nuclear cross sections. In any matter-antimatter mixture in which the atoms and antiatoms are not wholly ionized, rearrangement collisions between the atom and the antiatom can lead to bound states of the nucleus and antinucleus from which the annihilation can proceed. Since the cross sections for such collisions at low energies are considerably higher than the direct particle-antiparticle annihilation cross sections, atomic interactions play a dominant role in such a mixture.[7.15]

In many applications of the use of antiprotons for energy storage and propulsion, consideration is being given to annihilation of the antiprotons with heavier nuclei than protons. Since a neutron has the same baryon number as a proton and a free neutron will spontaneously decay into a proton, a neutron can be considered as an "excited state" of a proton. Thus, antiprotons, will annihilate with a neutron as well as a proton inside a heavy nucleus. Since the neutron has a neutral charge and charge must be conserved in the annihilation process, the reaction products from the annihilation of an antiproton in a heavy nucleus will produce different numbers of the various types of charged and uncharged pion and kaon particles.
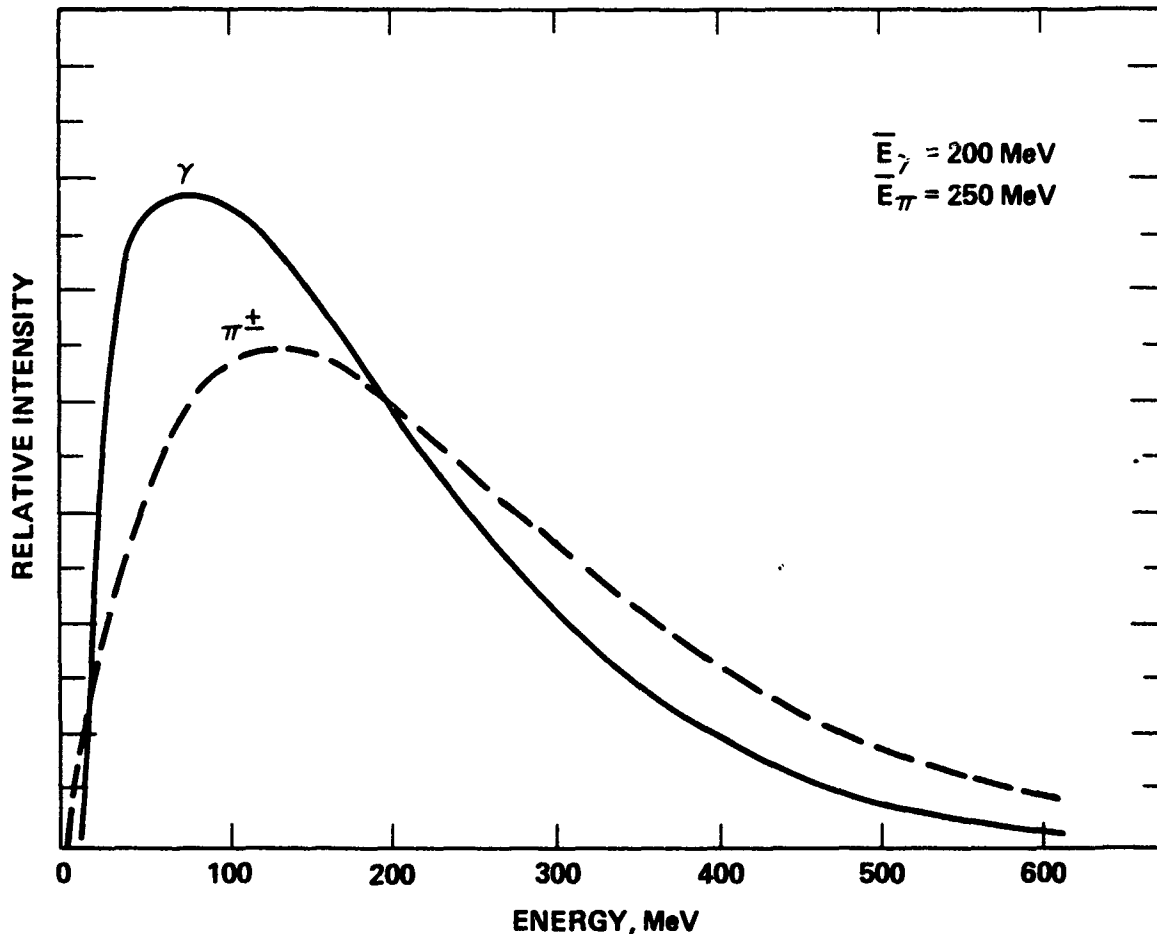
Fig. 7-3 <u>Antiproton-proton annihilation particle spectra.</u>

Annihilation inside a heavy nucleus has the potential for
increasing the efficiency of an antiproton annihilation
propulsion system, since the neutral pions are absorbed in the
nucleus instead of decaying into gamma rays. The annihilation
reaction will "heat up" the nucleus as well as cause
spallation fission of charged nuclear fragments. These
heavier charged particles would be yet another mechanism for
the transfer of the annihilation energy to a hydrogen working
fluid in a propulsion system.

Data for the reaction products of antiprotons with heavier
nuclei are sparse and of problematic accuracy, but ongoing
work with the LEAR antiprotons at CERN should soon produce
much better data. The available data to date include the 1972
experiments by Agnew, et al.[7.12] and 1982 calculations by
Clover, et al.[7.16]

111

		π^+	π^-	π^0	p	n
Agnew	(C^{12})	1.33	1.58	1.15		
Clover	(C^{12})	1.1	1.4	1.6	1.0	1.1
	(U^{238})	0.7	1.1	1.1	2.9	5.7

As can be seen, there are still disagreements in the numbers
of particles emitted from even the simple $\bar{p}$-p reaction. Thus,
research is still needed in the interaction of antiprotons
with protons, neutrons, and the nuclei of heavier elements.
The measurement of the annihilation-induced fission products
from the annihilation of antiprotons in heavy nuclei over a
broad range of nuclear masses is especially needed. These
data will help to determine if there is an optimum nucleus
that is better for propulsion than annihilating antiprotons
with hydrogen.

An ideal reaction would be one where the energy from the
antiproton annihilation causes the nucleus to break up into
doubly charged alpha particles that would rapidly couple their
kinetic energy to the hydrogen working fluid. A more
realistic reaction would have over half of the annihilation
energy showing up as charged nuclear fragments, a minimum
number of neutrons and neutral pions escaping, and most of the
rest of the energy showing up as charged pions.

References:

[7.11]The antiproton group at Los Alamos National Lab, private
communication (1984).

[7.12]L.E. Agnew, Jr., T. Elioff, W.B. Fowler, R.L. Lander, W.M.
Powell, E. Sergè, H.M. Steiner, H.S. White, C. Wiegand, and T.
Ypsilantis, "Antiproton interactions in hydrogen and carbon
below 200 MeV," Phys. Rev., 118, 1371 (1960).

[7.13]Lawrence Berkeley Laboratory Report LBL-58 (1972).

[7.14]G. Vulpetti, "A propulsion-oriented synthesis of the
antiproton-nucleon annihilation experimental results," J.
British Interplanetary Soc. 37, 124-134 (1984)

[7.15]D.L. Morgan, Jr. and V.W. Hughes, "Atom-antiatom
interactions," Phys. Rev. A7, 1811-1825 (1973).

[7.16]M.R. Clover, R.M. DeVries, N.J. DiGiacomo, and Y. Yariv,
"Low energy antiproton-nucleus interactions," Phys. Rev. C26,
2138-2151 (1982).

7.4 STOPPING OF PARTICLES

As we have seen in Section 7.3, the particles emitted from the annihilation of antiprotons with protons and neutrons are mainly pions. The neutral pions almost immediately decay into two gamma rays, however, so the particles that we must deal with are of two kinds: High-energy charged pions with an average kinetic energy of 250 MeV, and high-energy gamma rays with an average energy of 200 MeV. (See Figure 7-3.)

To utilize the energy in these particles for propulsion we need to either direct their momentum rearward from our vehicle to provide thrust, or we need to stop the particles and use their energy to heat a working fluid. We also need to provide shielding for the crew and the radiation sensitive components of the rocket engine.

7.4.1 Stopping of Charged Pions

The primary stopping mechanism for charged particles in matter is the electronic excitation and ionization of the atoms in the material. The stopping power depends largely on the atomic number (number of electrons per nucleus) of the stopping material, and the velocity and charge of the particle, but not on its mass.

For particles with large initial velocities the rate of energy deposition per unit path length is approximately independent of energy, then it rises rapidly as the energy approaches zero. The resultant integrated energy decrease produces a "range" for the particle in a particular stopping material that is a function of the energy. Because of statistical fluctuations, there will be a small spread of ranges for different particles with identical initial energies.

A great deal of data is available on the stopping power and range of protons, pions, and muons as a function of energy in various materials.[7.17], [7.18] Table 7-2 is an abbreviated list of this data giving the range of pions in a number of substances that might be of use in a first cut design of an antimatter rocket.

The range is first given in g/cm^2 of stopping material required to extract 100 MeV of energy, since that number is independent of the state of the material (gas, liquid, or solid). When multiplied by the density of the material it gives the range in centimeters of thickness of the material to produce a 100 MeV energy loss. The range is relatively constant down to 100 MeV, when it suddenly becomes much shorter.

113

Table 7-2 Range of Pions per 100 MeV of Energy.

Material	Density g/cm^3	Range for 100 MeV energy loss		Last 100 MeV	
		High Energy g/cm^2	cm	g/cm^2	cm
H$_2$ (100 atm)	0.009	24	2700	13	1400
H$_2$ (300 atm)	0.027	24	890	13	480
He (300 atm)	0.018	50	930	29	540
N$_2$ (100 atm)	0.125	55	440	32	250
Water	1.00	50	50	27	27
Be	1.85	61	33	33	18
Al	2.70	62	23	35	13
Fe	7.87	67	8.5	38	4.8
W	19.3	86	4.5	52	2.7
Pb	11.4	88	7.7	53	4.6

From Table 7-2 we can see that gases such as hydrogen, helium, and nitrogen, because of their low density, have a long interaction length with pions. It will be necessary to operate the reaction chamber at high pressures in order to get the density up so that the interaction range becomes shorter than the pion mean life range.

To calculate the fraction of the pion kinetic energy deposited in the working fluid requires a detailed calculation involving the pion energy spectrum, the density, temperature, and pressure of the working fluid, the containment losses, and other factors. As we can see from Table 7-2, nitrogen at 100 atm pressure gives a shorter range than either hydrogen or helium at 300 atm pressure. (The Space Shuttle Main Engines operate at 213 atm.) It may turn out that despite its higher molecular weight, nitrogen may be a preferred reaction gas because of its higher density.

Assuming that the containment losses are small and the temperatures not too high, it is possible to estimate the percentage of the pion energy that gets into the working fluid. The efficiency was found to be about 65% for hydrogen at 300 atm and 95% for nitrogen at 100 atm. Obviously, much more work needs to be done in this area since the lifetime and the stopping power both change with pion energy.

Using the detailed tables available in the literature[7.17] the ranges of the annihilation pions with their spectrum of possible initial energies were calculated and plotted in Figure 7-4 for hydrogen at 300 atm, nitrogen at 100 atm, and solid tungsten (for shielding). Also included are the pion mean life (not half-life) and the resulting mean range in vacuum as a function of energy. These last were calculated from Equations A.1 and A.2 in Appendix A.

114
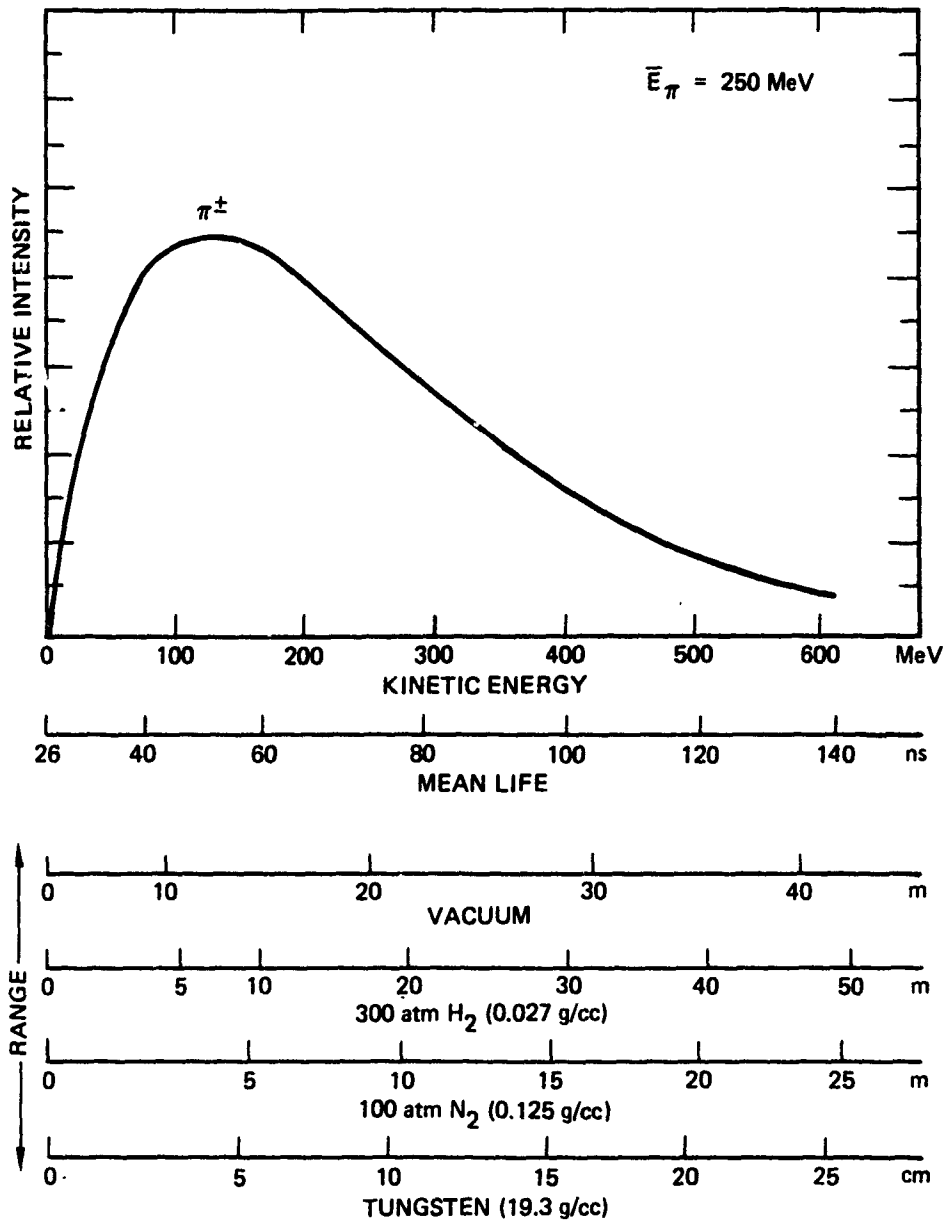
Fig. 7-4   Range of charged pions.

115

7.4.2 Stopping of Gamma Rays

The small numbers of prompt gamma rays produced by the antiproton-proton annihilation process and the large numbers of delayed gamma rays produced by the decay of the neutral pions are a major problem in the utilization of antiprotons for propulsion. As can be seen in Figure 7-3, the spectrum of the gamma rays peaks at around 70 MeV and extends out to many hundreds of MeV, with an average energy of about 200 MeV. The maximum energy gamma rays would be the small fraction (0.5%) of 938 MeV prompt gammas from the initial annihilation reaction.

Unlike charged particles, which have a definite range in matter, the gamma ray intensity is exponentially attenuated by matter. For the high-energy gammas the attenuation is predominantly due to pair production in the shield material.

From Figure 8e-11 in the AIP Handbook,[7.19] we find that for a heavy metal, the attenuation coefficient for gamma rays with an energy greater than 100 MeV is about 0.1 cm^2/g and slowly rises with energy. For tungsten, with a density of 19.3 g/cm^3, this gives an attenuation factor of 1.93 cm^{-1}. Table 7-3 gives the attenuation achieved for various thicknesses of tungsten.

Table 7-3   Attenuation of Gamma Rays by Tungsten.

x (cm)	Attenuation
2	2.1×10^{-2}
4	4.4×10^{-4}
6	9.4×10^{-6}
8	2.0×10^{-7}
10	4.2×10^{-9}
12	8.7×10^{-11}
14	1.8×10^{-12}
16	3.9×10^{-14}
18	8.2×10^{-16}
20	1.7×10^{-17}
22	3.6×10^{-19}
24	7.7×10^{-21}

This table can be used to obtain rough estimates of the amount of tungsten needed for various requirements. For example, if we wish to recover a majority of the neutral pion energy by capturing the decay gamma rays in a tungsten shield cooled with flowing hydrogen, then a thickness of only two centimeters is needed to capture 98% of the gamma rays.

116

7.4.3 Shielding of Vehicle and Crew

The gamma rays and the high-energy charged pions will cause heating and radiation damage if they are not shielded against. Fortunately, unlike neutrons, they will not cause the shielding material to become radioactive by transmutation of the nuclei in the shield. The components needing shielding are the crew, the electronics, the cryogenic tankage, and the magnetic coils for magnetically assisted rockets.

The radiation flux will be extremely high. A typical high performance antimatter rocket will probably operate at a thrust level of 10,000 N (pushing 10 metric tons at 1 m/s^2) and a specific impulse of 2000 s (exhaust velocity of 20 km/s). The power level of the exhaust coming from the charged pions is then 200 MW, with 100 MW of 200 MeV gamma rays coming from the neutral pions.

If we are concerned with shielding some superconducting coils that are generating magnetic fields to contain and direct the charged pions, then using Table 7-3 we find we will want to use a shield of about 10 cm thickness to attenuate the 100 MW of gamma ray energy down to a few watts that can be handled by the cryogenic coolers.

If we are interested in protecting personnel and electronics, then a shield thickness of 14 cm of tungsten will shield personnel at 10 meters from even a 100 MW source of gamma rays. To illustrate this last point, if we look at Table 8i-5 in the AIP Handbook[7.19], we find that the dose from a 1 Curie (3.7×10^{10} disintegrations/s) source of 100 MeV gamma rays at 1 m distance is 29 R/hr. Extrapolating from this data point, the dose from a 1 Curie source of 200 MeV gamma rays at 10 m distance would then be 0.58 R/hr.

Since a single 200 MeV gamma ray has an energy of 3.2×10^{-11} J, a 100 MW source of 200 MeV gamma rays produces 3×10^{18} gammas/s or 8.5×10^7 Curies. This would produce a dose of 4.9×10^7 R/hr at 10 m distance. From Table 7-3 we find that 14 cm of tungsten shielding would provide an attenuation of 1.8×10^{-12}. Thus, the dose rate at 10 m would be less than 0.1 mrad/hr, a reasonable dose for space missions.

A conceptual schematic of the shielding that might be used in a magnetic field assisted antiproton annihilation rocket is shown in Figure 7-5. The reaction chamber would be about 1 m in diameter. The pressure walls would have the thickness equivalent of 2 cm of tungsten so as to absorb most of the gamma ray energy and use it to heat hydrogen flowing through channels in the wall. The hot hydrogen would be used as a film flow to protect the nozzle from the ultrahot hydrogen plasma at the center of the chamber.

117

Each superconducting magnetic coil would be shielded by 10 cm of tungsten in a ring about 1.1 m in diameter. The crew would be protected by a shadow shield 14 cm thick and 0.6 m in diameter that is 0.6 m from the annihilation region. This would provide a shielded region 10 m in diameter at 10 m from the engine. The mass of the shadow shield is 800 kg, while each of the rings is 750 kg. At 2 cm thickness the pressure chamber mass is 2,200 kg.

References:

7.17 W.H. Barkas and M.J. Berger, **Tables of Energy Losses and Ranges of Heavy Charged Particles**, NASA SP-3013, STI Division, NASA, Washington, DC (1964).

7.18 Particle Data Group, "Review of particle properties," Rev. Mod. Phys. **56**, Part II (April 1984).

7.19 D.E. Gray, Ed., **American Institute of Physics Handbook**, Third Edition, McGraw-Hill, NY (1972).
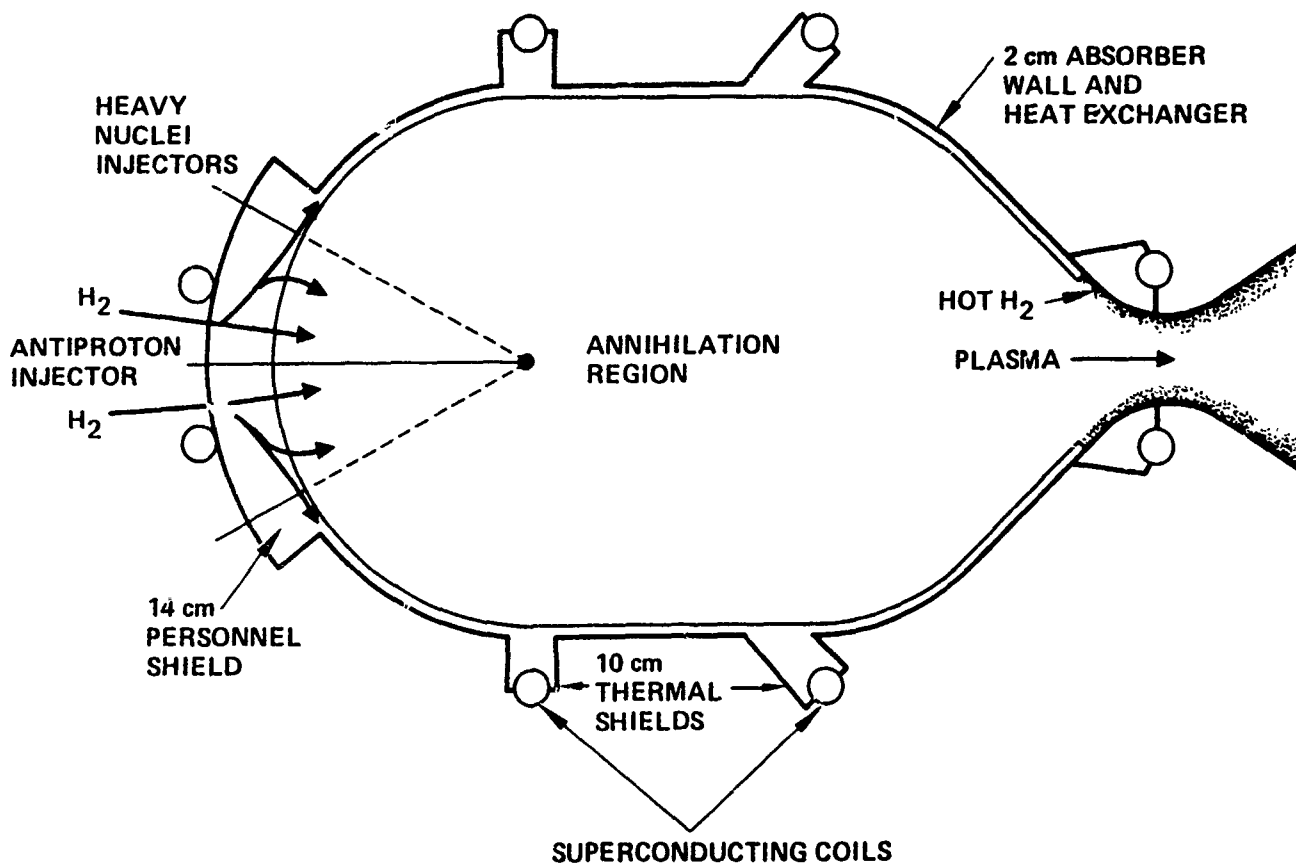
Fig. 7-5 Conceptual schematic for radiation shielding.

7.5 ANTIMATTER ROCKET ENGINE CONCEPTS

Antimatter fuel is so powerful that new types of rocket engines will have to be developed to fully utilize its potential. It should be emphasized, however, that the need for completely new engine designs is not unique to antimatter propulsion. Any new form of propulsion that produces high thrust at high specific impulse using a thermally expanded reaction fluid will have the same problem.

Laser plasma, solar plasma, fusion plasma, metallic hydrogen, atomic hydrogen, metastable helium, tetrahydrogen, and any other form of advanced propulsion that operates at high thrust with specific impulses over 1000 s will have to cope with chamber temperatures exceeding 3500 K. No known materials can survive these temperatures for long. If hydrogen is being used as the reaction mass, these temperatures will cause it to convert from a molecular gas to an atomic plasma of free protons and electrons.

Thus, any advanced thermal propulsion system will require the development of new types of reaction chambers and nozzles that can contain and direct a hot hydrogen plasma without direct contact with material walls. The best known technique for handling plasmas is the use of magnetic fields to guide and contain the charged particles in the plasma.

One type of magnetic engine design uses a solenoidal "magnetic bottle" where the magnetic field fills the entire chamber. In this design, the plasma ions tend to stay on the magnetic field lines and are kept away from the walls.

A less well known type of magnetically assisted engine uses a "picket fence" geometry where the walls of the chamber have ring magnets that alternate north and south in polarity. The magnetic fields go from one pole to another and stay near the walls, creating a "picket fence" of arching magnetic fields. In these designs, the ions in the plasma are free to move about in the chamber in any direction until they approach the wall. Since they find it difficult to cross the magnetic field lines near the wall, they are repelled back to the center of the chamber.

Much more research needs to be done on engines that can contain and control hot plasmas. This work is essentially independent of the source of the hot plasmas and can pay off in the future even if antiproton annihilation propulsion is not found to be practical.

7.5.1 Thermal Heat Exchanger Concept

One of the simplest antiproton propulsion systems would use a design similar to that of a nuclear thermal rocket. In a nuclear thermal rocket, the nuclear fission reactions were used to heat a high temperature material (graphite) which had cooling channels passing through it. Graphite was chosen as the core material because it best matched both the reactor nucleonics requirements (low neutron absorption) and the heat exchanger requirements (reasonable strength and high operating temperature). Hydrogen was passed through the cooling channels, keeping the reactor cool while the hydrogen was heated to many thousands of degrees. Specific impulse values close to 900 s were obtained by this technique.

In the antiproton annihilation version of the thermal heat exchanger rocket concept, the energy released by the annihilation reaction would be absorbed in the walls of a heat exchanger made out of refractory metal.[7.20] The heat exchanger would then heat hydrogen to produce thrust. As is shown in Figure 7-6, a heat exchanger made out of a cylinder of tungsten 28 cm in diameter and 28 cm long would only weigh 330 kg and would capture most of the energy in the gamma rays and pions, thus utilizing all of the annihilation energy.
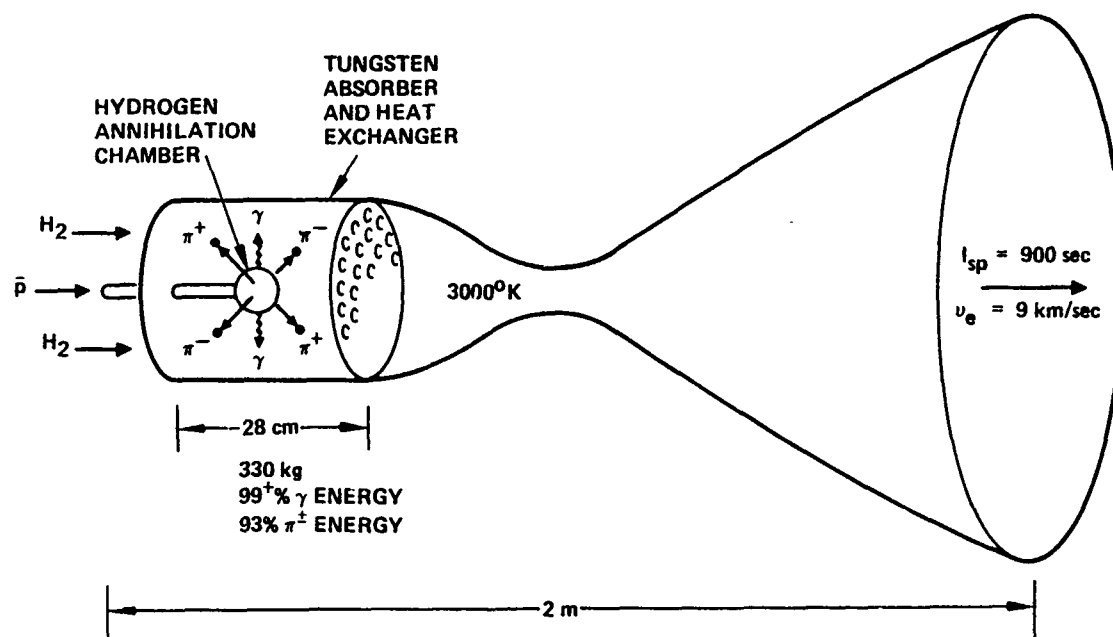
Fig. 7-6   First generation antimatter thermal rocket.

The maximum operating temperature of this rocket would be limited by the melting point of tungsten to about 3000 K, resulting in a maximum specific impulse of about 900 sec or an exhaust velocity of about 9 km/s. This specific impulse is considerably better than any chemical rocket or even a nuclear fission thermal rocket, but still does not utilize the high exhaust velocity potential of antiproton annihilation.

This first generation antimatter rocket engine would be optimum for many space missions in earth-lunar space and could be designed and tested using reasonable extrapolations of nuclear thermal rocket technology. The high risk engineering development of magnetic nozzles to control, contain, and direct the charged pions would be set aside for a second generation engine where higher specific impulse would be required.

References:

7.20 B.W. Augenstein, "Some examples of propulsion applications using antimatter," Rand Paper P-7113, Rand Corp., Santa Monica, CA 90406 (July 1985).

7.5.2 Hot Hydrogen Gas Engine Concept

The next level of sophistication in an antimatter rocket is to take the design for a hydrogen thermal rocket operating at high pressure and add a magnetic bottle to it. In this magnetically assisted engine, shown in Figure 7-7, hydrogen is contained by a pressure vessel while the charged pions from the annihilation reaction are contained by the magnetic bottle.[7.21] The pressure of the hydrogen is 100 atm (compared to the pressure in the Space Shuttle Main Engine of 213 atm).

In operation, hydrogen and antihydrogen are injected in the chamber and the antihydrogen annihilates with some of the hydrogen to produce pions. The neutral pions immediately convert into gamma rays. The gamma rays are considered lost in this design and no attempt is made to use their energy. In all probability, the pressure vessel will be designed to intercept as little of the gamma ray energy as possible to minimize heating problems.

The charged pions are trapped by the magnetic field and spiral back and forth in the magnetic bottle, transferring their energy to the hydrogen. The range of the average charged pion in hydrogen at 100 atm pressure is limited by its mean decay time. This varies from 45 ns at a kinetic energy of 100 MeV to 100 ns at 400 MeV.

At the 100 atm pressure assumed for the design shown in
Figure 7-7, the pion gives up about 25% of its kinetic energy
to the hydrogen before it decays into a muon and a neutrino.
The muon, with its much longer lifetime of 2.2 μs, then gives
up essentially all of its kinetic energy to the hydrogen
before decaying into an electron and two neutrinos.

In a complicated Monte Carlo calculation, it was estimated
that including losses of particles to the wall of the chamber
and out the ends of the magnetic bottle, 35% of the
annihilation energy ended up in the hydrogen working fluid.
As was pointed out in Section 7.4, it might be advantageous to
use nitrogen as the working fluid. Its higher density would
allow a higher percentage of the pion energy to be extracted.
This might be enough to overcome its larger molecular weight.

MAGNETIC FIELD ASSISTED
CONTAINMENT VESSEL

STANDARD REGENERATIVELY
COOLED 100:1 ROCKET NOZZLE

HYDROGEN AND
ANTIHYDROGEN

2 m

8 cm

P = 100 atmos

V_e = 5 km/sec

THRUST = 98 kN

300 kG

300 kG

50 kG
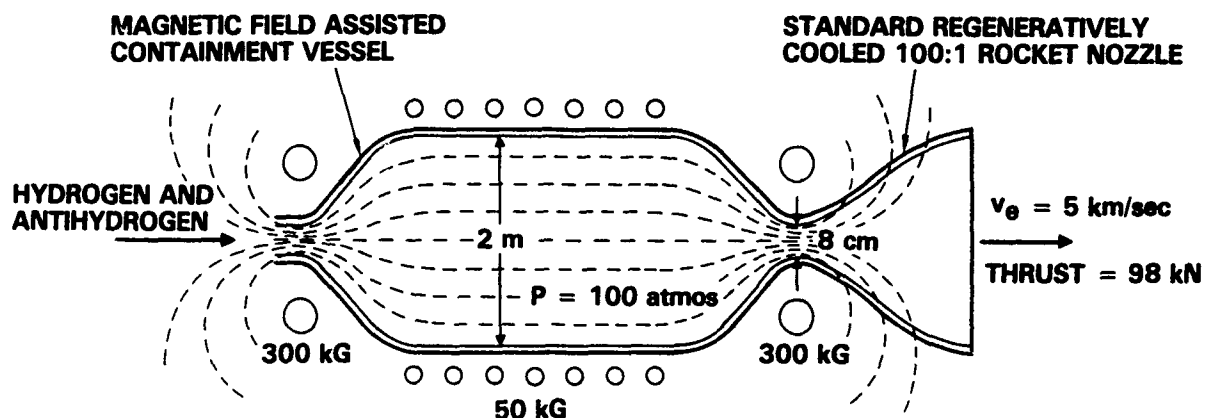
Fig. 7-7 Magnetic assisted antimatter heated hydrogen rocket.

Not all of the charged pions stay in the magnetic bottle.
Those which start out with a velocity vector at a small angle
to a magnetic field line will follow the magnetic field line
right out of the ends of the bottle and be lost. Those with
too high an initial velocity will have a large radius of
curvature and may hit the walls and be lost. As the pions
move through the hydrogen, and especially when they decay into
muons, the velocity vector will be changed and the particle
may find itself on a trajectory which leaves the confinement
volume.

If the antimatter is injected at a rate of 2.9 µg/s and the
hydrogen reaction mass at a rate of 29 kg/s, then the specific
impulse will be 350 s (compared to the Space Shuttle Main
Engine specific impulse of 460 s). The thrust level is 98 kN
and the power in the exhaust is 330 MW (1/20 the Space Shuttle
Main Engine power). The temperature of the hot hydrogen for
this relatively low specific impulse is only 460 K or 190 C
because of the low molecular weight of the pure hydrogen
exhaust.[7.21]

If the antimatter is injected at a rate of 12 µg/s and the
hydrogen reaction mass at a rate of 16 kg/s, then the specific
impulse will increase to 1000 s.[7.22] The temperature of the
hot hydrogen for this higher specific impulse is now 3700 K,
which is reaching the material limits of the pressure chamber.
At higher temperatures the hydrogen will also start to
disassociate and become ionized. We will than have to move to
newer engine designs that can work with a hot hydrogen plasma.

These hot hydrogen antimatter energized engines will require
significant advances in engine design. The pressure vessels
have to operate in a strong magnetic field and a high charged
particle and gamma ray environment. The high field strength
superconducting magnetic coils must be designed for minimum
mass and be shielded against the high thermal and radiation
environment. Yet for specific impulses below 1000 s, the
temperature of the hydrogen reaction mass is low enough that
standard pressure vessel designs and materials can be used, so
that much of the present rocket technology is applicable.
Much work remains to be done, but a great deal of it has
already been done.

References:

[7.21]B.N. Cassenti, "Antimatter Propulsion for OTV
Applications," AIAA Paper 84-1485, 20th Joint Propulsion
Conference, Cincinnati, Ohio, June 1984.

[7.22]B.N. Cassenti, personal communication (1983)

7.5.3 Magnetically Contained Plasma Engine Concept

In the previous design concept, the magnetic field was only
used to contain the high-energy charged pions, muons, and
electrons while they transferred their energy to the hydrogen
working fluid. Since the magnetic bottle exists, it can also
be used for containment of the working fluid if it is a
plasma.

There has been no detailed design yet of a magnetically
contained plasma rocket, independent of the method of heating
the plasma. There has been one preliminary design carried out
for an antimatter heated plasma rocket that uses heavy
elements as the working fluid. The conceptual design is shown
in Figure 7-8.[7.23]
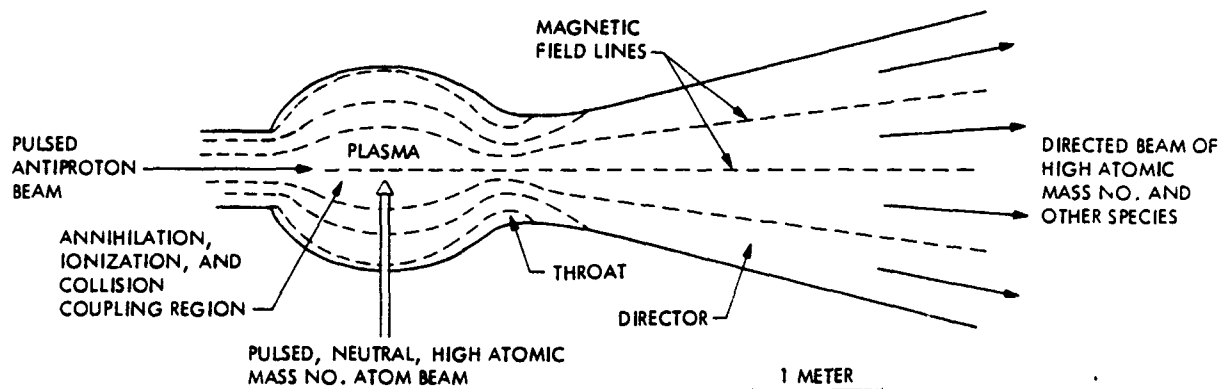
Fig. 7-8 High thrust magnetic containment antimatter rocket.

The magnetic field in this design is pulsed in the same manner as a pulsed fusion machine magnetic bottle. The full pulse cycle is 17 ms with the time of containment being 7 ms. The magnetic field in Figure 7-8 is shown in its maximum strength, or closed, configuration. At the start of each pulse, 5 μg of antiprotons are injected into the reaction chamber along with a stream of atoms of a heavy element such as lead or (depleted) uranium.

The antiprotons will annihilate with either a proton or a neutron in the nucleus of the heavy atom, producing pions. The pions immediately transfer their energy to the nucleus causing spallation, evaporation, or fission of the nucleus leading to the production of several light nuclides and individual particles, all of which have higher mass, lower velocity, and often higher charge than the pions. All of these characteristics lead to more rapid transfer of the kinetic energy to the rest of the working "fluid".

The beam of heavy atoms continues after the antiproton annihilation pulse until 60 g have been injected. The trapped charged particles circle about in the magnetic bottle until the excess matter becomes ionized due to collisions with the nuclear fragments and forms a plasma which is confined by the magnetic field.

After 7 ms the annihilation energy has been transferred to the working fluid, the field is opened and the hot plasma escapes out the nozzle, producing thrust. For an average input of 2×10^{20} antiprotons/s (0.3 mg/s) and 9×10^{24} U atoms/s (3.6 kg/s), the thrust of this engine design is 0.55 MN (124,000 lb).[7.23]

The specific impulse of this conceptual design for a high thrust plasma engine is a remarkable 14,000 s (140 km/s). The maximum temperature reached during a pulse is 2.6×10^8 K, but the average temperature is much less. The plasma confinement characteristics of the magnetic bottle are comparable to those of present day fusion plasma machines.

References:

[7.23]D.L. Morgan, "Concepts for the design of an antimatter annihilation rocket," J. British Interplanetary Soc. **35**, 405-412 (1982).

7.5.4 Magnetically Directed Annihilation Pion Rocket

In all the previous designs, a great deal of effort was spent developing mechanisms to ensure the transfer of the kinetic energy of the annihilation pions into some working fluid to lower the specific impulse and increase the thrust levels to match the performance characteristics of the antimatter rocket to space missions around earth and throughout the solar system. For deep space missions and missions to the stars, the higher specific impulse obtainable directly from the charged pions becomes more useful. A conceptual design for such a high exhaust velocity antiproton annihilation rocket is shown in Figure 7-9.[7.23]
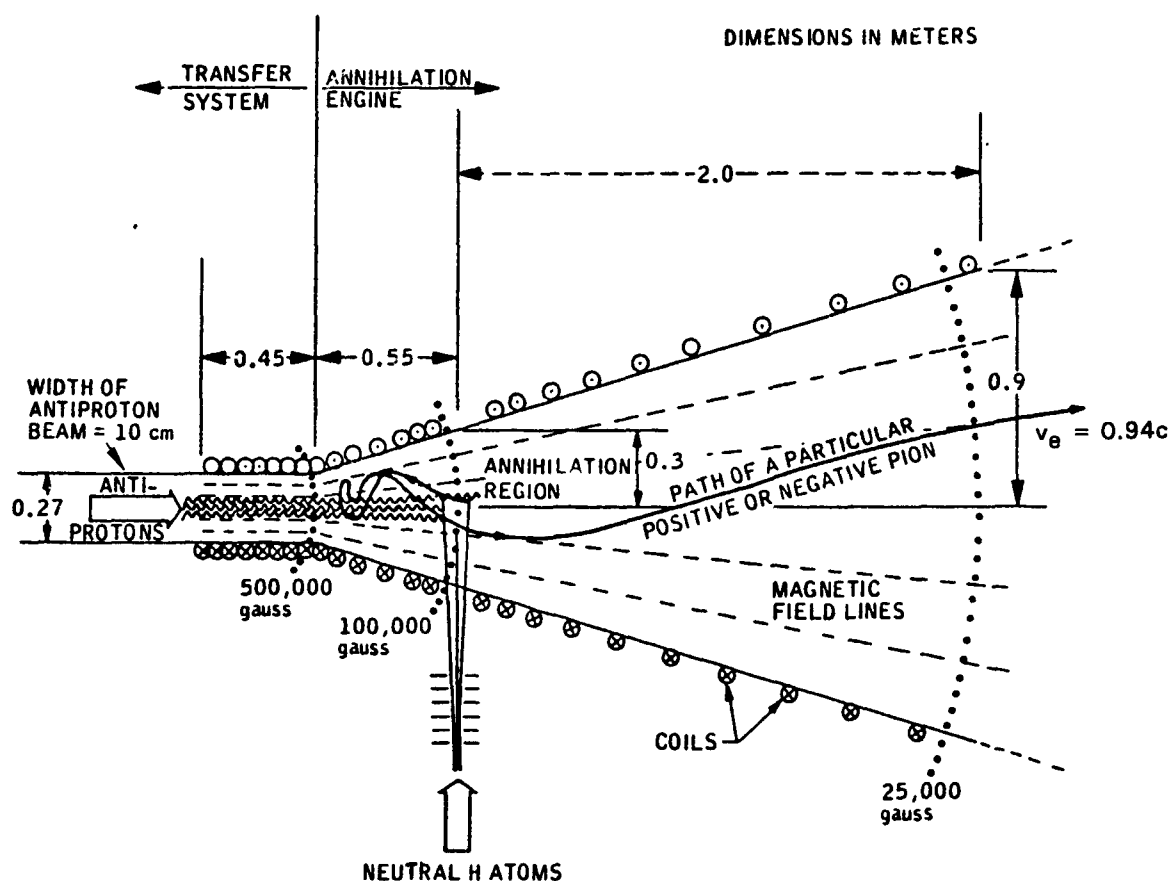
Fig. 7-9 High exhaust velocity antiproton rocket.

This rocket design concept uses a static magnetic field configuration in the shape of a conical rocket nozzle. The magnetic field is produced by the turns of a coil that increase in radius and separation so that the magnetic field lines form straight lines, all of which emanate from a common center on the axis. Within the field is space vacuum except for the antiproton beam, the hydrogen beam, and the annihilation products.

The beam of antiprotons enters from the left and collides at a right angle with a beam of hydrogen coming from below. If the two beams are $2x10^{20}$ ions/s each, then 95% of the antiproton ions are annihilated.[7.23] The ion current in each beam is approximately 30 A.

The charged pions produced by the $p\bar{p}$ annihilation follow paths that are along a cone whose vertex is the common center point of the magnetic field lines and whose surface is defined by the initial velocity vector of the pion. The vertex angle of the cone depends upon the velocity, charge, and mass of the pion and the strength of the magnetic field at the point of tangency.

The dynamics of the motion of the pion in the magnetic field confines the pion to the surface of the cone. If the pion velocity vector is to the right, the pion will spiral out of the engine to the right and produce thrust. If the pion velocity vector is to the left, it will spiral toward the vertex of the cone, circle around just below the tip, then reverse direction and spiral back out to the right and exit the nozzle. Only the small fraction of pions with a velocity vector nearly parallel to magnetic field line at its point of origin will be able to travel up the throat and out of the engine the wrong way.

The specific impulse of this engine is the velocity of the pions at their time of formation. For the mean kinetic energy of 250 MeV, this is a velocity of 94% the speed of light or a specific impulse of 28,800,000 s! The energy from the 30 A of antiproton ions will run this engine at the same power level as the three Space Shuttle Main Engines, 24 GW. With the high specific impulse, however, this 24 GW of power only produces 70 N of thrust. Such a design is probably best suited as the last stage in an interstellar probe design.

7.5.5 Magnetic Nozzle Antimatter Microexplosion Rocket

It has been suggested that it might be possible to direct a small amount of antimatter onto a pellet made of a heavy element and cause a microexplosion that would produce a hot, dense plasma.[7.24] Magnetic rocket nozzles that take hot, dense plasmas from microexplosions and convert them into

thrust have already been designed to convert the energy from a plasma formed by a laser fusion pellet microexplosion into directed thrust.[7.25] One version that uses a single large superconducting magnetic coil is shown in Figure 7-10. If antimatter microexplosions are ever proved feasible, a magnetic rocket exists to use them.

References:

[7.24]S. Polikanov, "Could antiprotons be used to get a hot, dense plasma?" pp. 851-853, **Physics at LEAR with Low-Energy Cooled Antiprotons**, U. Gastaldi and R. Klapisch, ed., Plenum Press, NY (1984).

[7.25]R. Hyde, L. Wood, and J. Nuckolls, "Prospects for rocket propulsion with laser induced fusion microexplosions," AIAA Paper 72-1063 (Dec 1972).

SHIELDING

SUPERCONDUCTOR
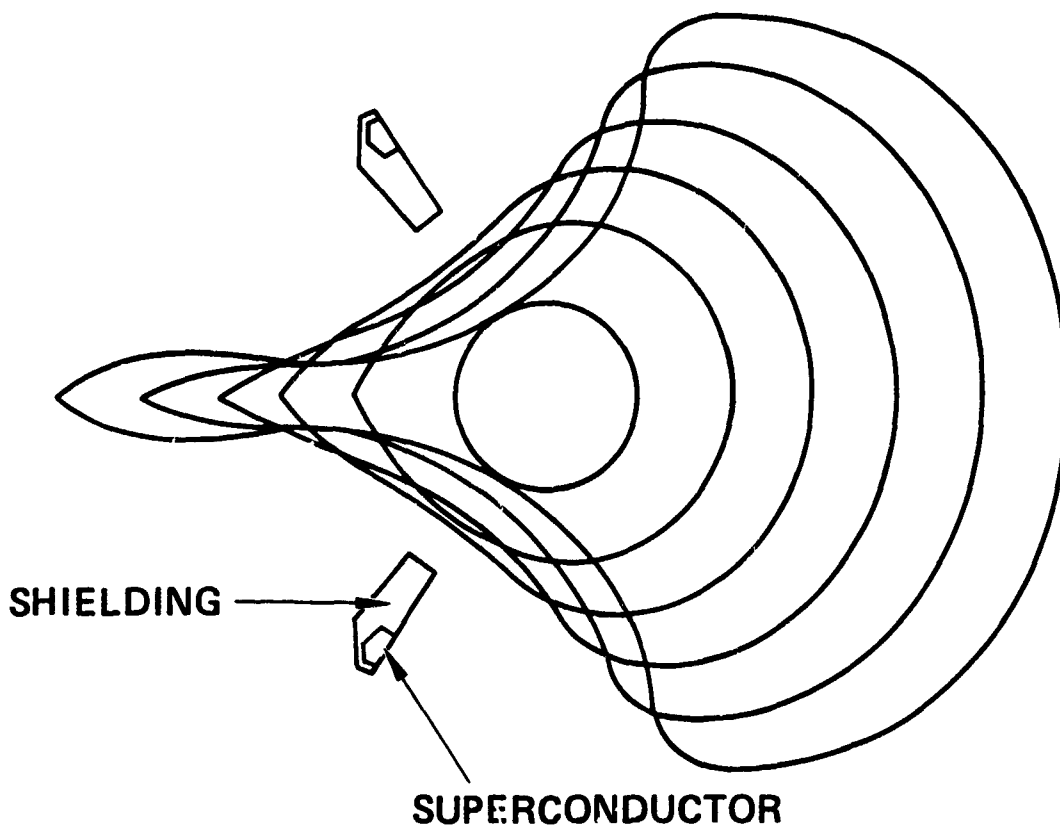
Fig. 7-10 Magnetic nozzle for microexplosion plasmas.

SECTION 8

ANTIMATTER MISSION STUDIES

The availability of antimatter as an energy source for space
propulsion will revolutionize the subject of mission analysis.
Many of the present assumptions that are implicit in the
design of a mission will no longer be valid, and mission
designers will have to develop a new set of assumptions to
replace them.

For example, the concept of mass ratio and staging mass
fractions plays an important part in the present design of
missions. Once a mission has been defined, there is a certain
characteristic velocity ΔV for that mission and once the fuel
is chosen, there is a fixed exhaust velocity v available from
that fuel. The total mission mass ratio R is then
automatically determined by the relation:

$$8.1) \qquad R = \frac{m_v + m_p}{m_v} = e^{\Delta V/v} = e^{\Delta V/g I_{sp}}$$

where m_v is the mass of the empty vehicle (including
payload) delivered to the destination and m_p is the mass of
the propellant exhausted at velocity v or specific impulse
I_{sp}, and $g=9.8$ m/s^2.

Thus, every different mission with a different characteristic
velocity requires a different mass ratio and a different
vehicle design. Also, if the mission characteristic velocity
starts to exceed five times the exhaust velocity, the mass
ratio starts to become greater than 100, and there is a
tendency to say that the mission is "impossible".

With antimatter powered rockets, the exhaust velocity can be
tailored to match the mission characteristic velocity, thus
minimizing the mass ratio and mission cost. As we shall see
in the next subsection, the mass ratio of an antimatter rocket
never exceeds 5:1, and mass ratios that minimize total mission
cost are typically 2.5:1 for any mission characteristic
velocity. Thus, the same vehicle can be used for all
missions, with the only difference being the amount of
antimatter used.

Another implicit assumption used by mission planners is that a high specific impulse automatically implies low thrust and long mission times. This is because present solar and nuclear electric systems are power limited by the heavy weight of their power source and the power density limitations of their thrusters. Long missions at high specific impulse may save money in lower mass ratios, but they are expensive in terms of ground support time and extra vehicle mass to insure crew health and safety.

Antimatter rockets are not inherently limited in their thrust levels. Assuming that new engines will be designed that can handle the antimatter, high thrust can be obtained at any specific impulse. With antimatter rockets, mission trajectories will no longer be modified Hohmann transfers, but nearly straight lines. Manned missions to Mars will no longer take years of time, but months of time, with significant savings in initial vehicle mass and ground support costs.

8.1 MINIMUM ANTIMATTER OPTIMIZATION

In this subsection, we will outline a mathematical proof for the optimization of an antimatter powered rocket mission in which the amount of antimatter used is minimized. The proof is simple, but has only been documented in journals[8.1] and reports[8.2] that are somewhat difficult to obtain, so we will repeat it here.

In an antimatter rocket, the source of propulsion energy is separate from the propellant or reaction fluid. Thus the total initial mass of the vehicle consists of the empty mass of the vehicle m_v, the mass of the reaction fluid m_r, and the mass of the energy source m_e, half of which is the mass of the antimatter m_a that we wish to minimize. The mass ratio is then:

$$8.2) \quad R = e^{\Delta V/v} = \frac{m_v + m_r + m_e}{m_v} .$$

The exhaust energy comes from the conversion of the energy source rest mass to kinetic energy with an efficiency e.

$$8.3) \quad e\,(m_e c^2) = \frac{1}{2}\,(m_r + m_e) v^2$$

130

Combining Equations 8.2 and 8.3 and rearranging we obtain:

$$8.4) \qquad m_e = \frac{m_v \, v^2}{2 \varepsilon \, c^2} \, (e^{\Delta V/v} - 1) = \frac{k}{x^2} \, (e^x - 1)$$

where $x = \Delta V/v$ and $k = m_v \Delta V^2 / 2 \varepsilon c^2$.

We now make the assumption that the antimatter costs dominate the reaction fluid costs and we want to minimize the amount of antimatter. By setting the derivative of Equation 8.4 with respect to x equal to zero and solving for x, it can be shown[8.1, 8.2] that the amount of antimatter is minimized when:

$$8.5) \qquad v = 0.63 \, \Delta V \quad .$$

This means that the mass ratio is a constant.

$$8.6) \qquad R = e^{\Delta V/v} = e^{1.59} = 4.9$$

Amazingly enough, this constant mass ratio is independent of the efficiency of the energy conversion, the mission characteristic velocity, and the molecular weight of the reaction fluid used. This constant mass ratio for minimum antimatter consumption holds for all conceivable missions in the solar system and only starts to deviate for interstellar missions where the mission velocity starts to approach the speed of light.[8.3]

The amount of antimatter needed for a specific mission is obtained by substituting Equation 8.5 into 8.4. It is found to be a function of the square of the mission characteristic velocity ΔV^2 (essentially the mission energy), the empty mass of the vehicle m_v, and the conversion efficiency ε:

$$8.7) \qquad m_a = \frac{1}{2} \, m_e = \frac{0.39}{\varepsilon} \frac{\Delta V^2}{c^2} \, m_v \quad .$$

For a typical antimatter mission, where the efficiency of conversion of antimatter energy to thrust is 0.32, only 120 mg of antimatter is needed to heat 39 metric tons of reaction fluid to an exhaust velocity of 19 km/s, which will suffice to accelerate a 10 ton vehicle to 30 km/s (0.0001 c). Thus, no matter what the mission, the vehicle will always use 3.9 tons of reaction fluid for each ton of vehicle and an insignificant amount (by weight, not cost) of antimatter.

131

References:

[8.1]L.R. Shepherd, "Interstellar flight," J. British Interplanetary Soc. **11**, 149-167 (1952).

[8.2]D.F. Dipprey, "Matter-Antimatter Annihilation as an Energy Source in Propulsion," Appendix in "Frontiers in Propulsion Research," JPL TM-33-722, D.D. Papailiou, Editor, Jet Propulsion Lab, Pasadena, CA 91109 (15 March 1975).

[8.3]B.N. Cassenti, "Optimization of relativistic antimatter rockets," J. British Interplanetary Soc., **37**, 483-490 (1984).

8.2 MINIMUM FUEL COST OPTIMIZATION

If instead of minimizing just the antimatter cost, we minimized the total fuel cost (the cost of the antimatter energy source plus the cost of the reaction fluid), we would find a new mass ratio optimum. This is because reaction fluid is not low cost once it has been lifted into low earth orbit.

An analysis was carried out (see Appendix B) to determine the optimum mass ratio for various missions. A typical result is shown in Figure 8-1. In this figure, we see that depending upon the relative cost of antimatter per milligram and reaction fluid per ton, the optimum mass ratio for minimum fuel cost will vary from 2:1 to 4:1, but will never be greater than 5:1. This compares favorably with the mass ratios for even the best chemical fuel, liquid hydrogen/liquid oxygen. For a H_2/O_2 chemical rocket the mass ratio rises exponentially with the mission characteristic velocity, exceeding 100:1 at 23 km/s and 1000:1 at 35 km/s.

Thus, mission analysts need to rethink those missions that have been labeled "impossible" because of the extreme mass ratios required using a chemical or nuclear system with a fixed specific impulse. Also, with these low mass ratios for antimatter propulsion, it may be beneficial to include other costs in the optimization, such as ground support costs and crew comfort and safety costs. Under such conditions, it may turn out to be more cost effective to increase the antimatter mass slightly and carry out the mission faster.
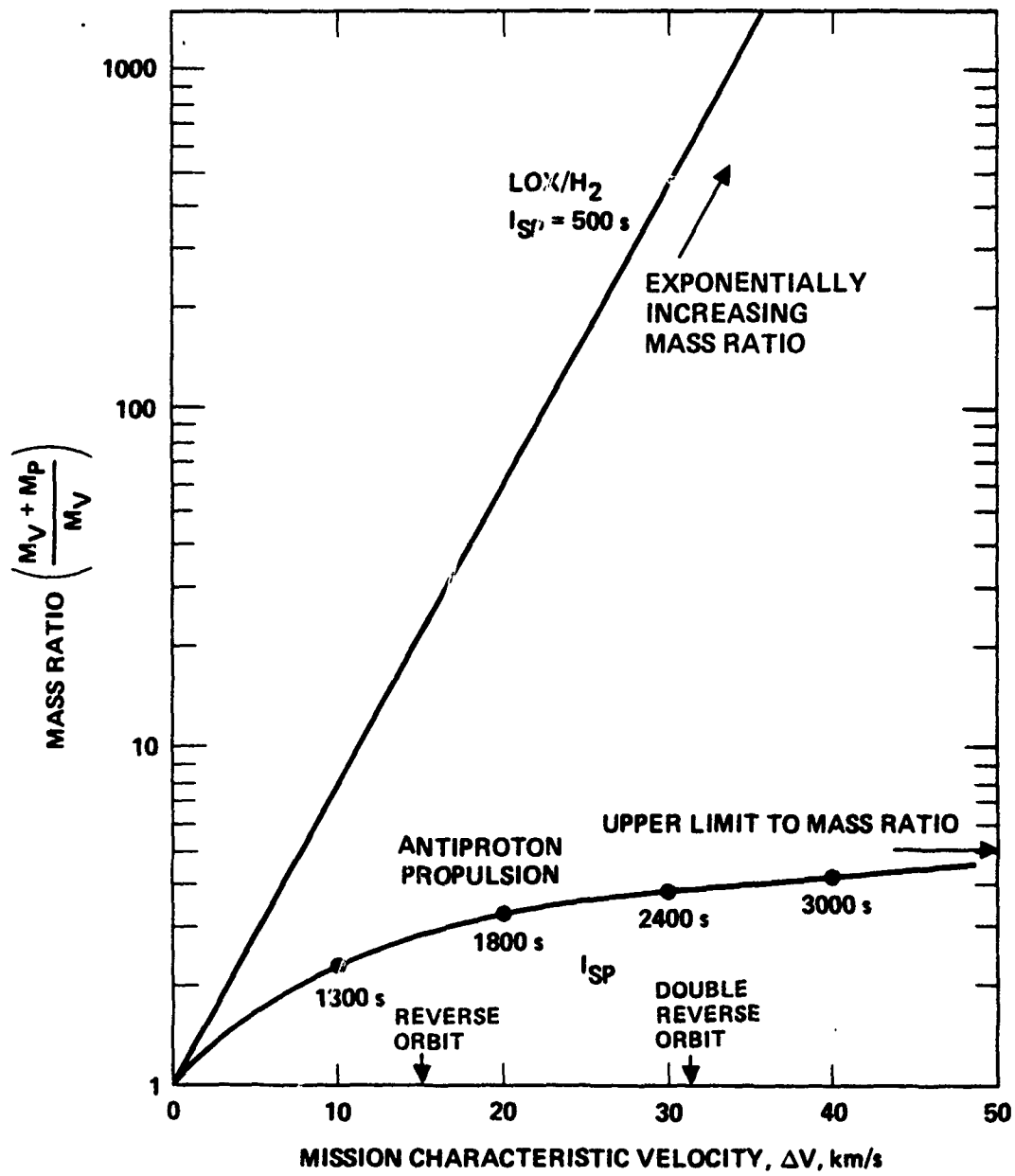
Fig. 8-1 Chemical and antimatter rocket mass ratios.

133

8.3 IMPOSSIBLE MISSIONS

There are missions in the solar system that would be desirable to accomplish for scientific purposes, but which are essentially impossible using chemical or even nuclear thermal rockets. One example is a solar impact mission, which requires the rocket to cancel out the orbital velocity of the earth so the vehicle can drop directly into the sun. This requires a mission characteristic velocity of 35 km/s, which is presently obtained by an out-of-the-way swingby of Jupiter, 5 AU and many years in the wrong direction. Another is a mission to the rings deep down in the gravity well of Saturn. This requires a mission characteristic velocity of 48 km/s.

There are even much simpler missions near earth that are nearly impossible using chemical rockets. One is the simple maneuver of rapidly reversing your orbital direction. This maneuver requires cancelling the initial orbital velocity and building it up again in the opposite direction. Since earth orbital velocity is 7.7 km/s, the total mission characteristic velocity of the reverse orbit maneuver is 15.5 km/s. If it is then desired to return to the initial orbit (to dock at an orbiting space station base), the process must be repeated with a total mission characteristic velocity of 31 km/s.

The mass ratios required for each type of rocket system to carry out each of these missions can be calculated from Equation 8.1. They are listed in Table 8-1. As can be seen, all of these mission require high mass ratios, with the more difficult ones requiring such large mass ratios that it is difficult, if not impossible, to imagine how one might build a vehicle to accomplish those missions using chemical or nuclear thermal rockets. All of those missions could be performed by an antimatter rocket with a mass ratio of 5:1 or less.

Table 8-1   Mass Ratios for Difficult Missions

	$I_{sp}=$ ΔV(km/s)	Total Mass Ratio		
		Storable 300 s	H_2/O_2 500 s	Nuclear 900 s
Reverse Orbit	15.5	175	22	6
Double Reverse Orbit	31	30,700	490	32
Solar Impact	35	117,000	1,100	49
Saturn Ring Rendezvous	48	8,900,000	15,000	200

134

8.4 COMPARATIVE COST STUDIES

We will now use the rocket equations to determine the total
fuel cost for a number of different propulsion systems. For
both storable and cryogenic chemical propulsion systems the
mass of the energy source is in the propellant. Thus the fuel
cost for the chemical rocket is just the cost of the
propellant mass in orbit.

For the case of a nuclear thermal rocket, the energy to heat
the reaction fluid is in the nuclear reactor. A reactor has
to have a certain minimum charge of uranium just to operate
and therefore carries much more uranium than will be used in
any reasonable mission. Therefore, we have assumed that the
mass and cost of the uranium is charged to the empty vehicle
mass and cost. The fuel cost for the nuclear thermal rocket
will just be the cost of the reaction fluid in orbit.

For the case of an antimatter rocket, the cost of the
antimatter part of the energy source is not negligible. The
total fuel cost for the antimatter rocket will be the cost of
the antimatter mass used plus the cost of the reaction fluid
in orbit.

8.4.1 Fuel Cost of a Chemical or Nuclear Thermal Mission.

The fuel cost C_c of a mission using a chemical or nuclear
thermal rocket system is the price of propellant or reaction
fluid per kilogram in low earth orbit p_p times the amount of
propellant or reaction fluid needed for the mission.

8.8)
$$C_c = p_p\, m_p$$
$$= p_p\, m_v\, (R - 1)$$
$$= p_p\, m_v\, (e^{\Delta V/v} - 1) \quad .$$

Since chemical and nuclear thermal propulsion systems have a
fixed specific impulse or exhaust velocity, we see from
Equation 8.8 that the cost of any chemical or nuclear thermal
rocket system rises exponentially with increasing mission
characteristic velocity as soon as the mission velocity
exceeds the exhaust velocity.

8.9)
$$C_c \xrightarrow{\Delta V > v} p_p\, m_v\, e^{\Delta V/v} .$$

135

8.4.2 Fuel Cost of an Antimatter Powered Mission

The fuel cost C_a of an antimatter powered mission consists of the price of the antimatter p_a times its mass m_a, plus the price of the reaction fluid p_r times its mass m_r.

$$8.10) \qquad C_a = p_r \, m_r + p_a \, m_a$$

In an antimatter rocket, the propulsion energy comes from the annihilation of the antimatter with a small amount of normal matter in the reaction fluid. The energy is twice the rest mass energy of the antimatter. Some fraction ϵ of the annihilation energy is then converted into kinetic energy of the reaction fluid.

$$8.11) \qquad 2\epsilon \, m_a \, c^2 = \frac{1}{2} \, m_r \, v^2 \qquad .$$

Substituting Equation 8.11 into Equation 8.10 we obtain:

$$8.12) \qquad C_a = (p_r + p_a \, \frac{v^2}{4\epsilon \, c^2}) \, m_r$$

$$= (p_r + p_a \, \frac{v^2}{4\epsilon \, c^2}) (e^{\Delta V/v} - 1) \, m_v \qquad .$$

Equation 8.12 can be used to find a cost minimum for an antimatter rocket. As the required mission ΔV increases, the cost of the mission tends to increase exponentially, since the amount of reaction fluid needed is rising exponentially, just as in a chemical rocket. In an antimatter rocket, however, this exponential rise in reaction fluid can be curbed by using more antimatter and increasing the reaction fluid exhaust velocity. How much more antimatter we use depends upon the relative price of antimatter and reaction fluid. For low exhaust velocity the second term becomes large, while at high exhaust velocity the first term becomes large. Thus, there is a cost minimum for each mission ΔV depending upon the relative price of reaction fluid and antimatter.

We were not able to find a simple analytic solution to the minimization of Equation 8.12 when the relative costs of the antimatter and the reaction fluid were comparable. Instead, a computer was used to calculate the total fuel cost, mass ratio, and antimatter mass used, as a function of the mission characteristic velocity over a range of exhaust velocities and relative fuel costs. The minimum in the total fuel cost was found on the computer printout and this determined the optimum values for the other quantities.

An important parameter in these parametric studies is the
ratio of the price of antimatter to the price of reaction
fluid in orbit. To be completely general, we should have
plotted the following curves in terms of a dimensionless price
ratio. Since the price ratios vary from 10^{10} to 10^8, however,
they are so large they are almost meaningless at first glance.
Instead, we fixed the price of reaction fluid or propellant in
orbit at the present day price of 5k$/kg and presented the
parametric curves in terms of the price of antimatter per
milligram. Thus, a curve which is labeled 5M$/mg is
equivalent to a relative price ratio of:

$$8.13) \qquad \frac{5M\$/mg}{5k\$/kg} = 10^9$$

8.4.3 Comparative Total Fuel Costs.

We next calculated the total fuel costs for a number of
different propulsion systems and compared the total fuel costs
as a function of mission characteristic velocity. The
propulsion systems considered were a storable chemical
propulsion system with a specific impulse of 300 s, a
cryogenic H_2/O_2 chemical propulsion system with a specific
impulse of 500 s, a nuclear thermal rocket system with a
specific impulse of 900 s, and three antimatter systems that
were optimized for lowest total fuel cost as a function of the
price of the antimatter.

Figure 8-2 shows the range of mission velocities that are
characteristic of present missions. The relative fuel cost
can be converted directly into millions of dollars per ton of
empty vehicle mass if chemical fuel for the chemical rockets
and reaction fluid for the nuclear and antimatter rockets is
assumed to cost 5k$/kg and the antimatter price is that
indicated for the various antimatter curves.

In examining Figure 8-2, we see that if the price of
antimatter can be brought down to 20M$/mg (or a relative cost
ratio of 4×10^9), an antimatter propulsion system is always
more fuel cost effective than a storable chemical propulsion
system. It is also better than the best chemical propulsion
system presently available (H_2/O_2) for any mission
characteristic velocity greater than 12 km/s. At a price of
10M$/mg (or a relative cost ratio of 2×10^9), antimatter
propulsion systems are better than any chemical propulsion
system at any mission velocity, but are not as cost effective
as nuclear thermal propulsion. If the price of antimatter
drops to 2M$/mg (relative price ratio of 4×10^8), then
antimatter propulsion is more cost effective than any other
known propulsion system at any mission velocity.

137
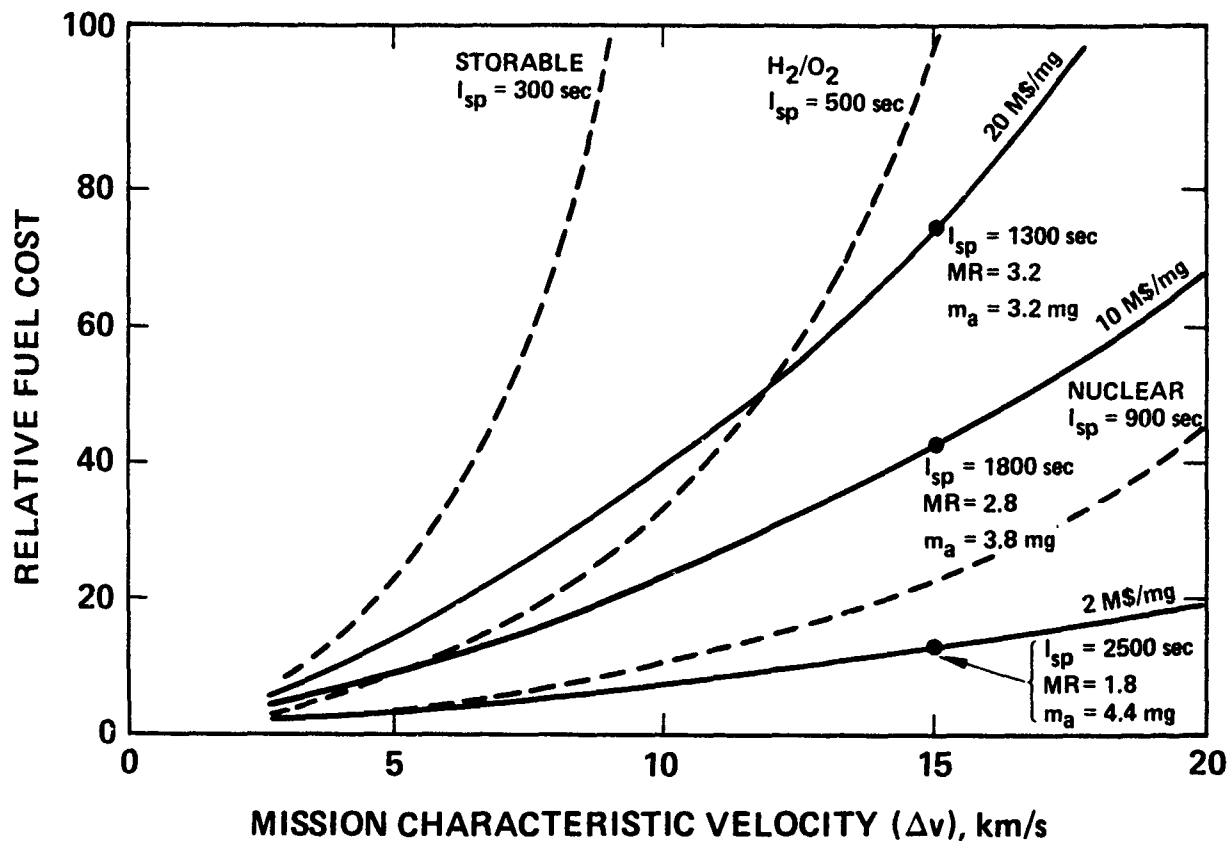
Fig. 8-2 Relative fuel cost vs. mission velocity.

Also shown in Figure 8-2 are some typical operational
parameters for a mission requiring a total velocity change of
15 km/s. At an antimatter price of 20M$/mg, to reach 15 km/s,
each ton of empty vehicle requires 3.2 mg of antimatter
costing 64M$ to heat 2.2 metric tons of reaction fluid costing
11M$ to a specific impulse of 1300 s. Thus, a vehicle can be
pushed to 15 km/s by an antimatter propulsion system for a
total fuel cost of 75M$ per ton of empty vehicle mass, while
to do the same job with a H_2/O_2 rocket would cost 100M$/T.

If the price of antimatter drops to 2M$/mg, then each ton of
delivered vehicle mass would require the use of 4.4 mg of
antimatter costing 8.8M$ to heat 0.8 tons of reaction fluid
costing 4M$ to a specific impulse of 2500 s. At this price
for antimatter, the total fuel cost to reach a velocity of
15 km/s would be only 12.8M$/T.

8.4.4 Antihydrogen Propulsion Enables "Impossible" Missions

In Figure 8-3 we broaden the range of the plot of relative fuel cost versus mission characteristic velocity to a scale that includes missions that are "impossible" using any chemical or nuclear thermal system. In Figure 8-3, the relative fuel cost scale can be converted into millions of dollars by assuming that the vehicle to be delivered has an empty mass of 5 metric tons and the cost of propellant or · reaction fluid in space is 5k$/kg or 5M$/T.

In this figure it is easier to see the differences in the shapes of the total fuel cost curves for the different types of propulsion systems. For those propulsion systems with a fixed specific impulse, the fuel cost rises exponentially with increasing mission characteristic velocity. Since the antimatter propulsion systems can vary the exhaust velocity to match the mission, the total fuel cost for an antimatter propulsion system only rises as the square of the mission characteristic velocity.

Thus, no matter what the cost of antimatter turns out to be, it will always be more cost effective than any propulsion system with a fixed exhaust velocity at sufficiently high mission velocity. For example, even at 10M$/mg, an antimatter propulsion system will cost less than a nuclear thermal rocket if the mission characteristic velocity desired is greater than 30 km/s (just off the top of Figure 8-3). If the price of antimatter can be brought down to 1M$/mg or less, then antimatter propulsion can open up the entire solar system and allow the performance of missions that are now impossible using any present propulsion system.

As a result of these comparative cost studies we find that if research on antiproton propulsion were successful in reducing the cost of antimatter to 10M$/mg or below, then antiproton annihilation would become a cost effective propulsion technique, in addition to reducing the size of the using vehicle. Thus, the primary objective of any antiproton propulsion research program should be to find cost effective, energy-efficient methods for making, controlling, and storing antimatter.

Once the research studies on the production and handling of antimatter have been completed, some 10 to 15 years from now, a reasonably firm estimate can be made of the cost of antimatter per milligram. If the cost estimate for antimatter is low enough that it is seen as a cost effective fuel for space propulsion, then the Air Force can, at that time, commit the major amounts of money needed for the design and fabrication of a special facility to produce milligram quantities of antimatter for propulsion.

139

HIGH THRUST, RAPID RESPONSE (NO ELECTRIC PROPULSION) ANY CHEMICAL FUEL COSTS 5 M$/T IN LEO
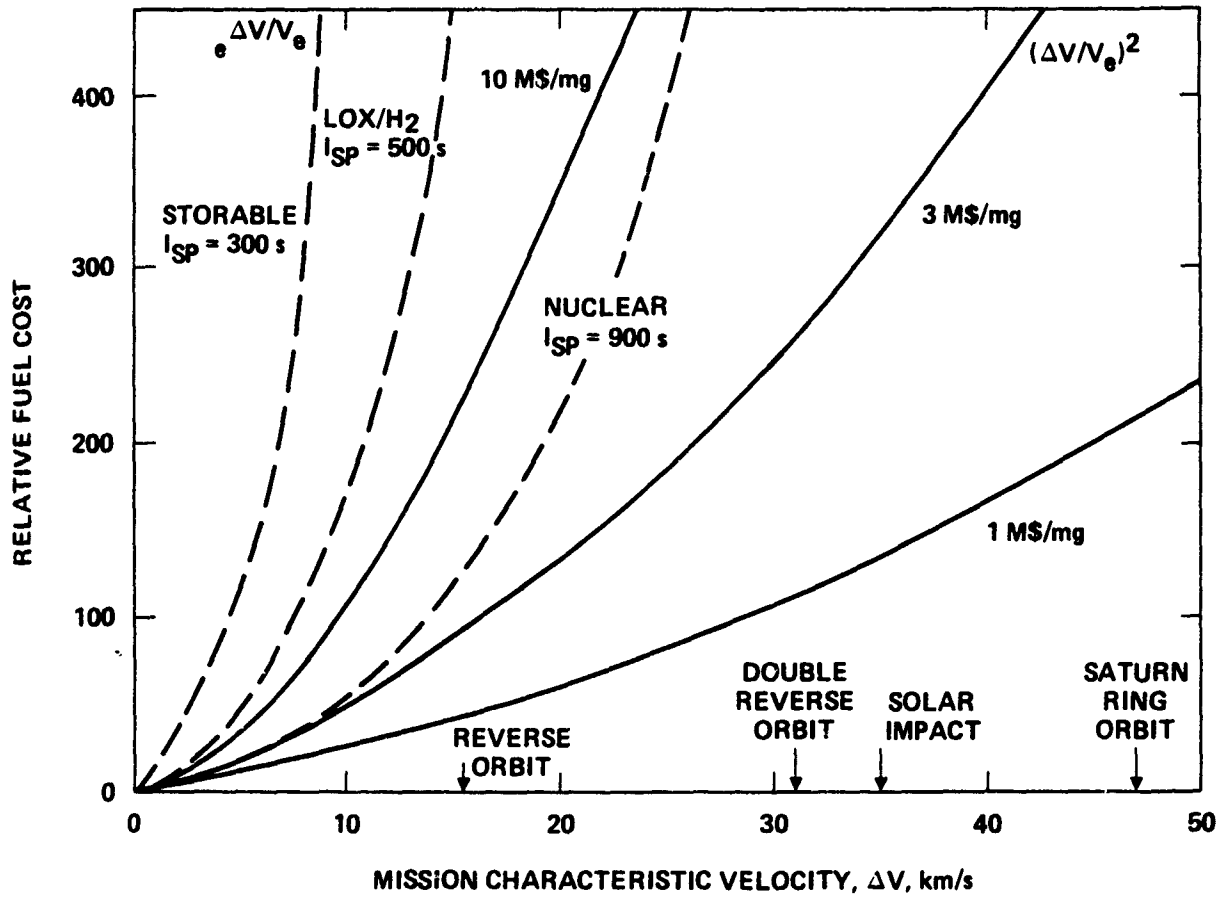
Fig. 8-3 Relative fuel c   .. expanded mission velocity.

SECTION 9

CONCLUSIONS AND RECOMMENDATIONS

9.1 CONCLUSIONS

The fundamental conclusion of this study is that antiproton
annihilation propulsion is feasible but expensive.

Because of the probable high expense, antiproton propulsion is
probably not cost competitive for propulsion on the earth's
surface or from earth to low earth orbit. It may, however, be
cost competitive for propulsion in space where any fuel is
expensive.

If antiproton annihilation propulsion could be made available
at a reasonable cost, it would revolutionize space travel and
would enable missions that are now deemed "too difficult" or
"too expensive" or "impossible" with present day propulsion
technology. Many of these difficult missions, such as a
simple sortie to inspect a spacecraft moving in the opposite
direction and returning to base, are exactly those missions
the Air Force may be called upon to carry out if there is a
future requirement for a manned military presence in space.

The present techniques for generating, capturing, cooling,
trapping, and using antiprotons are exceedingly inefficient.
Thus, the major thrust of antiproton propulsion research in
the near future should be on studies to determine the reasons
for the present low efficiencies, to develop methods for
improving those efficiencies, and to demonstrate
experimentally that the predicted efficiencies can be reached
at reasonable production rates and at reasonable cost.

9.2 RECOMMENDED RESEARCH INVESTIGATIONS

In this section we list some recommended investigations that
involve basic and applied research on the properties of
antimatter and the interaction of antimatter with fields and
particles. Many of these studies can be carried out using
normal matter instead of antimatter.

141

9.2.1 Trapping of Antiproton Ions

Antiprotons at low energy are available at the Low Energy
Antiproton Ring (LEAR) at CERN. It is recommended that
research be supported on techniques to slow the LEAR
antiprotons down and capture them in a Penning trap. This
research will result in the determination of the gravitational
and inertial mass, charge, spin, and lifetime of the
antiproton, and will provide a determination of the vacuum
level possible in a cryogenically cooled vacuum chamber.

9.2.2 Antiproton Production Spectrum

The absolute number of antiprotons produced from the
interaction of high energy protons with heavy metal targets is
probably not known to better than a factor of two. It is
recommended that experimental research be supported to measure
the antiproton production spectrum in energy and angle as a
function of the proton energy and the target parameters. The
proton energy range should cover from 26 GeV (the CERN energy)
to greater than 200 GeV. The only machine capable of carrying
out the experiments at the higher energies is the 400 GeV Main
Ring at Fermilab. If theoretical studies indicate that there
may be some benefit, the measurements should be repeated using
polarized protons and targets. This research will produce the
basic data needed to determine the maximum expected production
efficiency (and therefore minimum expected cost) of the
antiprotons. It will also aid in the engineering design of
the magnetic lenses and collector rings to capture the
antiprotons.

9.2.3 Annihilation Cross Sections at Low Energy

The annihilation cross section of an antiproton with protons,
hydrogen, and heavier atoms depends more on the Coulomb
interaction than on the nuclear interaction. It is
recommended that theoretical and experimental studies be
supported on the annihilation cross sections of antiprotons,
antihydrogen atoms, and antihydrogen molecules with various
nuclei at very low energies. This research will produce the
basic data needed to determine the "injection" and "ignition"
parameters for an antiproton annihilation rocket engine.

9.2.4 Annihilation Product Production Spectrum

When an antiproton annihilates with a proton, the reaction
products are typically 3 to 5 pions with an average kinetic
energy of 250 MeV, but the exact production spectrum is not
well known. The production spectrum for the annihilation of

142

an antiproton with heavier nuclei is even less known. It is
recommended that theoretical and experimental studies be
supported to determine the number and momentum spectrum of the
products from the annihilation of antiprotons and antihydrogen
with various nuclei. After the initial studies have been
completed to determine the number, energy, direction, and
lifetime of the various reaction products for unpolarized
antiparticles and particles, the research effort should be
expanded to study the effect of polarized antimatter and
polarized targets on the annihilation cross section and
production spectrum. This research will produce the basic
data needed to determine the "combustion" and "mixing"
parameters for an antiproton annihilation rocket engine.

9.2.5 Formation of Antihydrogen

Antihydrogen atoms can be formed by the spontaneous
recombination of antiprotons with positrons, and antihydrogen
molecules can be formed by the spontaneous recombination of
two antihydrogen atoms. It is recommended that theoretical
and experimental research be supported on these recombination
processes to determine the detailed mechanisms, rates, and
final states. This research could then be expanded to study
methods to enhance the rates or control the final states using
photons, fields, or other antimatter particles. Most of the
experimental work could be carried out using normal matter.
This research will produce the basic data needed to determine
the optimum method for conversion of antiprotons into ground
state antiparahydrogen with minimum loss and maximum
efficiency.

9.2.6 Slowing, Cooling, and Trapping of Antihydrogen

Lasers have been used to slow, cool, and stop a beam of sodium
atoms, and plans are underway to use lasers to trap a
collection of sodium atoms. It is recommended that
theoretical and experimental research be carried out on the
slowing, cooling, and trapping of both atomic and molecular
antihydrogen. The probable method will involve the use of a
tunable coherent source of ultraviolet photons, but other
techniques for slowing, cooling, and trapping using fields or
cold positrons should also be considered. In most cases, the
experimental studies can be carried out using normal matter.
The slowing, cooling, and trapping of molecular hydrogen is
recommended as a research project to be carried out at AFRPL.
It is discussed in further detail in Section 9.4. This
research will produce the basic data needed to determine the
optimum method for controlling and storing antihydrogen
without touching it with normal matter.

9.2.7 Crystal Nucleation from Antihydrogen Vapor

The techniques for slowing, cooling, and trapping of antihydrogen should produce a relatively dense gas of antiparahydrogen at a few millidegrees Kelvin. It would be desirable from a storage point to condense the gas into a solid. It is recommended that theoretical and experimental research be carried out on the molecular interaction mechanisms that will allow the nucleation of an antihydrogen crystal or amorphous solid from the vapor. The research should study the role of charged ions of antihydrogen in acting as nucleation sites and look at mechanisms for removing the latent heat of fusion energy from the resultant solid. The research should also identify the experimental parameters that control the crystal size and the final temperature of the solid. This research will produce the basic data needed to design the "fuel tanks" for the antiproton annihilation propulsion system.

9.2.8 Magnetic Properties of Antihydrogen

The magnetic susceptibility of gaseous and solid antihydrogen is predicted by theory to be negative with a strength two-thirds that of graphite. It is recommended that experimental measurements be carried out to determine the magnetic susceptibility of parahydrogen as a function of the temperature, density, physical state, and orthohydrogen impurity content. This research will produce the basic data needed to determine the feasibility of passive magnetic levitation for the antihydrogen "fuel tanks" in the antiproton annihilation propulsion system.

9.2.9 Levitation of Antihydrogen

Macroscopic particles have been levitated by electric fields, magnetic fields, and photon fields. All three levitation techniques should also be usable on antihydrogen. It is recommended that experimental studies be carried out of the levitation of normal matter parahydrogen ice by active feedback electrostatic fields and passive magnetic fields. The experiments should determine the optimum levitation parameters as a function of the field strength, the trap parameters, and the size, shape, surface charge, and composition of the parahydrogen. These studies will produce the engineering data needed to design the antihydrogen "fuel tanks" for an antiproton annihilation propulsion system.

144

9.3 RECOMMENDED ENGINEERING STUDIES

In this section we list some design and system studies that will generate a first cut at the operational parameters of an antimatter propulsion system. Antimatter is a synthetic fuel and present estimates of the production efficiency indicate that it is going to be an expensive synthetic fuel. Since the practical feasibility of the use of antimatter for propulsion depends strongly on the cost of the fuel, it is important, early in the program, to get estimates of the upper bound on the efficiency of production and utilization of antiprotons for propulsion. We will need studies of the "refining plant" that will manufacture the fuel, the rocket engines that will "burn" it to produce thrust, the new vehicles with their relatively small matter and antimatter "fuel tanks" that will use the engines, and the possible and "impossible" missions that can be carried out using these new vehicles.

9.3.1 Antiproton Factory Design

CERN, Fermilab, and IHEP have shown by a number of different techniques how to make, capture, cool, and store low intensity beams of antiprotons. It is recommended that an engineering study of the design of an antiproton "factory" be supported. This would involve the preliminary design of highly efficient high current proton accelerators, optimized target designs, new multilens arrays of magnetic collector lenses, stacks of collector rings, efficient stochastic and electron cooling rings, coherent decelerators that slow the antiprotons down and extract energy in the process, and closed-cycle beam dumps that extract energy from the particles that are not antiprotons. The objectives of the study would be to maximize the antiproton production rate and maximize the overall energy efficiency. The initial goal would be the design of a prototype factory that could produce a few milligrams of antiprotons a year for initial propulsion studies. Later designs would take into account physical limitations such as space charge or target destruction to design a factory "module" that is optimized in size to attain maximum efficiency. Higher production rates would then be attained by adding modules to the production facility.

9.3.2 Antiproton Annihilation Engine Design

Antimatter fuel is so powerful that new types of rocket engines will have to be developed to fully utilize its potential. This requirement for new rocket engine designs is not unique to antimatter propulsion. Any new form of propulsion that gives high thrust at high specific impulse (I_{sp} of 1000 s to 5000 s) will require the development of new

145

types of reaction chambers and nozzles that can contain and
direct a hot plasma without direct contact with material
walls. The best known technique for handling plasmas involves
the use of magnetic fields to guide and contain the charged
particles in the plasma. It is recommended that design
studies be supported on rocket engines that use magnetic
fields to assist in the containment of the plasma working
fluid. Both the magnetic "bottle" and "picket fence"
geometries should be studied along with the standard
regenerative cooling and film cooling concepts. Studies are
needed on the extraction of the antimatter from the "fuel
tank" and the "injection" of the jet of antimatter fuel at low
enough relative kinetic energy into the jet of ignition nuclei
so that rapid "ignition" takes place. Then the "mixing" of
the annihilation products with the working fluid needs study
to determine the optimum ignition nuclei and working fluid,
the optimum pressure, temperature, and density inside the
reaction chamber, optimum nozzle parameters, and optimum
magnetic field configuration. The effects on the engine
structure of the gamma rays and those charged pions that
escape the chamber also need to be included. The results of
this study should give relationships between the various
operational parameters of the rocket such as the size and
weight of the engine, the specific impulse, the thrust to
weight, and the efficiency of conversion of annihilation
energy into thrust.

9.3.3 Antiproton Annihilation Vehicle Design

Theoretically, the mass ratio of an antimatter rocket never
exceeds 5:1 and a vehicle for most solar system missions would
have a mass ratio of 2.5:1. It is recommended that
preliminary studies be supported on the design of a vehicle
that uses an antiproton annihilation rocket for propulsion.
The design effort would study the interaction of the various
parameters such as mass ratio, specific impulse, mission
characteristic velocity, thrust to weight, choice of reaction
fluid, tankage fraction, shielding, crew safety, and
antimatter storage on each other. The goal would be the
preliminary design of an antiproton annihilation powered
vehicle that could carry out most of the missions that it
would be desirable to do with an antimatter rocket.

9.3.4 Antimatter Powered Mission Design Studies

In Section 8 it was estimated that if the cost of antimatter
could be lowered to 10M$/mg, then antiproton annihilation
propulsion could be a cost-competitive method of propulsion
for the more difficult space missions of interest to the Air
Force and NASA. It is recommended that these studies be
expanded to include more realistic mission scenarios and

146

orbital parameters, a broader range of competing propulsion
systems, more realistic cost and weight estimates for vehicles
using different types of propulsion methods, more realistic
price estimates for reaction mass and chemical propellants as
delivered to LEO, and additional cost parameters such as
ground support costs and crew safety and health costs. The
objective of the studies would be to determine when antimatter
propulsion becomes more cost effective than competing forms of
propulsion as a function of the price of the antimatter and
the type of mission.

9.4 RECOMMENDED AFRPL IN-HOUSE RESEARCH PROJECT

Of the research topics discussed in Section 9.2, it is
recommended that the near-term in-house research project to be
carried out by personnel at the Air Force Rocket Propulsion
Laboratory be the experimental and theoretical investigation
of the slowing and cooling of neutral molecular hydrogen with
multiple photon interactions. The reasons for this
recommendation are as follows:

The project is basic in nature since it investigates the
interaction of intense photon fields with an elementary form
of matter. The intense fields open up new areas of physics
such as "dressed states," where the particles and photons must
be considered as a single system. The multiple vibrational
and rotational levels of each electronic level, plus the
alternate missing rotational levels due to the homonuclear
character of the hydrogen molecule make an investigation of
the physics of the transitions richer than similar
investigations of atoms. The basic nature of the research
makes it suitable for support by the Air Force Office of
Scientific Research.

The Principal Investigator can draw upon the extensive
existing base of knowledge at the National Bureau of Standards
and elsewhere on the slowing and cooling of sodium atoms.
These scientists can supply information on theory and
experimental techniques. The NBS also sponsors annual
workshops and conferences where the Principal Investigator can
maintain contact with the professional community.

Although the proposed research project is _similar_ to ongoing
projects elsewhere in that it uses intense beams of photons to
slow and cool neutral particles, it is significantly _different_
than the existing projects in that it concentrates on the
slowing and cooling of _molecular_ hydrogen. Slow molecules of
hydrogen are of little interest to the atomic hydrogen clock
and neutral atomic hydrogen particle beam weapon community, so
it is doubtful that the research will be carried out by anyone
else before the completion of the research effort at AFRPL.

147

9.5 REQUIRED FACILITIES

To carry out the recommended research program will require the collection and installation of a number of pieces of equipment. Although the specific items will change as new equipment becomes available and as the Principal Investigator defines the details of the exact experiments to be carried out, it is possible to list the equipment types needed for a representative experiment.

9.5.1 Ultra-High Vacuum System

This must be a custom system designed to accommodate the molecular hydrogen beam source at one end and the molecular hydrogen detector at the other end. There should be wide orthogonal VUV ports in the "cooling" region for transverse cooling and provision for inserting VUV radiation as near to the longitudinal axis of the beam as possible for longitudinal slowing and cooling. The VUV ports must be compatible with the tunable VUV photon source. Depending upon the cooling wavelength chosen, the ports may have a transmission window (with its accompanying losses) or the UHV system and the VUV system may have to be pumped down together. In addition there should be additional windows and ports for the insertion of diagnostic photon and electron beams.

9.5.2 Molecular Hydrogen Beam Source

The molecular hydrogen beam source should be a differentially pumped system that will use strong magnetic or electric gradient lenses to separate out the orthohydrogen molecules from the parahydrogen beam. The source should be able to produce a wide range of flow rates, with good control over beam divergence and longitudinal velocity.

9.5.3 Tunable Vacuum Ultraviolet Photon Source

Initial experiments could be done by using a single-frequency VUV laser, such as a molecular hydrogen laser. Ultimately, however, it will be necessary to buy or construct a high-power tunable photon source in the vacuum ultraviolet. Such a source is constructed by photon mixing of lower-frequency photons (at least one of which is tunable) in a nonlinear medium. Watts of power will be needed for a significant demonstration, so the primary laser sources should have kilowatts of peak power with long pulse lengths and high repetition rates. The photon source, especially the VUV output, should be designed to be compatible with the ports in the UHV system.

148

9.5.4 Molecular Hydrogen Diagnostics

The molecular hydrogen detector must be designed to give the velocity profile of the emerging slowed and cooled beam. Since the simulation experiments using normal hydrogen are only to prove that slowing and cooling have taken place, the beam can be disturbed during the diagnostic process. First, any ionized molecules must be diagnosed and removed from the beam by electric fields. Second, any excited molecules must be diagnosed and removed from the beam by diagnostic lasers tuned to interact preferentially with the excited state. Third, any molecules that have been converted to orthohydrogen must be removed by an electric or magnetic field and detected. Finally, the velocity profile of the neutral parahydrogen beam should be obtained. This may involve measurements of raman scattered photons, or excitation of an intermediate state by a frequency swept laser beam that picks molecules with a specific velocity, followed by another laser photon that produces an ionized molecule that is swept out by electric fields and counted. To carry out these diagnostic functions, it will be necessary to have a number of high quality laser sources and detectors for photons, electrons, and hydrogen.

9.6 AREAS OF CONCERN

During the study, some specific technological areas were uncovered where there may be a "show stopper". These are listed below. In assigning priorities, it would be important to make sure that these questionable areas are studied first. For if a major problem is uncovered in one of these areas that cannot be worked around, it may be concluded that antiproton annihilation propulsion is not feasible or is too costly, and it would be best if the research resources were used to study other topics.

The formation of antihydrogen ice crystals from a cold molecular hydrogen gas involves the production of heat from the latent heat of fusion. To carry this heat away requires a third body. When freezing hydrogen, this third body is usually the wall of the experimental chamber. It may be found impossible to force supercooled antihydrogen gas to nucleate.

Antihydrogen ice must be kept below 2 K to keep its vapor pressure low enough so that the antihydrogen molecules sublimating from its surface do not heat up the storage chamber walls. It may be found that radiation cooling to the cold chamber walls is not adequate for extracting heat from the ice generated by unavoidable heat leaks, and no other cooling technique works.

The present techniques for generating antiprotons in a target
with a high-energy proton beam and capturing them with
magnetic lenses and collecting rings are extremely
inefficient. It may be found impossible to engineer the
design of efficient proton accelerators, magnetic lenses, and
accumulator rings to raise the overall energy efficiency from
10^{-9} to the desired 10^{-4}. At 10^{-4} efficiency, antiprotons
cost 10M$/mg and antiproton annihilation propulsion is barely
cost effective. At 10^{-5} efficiency, antiprotons would cost
100M$/mg and there would be only limited use for antiproton
propulsion systems.

Antihydrogen annihilation propulsion only gives maximum
benefits to a military space program when the rocket engines
are operated at high thrust with specific impulses from 1000
to 3500 s. At these specific impulses the working fluid is a
hot ionized gas. It may be found to be impossible to design
and construct a reaction chamber and rocket nozzle that can
contain the pressures required to extract the energy from the
annihilation products and at the same time survive the heat
and radiation.

SECTION 10

ANTIPROTON ANNIHILATION PROPULSION BIBLIOGRAPHY

This section contains a partial listing of the bibliographic
references that were collected and read during this study as
well as pertinant bibliographic references collected from the
list of references in those papers. For the convenience of
the reader, the bibliography is grouped into three major
topics: 10.1 Production of Antiprotons and Antihydrogen, 10.2
Slowing, Cooling, and Trapping of Ions, Atoms, and Molecules,
and 10.3 Antimatter Annihilation and Propulsion.

10.1 PRODUCTION OF ANTIPROTONS AND ANTIHYDROGEN

V.V. Abramov, et al., "Production of hadrons with transverse
momentum 0.5-2.5 GeV/c in 70-GeV proton-nucleus collisions,"
Sov. J. Nuclear Phys. **31**, 343-346 (1980).

A.I. Ageyev, et al., "The IHEP accelerating and storage
complex (UNK) status report," pp. 60-70, Proc. 11th Int. Conf.
High Energy Accelerators, Geneva (1980).

H. Aihara and TPC Collaboration, "Charged hadron production in
e^+e^- annihilation at 29 GeV," LBL-17142 preprint, Lawrence
Berkeley Lab, Berkeley, California 94720 (December 1983)
Yu.M. Ado, E.A. Myae, A.A. Naumov, M.F. Ovchinnikov, O.N.
Radin, V.A. Teplyskov, V.G. Tishin, E.F. Troyanov, "Initial
operation of the IHEP proton synchrotron with a new ring
injector," Paper H50, 1985 Particle Accelerator Conf.,
Vancouver, B.C., Canada (13-16 May 1985) [To be published in
IEEE Trans. Nuclear Sci. (Oct 1985)].

M. Antinucci, A. Bertin, P. Capiluppi, M. D'Agostino-Bruno,
A.M. Rossi, G. Vannini, G. Giacomelli, and A. Bussiere,
"Multiplicities of charged particles up to ISR Energies,"
Lett. Nuovo Cimento **6**, 121-127 (1973).

R. Armenteros and B. French, "Antinucleon-nucleon
interactions," in **High Energy Physics - Vol. V**, E. Burhop,
ed., Academic Press, New York (1969), pp. 237-410.

E. Asseo, M. Boutheon, R. Cappi, G. Carron, M. Chanel, D. Dumollard, R. Garoby, R. Giannini, W. Hardt, et al. "Low energy antiprotons at the CERN PS," pp 20-23 (in Russian), Proc. 12th Int. Conf. High-Energy Accel., F.T. Cole and D. Donaldson, ed., Fermi National Accelerator Lab, Batavia, Illinois (1983).

B. Autin, "The future of the antiproton accumulator," pp. 573-582, Proc. Workshop on Proton-Antiproton Physics and the W discovery, La Plagne (1983).

V.E. Balakin and A.N. Skrinsky, "Project VLEPP," Akademiya Nauk USSR, Vestnik, No. 3, 66-77 (1983).

M.Q. Barton, et al., "Minimizing energy consumption of accelerators and storage ring facilities [panel discussion]," pp. 898-908, Proc. 11th Int. Conf. High Energy Accelerators, Geneva (1980).

B.F. Bayanov and G.I. Sil'vestrov, "Use of lithium to produce a strong cylindrical magnetic lens," Zh. Tekh. Fiz. **48**, 160-168 (1978) [English translation Sov. Phys. Tech. Phys. **23**, 94-98 (1978)].

B.F. Bayanov, A.D. Chernyakin, V.N. Karasyuc, G.I. Sil'vestrov, T.A. Vsevolozhskaya, V.G. Volohov, G.S. Willewald, "The antiproton target station on the basis of lithium lenses," pp. 362-368, Proc. 11th Int. Conf. High Energy Accelerators, Geneva (1980).

B.F. Bayanov, J.N. Petrov, G.I. Sil'vestrov, J.A. MacLachlan, and G.L. Nicholls, "A lithium lens for axially symmetric focusing of high energy particle beams," Nuclear Instr. & Methods, **190**, 9-14 (1981).

B.R. Bayanov, T.A. Vsevolozhskaya, Yu. N. Petrov, and G.I. Sil'vestrov, "The investigation and design development of lithium lenses with large operating lithium volume," pp. 587-590, Proc. 12th Int. Conf. High-Energy Accel., F.T. Cole and D. Donaldson, ed., Fermi National Accelerator Lab, Batavia, Illinois (1983).

M. Bell, J. Chaney, H. Herr, F. Krienen, P. Møller-Petersen, and G. Petrucci, "Electron cooling in ICE at CERN," Nuclear Instr. & Methods **190**, 237-255 (1981).

M. Bell and J.S. Bell, "Capture of cooling electrons by cool protons," Particle Accelerators, **12**, 49-52 (1982).

R. Billinge and M.C. Crowley-Milling, "The CERN proton-antiproton colliding beam facilities," IEEE Trans. on Nuclear Sci., **NS-26**, 2974-2977 (1979).

152

R. Billinge and E. Jones, "The CERN antiproton source," pp 14-16, Proc. 12th Int. Conf. High-Energy Accel., F. T. Cole and D. Donaldson, ed., Fermi National Accelerator Lab, Batavia, Illinois (1983).

R. Billinge, "CERN's p$\bar{\text{p}}$ source," CERN Publication 84-09, Proc. Fourth Topical Workshop on Proton-Antiproton Collider Physics, Berne, 5-8 March 1984, pp. 357-364 (8 August 1984).

U. Bizzarri, M. Conte, C. Ronsivalle, R. Scrimaglio, L. Tecchio, and A. Viganti, "High-energy electron cooling at LEAR p$\bar{\text{p}}$-collider," pp. 619-628, **Physics at LEAR with Low-Energy Cooled Antiprotons**, Workshop on Physics at LEAR with Low-Energy Cooled Antiprotons, Erice, Sicily, Italy, 9-16 May 1982, U. Gastaldi and R. Klapisch, ed., Plenum Press, NY (1984).

G. Brianti, "Experience with the CERN p$\bar{\text{p}}$ complex," IEEE Trans. Nuclear Sci. **NS-30**, 1950-1956 (August 1983).

P.J. Bryant, "Antiprotons in the ISR," IEEE Trans. Nuclear Sci. **NS-30**, 2047-2049 (August 1983)

G.I. Budker and A.N. Skrinsky, "Electron cooling and new possibilities in elementary particle physics," Usp. Fiz. Nauk **124**, 561-595 (1978) [English translation Sov. Phys. Usp. **21**, 277-296 (1978)].

D.C. Carey, et al., "Unified description of single-particle production in pp collisions," Phys. Rev. Lett. **33**, 330-333 (1974).

G. Carron, R. Johnson, S. van der Meer, C. Taylor, and L. Thorndahl, "Recent experience with antiproton cooling," IEEE Trans. Nuclear Sci. **NS-30**, 2587-2589 (1983).

CERN Courier editors, "When antimatter mattered," CERN Courier, **23**, 6-7 (January/February 1983).

CERN Courier editors, "LEAR arrives," CERN Courier, **23**, 314 (October 1983).

CERN Courier editors, "From AA to Z," CERN Courier, 23, 365-369 (November 1983).

CERN Courier editors, "Going for antiprotons," CERN Courier, **23**, 380-383 (November 1983).

CERN Courier editors, "First results from LEAR," CERN Courier, 23, 416-417 (December 1983).

CERN Courier editors, "Antiprotons in orbit," CERN Courier, **24**, 53-55 (March 1984).

CERN Proton Synchrotron Staff, "The CERN PS complex as an antiproton source," IEEE Trans. Nuclear Sci. **NS-30**, 2039-2041 (1983).

G. Chapline, "Antimatter Breeders?" J. British Interplanetary Soc., **35**, 423-424 (1982).

B.V. Chirikov, et al., "Optimization of antiproton fluxes from targets using hadron cascade calculations," Nuclear Instr. & Meth. **144**, 129-139 (1977).

D.B. Cline, et al., "Initial operation of the Fermilab antiproton cooling ring," IEEE Trans. Nuclear Sci. **NS-26**, 3158-3160 (1979).

D.B. Cline, "The development of bright antiproton sources and high energy density targeting," pp. 345-361, Proc. 11th Int. Conf. High Energy Accelerators, Geneva (1980).

D.B. Cline, C. Rubbia, and S. van der Meer, "The search for intermediate vector bosons," Scientific American **247**, No. 3, 48-59 (March 1982).

B. de Raad, "The SPS p-pbar collider, present performance and future prospects," CERN Publication 84-09, Proc. Fourth Topical Workshop on Proton-Antiproton Collider Physics, Berne, 5-8 March 1984, pp. 344-356 (8 August 1984).

T.W. Eaton, S. Hancock, C.D. Johnson, E. Jones, S. Maury, S. Milner, J.C. Schnuriger, and T.R. Sherwood, "Conducting targets for $\bar{p}$ production of ACOL, past experience and prospects," Paper X40, 1985 Particle Accelerator Conf., Vancouver, B.C., Canada (13-16 May 1985) [To be published in IEEE Trans. Nuclear Sci. (Oct 1985)].

T. Ellison, W. Kells, V. Kerner, F. Mills, R. Peters, T. Rathbun, D. Young, P.M. McIntyre, "Electron cooling and accumulation of 200-MeV protons at Fermilab," IEEE Trans. Nuclear Sci. **NS-30**, 2636-2638 (1983).

L.R. Evans, "Intrabeam scattering in the SPS proton antiproton collider," pp. 229-231, Proc. 12th Int. Conf. High-Energy Accel., F.T. Cole and D. Donaldson, ed., Fermi National Accelerator Lab, Batavia, Illinois (1983).

Fermilab staff, **Design Report: Tevatron 1 Project**, p. 4-13 to p. 4-16, Fermi National Accelerator Lab, Batavia, Illinois (September 1984).

D.C. Flander, C.D. Johnson, S. Maury, T.R. Sherwood, G. Dugan, C. Hojvat, and A. Lennox, "Beam tests of a 2 cm diameter lithium lens," Paper X39, 1985 Particle Accelerator Conf., Vancouver, B.C., Canada (13-16 May 1985) [To appear in IEEE Trans. Nuclear Sci. (Oct 1985)].

R. Forster, T. Hardek, D.E. Johnson, W. Kells, V. Kerner, H. Lai, A.J. Lennox, F. Mills, Y. Miyahara, L. Oleksiuk, T. Rhoades, D. Young, and P.M McIntyre, "Electron cooling experiments at Fermilab," IEEE Trans. Nuclear Sci. NS-28, 2386-2388 (1981).

J. Gareyte, "The CERN proton-antiproton complex," pp. 79-90, Proc. 11th Int. Conf. High Energy Accelerators, Geneva (1980).

U. Gastaldi and R. Klapish, Eds., **Physics at LEAR with Low-Energy Cooled Antiprotons**, Workshop on Physics at LEAR with Low-Energy Cooled Antiprotons, Erice, Sicily, Italy, 9-16 May 1982, Plenum Press, NY (1984).

M. Harrison, "The Fermilab $\bar{p}p$ collider," pp. 368-378, CERN Pub. 84-09, Fourth Topical Workshop on Proton-Antiproton Collider Physics, Berne, 5-8 March 1984, (8 August 1984).

H. Herr and C. Rubbia, "High energy cooling of protons and antiprotons for the SPS collider," pp. 825-829, Proc. 11th Int. Conf. on High Energy Accelerators, Geneva, Switzerland (1980).

H. Herr, "A small deceleration ring for extra low energy antiprotons (ELENA)," pp. 633-642, **Physics at LEAR with Low-Energy Cooled Antiprotons**, Workshop on Physics at LEAR with Low-Energy Cooled Antiprotons, Erice, Sicily, Italy, 9-16 May 1982, U. Gastaldi and R. Klapisch, ed., Plenum Press, NY (1984).

H. Herr, D. Mohnl, and A. Winnacker, "Production of and experimentation with antihydrogen at LEAR," pp. 659-676, **Physics at LEAR with Low-Energy Cooled Antiprotons**, Workshop on Physics at LEAR with Low-Energy Cooled Antiprotons, Erice, Sicily, Italy, 9-16 May 1982, U. Gastaldi and R. Klapisch, ed., Plenum Press, NY (1984).

C. Hojvat and A. Van Ginneken, "Calculation of antiproton yields for the Fermilab antiproton source," Nuclear Instr. & Methods 206, 67-83 (1983).

C. Hojvat, G. Biallas, R. Hanson, J. Heim, and F. Lange, "The Fermilab Tevatron I project target station for antiproton production," Fermilab TM-1174, 1983 Particle Accelerator Conf., Santa Fe, NM (21-24 March 1983).

H. Hora, "Estimates for the efficient production of antihydrogen by lasers of very high intensities," Opto-Electronics 5, 491-501 (1973).

H. Hora, "Theory of relativistic self-focusing of laser radiation in plasmas," J. Opt. Soc. Am. **65**, 882-886 (1975).

L. Hütten, H. Poth and A. Wolf, "The electron cooling device for LEAR," pp. 605-618, **Physics at LEAR with Low-Energy Cooled Antiprotons**, Workshop on Physics at LEAR with Low-Energy Cooled Antiprotons, Erice, Sicily, Italy, 9-16 May 1982, U. Gastaldi and R. Klapisch, ed., Plenum Press, NY (1984).

C.D. Johnson, "Antiproton yield optimization in the CERN antiproton accumulator," IEEE Trans. Nuclear Sci. **NS-30**, 2821-2826 (August 1983).

R.P. Johnson and J. Marriner, "Stochastic stacking without filters," Fermilab $\bar{p}$ Note 226, Fermi National Accelerator Lab, Batavia, Illinois (17 August 1982).

E. Jones, S. van der Meer, R. Rohner, J.C. Schnuriger, and T.R. Sherwood, "Antiproton production and collection for the CERN antiproton accumulator," IEEE Trans. Nuclear Sci. **NS-30**, 2778-2780 (August 1983).

N.G. Jordan and P.V. Livdahl, "Costs to build Fermilab in 1984 dollars," Fermilab Technical Memo TM-1242, 0002.000 (1984).

W. Kells, P. McIntyre, L. Oleksiuk, N. Dikansky, I. Meshkov, V. Parkhomchuk, and W. Herrmannsfeldt, "Studies of the electron beam for the Fermilab electron cooling experiment," pp. 814-818, Proc. 11th Int. Conf. on High Energy Accelerators, Geneva, Switzerland (1980).

W. Kells, "Advanced stochastic cooling mechanisms," IEEE Trans. Nuclear Sci. **NS-28**, 2459-2461 (1981).

W. Kells, F. Krienen, F. Mills, L. Oleksiuk, J. Peoples, and P.M. McIntyre, "Electron cooling for the Fermilab $\bar{p}$ source," IEEE Trans. Nuclear Sci. **NS-28**, 2583-2584 (1981).

W. Kells, G. Gabrielse, and K. Helmerson, "On achieving cold antiprotons in a Penning trap," FERMILAB-Conf-84/68-E, Fermi National Accelerator Lab, Batavia, Illinois (August 1984). [Preprint submitted to the IX Int. Conf. on Atomic Physics, Seattle, Washington (23-27 July 1984).]

K. Kilian, "Physics with antiprotons at LEAR," pp. 324-341, CERN Publication 84-09, Proc. Fourth Topical Workshop on Proton-Antiproton Collider Physics, Berne, 5-8 March 1984, (8 August 1984).

T.B.W. Kirk, "Antiproton production target studies - numerical calculations," Fermilab TM-1011 (14 Nov 1980).

E. Knapp, "Accelerator Costs and Efficiency," **Proc. Information Meeting on Accelerator Breeding,** Brookhaven, NY, p. 294, (Jan 1977).

H.J.C. Kouts, Chairman, **Proceedings of an Information Meeting on Accelerator Breeeding,** Brookhaven National Laboratory, Upton, New York, 18-19 Jan 1977.

F. Krienen, "Initial cooling experiments (ICE) at CERN," pp. 781ff, Proc. 11th Int. Conf. High Energy Accelerators, Geneva (1980).

F. Krienen and J.A. MacLachlan, "Antiproton collection from a production target," IEEE Trans. Nuclear Sci. **NS-28,** 2711-2716 (1981).

G. Lambertson, et al., "Experiments on stochastic cooling of 200 MeV protons," IEEE Trans. Nuclear Sci. **NS-28,** 2471-2473 (1981).

P. Lefèvre, D. Möhl, G. Plass, "The CERN low energy antiproton ring (LEAR) project," pp. 819-823, Proc. 11th Int. Conf. High Energy Accelerators, Geneva (1980).

J.A. MacLachlan, "Current carrying targets and multitarget arrays for high luminosity secondary beams," FN-334, 8055.000, Fermi National Accelerator Lab, Batavia, Illinois (April 1982).

E. Malamud, "The Fermilab p̄p Collider: Machine and Detectors," Fermilab p̄ Note #421, Fifth Topical Conf. on Proton-Antiproton Collisions, St. Vincent, Italy (26 Feb 1985).

J.P. Marriner, "The Fermilab p̄p collider," pp. 583-592, Proc. Workshop on Proton-Antiproton Physics and the W discovery," La Plagne, (1983).

H.-J. Möhring and J. Ranft, "Antiproton production from extended targets using a weighted Monte Carlo hadron cascade model," Nuclear Instr. & Methods **201,** 323-327 (1982).

R. Neumann, H. Poth, A. Winnacker, and A. Wolf, "Laser-enhanced electron-ion capture and antihydrogen formation," Z. Phys. A, **313,** 253-262 (1983).

J. Peoples, "The Fermilab antiproton source," IEEE Trans. Nuclear Sci. **NS-30,** 1970-1975 (1983).

E. Peschardt and M. Studer, "Stochastic cooling in the CERN ISR during p$\bar{\text{p}}$ colliding beam physics," IEEE Trans. Nuclear Sci. **NS-30**, 2584-2586 (August 1983).

Physics Today editors, "CERN builds proton-antiproton ring; Fermilab plans one," Search and Discovery Section, Physics Today, 32, No. 3, 17-19 (March 1979).

Physics Today editors, "CERN SPS now running as 540-GeV $\bar{\text{p}}$p collider," Search and Discovery Section, Physics Today, 35, No. 2, 17-20 (February 1982).

Physics Today editors, "p$\bar{\text{p}}$ collisions yield intermediate boson at 80 GeV, as predicted," Search and Discovery Section, Physics Today, **35**, No. 4, 17-20 (April 1982).

Physics Today editors, "Fermilab's superconducting synchrotron strives for 1 TeV," Search and Discovery Section, Physics Today, **37**, No. 3, 17-20 (March 1984).

A.L. Robinson, "CERN sets intermediate vector boson hunt," Science **213**, 191-194 (10 July 1981).

R.E. Shafer, "The Fermilab antiproton debuncher betatron cooling system," pp. 581-583, Proc. 12th Int. Conf. High-Energy Accel., F.T. Cole and D. Donaldson, ed., Fermi National Accelerator Lab, Batavia, Illinois (1983).

P. Sievers, R. Bellone, A. Ijspeert, P. Zanasco, "Development of lithium lenses at CERN," Paper X41, 1985 Particle Accelerator Conf., Vancouver, B.C., Canada (13-16 May 1985) [To be published in IEEE Trans. Nuclear Sci. (Oct 1985)].

A.H. Sørensen, "Theory of electron cooling in a magnetic field," pp. 599-604, **Physics at LEAR with Low-Energy Cooled Antiprotons**, Workshop on Physics at LEAR with Low-Energy Cooled Antiprotons, Erice, Sicily, Italy, 9-16 May 1982, U. Gastaldi and R. Klapisch, ed., Plenum Press, NY (1984).

F.E. Taylor, et al., "Analysis of radial scaling in single-particle inclusive reactions," Phys. Rev. **D14**, 1217-1242 (1976).

S. van der Meer, "Stochastic cooling in the CERN antiproton accumulator," IEEE Trans. Nuclear Sci. **NS-28**, 1194-1998 (1981).

S. van der Meer, "Practical and foreseeable limitations in usable luminosity for the collider," CERN Publication 83-04, Proc. Third Topical Workshop on Proton-Antiproton Collider Physics, Rome, 12-14 January 1983, pp. 555-561 (10 May 1983).

G.S. Villeval'd, V.N. Karasyuk, and G.I. Sil'vestrov, "Magnetic field limited parabolic lens," Sov. Phys. Tech. Phys. **23**, 332-336 (1978).

T.A. Vsevolozhskaya and G.I. Sil'vestrov, "Optical properties of fast parabolic lenses," Zh. Tekh. Fiz. **43**, 61-70 (1973) [English translation Sov. Phys. Tech. Phys. **18**, 38-43 (1973)].

T.A. Vsevolozhskaya, M.A. Lyubimova, and G.I. Sil'vestrov, "Optical properties of cylindrical lenses," Zh. Tekh. Fiz. **45**, 2494-2507 (1975) [English translation Sov. Phys. Tech. Phys. **20**, 1556-1563 (1976)].

T. Vsevolozhskaya, B. Grishanov, Ya. Derbenev, N. Dikansky, I. Meshkov, V. Parkhomchuk, D. Pesrikov, G. Sil'vestrov, A. Skrinsky, "Antiproton source for the accelerator-storage complex, UNK-IHEP," Fermilab Report FN-353 8000.00 (June 1981), a translation of INP Preprint 80-182 (December 1980).

T.A. Vsevolozhskaya, "The optimization and efficiency of antiproton production within a fixed acceptance," Nuclear Instr. & Methods **190**, 479-486 (1981).

E.J.N. Wilson, "The CERN antiproton accumulator," pp. 567-571, Proc. Workshop on Proton-Antiproton Physics and the W discovery," La Plagne (1983).

D.E. Young, "Progress on beam cooling at Fermilab," pp. 800 ff, Proc. 11th Int. Conf. High Energy Accelerators, Geneva (1980).

D.E. Young, "The Fermilab proton-antiproton collider," IEEE Trans. Nuclear Sci. **NS-28**, 2008-2012 (1981)

D. Young, F. Mills, and G. Michelassi, "Information relevant to the optimization of electric power versus equipment costs," Fermilab p̄-Note 189 (1984?)

10.2 SLOWING, COOLING, AND TRAPPING OF IONS, ATOMS, AND MOLECULES

S.V. Adreev, V.I. Balykin, V.S. Letokhov, and V.G. Minogin, "Radiative slowing and reduction of the energy spread of a beam of sodium atoms to 1.5 K in an oppositely directed laser beam," Pis'ma Zh. Eksp. Teor. Fiz. **34**, 463-467 (1981) [English translation Sov. Phys. JETP Lett. **34**, 442-445 (1981)].

A. Ashkin, "Acceleration and trapping of particles by radiation pressure," Phys. Rev. Lett. **24**, 156-159 (1970).

A. Ashkin, "Atomic-beam deflection by resonance-radiation pressure," Phys. Rev. Lett. **25**, 1321-1324 (1970).

A. Ashkin, "Trapping of atoms by resonance radiation pressure," Phys. Rev. Lett. **40**, 729-732 (1978).

A. Ashkin and J.M. Dziedzic, "Optical levitation in high vacuum," Appl. Phys. Lett., **28**, 333-335 (1976).

A. Ashkin and J.M. Dziedzic, "Observation of radiation-pressure trapping of particles by alternating light beams," Phys. Rev. Lett. **54**, 1245-1248 (1985).

A. Ashkin and J.P. Gordon, "Cooling and trapping of atoms by resonance radiation pressure," Optics Lett. **4**, 161-163 (1979).

A. Ashkin and J.P. Gordon, "Stability of radiation-pressure particle traps: an optical Earnshaw theorem," Optics Lett. **8**, 511-513 (1983).

V.I. Balykin, V.S. Letokhov, and V.I. Mishin, "Observation of the cooling of free sodium atoms in a resonance laser field with a scanning frequency," Pis'ma Zh. Exp. Teo. Fiz. **29**, 614-618 (1979) [English translation JETP Lett. **29**, 561-564 (1979)].

V.I. Balykin, V.S. Letokhov, and V.I. Mishin, "Cooling of sodium atoms by resonant laser emission," Zh. Exp. Teo. Fiz. **78**, 1376-1385 (1980) [English translation Sov. Phys. JETP **51**, 692-696 (1980)].

V.I. Balykin, "Cyclic interaction of Na atoms with circularly polarized laser radiation," Optics Comm. **33**, 31-36 (1980).

A. Bernard, J.P. Canny, T. Juillerat, and P. Touboul, "Electrostatic suspension of samples in microgravity," Proc. 35th Congress of International Astronautical Federation, Lausanne, Switzerland (7-13 October 1984).

A.F. Bernhardt and B.W. Shore, "Coherent atomic deflection by resonant standing waves," Phys. Rev. 23A, 1290-1301 (1981).

N. Beverini, L. Bracci, V. Lagomarsino, G. Manuzio, R. Parodi, and G. Torelli, "A Penning trap to store antiprotons," pp. 771-778, **Physics at LEAR with Low-Energy Cooled Antiprotons**, Workshop on Physics at LEAR with Low-Energy Cooled Antiprotons, Erice, Sicily, Italy, 9-16 May 1982, U. Gastaldi and R. Klapisch, ed., Plenum Press, NY (1984).

J.H. Billen, K.R. Crandall, T.P. Wangler, M. Weiss, "An RFQ as a particle decelerator," Los Alamos National Lab Preprint LA-UR-85-140, Third LEAR Workshop, Tignes-Savoie, France (19-26 Jan 1985).

J.E. Bjorkholm, R.R. Freeman, A. Ashkin, and D.B. Pearson, "Observation of focusing of neutral atoms by the dipole forces of resonance-radiation pressure," Phys. Rev. Lett. 41, 1361-1364 (1978).

J.E. Bjorkholm, R.R. Freeman, and D.B. Pearson, "Efficient transverse deflection of neutral atomic beams using spontaneous resonance-radiation pressure," Phys. Rev. 23A, 491-497 (1981).

R. Blatt, W. Ertmer, and J.L. Hall, "Cooling of an atomic beam with frequency-sweep techniques," pp. 142-153, **Laser-Cooled and Trapped Atoms**, NBS SP-653, W.D. Phillips, ed. (1983).

J.J. Bollinger, J.D. Prestage, W.N. Itano, and D.J. Wineland, "Laser-cooled atomic frequency standard," Phys. Rev. Lett. 54, 1000-1003 (1985).

T. Breeden and H. Metcalf, "Stark acceleration of Rydberg atoms in inhomogeneous electric fields," Phys. Rev. Lett. 47, 1726-1729 (1981).

L.N. Breusova, I.N. Knyazev, V.G. Movshev, and T.B. Fogel'son, "Vacuum ultraviolet H_2 laser with a sealed gas-discharge cell," Kvant. Elektron. 6, 2458-2460 (1979) [English translation Sov. J. Quantum Elec. 9, 1452-1453 (1979)].

L. Campbell, W.R. Gibbs, T. Goldman, D.B. Holtkamp, M.V. Hynes, N.S.P. King, M.M. Nieto, A. Picklesimer, and T.P. Wangler, "Basic research in atomic, nuclear and particle physics," LA-UR-84-3572, Los Alamos National Lab, Los Alamos, New Mexico (1984).

R.W. Cline, et al., "Magnetic confinement of spin-polarized atomic hydrogen," Phys. Rev. Lett., 45, 2117-2120 (1980).

R.J. Cook and R.K. Hill, "An electromagnetic mirror for neutral atoms," Optics Comm. **43**, 258-260 (1982).

J. Dalibard, S. Reynaud, and C. Cohen-Tannoudji, "Proposals of stable optical traps for neutral atoms," Optics Comm. **47**, 395-399 (1983).

R.W. Dreyfus, "Molecular hydrogen laser: 1098-1613 Angstrom," Phys. Rev. **A9**, 2635 (1974).

P. Ekstron and D. Wineland, "The isolated electron," Sci. Am. **243**, 105-121 (August 1980).

W. Ertmer, R. Blatt, J.L. Hall, and M. Zhu, "Laser manipulation of atomic beam velocities: Demonstration of stopped atoms and velocity reversal," Phys. Rev. Lett. 54, 996-999 (1985).

R. Evrard and G.-A. Boutry, "An absolute micromanometer using diamagnetic levitation," J. Vacuum Sci. and Tech. **6**, 279 (1969).

Fermilab, **Design Report: Tevatron 1 Project**, pp. 4-13 to 1-16, Fermi National Accelerator Lab, Batavia, Illinois (September 1984).

H. Friedman and A.D. Wilson, "Isotope separation by radiation pressure of coherent pi pulses," Appl. Phys. Lett. **28**, 270 (1976).

G. Gabrielse, "Detection, damping, and translating the center of the axial oscillation of a charged particle in a Penning trap with hyperbolic electrodes," Phys. Rev. **29A**, 462-469 (1984).

T. Goldman and M.M. Nieto, "Gravitational properties of antimatter," Los Alamos National Lab Preprint LA-UR-85-1092, Third LEAR Workshop, Tignes-Savoie, France (19-26 Jan 1985).

J.P. Gordon and A. Ashkin, "Motion of atoms in a radiation trap," Phys. Rev. **A21**, 1606-1617 (1980).

T.W. Hänsch and A.L. Schawlow, "Cooling of gases by laser radiation," Optics Comm. **13**, 68-69 (1975).

H.F. Hess, D.A. Bell, G.P. Kochanski, R.W. Cline, D. Kleppner, and T.J. Greytak, "Observation of three-body recombination in spin-polarized hydrogen," Phys. Rev. Lett. **51**, 483-486 (1983).

G. Herzberg, **Molecular Spectra and Molecular Structure - I. Spectra of Diatomic Molecules**, 2nd Ed., D. Van Nostrand, Princeton, NJ (1950).

162

R.T. Hodgson, "VUV laser action observed in the Lyman band of molecular hydrogen," Phys. Rev. Lett. 25, 494 (1970).

M.V. Hynes, "Physics with low temperature antiprotons," Los Alamos National Lab preprint LA-UR-85-1060, Third LEAR Workshop, Tignes, France (19-26 Jan 1985).

R.P. Johnson and J. Marriner, "Stochastic stacking without filters," Fermilab p̄ Note 226, Fermi National Accelerator Lab, Batavia, Illinois (17 August 1982).

A.P. Kazantsev, "The acceleration of atoms by light," Sov. Phys. JETP, **39**, 784-790 (1974).

W. Kells, G. Gabrielse, and K. Helmerson, "On achieving cold antiprotons in a Penning trap," FERMILAB-Conf-84/68-E, Fermi National Accelerator Lab, Batavia, Illinois (August 1984). [Preprint submitted to the IX Int. Conf. on Atomic Physics, Seattle, Washington (23-27 July 1984).]

J. F. Lam, R.A. McFarlane, A.J. Palmer, and D.G. Steel, "Experimental and theoretical studies of laser cooling and emittance control of neutral beams," Hughes Research Laboratories, Malibu, California, Annual Report on AFOSR Contract F49620-82-C-0004, (September 1983).

V.S. Letokhov, V.G. Minogin and B.D. Pavlik, "Cooling and capture of atoms and molecules by a resonant light field," Sov. Phys. JETP, **45**, 698-705 (1977).

V.S. Letokhov and V.G. Minogin, "Possibility of accumulation and storage of cold atoms in magnetic traps," Optics Comm., **35**, 199-202 (1980).

V.S. Letokhov and V.G. Minogin, "Laser radiation pressure on free atoms," Phys. Reports **73**, 1-65 (1981) [review].

M.S. Lubell and K. Rubin, "Velocity compression and cooling fo a sodium atomic beam using a frequency modulated ring laser," pp. 125-136, **Laser-Cooled and Trapped Atoms**, NBS SP-653, W.D. Phillips, ed. (1983).

H.J. Metcalf, "Magnetic trapping of decelerated neutral atoms," **Laser-Cooled and Trapped Atoms**, NBS SP-653, W.D. Phillips, ed. (1983).

R.A. McFarlane, D.G. Steel, R.S. Turley, J.F. Lam, and A.J. Palmer, "Experimental and theoretical studies of laser cooling and emittance control of neutral beams," Hughes Research Laboratories, Malibu, CA 90265, Annual report on contract F49620-82-C-0004, AFOSR, Bolling AFB, DC 20332 (Oct 1984).

163

R. D. McCarty, "Hydrogen technological survey," Thermophysical Properties," NASA SP-3089 [550 pages] (1975).

R.D. McCarty, J. Hord, and H.M. Roder, Edited by J. Hord, "Selected properties of hydrogen (engineering design data)," Center for Chemical Engineering, National Engineering Lab, National Bureau of Standards, Boulder, Colorado (February 1981).

J.C. Mullins, W.T. Ziegler, and B.S. Kirk, "The thermodynamic properties of parahydrogen from 1 to 22 K," Tech. Report No. 1, Project No. A-593, Contract CST-7339, National Bureau of Standards, Boulder, Colorado (1 November 1961).

I. Nebenzahl and A. Szöke, "Deflection of atomic beams by resonance radiation using stimulated emission," Appl. Phys. Lett. 25, 327-329 (1974).

W. Neuhauser, M. Hohenstatt, P. Toschek, and H. Dehmelt, "Optical-sideband cooling of visible atom cloud confined in parabolic well," Phys. Rev. Lett. 41, 233-236 (1978).

W. Neuhauser, M. Hohenstatt, P.E. Toschek, and H.G. Dehmelt, "Visual observation and optical cooling of electrodynamically contained ions," Appl. Phys. 17, 121-129 (1978).

W. Neuhauser, M. Hohenstatt, P.E. Toschek, and H. Dehmelt, "Localized visible Ba^+ mono-ion oscillator," Phys. Rev. 22A, 1137-1140 (1980).

F.J. Northrop, et al., "VUV laser-induced fluorescence of molecular hydrogen," Chem. Phys. Let. 105, 34-37 (1984).

A.J. Palmer and J.F. Lam, "Radiation cooling with pi-pulses," Paper WG1, Annual Meeting Optical Soc. Am., San Diego (1984) [submitted to J. Opt. Soc. Am. (1985)].

D.B. Pearson, R.R. Freeman, J.E. Bjorkholm, and A. Askin, "Focusing and defocusing of neutral atomic beams using resonance-radiation pressure," Appl. Phys. Lett. 36, 99-101 (1980).

W.D. Phillips and H.J. Metcalf, "Laser deceleration of an atomic beam," Phys. Rev. Lett., 48, 596-599 (1982).

W.D. Phillips, ed., **Laser-cooled and trapped atoms**, NBS Special Publication 653, Proc. Workshop on Spectroscopic Applications of Slow Atomic Beams, NBS Gaithersburg, MD (14-15 April 1983).

164

W.D. Phillips, J.V. Prodan, and H.J. Metcalf, "Neutral atomic beam cooling experiments at NBS," pp. 1-8, **Laser-Cooled and Trapped Atoms**, NBS SP-653, W.D. Phillips, ed. (1983).

J.V. Prodan, W.D. Phillips, and H.J. Metcalf, "Laser production of a very slow monoenergetic atomic beam," Phys. Rev. Lett. **49**, 1149-1153 (1982).

J.V. Prodan and W.D. Phillips, "Chirping the light -- fantastic?," pp. 137-141, **Laser-Cooled and Trapped Atoms**, NBS SP-653, W.D. Phillips, ed. (1983).

J. Prodan, A. Migdall, W.D. Phillips, I. So, H. Metcalf, and J. Dalibard, "Stopping atoms with laser light," Phys. Rev. Lett. **54**, 992-995 (1985).

W-K Rhim, M.M. Saffren, and D.D. Elleman, "Development electrostatic levitator at JPL," pp. 115-119 of **Materials Processing in the Reduced Gravity Environment of Space**, G.E. Rindone, ed., Elsevier Science (1982)

H.M. Roder, G.E. Childs, R.D. McCarty and P.E. Angerhafer, "Survey of properties of H isotopes below their critical temperatures," TN 641, National Bureau of Standards, Boulder, Colorado (1973).

F. Schmidt, "Diffusion and ortho-para conversion in solid hydrogen," Phys. Rev. **D10**, 4480-4484 (1974).

P.B. Schwinberg, R.S. Van Dyck, Jr., and H.G. Dehmelt, "New comparison of the positron and electron g factors," Phys. Rev. Lett. **47**, 1679-1682 (1981).

I.F. Silvera, "The solid molecular hydrogens in the condensed phase: Fundamentals and static properties," Rev. Mod. Phys. **32**, 393-452 (1980).

I.F. Silvera and J. Walraven, "The stabilization of atomic hydrogen," Sci. Am. **246**, 66-74 (January 1982).

I. Simon, et al., "Sensitive tiltmeter utilizing a diamagnetic suspension," Rev. Sci. Inst. **39**, 1666 (1968).

R. Sprik, J.T.M. Walraven, and I.F. Silvera, "Compression of spin-polarized hydrogen to high density," Phys. Rev. Lett. **51**, 479-482 (1983).

D.G. Steel, J.F. Lam, R.A. McFarlane, "Studies of laser enhanced relativistic ion beam neutralization," White Paper, Hughes Research Laboratories, Malibu, California (October 1983).

W.C. Stwalley, "A hybrid laser-magnet trap for spin-polarized atoms," pp. 95-102, **Laser-Cooled and Trapped Atoms**, NBS SP-653, W.D. Phillips, ed. (1983).

W. Thompson and S. Hanrahan, "Characteristics of a cryogenic extreme high-vacuum chamber," J. Vac. Sci. Technol. **14**, 643-645 (1977).

R.D. Waldron, "Diamagnetic levitation using pyrolytic graphite," Rev. Sci. Inst. **37**, 29-34 (1966).

R.S. Van Dyck, Jr., D.J. Wineland, P.A. Ekstron, and H.G. Dehmelt, "High mass resolution with a new variable anharmonicity Penning trap," Appl. Phys. Lett. **28**, 446-448 (1976).

R. W. Waynant, J.D. Shipman, Jr., R.C. Elton, and A.W. Ali, "VUV laser emission from molecular hydrogen," Appl. Phys. Lett. **17**, 383 (1970).

M.J. Weber, Ed., **CRC Handbook of Laser Science and Technology**, pp. 282-286, CRC Press, Boca Raton, Florida.

D.J. Wineland and H.G. Dehmelt, "Principles of the stored ion calorimeter," J. Appl. Phys. **46**, 919-930 (1975).

D.J. Wineland, R.E. Drullinger, and F.L. Walls, "Radiation-pressure cooling of bound resonant absorbers," Phys. Rev. Lett. **40**, 1639-1642 (1978).

D.J. Wineland, "Trapped ions, laser cooling, and better clocks," Science **226**, 395-400 (26 Oct 1984).

W.H. Wing, "Electrostatic trapping of neutral atomic particles," Phys. Rev. Lett., **45**, 631-634 (1980).

W.H. Wing, "Some problems and possibilities for quasistatic neutral particle trapping," pp. 74-93, **Laser-Cooled and Trapped Atoms**, NBS SP-653, W.D. Phillips, ed. (1983).

W.H. Wing, "Gravitational effects in particle traps," p. 94, **Laser-Cooled and Trapped Atoms**, NBS SP-653, W.D. Phillips (editor) (1983).

10.3 ANTIMATTER ANNIHILATION AND PROPULSION

L.E. Agnew, Jr., T. Elioff, W.B. Fowler, R.L. Lander, W.M. Powell, E. Sergè, H.M. Steiner, H.S. White, C. Wiegand, and T. Ypsilantis, "Antiproton interactions in hydrogen and carbon below 200 MeV," Phys. Rev., **118**, 1371 (1960).

B.W. Augenstein, "Concepts, problems, and opportunities for use of annihilation energy: an annotated briefing on near-term RDT&E to assess feasibility," Rand Note N-2302-AF/RC, Rand Corp., Santa Monica, CA 90406 (June 1985).

B.W. Augenstein, "Some examples of propulsion applications using antimatter," Rand Paper 7113, Rand Corp., Santa Monica, CA 90406 (July 1985).

H. Barkas and M.J. Berger, **Tables of Energy Losses and Ranges of Heavy Charged Particles**, NASA SP-3013, STI Division, NASA, Washington, DC (1964).

B.N. Cassenti, "Design considerations for relativistic antimatter rockets," J. British Interplanetary Soc., **35**, 396-404 (1982).

B.N. Cassenti, "Antimatter propulsion for OTV applications," AIAA preprint 84-1485, AIAA/SAE/ASME 20th Joint Propulsion Conference, Cincinnati, Ohio (11-13 June 1984).

B.N. Cassenti, "Optimization of relativistic antimatter rockets," J. British Interplanetary Soc., **37**, 483-490 (1984).

F.R. Chang and J.L. Fisher, "The hybrid plume plasma rocket," Draper Lab preprint (1983).

M.R. Clover, R.M. DeVries, N.J. DiGiacomo, and Y. Yariv, "Low energy antiproton-nucleus interactions," Phys. Rev. **C26**, 2138-2151 (1982).

R.M. DeVries and N.J. DiGiacomo, "The annihilation of low-energy antiprotons in nuclei," pp. 543-560, **Physics at LEAR with Low-Energy Cooled Antiprotons**, Workshop on Physics at LEAR with Low-Energy Cooled Antiprotons, Erice, Sicily, Italy, 9-16 May 1982, U. Gastaldi and R. Klapisch, ed., Plenum Press, NY (1984).

D.F. Dipprey, "Matter-Antimatter Annihilation as an Energy Source in Propulsion," Appendix in "Frontiers in Propulsion Research," JPL TM-33-722, D.D. Papailiou, Editor, Jet Propulsion Lab, Pasadena, CA 91109 (15 March 1975).

R.L. Forward, "Interstellar flight systems," AIAA Reprint 80-0823, AIAA Int. Meeting, Baltimore, MD (1980).

R.L. Forward, "Antimatter propulsion," J. British Interplanetary Soc., 35, 391-395 (1982).

R.L. Forward, Alternate Propulsion Energy Sources, AFRPL-TR-83-067, Final Report on Contract F04611-83-C-0013, Air Force Rocket Propulsion Lab, Edwards, CA 93523 (December 1983)
R.L. Forward, "Antiproton annihilation propulsion," AIAA preprint 84-1482, AIAA/SAE/ASME 20th Joint Propulsion Conference, Cincinnati, Ohio (11-13 June 1984) [To be published in J. Propulsion and Power].

R. Hyde, L. Wood, and J. Nuckolls, "Prospects for rocket propulsion with laser induced fusion microexplosions," AIAA Paper 72-1063 (Dec 1972).

W. Kolos, D.L. Morgan, D.M. Schrader, and L. Wolniewicz, "Hydrogen-antihydrogen interactions," Phys. Rev. A11, 1792-1796 (1975).

H. Löb, "Sinn oder Unsinn der Photonenrakete," Astronautik 8, 39-47 (1971).

E. Mallove, R.L. Forward, Z. Paprotny, and J. Lehmann, "Interstellar travel and communication: a bibliography," J. British Interplanetary Soc., 33, 201-248 (1980) [entire issue].

P.F. Massier, "The need for expanded exploration of matter-antimatter annihilation for propulsion application," J. British Interplanetary Soc., 35, 387-390 (1982).

D.L. Morgan and V.W. Hughes, "Atomic processes involved in matter-antimatter annihilation," Phys. Rev. D2, 1389-1399 (1970).

D.L. Morgan and V.W. Hughes, "Atom-antiatom interactions," Phys. Rev. A7, 1811-1825 (1973).

D.L. Morgan, "Rocket thrust from antimatter annihilation," JPL Contractor Report CC-571769, Jet Propulsion Lab, Pasadena, Calif. (1975).

D.L. Morgan, "Coupling of annihilation energy to a high momentum exhaust in a matter-antimatter annihilation rocket," JPL Contract Report JS-651111 (1976)

D.L. Morgan, "Concepts for the design of an antimatter annihilation rocket," J. British Interplanetary Soc., 35, 405-412 (1982).

168

Particle Data Group, "Review of particle properties," Rev. Mod. Phys. 56, Part II (April 1984).

G. Piragino, "Antiproton annihilation in nuclear matter: multipion-nucleus interactions and exotic phenomena," pp. 855-860, **Physics at LEAR with Low-Energy Cooled Antiprotons,** Workshop on Physics at LEAR with Low-Energy Cooled Antiprotons, Erice, Sicily, Italy, 9-16 May 1982, U. Gastaldi and R. Klapisch, ed., Plenum Press, NY (1984).

S. Polikanov, "Could antiprotons be used to get a hot, dense plasma?," pp. 851-853, **Physics at LEAR with Low-Energy Cooled Antiprotons,** Workshop on Physics at LEAR with Low-Energy Cooled Antiprotons, Erice, Sicily, Italy, 9-16 May 1982, U. Gastaldi and R. Klapisch, ed., Plenum Press, NY (1984).

E. Sänger, "The theory of photon rockets," Ing. Arch. 21, 213 (1953) [in German].

L.R. Shepherd, "Interstellar flight," J. British Interplanetary Soc. 11, 149-167 (1952).

G. Vulpetti, "Relativistic astrodynamics: The problem of payload optimization in a two-star exploration flight with and intermediate powered swing-by," IAF Paper 83-327, 34th IAF Congress, Budapest, Hungary (Oct 1983).

G. Vulpetti, "A concept of low-thrust relativistic jet speed high efficiency matter-antimatter annihilation propulsion system," IAF Paper 83-397, 34th IAF Congress, Budapest, Hungary (Oct 1983).

G. Vulpetti, "A propulsion-oriented synthesis of the antiproton-nucleon annihilation experimental results," J. British Interplanetary Soc. 37, 124-134 (1984)

G. Vulpetti, "An approach to the modeling of matter-antimatter propulsion systems," J. British Interplanetary Soc., 37, 403-409 (1984).

M. Wade and V.G. Lind, "Ratio of antiproton annihilations on neutrons and protons in carbon for low-energy and stopped antiprotons," Phys. Rev. D14, 1182-1187 (1976).

R.R. Zito, "The cryogenic confinement of antiprotons for space propulsion systems," J. British Interplanetary Soc., 35, 414-421 (1982).

R.R. Zito, "Chain reactions in a hydrogen-antiproton pile," J. British Interplanetary Soc., 36, 308-310 (1983).

APPENDIX A

SOME USEFUL DATA AND CONVERSION FACTORS

FUNDAMENTAL CONSTANTS

Some useful fundamental constants are:[A.1]

c = 2.997925×10^8 m/s   speed of light

e = 1.602192×10^{-19} C   electronic charge

h = 6.626196×10^{-34} J·s   Planck's constant
$\hbar$ = $h/2\pi$

m = 9.109558×10^{-31} kg   electron mass
   = 5.110041×10^5 eV   electron rest mass energy

M = 1.672614×10^{-27} kg   (anti)proton mass
   = 9.382592×10^8 eV   (anti)proton rest mass energy

$m_{\pi^{\pm}}$ = 2.48823×10^{-28} kg   charged pion mass
   = 1.39578×10^8 eV   charged pion rest mass energy
   = 2.60×10^{-8} s   charged pion mean lifetime

m_{π^0} = 2.40617×10^{-28} kg   neutral pion rest mass
   = 1.34975×10^8 eV   neutral pion rest mass energy
   = 8.9×10^{-17} s   neutral pion mean lifetime

m_μ = 1.88356×10^{-28} kg   muon rest mass
   = 1.05659×10^8 eV   muon rest mass energy
   = 2.198×10^{-6} s   muon mean lifetime

k = 1.380622×10^{-23} J/K   Boltzmann's constant

σ = 5.669620×10^{-8} W/m^2·K^4 Stefan-Boltzmann constant

μ_e = 9.274096×10^{-24} J/T   Bohr (electron) magneton
   = 9.274096×10^{-21} erg/G

μ_n = 5.050951×10^{-27} J/T   nuclear magneton
   = 5.050951×10^{-23} erg/G

References:

[A.1] D.E. Gray, Ed., **American Institute of Physics Handbook**, Third Edition, McGraw-Hill, NY (1972).

ENERGY CONVERSION FACTORS

Some energy conversion factors to help understand atomic and molecular spectra and energy level diagrams.[A.1]

$$1 \text{ eV} = 1.602192 \times 10^{-19} \text{ J}$$

1.602192×10^{-12}	erg	
1.782679×10^{-36}	kg	mass
2.417966×10^{14}	Hz	frequency
8.065465×10^{5}	m^{-1}	wavelength
8.065465×10^{3}	cm^{-1}	wavelength
1.160485×10^{4}	K	temperature

HEAT ENERGY CONVERSION FACTORS

$$1 \text{ calorie} = 4.1840 \text{ absolute Joules}$$
$$= 4.1833 \text{ international Joules}$$

PRESSURE CONVERSION FACTORS

$$1 \text{ atm} = 1.01325 \text{ bar}$$
$$= 14.70 \text{ psi}$$
$$= 29.92 \text{ inHg}$$
$$= 406.78 \text{ inH}_2\text{O}$$
$$= 760.0 \text{ Torr (mmHg)}$$
$$= 101,325 \text{ Pascal (Pa)}$$

SELECTED PROPERTIES OF HYDROGEN

Triple Point[A.2]
    T = 13.800 K
    P = 7.0420875 kPa   (0.0695 atm)
    d = 86.51 kg/m^3 (solid)
      = 77.04 kg/m^3 (liquid)
      = 0.12558 kg/m^3 (vapor)

Normal Boiling Point
    T = 20.278 K   (P = 1 atm)

Heat of Vaporization
    H_v = 214.8 cal/gm-mole = 449.4 J/gm   (P = 1 atm)

Heat of Fusion
    H_f = 28.03 cal/gm-mole = 58.64 J/gm

Calculated Properties of Saturated Parahydrogen[A.3]

Temperature K	Pressure Torr	Heat of Sublimation cal/gm-mole	Heat Capacity cal/K·gm-mole
13.813	52.89	244.90	1.360
13.000	30.13	242.30	1.164
12.000	13.78	238.71	9.438×10^{-1}
11.000	5.567	234.76	7.471×10^{-1}
10.000	1.917	230.55	5.751×10^{-1}
9.000	5.343×10^{-1}	226.12	4.280×10^{-1}
8.000	1.118×10^{-1}	221.53	3.054×10^{-1}
7.000	1.561×10^{-2}	216.82	2.065×10^{-1}
6.000	1.198×10^{-3}	212.02	1.301×10^{-1}
5.000	3.570×10^{-5}	207.15	7.420×10^{-2}
4.000	2.080×10^{-7}	202.24	3.799×10^{-2}
3.000	4.832×10^{-11}	197.30	1.603×10^{-2}
2.000	3.985×10^{-18}	192.34	4.749×10^{-3}
1.000	8.255×10^{-39}	187.37	5.936×10^{-4}
T	$P = 1924 e^{-95.25/T}$		$C_p = 5.936 \times 10^{-4} T^3$

References

[A.2] R.D. McCarty, J. Hord, and H.M. Roder, Edited by J. Hord, "Selected properties of hydrogen," Center for Chemical Engineering, National Engineering Lab, National Bureau of Standards, Boulder, Colorado (February 1981).

[A.3] J.C. Mullins, W.T. Ziegler, and B.S. Kirk, "The thermodynamic properties of parahydrogen from 1 to 22 K," Technical Report No. 1, Project No. A-593, Contract CST-7339, National Bureau of Standards, Boulder, Colorado (1 November 1961).

RELATIVISTIC MASS INCREASE AND TIME DILATION

The mass m and the lifetime t of a particle increase over the rest mass m_O and the resting lifetime t_O with increased total energy E_t according to the relativistic equations:

$$\text{A.1)} \quad \frac{t}{t_O} = \frac{m}{m_O} = \frac{E_t}{E_O} = \gamma = \frac{1}{(1 - \beta^2)^{1/2}} = 1 + \frac{E_k}{E_O}$$

where $E_O = mc^2$ is the rest mass energy of the particle and E_k is the kinetic energy.

The distance of travel d of the particle in vacuum is then just the velocity of the particle $v = \beta c$ times the relativistic lifetime of the particle $t = \gamma t_O$ or:

$$\text{A.2)} \quad d = vt = \gamma \beta c \, t_O \quad .$$

CENTER OF MASS ENERGIES

When a proton strikes a target with an incident energy E, the center of mass energy $s^{1/2}$ for the reaction $p \rightarrow p$ is:

$$\text{A.3)} \quad E_{cm} = s^{1/2} = (2mc^2 E + 2m^2 c^4)^{1/2}$$

where $mc^2 = 0.938$ GeV. The same reaction could have been obtained by colliding the two protons head on, with each proton at the energy $s^{1/2}/2$.

For very high energies this reduces to:

$$\text{A.4)} \quad s^{1/2} = (2mc^2 E)^{1/2} \quad .$$

In GeV units, where c=1 and m=1, this reduces to

$$\text{A.5)} \quad s^{1/2} = (2E)^{1/2}$$

so that at high energies the center of mass energy in a stationary target system only goes as the square root of the incident proton energy.

For example, the Fermilab 400 GeV Main Ring gives center of mass energies of 90 GeV, while the colliding beams at CERN of 270 GeV give a center of mass energy of 540 GeV. When Fermilab achieves collisions of 1000 GeV (1 TeV) protons on 1 TeV antiprotons, the center of mass energy will be 2 TeV. It would take an accelerator capable of reaching 2000 TeV to achieve the same results using a stationary target.

RELATIONS BETWEEN BEAM ENERGY AND MOMENTUM

The total energy E_t of an (anti)proton is related to the momentum p by the relativistic equation:

A.6) $E_t^2 = m^2c^4 + p^2c^2$

where m is the (anti)proton mass and c is the speed of light. For the (anti)proton, the rest mass energy is given by $mc^2 = 0.938$ GeV, while $m^2c^4 = 0.880$ GeV^2.

The total energy of the (anti)proton consists of the rest mass energy $E_o = mc^2$ plus the kinetic energy E_k:

A.7) $E_t = E_k + E_o = E_k + mc^2$.

Thus, the momentum of the (anti)proton in terms of the kinetic energy is:

A.8) $p^2 = 2mE_k + E_k^2/c^2$.

For kinetic energies well below the rest mass energy of the (anti)proton, the kinetic energy is given by the usual relation:

A.9) $E_k \sim p^2/2m$

or

A.10) $p \sim (2mE_k)^{1/2}$.

For kinetic energy well above the rest mass energy of the (anti)protons, the kinetic energy is approximately equal to the total energy

A.11) $E_k \sim E_t \sim pc$.

Thus, for energies much higher than the approximately 1 GeV rest mass energy of the (anti)proton, the numerical value of the energy in GeV and the momentum in units of GeV/c are roughly the same. For energy values below 1 GeV they differ significantly as is shown in Figure A-1.

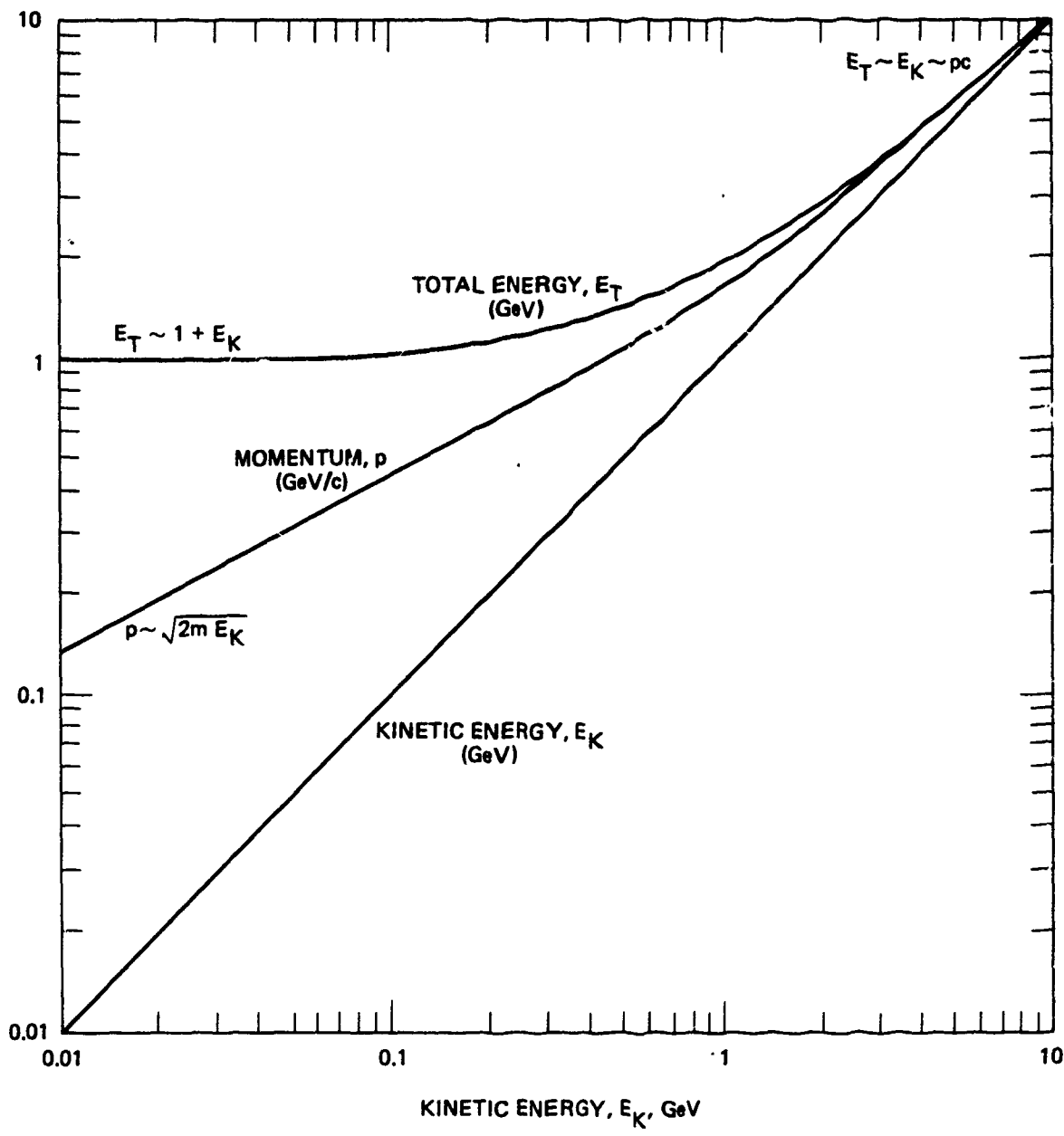Figure A-1 – Total energy and momentum vs. kinetic energy.

A-6

APPENDIX B

COST COMPARISON OF

CHEMICAL AND ANTIHYDROGEN PROPULSION SYSTEMS

FOR HIGH ΔV MISSIONS

This paper was presented at the AIAA/SAE/ASME/ASEE 21st Joint Propulsion Conference, Monterey, California (8-10 July 1985).

AIAA'85

AIAA-85-1455

COST COMPARISON OF CHEMICAL AND ANTIHYDROGEN PROPULSION SYSTEMS FOR HIGH ΔV MISSIONS

ROBERT L. FORWARD
HUGHES RESEARCH LABORATORIES
MALIBU, CALIFORNIA

BRICE N. CASSENTI
UNITED TECHNOLOGY RESEARCH CENTER
EAST HARTFORD, CONNECTICUT

DAVID MILLER
PURDUE UNIVERSITY
WEST LAFAYETTE, INDIANA

AIAA/SAE/ASME/ASEE 21st Joint Propulsion Conference
July 8-10, 1985 / Monterey California

COST COMPARISON OF CHEMICAL AND
ANTIHYDROGEN PROPULSION SYSTEMS FOR HIGH ΔV MISSIONS

Robert L. Forward
Hughes Research Laboratories
Malibu, California

Brice N. Cassenti
United Technology Research Center
East Hartford, Connecticut

David Miller
Purdue University
West Lafayette, Indiana

Abstract

Recent studies have indicated that it may be possible to make and store antimatter in the form of solid antihydrogen. For space propulsion, milligrams of antihydrogen would be used to heat tons of hydrogen reaction fluid to produce a specific impulse of 1000 to 3500 s tailored to the mission characteristic velocity ΔV. For typical deep space missions 1 milligram of antihydrogen would give the propulsion energy of 6 tons of liquid oxygen/liquid hydrogen fuel. In this paper we carry out a detailed parametric study of the comparative cost of chemical, nuclear thermal, and antihydrogen propulsion systems as a function of the mission characteristic velocity and the relative price of antihydrogen and propellant or reaction fluid in low earth orbit. We find that since the fuel cost of an antihydrogen propulsion system does not rise exponentially with mission characteristic velocity, ΔV, but only as the square of ΔV, antihydrogen propulsion will always be more cost effective than chemical propulsion at sufficiently high mission characteristic velocities.

Introduction

There has recently been a series of publications on the feasibility of using antimatter in the form of antihydrogen for space propulsion.[1-9] The annihilation of antihydrogen with hydrogen will produce large amounts of energy. The annihilation of a milligram of antihydrogen with a milligram of hydrogen produces the same amount of energy as 40 metric tons of TNT or 12 metric tons of liquid oxygen/liquid hydrogen fuel.

The antiprotons in antihydrogen are preferred over antielectrons for propulsion, since two-thirds of the annihilation energy appears as kinetic energy in the form of charged particles (pions). The charged particles can then transfer their kinetic energy to a hydrogen working fluid, which can be used to provide thrust. Only milligrams of antihydrogen will be needed to heat tons of hydrogen, and overall propulsion efficiencies (annihilation power to thrust power) of 25 to 50% have been predicted. For a typical mission, one extra milligram of antihydrogen allowed a mission to be done with 6 metric tons less hydrogen reaction mass.

Antimatter in the form of antiprotons is being made and stored today in very small amounts.[10-12] The publications on antihydrogen propulsion make the case that it should be possible to significantly increase the efficiency of the present production methods, turn the antiprotons into antihydrogen, and store the antihydrogen as charged ice crystals electrostatically levitated in a small cryogenically cooled chamber. If the production energy efficiencies (annihilation energy

out divided by ac mains power in) could be raised from the present 10^{-9} to 10^{-4}, then antihydrogen could be produced for an estimated 10M$/mg.[7,9]

At present, the cost to lift anything into space is 5k$/kg or 5M$/T. If the propulsion effectiveness of antihydrogen fuel to matter fuel remains at 1 mg per 6 T, then the cost of the 6 T of reaction mass would be 30M$, while the price of 1 mg of antihydrogen fuel would be only 10M$. Thus, based on fuel cost alone, antihydrogen would seem to be cost effective for space missions.

The previous estimates of the relative fuel costs for antihydrogen and other propulsion systems were limited in scope. The purpose of this paper is to look in detail at the relative fuel costs of various different missions and determine a price at which antihydrogen becomes cost effective for those different missions.

Thesis and Assumptions

The question we address in this paper is deliberately limited: "What is the relative total fuel cost of chemical, nuclear thermal, and antihydrogen propulsion systems for orbit transfer and other high velocity missions?" To keep the study from getting too complex, we have made a number of assumptions:

- The mission is entirely in space. There are no landing scenarios or aerobraking maneuvers.

- The simple rocket equations relating the mass ratio of the vehicle to the mission characteristic velocity and the propellant exhaust velocity are adequate to describe the actual performance of the propulsion system.

- Only fuel costs will be compared. The cost of designing and building the space vehicle itself will not be considered. No vehicle capable of handling antihydrogen or hot hydrogen reaction mass at specific impulses from 1000 to 3500 s has yet been built, while designs exist for chemical and nuclear thermal rockets. The cost of building the first antihydrogen powered rocket will be large, but it will not be included in these cost comparisons.

- The mission is time urgent. Long orbit-raising maneuvers and long, low thrust missions are not considered. This eliminates from consideration solar electric and nuclear electric propulsion as well as solar sails. Of course, solar sails with their zero use of fuel will always have the lowest fuel cost per mission and should always be used if time is not a consideration.

- The ratio of delivered payload to empty vehicle mass is the same for all the systems. Storable chemical and liquid oxygen/liquid hydrogen chemical propulsion systems will need more tankage than the other concepts. A nuclear thermal propulsion system will have a heavy reactor and shielding. An antihydrogen propulsion system will have a heavy reaction chamber and will also require some shielding.

- The specific impulses of chemical and nuclear thermal rockets are fixed by the inherent properties of the propulsion system. For storable chemical propellants we will assume a maximum specific impulse of 300 s or an exhaust velocity of 3 km/s. For a cryogenic liquid oxygen/liquid hydrogen propellant system we will assume a maximum specific impulse of 500 s or an exhaust velocity of 5 km/s. Although theoretically a nuclear rocket can have any specific impulse, we will assume that it is limited by the melting point of the reactor/heat exchanger to 900 s or an exhaust velocity of 9 km/s.

- An antihydrogen rocket can be operated at any desired specific impulse. Real antihydrogen rockets will have an upper limit to the specific impulse that is determined by temperature considerations. Proposed antihydrogen rocket designs will operate at temperatures where the reaction fluid has turned into a plasma and the plasma is contained and directed by magnetic fields. We will assume that such engines can be built and that they can produce high thrust at high exhaust velocities. We will not give the same benefit to the nuclear thermal rocket, but will assume it would use the present thermal reactor core design that is limited by the melting point of the core to specific impulses of less than 900 s.

Rocket Equations

We will assume that the performance of the propulsion systems is based on the following simplified equations. The exhaust velocity, v, of the propellant is related to the specific impulse, I_{sp}, by the relation,

$$v = g I_{sp} \qquad (1)$$

where $g = 9.8$ m/sec^2.

The mass ratio, R, is defined as the ratio of the mass of the empty vehicle (including payload), m_v, plus the mass of the propellant, m_p, divided by the mass of the empty vehicle. If the propulsion system has its energy source separate from its reaction fluid, as is the case with both the nuclear thermal and antihydrogen propulsion

systems, then the mass of the propellant consists of the mass of the reaction fluid, m_r, and the mass of the energy source, m_e:

$$R = \frac{m_v + m_p}{m_v} = \frac{m_v + m_r + m_e}{m_v} \qquad (2)$$

or

$$m_p = m_r + m_e = (R - 1)m_v \qquad (3)$$

The mass ratio, R, is related to the average exhaust velocity, v, of the propellant or the reaction fluid plus energy source mass through the relation,

$$R = e^{\Delta V/v} , \qquad (4)$$

$$= e^{\Delta V/gI_{sp}}$$

where the mission characteristic velocity, ΔV, is the sum of all the velocity changes that are required by the mission.

"Impossible" Missions

There are some missions in the solar system that would be desirable to accomplish for scientific purposes but which are essentially impossible using chemical or even nuclear thermal rockets because of the exponential growth of the mass ratio with increasing mission characteristic velocity. One example is a solar impact mission, which requires the rocket to cancel out the orbital velocity of the earth so the vehicle can drop directly into the sun. This requires a mission characteristic velocity of $\Delta V = 35$ km/s. Another is a rendezvous mission to the rings deep down in the gravity well of Saturn. This mission requires a ΔV of 48 km/s.

There are even simpler missions near earth that are nearly impossible using chemical rockets. One is the simple maneuver of leaving an orbiting base to inspect or pick up a satellite orbiting in the opposite direction. This maneuver requires canceling the initial orbital velocity and providing it again in the opposite direction. Since orbital velocity about the earth is 7.7 km/s, the total mission characteristic velocity of the reverse orbit maneuver is 15.3 km/s. If it is then desired to return to the orbiting base, the process must be repeated for a total ΔV of 31 km/s.

The mass ratios required for each type of rocket system to carry out these missions can be calculated from Equation (4) and are listed in Table 1. All of these missions require high mass ratios, the more difficult ones requiring such large mass ratios that it is extremely difficult to imagine how one might build a vehicle to accomplish such missions using chemical or even nuclear

Table 1. Mass Ratios for Difficult Missions

		TOTAL MASS RATIO, R		
	ΔV(km/s)	STORABLE 300 s	O_2/H_2 500 s	NUCLEAR 900 s
REVERSE ORBIT	15.5	175	22	6
DOUBLE REVERSE ORBIT	31.0	30,700	490	32
SOLAR IMPACT	35.0	117,000	1,100	49
SATURN RING RENDEZVOUS	48.0	8,900,000	15,000	200

thermal rockets. As we shall see later, all of these missions could be performed by an antihydrogen rocket with a mass ratio of 5:1 or less.

Minimum Antihydrogen Optimization

In this subsection, we will outline a mathematical proof for the optimization of an antihydrogen powered rocket mission in which the amount of antihydrogen used is minimized. The proof is simple, but has only been documented in journals[13] and reports[14] that are somewhat difficult to obtain, so we will repeat it here.

In an antihydrogen rocket, the source of propulsion energy is separate from the reaction fluid. Thus the total initial mass of the vehicle consists of the empty mass of the vehicle, m_v, the mass of the reaction fluid, m_r, and the mass of the energy source, m_e, half of which is the mass of the antihydrogen, m_a, that we wish to minimize. The mass ratio is then

$$R = e^{\Delta V/v} = \frac{m_v + m_r + m_e}{m_v} \quad (5)$$

The energy in the exhaust comes from the conversion of the fuel rest mass energy to kinetic energy with an efficiency, ϵ:

$$(m_e c^2)\epsilon = \frac{1}{2}(m_r + m_e)v^2 \sim \frac{1}{2}m_r v^2 \quad (6)$$

Combining Equations (5) and (6) and rearranging we obtain

$$m_e = \frac{m_v v^2}{2\epsilon c^2}(e^{\Delta V/v} - 1) = \frac{k}{x^2}(e^x - 1) \quad , \quad (7)$$

where $x = \Delta V/v$ and $k = m_v \Delta V^2/2\epsilon c^2$.

We now make the assumption that fuel costs dominate the reaction fluid costs and we want to minimize the amount of antihydrogen. By setting the derivative of Equation (7) with respect to x equal to zero and solving for x, it can be shown[13,14] that the fuel is minimized when

$$v = 0.63 \Delta V \quad . \quad (8)$$

This means that the mass ratio is a constant. Amazingly, this constant mass ratio is independent of the efficiency of the energy conversion and independent of the mission characteristic velocity:

$$R = e^{\Delta V/v} = e^{1.59} = 4.9 \quad . \quad (9)$$

This constant mass ratio for minimum antihydrogen consumption holds for all conceivable missions in the solar system and only starts to deviate significantly for interstellar missions where the mission characteristic velocity starts to approach the speed of light.[15]

The amount of antihydrogen needed for a specific mission is obtained by substituting Equation (8) into (7) to get the mass of the energy source, m_e. The antimatter is just half of this. It is found to be a function of the square of the mission characteristic velocity, ΔV^2 (essentially the mission energy), the empty mass of the vehicle, m_v, and the conversion efficiency, ϵ:

$$m_a = \frac{1}{2}m_e = \frac{0.39 \Delta V^2}{\epsilon c^2} m_v \quad . \quad (10)$$

For a typical antihydrogen mission where the antihydrogen energy to thrust energy conversion efficiency, ϵ, equals 0.3, only 12 mg of antihydrogen and 3.9 metric tons of propellant are needed to accelerate 1 ton of payload to 30 km/s (0.0001 c). Thus, no matter what the mission, the vehicle will always use 3.9 tons of propellant for each ton of payload and an insignificant amount (by weight, not cost) of antihydrogen.

Cost Equations

We now use the rocket equations to compare the total fuel cost for a number of different propulsion systems. For both storable and cryogenic chemical propulsion systems, the mass of the energy source is in the propellant. Thus, the fuel cost for the chemical rocket is just the cost of the propellant mass in orbit. For a nuclear thermal rocket, the energy to heat the reaction fluid is in the nuclear reactor. A reactor must have a certain minimum charge of uranium just to operate, and carries much more uranium than will be used in any reasonable mission. Therefore, we have assumed that the mass and cost of the uranium energy source is charged to the empty vehicle mass and cost. The fuel cost for the nuclear thermal rocket will be the cost of the reaction fluid mass in orbit. For an antihydrogen rocket, the cost of the antihydrogen part of the energy source is not negligible. The total fuel cost for the antihydrogen rocket will be the cost of the antihydrogen plus the cost of the reaction fluid mass.

Fuel Cost of a Chemical or Nuclear Thermal Mission

The fuel cost, C_c, of a mission using a chemical propulsion system is the price of propellant per kilogram in low earth orbit, p_p, times the propellant mass, m_p, needed for the mission:

$$C_c = p_p \, m_p \tag{11}$$

$$= p_p \, m_v \, (R - 1)$$

$$= p_p \, m_v \, (e^{\Delta V/v} - 1)$$

$$= p_p \, m_v \, (e^{\Delta V/g I_{sp}} - 1) \quad .$$

Since the chemical propulsion system has a fixed specific impulse or exhaust velocity, we see from Equation (11) that the cost of any chemical or nuclear thermal rocket system rises exponentially with increasing mission characteristic velocity as soon as the mission velocity exceeds the exhaust velocity:

$$C_c \xrightarrow{\Delta V > v} p_p \, m_v \, e^{\Delta V/v} \quad . \tag{12}$$

A similar conclusion can be derived for the nuclear thermal rocket. Although the nuclear reactor still has plenty of energy left, if the exhaust velocity is limited by thermal considerations, then an exponentially growing amount of reaction mass will be needed for the more difficult missions. It is this exponential growth of mass ratio and the fuel costs associated with it that has led to the labeling of some missions as "impossible."

Fuel Cost of an Antihydrogen Powered Mission

The fuel cost, C_a, of an antihydrogen rocket consists of the price of the antihydrogen, p_a, times the mass of antihydrogen, m_a, used plus the price of the reaction fluid, p_r, times the mass of the reaction fluid, m_r, heated by the energy from the antihydrogen:

$$C_a = p_r \, m_r + p_a \, m_a \quad . \tag{13}$$

In an antihydrogen rocket, the propulsion energy comes from the annihilation of the antihydrogen with a small amount of the normal matter in the propellant. The energy obtained is thus twice the rest mass energy of the antihydrogen. Some portion, ϵ, of this annihilation energy is then converted into kinetic energy of the propellant:

$$2\epsilon \, m_a c^2 = \frac{1}{2} \, m_r v^2 \quad . \tag{14}$$

Substituting Equation (14) into Equation (13) we obtain:

$$C_a = (p_r + p_a \frac{v^2}{4\epsilon \, c^2}) \, m_r \tag{15}$$

$$= (p_r + p_a \frac{v^2}{4\epsilon \, c^2}) \, (e^{\Delta V/v} - 1) \, m_v \quad .$$

In examining Equation (15) we see that there is a cost minimization possible for an antihydrogen rocket. As the required mission characteristic velocity increases, the cost of the mission tends to increase exponentially since the amount of reaction fluid mass needed is rising exponentially,

just as in a chemical rocket. In an antihydrogen rocket, however, this exponential rise in reaction fluid mass can be curbed by using more antihydrogen and increasing the reaction fluid exhaust velocity. Thus, for low exhaust velocity the second term becomes large, while at high exhaust velocity the first term becomes large. There is a cost minimum for each mission characteristic velocity, depending on the relative price in low earth orbit of hydrogen and antihydrogen.

Parametric Studies

In this section we carry out a parametric analysis of Equation (15) to determine the total fuel cost for an antihydrogen propulsion system for various values of the parameters of mission characteristic velocity and relative price ratio of antihydrogen to propellant or reaction fluid.

By varying the parameters we were able to establish a fuel cost minimum at each relative price ratio for various mission characteristic velocities. These total fuel cost minimum values for the antihydrogen propulsion system are then compared with the total fuel costs for chemical and nuclear thermal rockets given by Equation (11).

If antihydrogen is extremely expensive and the price ratio is high, then Equation (15) has the same form as Equation (7). We can then use the same technique that was used to minimize the amount of antihydrogen to minimize the total fuel cost. The optimum exhaust velocity, mass ratio, and antihydrogen mass used for minimum cost are those given by Equations (8), (9), and (10). Those optimum values for those parameters are indicated as the "asymptotic limits" in the figures that follow.

We were not able to find a simple analytic solution to the minimization of the cost expressed by Equation (15) when the relative costs of the antihydrogen and reaction fluid were comparable. Instead, a computer was used to calculate the total fuel cost, mass ratio, and antihydrogen mass used, as a function of the mission characteristic velocity over a range of specific impulses or exhaust velocities and a range of relative fuel costs. The minimum in the fuel cost was found and this determined the optimum values for the other quantities.

An important parameter in these studies is the ratio of the price of antihydrogen to the price of propellant or reaction mass in orbit. To be more general, we should have plotted the following curves in terms of a dimensionless price ratio. Since the price ratios vary from 10^{10} to 10^{0}, however, they are so large that they are almost meaningless. Instead, we fixed the price of either propellant or reaction mass in orbit at the present-day price of 5k\$/kg or 5M\$/T to lift mass into low earth orbit and presented the parametric curves in terms of the price of antihydrogen per milligram. Thus, a curve which is labeled 5M\$/mg is equivalent to a relative price ratio of

$$\frac{5M\$/mg}{5k\$/kg} = 10^9 \quad . \tag{16}$$

Optimum Mass Ratio

Figure 1 is a plot of the mass ratio of a number of different high thrust, fast response propulsion systems as a function of the mission characteristic velocity. The lines for a storable chemical system with a specific impulse of 300 s, a cryogenic O_2/H_2 chemical system with a specific impulse of 500 s, and a nuclear thermal rocket system with a specific impulse of 900 s were all obtained using the mass ratio expression given in Equation (4).

Also included in Figure 1 is the asymptotic limit of 4.9 for the mass ratio of an antihydrogen rocket using the minimum amount of antimatter and a set of curves giving the optimum mass ratios determined in our parametric studies as a function of the price of antihydrogen.

In Figure 1 we see that as the mission becomes more difficult with increasing ΔV, the mass ratios of the chemical and nuclear thermal systems rise exponentially. If we assume that it is difficult to build or stack a vehicle with an overall mass ratio much greater than 100, then storable chemical fuels cannot be used for missions with a characteristic velocity greater than 15 km/s. A cryogenically cooled O_2/H_2 propulsion system could be used instead, but even this most energetic of chemical fuels begins to fail for missions requiring a ΔV of 25 km/s. If a nuclear rocket could be built and flown with a specific impulse of 900 s, then it could be used for the more difficult missions, but even it begins to fail when the ΔV exceeds 40 km/s.

In contrast, all of the antihydrogen propulsion systems have mass ratios of less than 5. Depending on the relative price of antihydrogen and propellant or reaction fluid, and the difficulty of the mission, the values for the mass ratio are significantly less than 5, with a typical mass ratio value being 3:1.

Optimum Exhaust Velocity

Figure 2 illustrates the optimum exhaust velocity of an antihydrogen rocket as a function of the mission characteristic velocity for various antihydrogen prices. The asymptotic limit for high antihydrogen prices is the bottom line with a slope given by Equation (8).

As the price of antihydrogen drops below $50M\$/mg$ (relative price ratio of 10^{10}), the parametric studies indicate that the total fuel cost can be minimized by using more antihydrogen to heat the reaction fluid hotter, thereby obtaining a higher specific impulse and exhaust velocity and decreasing the amount of reaction fluid required.

The interesting characteristic of these optimum exhaust velocity curves is that they are nearly parallel to the asymptotic limit line. The slopes are slightly different, however, and they will intersect with the asymptotic line at very high mission velocities. As an example, the top line in Figure 2 for the optimum exhaust velocity when the price of antihydrogen is $1M\$/mg$ (relative price ratio 2×10^8) can be represented by the equation,

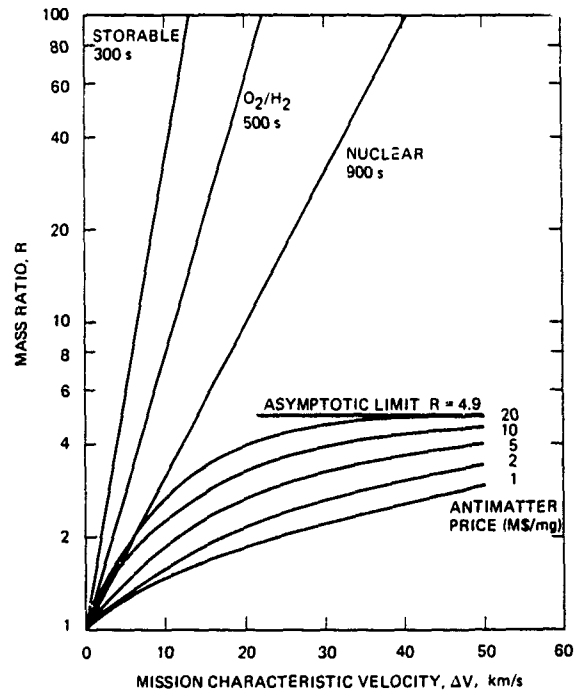$$v = 25 \text{ km/s} + 0.50 \ \Delta V \ . \qquad (17)$$

Fig. 1 Mass ratio vs mission characteristic velocity.
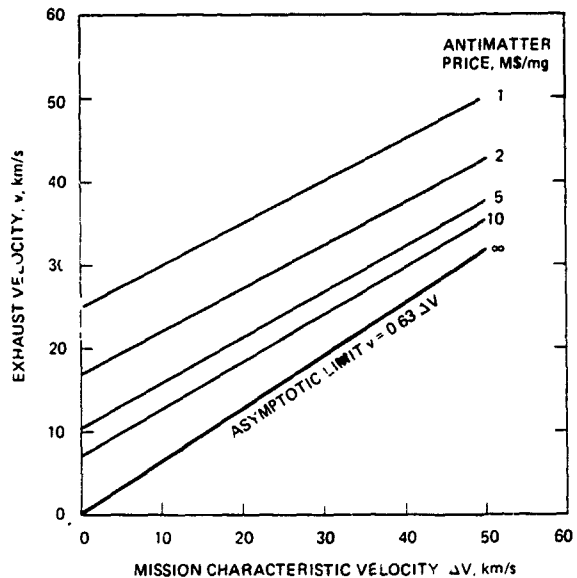

Fig. 2 Exhaust velocity vs mission characteristic velocity.

At the probable price of antihydrogen of $10M\$/mg$ the specific impulse required to carry out any mission in the solar system is seen to range from 1000 to 3500 s.

Optimum Antihydrogen Mass

Although the optimum exhaust velocity jumps with each decrease in the relative price of antihydrogen to reaction fluid, the amount of antihydrogen does not change in the same fashion. Figure 3 shows the optimum amount of antihydrogen needed per ton of empty vehicle mass, m_a, to produce the minimum total fuel cost. The bottom line is the asymptotic limit when the price of antihydrogen is high. The asymptotic limit rises as the square of the mission characteristic velocity (essentially the energy of the mission). The asymptotic limit for the amount of antihydrogen needed is also a function of the efficiency of conversion of annihilation energy into thrust.

We have assumed for the parametric studies that the overall efficiency of the conversion of annihilation energy into thrust is 30%. This efficiency estimate consists of a 67% conversion of annihilation energy into charged particles, a 50% efficiency of conversion of the energy of the charged particles into energy in the working fluid, and a nozzle expansion efficiency of 90%. Variations in this efficiency will not affect the mass ratio or exhaust velocity optimums, but will directly affect the amount of antihydrogen needed for a given mission and the total fuel costs for the mission.

From plots of the optimum amounts of antihydrogen as a function of its price we see that at the probable price of antihydrogen, 10M$/mg (relative price ratio of 2 x 10⁹), the amount of antihydrogen needed drops to the asymptotic limit at mission characteristic velocities greater than 20 km/s. Yet from Figure 2, the exhaust velocity is still significantly higher than the asymptotic exhaust velocity, because in optimizing the total fuel cost it was found to be more cost effective to decrease the amount of reaction fluid rather than increase the amount of antihydrogen. The decreased amount of reaction fluid is then ejected at a higher velocity. The mass ratio of the vehicle is less than the asymptotic limit, while the exhaust velocity is greater than the asymptotic limit. The interesting feature of Figure 3 is that the mass of antihydrogen required for a mission does not depend significantly on the cost of the antihydrogen for any of the difficult missions ($\Delta V > 10$ km/s) that antihydrogen rockets are best suited for.

Comparative Total Fuel Costs

We next calculated the total fuel costs for a number of different propulsion systems and compared the total fuel costs as a function of mission characteristic velocity. The propulsion systems considered were the storable chemical propulsion system with a specific impulse of 300 s, a cryogenic O_2/H_2 chemical propulsion system with a specific impulse of 500 s, a nuclear thermal rocket system with a specific impulse of 900 s, and three antihydrogen systems that were optimized for lowest total fuel cost as a function of the price of the antihydrogen.

Figure 4 presents the range of mission characteristic velocities that are typical of present-day missions. The ordinate showing relative fuel cost can be converted directly into millions of dollars per ton of empty vehicle mass if propellant for the chemical rockets and reaction
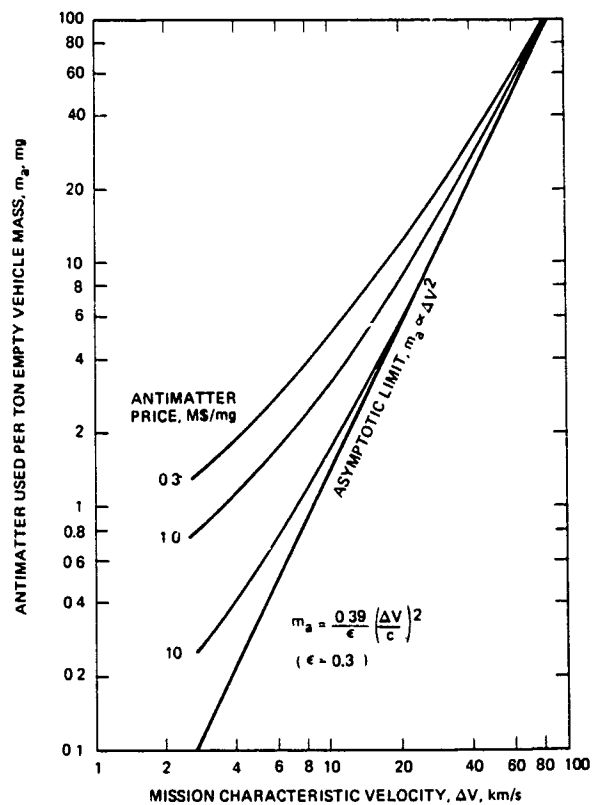

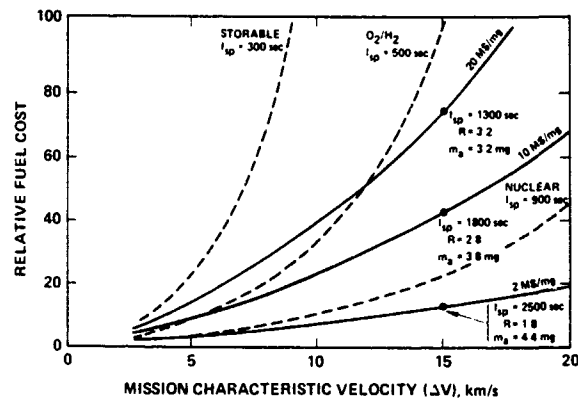
Fig. 3 Antihydrogen needed vs mission velocity.

Fig. 4 Relative fuel cost vs mission characteristic velocity.

fluid for the nuclear and antihydrogen rockets is assumed to be 5k$/kg and the antihydrogen price is that indicated for the various antihydrogen curves.

In examining Figure 4, we see that if the price of antihydrogen can be brought down to 20M$/mg (or a relative cost ratio of 4 x 10⁹), then an antihydrogen propulsion system is always more fuel cost effective than a storable chemical propulsion system. It is also better than the best chemical

propulsion system now available (O_2/H_2) for any mission characteristic velocity greater than 12 km/s. At a price of 10M$/mg (or a relative cost ratio of 2×10^9), antihydrogen propulsion systems are better than any chemical propulsion system at any mission velocity, but are not as cost effective as nuclear thermal propulsion. If the price of antihydrogen drops to 2M$/mg (relative price ratio of 4×10^8), then antihydrogen propulsion is more cost effective than any other known propulsion system at any mission velocity.

Also shown in Figure 4 are some typical operational parameters for a mission requiring a total ΔV of 15 km/s. At an antihydrogen price of 20M$/mg, each ton of empty space vehicle requires only 3.2 mg of antihydrogen costing $64M to heat 2.2 metric tons of reaction fluid costing $11M to a specific impulse of 1300 s. Thus, one ton of vehicle can be pushed to 15 km/s by an antihydrogen propulsion system for a total fuel cost of $75M, while to do the same job with a O_2/H_2 rocket would cost $100M. If the price of antihydrogen drops to 2M$/mg, then each ton of delivered vehicle mass would require the use of 4.4 mg of antihydrogen costing $8.8M to heat 0.8 tons of reaction fluid costing $4M to a specific impulse of 2500 s. At this price for antihydrogen, the total fuel cost to push a ton to a velocity of 15 km/s would be only $12.8M.

Antihydrogen Propulsion Enables "Impossible" Missions

In Figure 5 we expand the scale of the plot of relative fuel cost versus mission characteristic velocity from the scale of Figure 4, which shows the missions that are being considered in the near future, to a scale that includes missions that are "impossible" using any chemical or nuclear thermal system. In Figure 5 the relative fuel cost scale can be converted into millions of dollars per ton of delivered empty vehicle mass if the cost of propellant or reaction fluid in space is 5k$/kg or 5M$/T.

In this figure it is easier to see the differences in the shapes of the total fuel cost curves for the different types of propulsion systems. For those propulsion systems with a fixed specific impulse, the fuel cost rises exponentially with increasing mission characteristic velocity. Since the antihydrogen propulsion systems can vary the exhaust velocity to match the mission, the total fuel cost for an antihydrogen propulsion system only rises as the square of the mission characteristic velocity. Thus, no matter what the cost of antihydrogen, it will always be more cost effective than any propulsion system with a fixed exhaust velocity at sufficiently high enough mission velocity. For example, even at 10M$/mg, an antihydrogen propulsion system will cost less than a nuclear thermal rocket if the mission characteristic velocity desired is greater than 30 km/s (just off the top of Figure 5).

If the price of antihydrogen can be brought down to 1M$/mg or less, then antihydrogen propulsion can open up the entire solar system and allow the performance of missions that are now impossible to consider using any present propulsion system. For example, at 1M$/mg, an antihydrogen
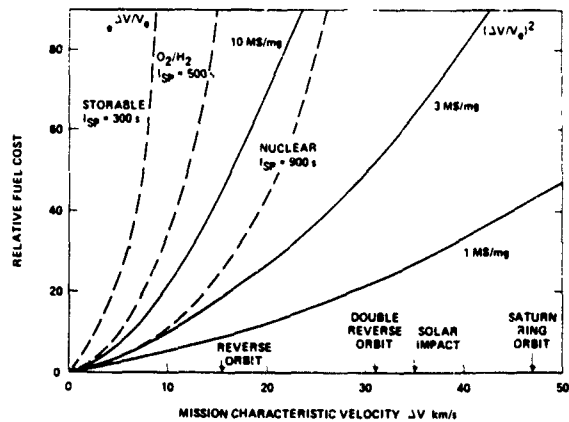

Fig. 5 Relative fuel cost vs expanded mission velocity.

propulsion system can deliver a 5 T vehicle to the rings of Saturn for a total fuel cost of just $200M and complete the mission in months instead of years.

Conclusions

In this paper we have carried out a parametric study of the comparative total fuel costs for storable chemical, cryogenic chemical, nuclear thermal, and antihydrogen propulsion systems for various mission characteristic velocities and various relative price ratios for antihydrogen and propellant or reaction fluid in space. Under several restrictive assumptions we have shown the following:

• Since an antihydrogen propulsion system can operate at any specific impulse by changing the ratio of antihydrogen to hydrogen, the total fuel cost only rises as the square of the mission characteristic velocity. Chemical and nuclear thermal systems with a fixed exhaust velocity have a fuel cost that rises exponentially with mission characteristic velocity. Thus, antihydrogen propulsion will always be more cost effective than other forms of propulsion at sufficiently high mission characteristic velocity.

• Chemical propulsion systems are nearly always more cost effective for mission characteristic velocities of less than 5 km/s.

• If the price ratio of antihydrogen to propellant or reaction fluid is greater than 4×10^9 (20M$/mg), then antihydrogen propulsion systems are more cost effective than chemical propulsion systems for mission characteristic velocities of greater than 12 km/s.

• If the cost of antihydrogen to propellant or reaction mass is less than 2×10^8 (1M$/mg), then antihydrogen propulsion

B-9

systems are more cost effective than chemical propulsion systems and even nuclear thermal propulsion systems for any mission characteristic velocity over 5 km/s.

Acknowledgments

References

1. R.L. Forward, "Interstellar flight systems," AIAA Reprint 80-0823, AIAA Int. Meeting, Baltimore, MD (1980).

2. P.F. Massier, "The need for expanded exploration of matter-antimatter annihilation for propulsion application," J. British Interplanetary Soc. 35, 387-390 (1982).

3. R.L. Forward, "Antimatter propulsion," J. British Interplanetary Soc. 35, 391-395 (1982).

4. B.N. Cassenti, "Design considerations for relativistic antimatter rockets," J. British Interplanetary Soc. 35, 396-404 (1982).

5. D.L. Morgan, "Concepts for the design of an antimatter annihilation rocket," J. British Interplanetary Soc. 35, 405-412 (1982).

6. G. Vulpetti, "A propulsion-oriented synthesis of the antiproton-nucleon annihilation experimental results," J. British Interplanetary Soc. 37, 124-134 (1984).

7. R.L. Forward, "Antiproton annihilation propulsion," AIAA preprint 84-1482, AIAA/SAE/ASME 20th Joint Propulsion Conference, Cincinnati, Ohio (11-13 June 1984).

8. B.N. Cassenti, "Antimatter propulsion for OTV applications," AIAA preprint 84-1485, AISS/SAE/ASME 20th Joint Propulsion Conference, Cincinnati, Ohio (11-13 June 1984).

9. R.L. Forward, Alternate Propulsion Energy Sources, AFRPL-TR-83-067, Final Report on Contract F04611-83-C-0013, Air Force Rocket Propulsion Lab, Edwards, CA 93523 (December 1983) [Distribution limited to U.S. Government and Contractors.]

10. CERN Proton Synchrotron Staff, "The CERN PS complex as an antiproton source," IEEE Trans. NS-30, 2039-2041 (1983).

11. J. Peoples, "The Fermilab antiproton source," IEEE Trans. NS-30, 1970-1975 (1983).

12. T.A. Vsevolozhskaya, B. Grishanov, Ya. Derbenev, N. Dikansky, I. Meshkov, V. Parkhomchuk, D. Pesrikov, G. Sil'vestrov, and A. Skrinsky, "Antiproton source for the accelerator-storage complex, UNK-IHEP," Fermilab Report FN-353 8000.00 (June 1981), a translation of INP Preprint 80-182 (December 1980).

13. L.R. Shepherd, "Interstellar flight," J. British Interplanetary Soc. 11, 149-167 (1952).

14. D.F. Dipprey, "Matter-Antimatter Annihilation as an Energy Source in Propulsion," Appendix in Frontiers in Propulsion Research, JPL TM-33-722, D.D. Papailiou, Ed. (Jet Propulsion Lab, Pasadena, CA (15 March 1975).

15. B.N. Cassenti, "Optimization of relativistic antimatter rockets," J. British Interplanetary Soc. 37, 483-490 (1984).

APPENDIX C

ANTIPROTON ANNIHILATION PROPULSION

This paper was prepared and presented under the present contract although a good deal of. the material used was based on the results of a previous contract[C.1] with the Air Force Rocket Propulsion Laboratory. It was first presented[C.2] at the AIAA/SAE/ASME 20th Joint Propulsion Conference in Cincinnati, Ohio on 11-13 June 1984, and a shorter version was presented[C.3] at the 35th Congress of the International Astronautical Federation in Lausanne, Switzerland on 7-13 October 1984. It was submitted to the Journal of Propulsion and Power and was accepted for publication after reduction in length, number of figures, and number of references. The reduced version that will appear in a future issue of the Journal of Propulsion and Power (late 1985 or early 1986) is reproduced in the following pages.

[C.1]R.L. Forward, "Alternate Propulsion Energy Sources," AFRPL-TR-83-067, Final Report on Contract F04611-83-C-0013, Air Force Rocket Propulsion Lab, Edwards, CA 93523, December 1983,

[C.2]R.L. Forward, "Antiproton annihilation propulsion," AIAA Paper 84-1482, AIAA/SAE/ASME 20th Joint Prop. Conf., Cincinnati, Ohio (11-13 June 1984).

[C.3]R.L. Forward, "Antiproton propulsion," IAF Paper 84-318, 35th Congress of the Int. Astronaut. Fed., Lausanne, Switzerland (7-13 October 1984)

ANTIPROTON ANNIHILATION PROPULSION

Robert L. Forward[*]

Abstract

Antimatter represents a highly concentrated form of energy storage since the antimatter converts all of its mass to energy upon annihilation with normal matter. The antimatter should be in the form of antiprotons since, unlike positrons or antielectrons, the antiproton does not convert into gamma rays upon annihilation, but instead two-thirds of the energy is emitted as charged particles (pions) whose kinetic energy can be converted into thrust by interaction with a magnetic field nozzle or a working fluid. Antiprotons are already being generated, captured, cooled, and stored at a number of particle physics laboratories around the world, albeit in small quantities. A number of techniques for the efficient generation, long-term storage, and effective utilization of milligram quantities of antiprotons for space propulsion are discussed.

---

[*] Associate Fellow, AIAA

Introduction

In this paper I discuss a new high specific impulse, high thrust propulsion system based on the generation, storage, and utilization of antiprotons. It has long been realized that antimatter would be a valuable propulsion energy source because it allows for the complete conversion of mass to energy. Early studies of the concept by Sänger[1] assumed that the antimatter would be antielectrons (positrons), which interact with electrons to produce 0.511 MeV gamma rays. Sänger unsuccessfully tried to invent electron-gas mirrors to direct these short wavelength gamma rays to produce a photon rocket.

The antiproton is much more suitable than the antielectron for propulsion systems. The annihilation of an antiproton by a proton (or neutron) does <u>not</u> produce gamma rays immediately. Instead the products of the annihilation are from three to seven pions. On the average there are 3.2 charged pions and 1.6 neutral pions.[2] The neutral pions have a lifetime of only 90 attoseconds and almost immediately convert into two high-energy (200 MeV) gamma rays. The charged pions have a normal half-life of 26 nanoseconds, but because they are moving at 94% the speed of light, their lives are lengthened to 70 nanoseconds. Thus, they travel an average of 21 meters before they decay. This time and interaction length is easily long enough to collect the charged pions in a thrust chamber constructed of magnetic fields and direct the isotropic microexplosion into a unidirectional flow. Even after the charged pions decay, they decay into energetic charged muons, which have even longer lifetimes and interaction lengths for further conversion into thrust. Thus, if sufficient quantities of antiprotons could be made, captured, and stored, then present known physical principles show that they can be used as a highly efficient propulsion fuel.

Because of the extreme difficulty in obtaining significant quantities of antimatter, the idea of an antimatter rocket has usually remained in the "science fiction" category. Any papers before 1980 [see 27 references in section 02.01 of bibliography by Mallove, et al.[3]] were usually concerned with interstellar missions and glossed over the problems of generating, storing, and using the antimatter. Recent progress in particle physics on methods for obtaining intense antiproton beams, however, have caused those in the space propulsion community to take another look at the concept of antimatter propulsion to see if the concept can be removed from the "science fiction" category to the "technically difficult and very costly" category, at which point the military services or NASA could begin considering its use.

The last five years have seen the presentation of a number of papers on antimatter propulsion,[4-8] including a special issue of the Journal of the British Interplanetary Society on the subject of antimatter propulsion.[9-14]

The problems to be solved in making antiproton annihilation propulsion feasible can be listed as:

Antiproton Generation
Antiproton Capture
Cooling at Relativistic Velocities
Deceleration from Relativistic to Subrelativistic Velocities
Cooling and Slowing at Subrelativistic Velocities
Conversion of Antiproton Beam to Antihydrogen Beam
Cooling and Slowing of Antihydrogen Beam
Conversion of Antihydrogen Atoms to Antihydrogen Molecules
Cooling and Slowing of Molecular Antihydrogen Beam
Stopping of Antihydrogen Molecules
Trapping and Cooling of Antihydrogen Molecules
Conversion of Antihydrogen Gas to Antihydrogen Ice
Long Term Storage of Antihydrogen Ice
Extraction of Antihydrogen from Storage
Annihilation of Antihydrogen
Transfer of Annihilation Energy to Working Fluid
Conversion of Working Fluid Energy to Thrust

Solutions to some of these problems, such as generation, capture, relativistic cooling, deceleration, and subrelativistic cooling have already been demonstrated. I can see solutions to most of the rest of the problems, although not all of them. In the remainder of this paper we will see what is the present state of the art, what are the problems yet to be solved, and how one might approach a solution to those problems.

Present Production Facilities

Antimatter in the form of antiprotons is being made and stored today, albeit in small quantities. The two major producers are the Institute for High Energy Physics (IHEP) in the USSR[15] and the Centre Européenne pour la Recherche Nucléaire (CERN) in Europe.[16] Fermilab in the US has started construction of their antiproton facility and expects to be in operation in 1985.[17] In these facilities, the antiprotons are generated by sending a high-energy beam of protons into a metal target. When the relativistic protons strike the dense metal nuclei, their kinetic energy, which is many times their rest-mass energy, is converted into a spray of particles, some of which are antiprotons. A magnetic field focuser and selector separates the antiprotons from the resulting debris and directs it to a storage ring.

When the antiprotons are generated, they have a wide spread of energies. This makes it difficult to decelerate them to subrelativistic velocities, so it is necessary to "cool" the beam so that all the antiprotons have the same energy. Two techniques for reducing the velocity spread have been successfully demonstrated. In the stochastic cooling scheme,[18] the radio noise generated by fluctuations in the beam are detected. This noise is amplified, phase shifted, then transmitted across the diameter of the ring to an electromagnetic kicker that suppresses the fluctuation. In the electron cooling scheme[19] a beam of monoenergetic electrons is inserted in the ring with the antiprotons. Those antiprotons moving too slowly will be accelerated by electromagnetic interactions with the negative charge on the electrons and those moving too fast will be decelerated. These cooled antiprotons could then go through another stage of deceleration and cooling to bring them down to speeds suitable for capture, control, and cooling by other techniques. The accelerator at CERN generates 3.5 GeV antiprotons using a 26 GeV proton beam and has stored as many as 10^{12} antiprotons for days at a time in their magnetic ring "racetrack" antiproton accumulator.[20]

To give some scale as to what has already been accomplished at these research facilities, 10^{12} antiprotons have a mass of 1.7 picograms. When this amount of antimatter is annihilated with an equivalent amount of normal matter, it will release 300 joules, a significant quantity of energy from an engineering viewpoint. To obtain this "firecracker" amount of annihilation energy required the use of multimillion dollar machines that used an enormous amount of electric energy. Yet it is important to recognize that scientists working in basic physics, using research tools not designed for the job, have produced and continue to produce significant quantities of annihilation energy.

Present Production Rates

The capture efficiencies of the present antiproton facilities are abysmally low. The situation is summarized by Figure C-1 from a recent paper.[21] The upper part of the figure shows the total number of antiprotons generated per GeV of antiproton momentum per steradian of solid angle at the central portion of the antiproton beam. Integrating the curve over the antiproton momenta shows that each proton produces 7.7 antiprotons per steradian. The number of antiprotons per GeV of antiproton momentum for two different angular acceptances is shown in the lower two curves. In the paper, the number of antiprotons per GeV of antiproton momentum is estimated assuming that first antiproton collector at Fermilab can only accept those antiprotons with an angular spread off the axis of 30 mrad (0.0028 steradians).
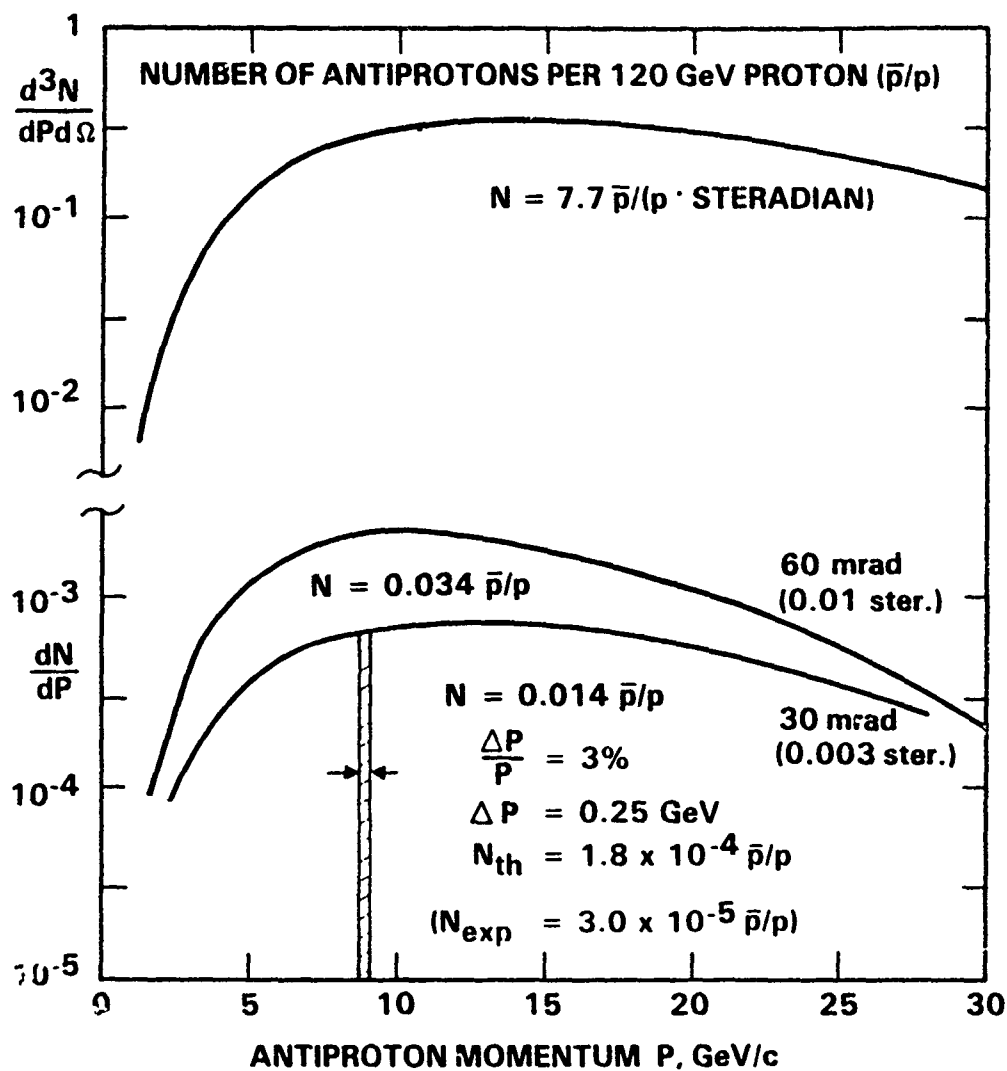
Fig. C-1   Present antiproton capture efficiencies

When the 30 mrad curve is integrated over the antiproton
momenta we find a total of only 0.014 antiprotons per proton
in this narrow angular acceptance. Then, of this small
angular spread the Fermilab collector is able to capture only
those with a momentum (velocity) spread of 3% or 0.25 GeV
around 8.9 GeV. Thus, ideally, they would expect to capture
about 1.8×10^{-4} antiprotons per proton, with an estimated
actual capture rate (including mismatch and transport losses)
of 3×10^{-5} antiprotons per proton. If we compare the
annihilation energy we get from using the antiproton ($2m_p c^2 =$
1.87 GeV) with the energy in the 120 GeV protons required to
make that antiproton, we get an energy efficiency of 5×10^{-7}.
Since a typical synchrotron is only about 5% efficient, the
"wall-plug" energy efficiency for antiproton production of
present machines is only about 2×10^{-8}.

Future Production Rates

Data on the antiproton production spectrum of high-energy
protons impacting heavy metal targets are available only for
small angles about the forward direction. These data are
sufficient for the design of the present antiproton collector
systems that only attempt to capture the antiprotons emitted
around the forward peak. To design systems that will capture
a higher percentage of the antiprotons, it will be necessary
to know the antiproton spectrum as a function of angle and
incident proton energy over a greater angular spread. Such
data do not seem to exist and there are no present plans to
make these measurements since obtaining the data would require
an extensive amount of time on the large synchrotron machines.
The particle physics community prefers to use the machine time
to study issues more important to particle physics. As a
result of this lack of detailed knowledge of the spectrum, the
total number of antiprotons generated is also unknown (to
probably a factor of two).

The last collection of experimental data on total antiproton
production rates was done over a decade ago and published in a
review paper by Antinucci, et al.[22] The measurements were
made using colliding beams of protons, so the data are only
partially relevant to the problem of colliding protons with
heavy nuclei, which is known to give a higher antiproton
production rate. The data from the table in the Antinucci
paper for the total antiproton production rate are the large
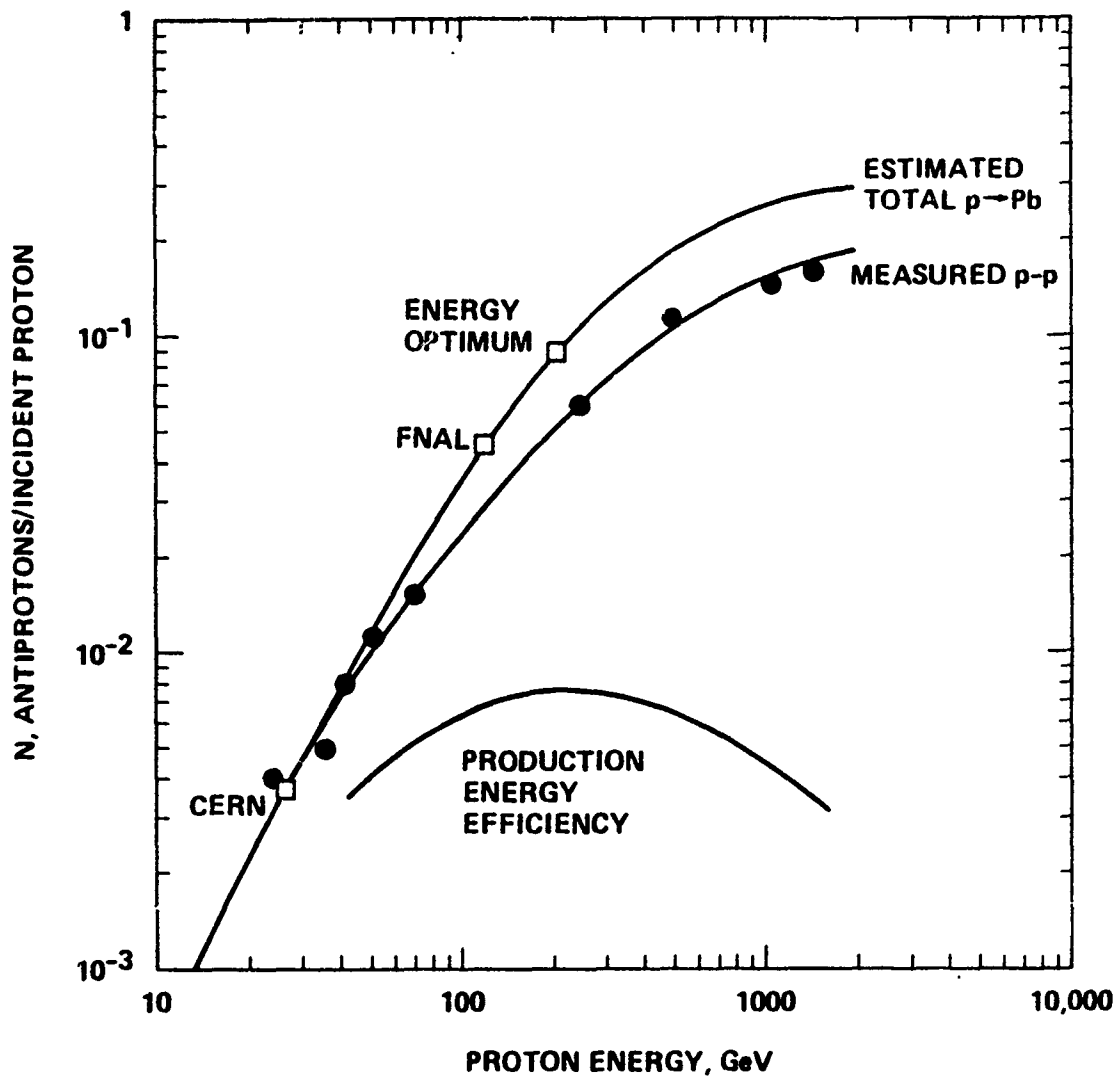dots in Figure C-2.

Fig. C-2   Total antiproton production rates.

Using the known ratio of antiproton production in the forward direction from heavy nuclei and hydrogen targets,[21] I was able to modify the Antinucci hydrogen target data to obtain the upper curve which gives the predicted antiproton production rates as a function of energy for protons incident on metal targets.

If we now take the upper curve giving the number efficiency for producing antiprotons and divide it by the energy of the proton making the antiprotons, we obtain the bottom curve. This is the energy efficiency for producing antiprotons. Note that it has a broad peak around 200 GeV. Although the number of antiprotons produced continues to increase as the incident proton energy is increased, above 200 GeV the gain in production is not enough to offset the increased proton energy required.

From Figure C-2 we see that the maximum energy efficiency production rate occurs for an incident proton energy of 200 GeV and is 0.085 antiprotons/proton. (There are roughly 5 K mesons, 50 pi mesons, and large numbers of positrons and electrons produced for each antiproton generated.) This antiproton production rate is 2 times the production at the Fermilab energy of 120 GeV and 20 times the production at the CERN energy of 26 GeV. It should be emphasized that the curves in Figure C-2 are based on sparse data and that actual measurements of antiproton production spectra as a function of angle and proton energy are needed before any major engineering studies on antiproton production are done.

Antiproton Factory

Figure C-3 shows a conceptual design for an antiproton factory which would utilize the technologies being developed at CERN, Fermilab, and IHEP, but on a much larger scale and with the design optimized for energy efficiency. First, the proton accelerator should be a high current rf linear accelerator (linac) with a wallplug efficiency of 50%, rather than the low current, low efficiency, but high energy resolution synchrotron preferred as a research tool by particle physicists. There would be more than one proton beam with each beam operated at the optimum beam current for the particular target design chosen. Each proton beam would strike a metal target and the resulting particles would be sorted by an array of wide-angle collecting lenses to extract the antiprotons and positrons. The positrons with the right energy would be picked off and sent to the antihydrogen generator, while all the antiprotons possible would be sorted by energy and sent to a stack of stochastic coolers, each optimized for a particular central antiproton momentum.
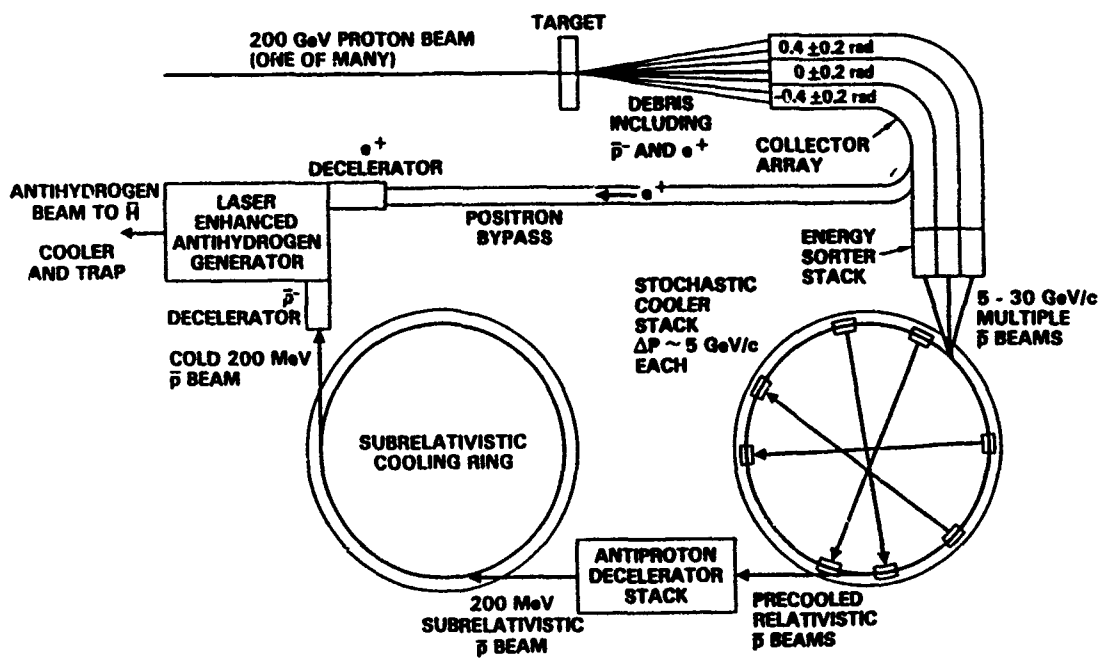
Fig. C-3   Antiproton factory (one segment)

After stochastic cooling, the stack of beams at different
energies would go to a decelerator stack that would reduce all
the antiproton energies to the same subrelativistic energy
(200 MeV). The combined beam would then be sent to a
subrelativistic cooling ring using either stochastic or
electron cooling before being further decelerated and sent on
to the antihydrogen generator where the antiprotons are
combined with the positrons to make antihydrogen atoms.

Antihydrogen

The antihydrogen generator would follow the general concepts
described in a recent research publication at CERN.[23] As
shown in Figure C-4, if a beam of positrons were traveling
along with a beam of antiprotons at the same speed, they would
attract one another and recombine to form antihydrogen. This
natural process can be enhanced by factors of 100 or more by
stimulating the capture process with photons at the right
wavelength.

Once an antihydrogen beam has been formed, there are a number
of techniques available for cooling the electrically neutral
antihydrogen down, slowing it to a stop, and storing it in a
trap. Traps for atoms were first proposed by Letokov[24] and
Ashkin.[25] These traps use laser beams tuned just below the
first optical resonance line of the atom. Those atoms trying
to move toward the laser will see the laser photons shifted
upward into resonance with the optical absorption line. The
atoms will absorb the Doppler-shifted laser photons, slowing
down slightly in the process. The atom then reradiates each
photon, but in a random direction, so the recoils from the
reradiated photons will average out. Thus, after many
absorptions and reradiations, the atom has stopped moving.
Once the atom is stationary, it no longer absorbs the off-
resonant laser photons and stays trapped.

Lasers have also been used to "push" a beam of sodium atoms to
one side, "cool" the beam both longitudinally and transversely
until all the atoms have the same speed, and slow down, halt,
and reverse the direction of an atomic beam. The activities
in the field of cooling and trapping atoms has progressed to
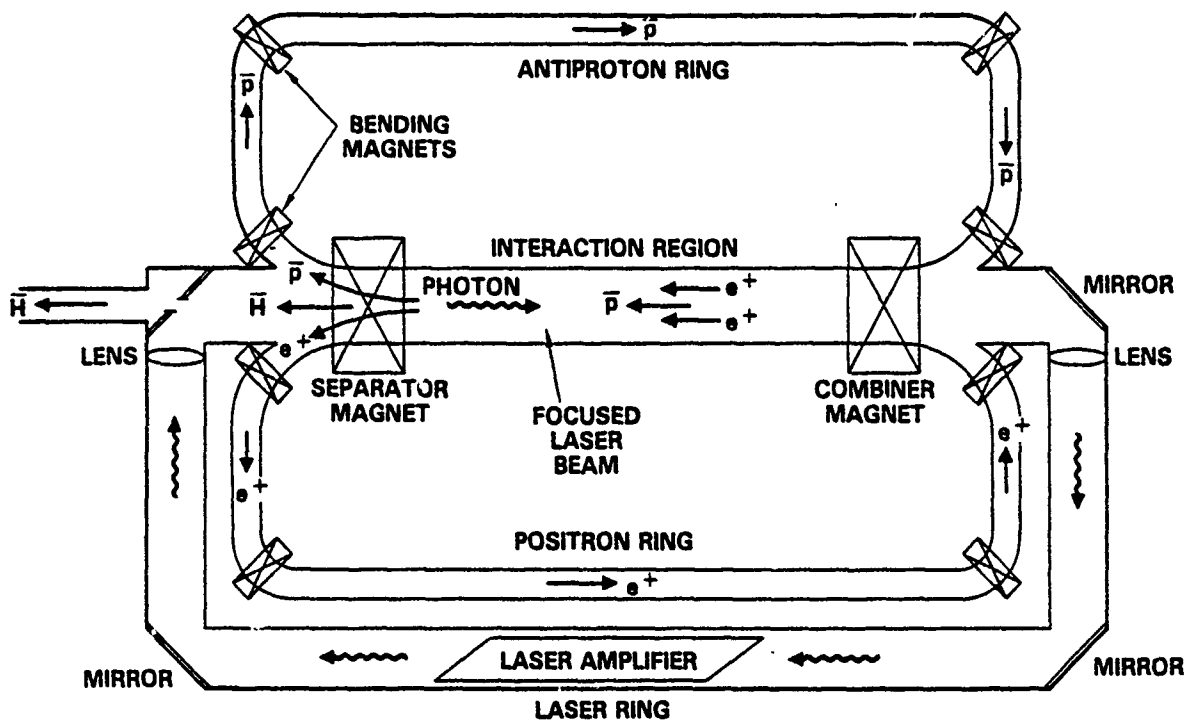the point where there are periodic workshops on laser cooling
and trapping.[26]

Fig. C-4   Laser-aided antihydrogen formation

Although it might be possible to store antihydrogen as an atomic gas,[27] the atomic form of antihydrogen is more difficult to control, cool, and trap than sodium since the first resonance line in atomic hydrogen is in the vacuum ultraviolet (the Lyman alpha line). The fundamental problem is that while one Lyman alpha photon will excite an antihydrogen atom, if a second photon arrives before the atom has decayed back into its ground state, the second photon may ionize the antihydrogen atom. Although proprietary ideas exist for overcoming these problems, it will likely be found necessary to convert the antihydrogen atoms into antihydrogen molecules, then store them as antihydrogen ice.

The conversion of antihydrogen atoms to antihydrogen molecules takes place naturally (with the release of lots of energy, which is why spin-polarized normal hydrogen is being looked at as a potential rocket fuel). A large number of the molecules remain in a metastable orthohydrogen state. Left to themselves, cold antihydrogen molecules will ultimately all convert to parahydrogen, the ground state of the molecule, but unless a catalyst is used, the process takes many days. Research is needed on the use of lasers and magnetic fields with high gradients to convert the antihydrogen atoms into antihydrogen molecules. These antihydrogen molecules can then be further cooled and trapped using lasers operating on a molecular hydrogen line, then turned into antihydrogen ice in the preferred parahydrogen state. Research is also needed on turning a cold antihydrogen vapor into ice crystals, since there is a heat of fusion generated during the formation of the ice. Fortunately, all of these research problems on manipulation of antihydrogen can be studied using normal hydrogen (and would make excellent thesis topics).

Antihydrogen Traps

Antihydrogen ice, like hydrogen ice, is diamagnetic, with a negative magnetic susceptibility that is two-thirds that of graphite. A simple passive trap for a ball of antihydrogen ice could be made of magnetic fields. There are a number of different ways to configure permanent magnets and coils to produce a magnetic field minimum that will attract and trap a diamagnetic material such as graphite[28] or hydrogen. One simple example consists of two superconducting coils spaced so that there is a magnetic minimum midway between them.[29] This kind of trap would be completely stable and require no power. It is not very deep, however, and although quite suitable for storage of antihydrogen ice in free fall, it might not be able to levitate the antihydrogen ice at high acceleration levels.

For high acceleration levels, a more suitable trap would be a servocontrolled dc voltage electrostatic levitation mechanism such as those made at JPL.[30]   These traps have levitated electrically charged 20 mg millimeter sized spheres of water ice in the earth's field. Antihydrogen ice will have a density of 0.0763 g/cm^3, which is 13 times less than water ice.   Thus, the same electrostatic suspension could hold milligram-sized balls of antihydrogen ice at accelerations up to 13 gees. Since the antihydrogen ice will be formed at millidegrees or below, and the heat input from the electric levitator will be low, the sublimation pressure of the antihydrogen will be so low (10^{-39} torr at 1 K) that the antihydrogen ice ball should last for years.

Utilizing Antihydrogen For Propulsion

There are a number of techniques for extracting the antihydrogen from the storage trap and directing it into the rocket engine under control. If the antihydrogen is in the form of a large ball many milligrams in size, the antiprotons can be extracted from the ice ball by irradiating the ice with ultraviolet, driving off the positrons, extracting the excess antiprotons by field emission with a high intensity electric field, then directing them to the thrust chamber.[12]   It might be more desirable if the antihydrogen could be formed as a cloud of charged microcrystals, each a microgram and containing the energy equivalent of 20 kg of chemical fuel. Then, using a directed beam of ultraviolet light to drive off a few more positrons, an individual microcrystal could be made more highly charged, preferentially extracted from the microcrystal cloud using electric fields, and directed down a vacuum line to the thrust chamber. Since the position of the charged microcrystal in the injection line can be sensed, mechanical shutters can allow the passage of the microcrystal without breaking vacuum.

Antimatter fuel is so powerful that new types of rocket engines will have to be developed to fully utilize its potential. One of the simplest antiproton propulsion systems would use a design similar to that of a nuclear thermal rocket. In a nuclear thermal rocket hydrogen gas is heated by passing it through the core of a fission reactor. The hot hydrogen is then used to provide thrust. In the antiproton annihilation version, the energy released by the annihilation reaction would be absorbed in the walls of a heat exchanger made out of refractory metal. The heat exchanger would then heat hydrogen to produce thrust.[31]   A heat exchanger made out of a cylinder of tungsten 28 cm in diameter and 28 cm long would only weigh 330 kg and would capture most of the energy in the gamma rays and pions emitted by the antiproton-proton annihilation process, thus utilizing all of the energy in the

annihilation reaction. The maximum temperature would be limited by the melting point of tungsten to about 3000 K, resulting in a maximum specific impulse of about 900 sec or an exhaust velocity of about 9 km/s. This is considerably better than any chemical rocket or even a nuclear fission thermal rocket, but still does not use the high exhaust velocity potential of antiproton annihilation.

The plasma created from the heating of the hydrogen working fluid by the pions emitted from the annihilation process is too hot to be contained and directed by thrust chambers and nozzles made of solid material. Fortunately, most of the particles generated are charged and can be contained and directed by strong magnetic fields. The first example of a design for a magnetic field antiproton rocket engine can be found in the paper by Morgan.[12]

Minimum Antimatter Optimization

When antiprotons interact with protons (hydrogen), the resultant annihilation products are pions with an average kinetic energy of 250 MeV. This translates into an exhaust velocity of 94% of the speed of light. Thus, pure antimatter rockets are best suited for relativistic missions. In order to use the minimum amount of antimatter for the mission, the best way to use the antimatter is not to use equal amounts of matter and antimatter. Instead, the antimatter should be used to heat a much larger amount of propellant. It has been shown,[32] that except for extreme relativistic spacecraft speeds (>0.5 c), the reaction mass needed is always four times the spacecraft payload mass, or an overall ratio of launch mass to payload mass of 5:1. The mass of the antimatter needed increases as the square of the mission total velocity change, but is always a negligible fraction of the total mass. Because the mass ratio of an antimatter powered space vehicle will always be less than 5:1 (typically 2-3:1), mission analysts need to rethink those mission that have been labeled "impossible" because of the extreme mass ratios required to accomplish the mission using a chemical or nuclear system with a fixed specific impulse.

Antimatter Powered Mission Analyses

In some preliminary studies of an antihydrogen/hydrogen rocket, Cassenti has estimated some of the parameters in an antimatter powered orbit transfer mission. The mission was to take a 10 ton spacecraft from LEO to GEO back to LEO (using aeroassist).[6] The mission velocity change was assumed to be 5.5 km/sec. Using the minimum antimatter optimization, Cassenti found that the optimum exhaust velocity was

3.4 km/sec (specific impulse of only 350 sec), the reaction
mass required was 40 tons, and the amount of antihydrogen
needed was only 6 mg. If the amount of antihydrogen used is
raised from 6 mg to 10 mg, the amount of hydrogen reaction
mass drops dramatically, from 40 tons to 15 tons, giving a
mass ratio of 2.5:1, while the exhaust velocity rose to
5 km/sec. Thus, in this range of the parameters, an
additional 4 mg of antihydrogen saves 25 tons of reaction
mass. Whether this trade-off is worth it depends upon the
relative cost of antihydrogen per milligram compared to the
cost of hydrogen per ton in LEO. In a recently completed
study[33] it was estimated that a well-designed factory for
producing antihydrogen should be able to operate at an energy
efficiency of better than 10^{-4} (compared to the present
efficiency of $2x10^{-8}$). The cost of the antimatter was
estimated to be about $10M per milligram, while reaction mass
in LEO was estimated to cost $5M per ton. Thus, using the
numbers from the Cassenti study, an additional 4 milligrams
($40M) of antimatter fuel in the rocket saved 25 tons ($125M)
of reaction mass. Although these cost estimates are far from
firm, it looks as though antimatter might be a cost-effective
fuel for space propulsion. ·

Conclusions

Our major conclusion about antiproton propulsion is that the
concept is feasible but difficult and expensive. Yet, despite
the high cost of antimatter, it may be a cost effective fuel
in space where any fuel is expensive. There is high risk in
the development of antiproton propulsion. The major
uncertainties seem to be in the production and capture of the
antiprotons at high efficiency, and the conversion of
antiprotons into frozen antihydrogen without excessive losses.
The storage problems look tractable. The problems that need
working on first are to determine the total antiproton
production rate and spectrum versus proton energy, the maximum
feasible limits to antiproton capture efficiencies of
physically feasible lenses and accumulator rings, and the
maximum efficiency of the antimatter rocket that uses the
antiproton fuel. It is important to recognize that many of
the problems of capturing, cooling, slowing, trapping, and
storing of antiprotons (antihydrogen) can be done as thesis
topics using normal protons and hydrogen.

Acknowledgments

References

[1] Sänger, E., "The Theory of Photon Pockets," _Ing. Arch._, Vol. 21, 1953, pp. 213 ff.

[2] Agnew, L.E., et al., "Antiproton Interactions in Hydrogen and Carbon Below 200 MeV," _Physical Review_, Vol. 118, 1960, pp. 1371 ff.

[3] Mallove, E.F., Forward, R.L., Paprotny, Z., and Lehmann, J., "Interstellar Travel and Communication: A Bibliography," _Journal of the British Interplanetary Society_, Vol. 33, June 1980, pp. 201-248 (entire issue).

[4] Forward, R.L., "Interstellar Flight Systems," AIAA Paper 80-0823, AIAA International Meeting, Baltimore, Md., May 1980, pp. 6-8.

[5] Cassenti, B.N., "Antimatter Propulsion for OTV Applications," AIAA Paper 84-1485, 20th Joint Propulsion Conference, Cincinnati, Ohio, June 1984.

[6] Cassenti, B.N., "Optimization of Relativistic Antimatter Rockets," _Journal of the British Interplanetary Society_, Vol. 37, November 1984, pp. 483-490.

[7] Vulpetti, G., "A Propulsion-Oriented Synthesis of the Antiproton-Nucleon Annihilation Experimental Results," _Journal of the British Interplanetary Society_, Vol. 37, March 1984, pp. 124-134.

[8] Vulpetti, G., "An Approach to the Modeling of Matter-Antimatter Propulsion Systems," _Journal of the British Interplanetary Society_, Vol. 37, September 1984, pp. 403-409.

[9] Massier, P.F., "The Need for Expanded Exploration of Matter-Antimatter Annihilation for Propulsion Application," _Journal of the British Interplanetary Society_, Vol. 35, September 1982, pp. 387-390.

[10]Forward, R.L., "Antimatter Propulsion," *Journal of the British Interplanetary Society*, Vol. 35, September 1982, pp. 391-395.

[11]Cassenti, B.N., "Design Considerations for Relativistic Antimatter Rockets," *Journal of the British Interplanetary Society*, Vol. 35, September 1982, pp. 396-404.

[12]Morgan, D.L., "Concepts for the Design of an Antimatter Annihilation Rocket," *Journal of the British Interplanetary Society*, Vol. 35, September 1982, pp. 405-412.

[13]Zito, R.R., "The Cryogenic Confinement of Antiprotons for Space Propulsion Systems," *Journal of the British Interplanetary Society*, Vol. 35, September 1982, pp. 414-421.

[14]Chapline, G., "Antimatter Breeders?" *Journal of the British Interplanetary Society*, Vol. 35, September 1982, pp. 423-424.

[15]Vsevolozskaya, T.A., et al., "Antiproton Source for the Accelerator-Storage Complex, UNK-IHEP," Fermilab Report FN-353 8000.00, June 1981, a translation of INP Preprint 80-182, December 1980.

[16]The Proton Synchrotron Staff, "The CERN PS Complex as an Antiproton Source," *IEEE Transactions on Nuclear Science*, Vol. NS-30, August 1983, pp. 2039-2041.

[17]Peoples, J., "The Fermilab Antiproton Source," *IEEE Transactions on Nuclear Science*, Vol. NS-30, August 1983, pp. 1970-1975.

[18]Van der Meer, S., "Stochastic Cooling in the CERN Antiproton Accumulator," *IEEE Transactions on Nuclear Science*, Vol. NS-28, 1981, pp. 1994-8.

[19]Bell, M., et al. "Electron Cooling in ICE at CERN," *Nuclear Instrumentation and Methods*, Vol. 190, 1981, pp. 237-255.

[20]Cline, D.B., Rubbia, C., and Van der Meer, S., "The Search for Intermediate Vector Bosons," *Scientific American*, Vol. 247, No. 3, March 1982, pp. 48-59.

[21]Hojvat, C., and Van Ginneken, A., "Calculation of Antiproton Yields for the Fermilab Antiproton Source," *Nuclear Instrumentation and Methods*, Vol. 206, 1983, pp. 67-83.

[22]Antinucci, M., et al., "Multiplicities of Charged Particles up to ISR Energies," *Letters Nuovo Cimento*, Vol. 6, 1972, pp. 121-127.

[23]Neumann, R., Poth, H., Winnacker, A. and Wolf, A., "Laser-Enhanced Electron-Ion Capture and Antihydrogen Formation," Zeitschrift für Physik A, Vol. 313, 1983, pp. 253-262.

[24]Letokhov, V.S. and Minogin, V.G., "Laser Radiation Pressure on Free Atoms," Physics Reports, Vol. 73, 1981, pp. 1-65.

[25]Ashkin, A. and Gordon, J.P., "Cooling and Trapping of Atoms by Resonance Radiation Pressure," Optics Letters, Vol. 4, 1979, pp. 161-163.

[26]Phillips, W.D. (editor), Laser-Cooled and Trapped Atoms, NBS Special Publication 653, Proceedings of Workshop on Spectroscopic Applications of Slow Atomic Beams, NBS Gaithersburg, MD, April 1983.

[27]Cline, R.W., et al, "Magnetic Confinement of Spin-Polarized Atomic Hydrogen," Physical Review Letters, Vol. 45, 1980, pp. 2117-2120.

[28]Waldron, R.D., "Diamagnetic Levitation Using Pyrolytic Graphite," Reviews of Scientific Instruments, Vol. 37, 1966, pp. 29-34.

[29]Letokhov, V.S. and Minogin, V.G., "Possibility of Accumulation and Storage of Cold Atoms in Magnetic Traps," Optics Communications, Vol. 35, 1980, pp. 199-202.

[30]Rhim, W.-K., Saffren, M.M., and Elleman, D.D., "Development of Electrostatic Levitator at JPL," Materials Processing in the Reduced Gravity Environment of Space, G.E. Rindone, Editor, Elsevier Science, 1982, pp. 115-119.

[31]Augenstein, B.W., "Some Examples of Propulsion Applications Using Antimatter," Rand Paper P-7133, The Rand Corp., Santa Monica, CA 90406 (July 1985).

[32]Shepherd, L.R., "Interstellar Flight," Journal of the British Interplanetary Society, Vol. 11, July 1952, pp. 149-167.

[33]Forward, R.L., "Alternate Propulsion Energy Sources," AFRPL-TR-83-067, Final Report on Contract F04611-83-C-0013, Air Force Rocket Propulsion Lab, Edwards, CA 93523, December 1983,

APPENDIX D

MATERIAL ENTHALPY ASCENT/DESCENT (MEAD) MODULE

ABSTRACT

This novel non-conventional propulsion concept resulted from a discussion on 3 January 1985 between the contract Principal Investigator, Dr. Robert L. Forward and the Task Manager, Dr. Franklin B. Mead, Jr. on the feasiblity of storing thermal energy in the heat capacity of high temperature materials. In the 1950's Dr. Mead had looked into the storage of heat energy in the specific heat capacity of graphite. The amount of heat that could be stored in graphite was significant, but the amount of propulsion obtainable was not competitive with liquid fuels. During the discussion, however, it was realized that the amount of energy stored in the latent heats of the phase changes to the liquid and vapor states of a material could be many times greater than the energy stored in the specific heat alone. For example, the latent heat of vaporization of some materials can release up to four times as much heat energy per kilogram as any chemical reaction can.

There was not enough time left on the contract to give this concept more than a cursory evaluation. The concept looks promising as an energy storage technique. It is recommended that the Air Force study the concept further to determine its technical feasiblity as an energy storage technique and the feasibility of utilizing the stored energy to heat a working fluid for propulsion.

MATERIAL ENTHALPY ASCENT/DESCENT (MEAD) MODULE

Dr. Franklin B. Mead, Jr. of AFRPL has observed that a great deal of energy can be stored as heat energy in the specific heat capacity of refractory materials. If that heat could be efficiently transferred to a propellant, such as hydrogen, then the hot hydrogen could propel a rocket. Whether such a rocket makes sense would depend upon the amount of heat stored, the efficiency of transfer of the energy to the propellant, and the weight of the storage material, tankage, and insulation.

As an example, the specific heat of graphite at high temperatures is roughly 2 J/gm·K. Graphite melts (sublimates) at 3820 K. The amount of heat energy released by graphite as it is cooled from 3820 to 820 K is 6 kJ/gm. This is about half the energy released by the combustion of LOX/H_2.

If the energy in the graphite is used to heat a working fluid such as hydrogen, then because of its low molecular weight, the specific impulse of the hydrogen is significant, ranging from 1000 sec at 3820 K to 470 sec at 820 K. However, because the specific heat of hydrogen at high temperatures is about 15 J/gm·K, it would take a number of grams of hot graphite to heat one gram of hydrogen (depending upon the exhaust temperature and I_{sp} that we wanted). The weight of the graphite makes it doubtful that a rocket using a MEAD module containing hot solid graphite could compete with a rocket using chemical fuels.

An alternate approach is to use the latent heat of fusion or the latent heat of vaporization of a material as the storage mechanism for the heat energy. A review of standard chemistry and physics handbooks led to the conclusion that the latent heat of vaporization is much better than the latent heat of fusion.

It was found in the handbooks that certain materials, upon condensing from a vapor to a liquid, can release four times as much energy as the combustion of LOX/H_2. The four elements that store the most energy per gram are listed below:

Element	Mol. Wt.	Temp. Vap. (K)	Heat of Vap. (kJ/gm)
C	12.01	5100	60
B	10.81	2820	53
Be	9.01	3240	36
Li	6.94	1615	23

Boron looks like a promising candidate for a metal vapor version of a MEAD module. The boron in the insulated MEAD module would be preheated on the ground over a long period of time until it turned into vapor at a temperature of 2820 K or greater (depending upon the pressure). At this temperature it could be contained in a pressure vessel made of graphite, which has a melting point of 3820 K.

The MEAD module and a tank of liquid hydrogen would then be attached to a single-stage-to-orbit vehicle just before takeoff. The hot vapor from the MEAD module would be sent to a heat exchanger in the rocket engine of the vehicle using rhenium tubing (similar to that used in the AFRPL/Rocketdyne solar thermal rocket). The hot boron vapor would heat the hydrogen to about 2820 K (the same temperature expected in the solar thermal rocket) to produce a specific impulse of about 800 sec. Each gram of boron vapor at 2820 K has enough energy to raise a gram of hydrogen to 2820 K with 10 kJ/gm left over to cover losses. The condensed boron liquid would drain off, allowing more hot boron vapor to reach the heat exchanger tubes. After all the boron vapor has condensed, there is still 4 to 6 kJ/gm of heat energy left in the specific heat of the liquid boron that can be used for further propulsion at lower specific impulse.

I was unable to find data on the critical temperature (T_c), pressure (P_c), and density (d_c) of boron. But from the data on lead, silver, and gallium, I estimate that T_c=6000 K, P_c=250 atm, and d_c=1 gm/cc for boron. This would mean that at a temperature of 3000 K and a pressure of 30 atm, the density of the vapor would be about 0.25 gm/cc. At this density, 100 tons of hot boron would fit into a tank 5 m in diameter by 20 m long (the size of the body of the Shuttle), while 100 tons of liquid hydrogen propellant would take up the same room as the 100 tons flown in the present STS external tank (8.4 m diameter by 25 m long). Different storage pressures for the boron would give different volumes for the MEAD module, since the boron is being stored as a gas.

It is not possible to know at this time if this concept makes sense as a single-stage-to-orbit rocket. Since the energy source for the rocket (the hot boron) is heavy and is kept on board instead of being exhausted with the propellant, the basic rocket equations to describe the situation have to be rederived with the new assumptions. The density of boron vapor at high temperature and pressures has to be determined. Then the weight of the structure and insulation for the hot, high pressure tankage in the MEAD module needs to be estimated. The final design may turn out to be too heavy to fly, but any concept that gives high thrust at 800 sec in a compact package is certainly worth looking at further.